

# LINEAR CONVERGENCE OF THE SUBSPACE CONSTRAINED MEAN SHIFT ALGORITHM: FROM EUCLIDEAN TO DIRECTIONAL DATA

BY YIKUN ZHANG<sup>1,\*</sup> AND YEN-CHI CHEN<sup>1,†</sup>

<sup>1</sup>*Department of Statistics, University of Washington*

<sup>\*</sup>*yikun@uw.edu*; <sup>†</sup>*yenchi@uw.edu*

This paper studies linear convergence of the subspace constrained mean shift (SCMS) algorithm, a well-known algorithm for identifying a density ridge defined by a kernel density estimator. By arguing that the SCMS algorithm is a special variant of a subspace constrained gradient ascent (SCGA) algorithm with an adaptive step size, we derive linear convergence of such SCGA algorithm. While the existing research focuses mainly on density ridges in the Euclidean space, we generalize density ridges and the SCMS algorithm to directional data. In particular, we establish the stability theorem of density ridges with directional data and prove the linear convergence of our proposed directional SCMS algorithm.

**1. Introduction.** Identifying meaningful lower dimensional structures from a point cloud has long been a popular research topic in Statistics and Machine Learning (Izenman, 2012; Wasserman, 2018). One reliable characterization of such a low-dimensional structure is the *density ridge*, which can be feasibly estimated by a kernel density estimator (KDE) from point cloud data (Eberly, 1996; Genovese et al., 2014). Loosely speaking, an estimated density ridge signifies a high-density curve or surface in a point cloud; see the left panel of Figure 1. Let  $p$  be the underlying probability density function that generates the data in the Euclidean space  $\mathbb{R}^D$ . Its order- $d$  density ridge  $R_d$  with  $0 \leq d < D$  is the set of points

$$(1) \quad R_d = \{ \mathbf{x} \in \mathbb{R}^D : V_d(\mathbf{x})^T \nabla p(\mathbf{x}) = \mathbf{0}, \lambda_{d+1}(\mathbf{x}) < 0 \},$$

where  $\lambda_1(\mathbf{x}) \geq \dots \geq \lambda_D(\mathbf{x})$  are the eigenvalues of Hessian  $\nabla \nabla p(\mathbf{x})$  and  $V_d(\mathbf{x}) \in \mathbb{R}^{D \times (D-d)}$  has its columns as the last  $D - d$  orthonormal eigenvectors. The notion of density ridges has appeared in various scientific fields, such as medical imaging (You et al., 2011), seismology (Sasaki et al., 2017), and astronomy (Sousbie et al., 2007; Chen et al., 2016). To locate an estimated density ridge defined by (Euclidean) KDE, Ozertem and Erdogmus (2011) proposed a practical method called *subspace constrained mean shift (SCMS) algorithm*.

While the statistical estimation and asymptotic theories of density ridges in  $\mathbb{R}^D$  have been well-studied (Genovese et al., 2014; Chen et al., 2015; Qiao and Polonik, 2016; Chen et al., 2015a; Qiao, 2020; Qiao and Polonik, 2021), the literature falls short of addressing the algorithmic properties of the ridge-finding method, *i.e.*, the SCMS algorithm. To the extent of our knowledge, Ghassabeh et al. (2013); Ghassabeh and Rudzicz (2020) were the only available works to investigate the SCMS algorithm (and its modified version) from an algorithmic perspective. However, they only proved a non-decreasing property of density estimates and the validity of two stopping criteria for the SCMS algorithm. The algorithmic convergence rate of the SCMS algorithm remains an open question. There are two challenges to answering this question. First, because every iteration of the SCMS algorithm involves a projection matrix defined by the (estimated) Hessian, it is no longer a conventional first-order method in optimization. Second, estimating a density ridge in practice is a nonconvex/nonconcave

*MSC2020 subject classifications:* Primary 62G05; secondary 49Q12, 62H11.

*Keywords and phrases:* Ridges, subspace constrained mean shift, directional data, optimization on a manifold.

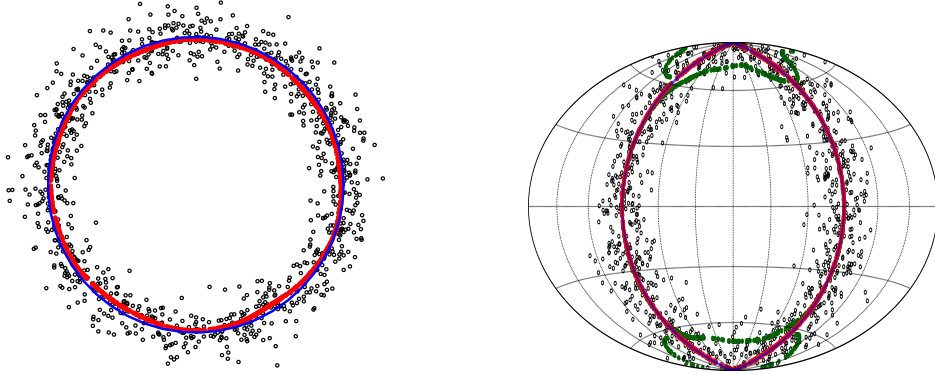


Fig 1: Synthetic data samples (drawn as black points) with hidden circular manifold structures (indicated by blue curves) in  $\mathbb{R}^2$  and on the unit sphere  $\Omega_2 \subset \mathbb{R}^3$  as well as the associated (directional) density ridges. **Left:** The red points indicate the estimated ridge obtained by the Euclidean SCMS algorithm. **Right:** The red points represent the estimated directional ridge identified by our directional SCMS algorithm, while the green points indicate the estimated ridge obtained by the Euclidean SCMS algorithm. The right panel is presented under the Hammer projection; see Appendix C of the supplement (Zhang and Chen, 2021) for details.

optimization problem. Thus, the first objective of this paper is to provide a theoretical study on the algorithmic (linear) rate of convergence.

In stark contrast to abundant research papers about density ridges in an Euclidean space, little work has been done to examine the statistical properties and any practical algorithm of estimating density ridges on the unit hypersphere  $\Omega_q = \{\mathbf{x} \in \mathbb{R}^{q+1} : \|\mathbf{x}\|_2 = 1\} \subset \mathbb{R}^{q+1}$ . In many scientific fields of study, such as seismology and astronomy, the available data may consist of i.i.d. (independently and identically distributed) observations on  $\Omega_q$ , which is generally known as *directional data* in the statistical literature (Mardia and Jupp, 2000; Ley and Verdebout, 2017). More importantly, identifying an estimated density ridge from directional data on  $\Omega_2$  by the Euclidean SCMS algorithm always suffers from high bias near the two poles of  $\Omega_2$ ; see the right panel in Figure 1 for a preview and Section B in the supplement (Zhang and Chen, 2021) for detailed discussions. Hence, the second objective of this paper is to generalize density ridges and the SCMS algorithm to directional data.

#### Main Results.

- We prove the linear convergence of the SCMS algorithm with Euclidean data (Theorem 5 and its related discussion):

$$\left\| \hat{\mathbf{x}}^{(t)} - \hat{\mathbf{x}}^* \right\|_2 \leq \Upsilon^t \left\| \hat{\mathbf{x}}^{(0)} - \hat{\mathbf{x}}^* \right\|_2,$$

where  $\{\hat{\mathbf{x}}^{(t)}\}_{t=0}^\infty$  is a sequence of points generated by the SCMS algorithm,  $\hat{\mathbf{x}}^*$  is the limit point of the sequence, and  $0 < \Upsilon < 1$  is a constant.

- We generalize density ridges and the SCMS algorithm to directional data on  $\Omega_q$  (Section 4).
- We prove the convergence rate of a ridge estimator on  $\Omega_q$  defined by directional KDE (Theorem 6):

$$\text{Haus}(\underline{R}_d, \hat{\underline{R}}_d) = O(h^2) + O_P\left(\sqrt{\frac{|\log h|}{nh^{q+4}}}\right),$$

where  $\underline{R}_d$  and  $\widehat{\underline{R}}_d$  are the population and estimated directional density ridges, respectively, Haus is the Hausdorff distance, and  $q$  is the dimension of the sphere  $\Omega_q$ .

- We prove the linear convergence of the directional SCMS algorithm (Theorem 10):

$$d_g(\widehat{\underline{x}}^{(t)}, \widehat{\underline{x}}^*) \leq \Upsilon^t \cdot d_g(\widehat{\underline{x}}^{(0)}, \widehat{\underline{x}}^*),$$

where  $\{\widehat{\underline{x}}^{(t)}\}_{t=0}^\infty$  is the sequence of points generated by our directional SCMS algorithm,  $\widehat{\underline{x}}^*$  is the convergence point,  $0 < \Upsilon < 1$  is a constant, and  $d_g$  is the geodesic distance on  $\Omega_q$ .

*Other Related Literature.* The problem of density ridge estimation has its unique standing in both the computer science and statistics literature; see Hall et al. (1992); Eberly (1996); Damon (1999); Hall et al. (2001) and references therein. The SCMS algorithm for identifying an estimated density ridge first appeared in the field of computer vision (Saragih et al., 2009) before its introduction to the statistical community by Ozertem and Erdogmus (2011). Among various definition of density ridges (Norgard and Bremer, 2012; Peikert et al., 2013), our definition follows from Eberly (1996); Genovese et al. (2014); Chen et al. (2015), because its statistical estimation theory has been well-established and it is feasible to be directly generalized to directional densities. Qiao and Polonik (2021) proposed a new method for finding ridges based a gradient descent of the ridgeness, which shows connection to solution manifolds (Chen, 2020). Practically, our directional SCMS algorithm is extended from the directional mean shift algorithm (Oba et al., 2005; Kafai et al., 2010; Yang et al., 2014). As we cast the (directional) SCMS algorithms into subspace constrained gradient ascent (SCGA) algorithms (on a hypersphere), it is worth mentioning that one should not confuse such SCGA algorithm with the projected gradient ascent/descent method for a constrained problem in the standard optimization theory; see Section 3.2 in Bubeck (2015) for some references of the latter one. The SCGA algorithm discussed in this paper is a gradient ascent algorithm but with a subspace constrained gradient. When the subspace coincides with alternating one-dimensional coordinate spaces, the SCGA algorithm reduces to the well-known coordinate ascent/descent method (Wright, 2015). Some linear convergence results of the coordinate descent algorithms were previously established by Luo and Tseng (1992); Beck and Tetruashvili (2013). Other related work includes Kozak et al. (2019, 2020), though, in their problem setups, the projection matrix onto the subspace is random and has its expectation equal to the identity matrix. Our interested SCGA algorithm always has a deterministic constrained subspace defined by the eigenspace associated with the last several eigenvalues of the Hessian of the density  $p$ .

*Outlines and Notations.* Section 2 introduces the definitions of Euclidean and directional KDEs and reviews some preliminary concepts of differential geometry on  $\Omega_q$ . We discuss the assumptions on Euclidean density ridges and establish the linear convergence of SCMS/SCGA algorithms in Section 3. In Section 4, we generalize the definition of density ridges to the directional data scenario and prove the linear convergence of SCMS/SCGA algorithms on  $\Omega_q$ . We conclude the paper and discuss some potential impacts in Section 5. Simulation studies and real-world applications of Euclidean and directional SCMS algorithms are deferred to Appendix C in the supplement (Zhang and Chen, 2021), whose code is available at <https://github.com/zhangyk8/EuDirSCMS>.

Throughout the paper we use  $d$  as the intrinsic dimension of density ridges, whose ambient spaces are  $\mathbb{R}^D$  in Euclidean data cases and  $\Omega_q = \{\mathbf{x} \in \mathbb{R}^{q+1} : \|\mathbf{x}\|_2 = 1\}$  in directional data cases. Notice that *a quantity under the directional data setting that has its counterpart in the Euclidean data case will be denoted by the same notation with an extra underline*. For instance,  $R_d$  is a ridge of density  $p$  in the Euclidean space  $\mathbb{R}^D$  while  $\underline{R}_d$  refers to a ridge of directional density  $f$  on the sphere  $\Omega_q$ .

Let  $f : \mathbb{R}^D \rightarrow \mathbb{R}$  be a smooth function and  $[\alpha] = (\alpha_1, \dots, \alpha_D)$  be a multi-index (that is,  $\alpha_1, \dots, \alpha_D$  are nonnegative integers and  $||[\alpha]|| = \sum_{i=1}^D \alpha_i$ ). Define  $D^{[\alpha]} = \frac{\partial^{\alpha_1}}{\partial x_1^{\alpha_1}} \cdots \frac{\partial^{\alpha_D}}{\partial x_D^{\alpha_D}}$  to

be the  $[[\alpha]]$ -th order partial derivative operator, where  $D^{[\alpha]}f$  is often written as  $f^{(\alpha)}$ . For  $j = 0, 1, \dots$ , we define the functional norms  $\|f\|_\infty^{(j)} = \max_{\alpha: [[\alpha]] = j} \sup_{\mathbf{x} \in \mathbb{R}^D} |f^{(\alpha)}(\mathbf{x})|$ . When  $j = 0$ , this becomes the infinity norm of  $f$ ; for  $j > 0$ , the above norms are indeed some semi-norms. We also define  $\|f\|_{\infty, k}^* = \max_{j=0, \dots, k} \|f\|_\infty^{(j)}$ .

The (total) gradient and Hessian of  $f$  are defined as  $\nabla f(\mathbf{x}) = \left( \frac{\partial f(\mathbf{x})}{\partial x_1}, \dots, \frac{\partial f(\mathbf{x})}{\partial x_D} \right)^T$  and  $\nabla \nabla f(\mathbf{x}) = \left( \frac{\partial^2 f(\mathbf{x})}{\partial x_i \partial x_j} \right)_{1 \leq i, j \leq D}$ . Inductively, the third derivative of  $f(\mathbf{x})$  is a  $D \times D \times D$  array given by  $\nabla^3 f(\mathbf{x}) = \left( \frac{\partial^3}{\partial x_i \partial x_j \partial x_k} f(\mathbf{x}) \right)_{1 \leq i, j, k \leq D}$ . When  $f$  is a directional density supported on  $\Omega_q$ , the preceding functional norms are defined via the Riemannian gradient, Hessian, and high-order derivatives of  $f(\mathbf{x})$  within the tangent space  $T_{\mathbf{x}}$  at  $\mathbf{x} \in \Omega_q$ , and the supremum will be taken over  $\Omega_q$  instead of  $\mathbb{R}^D$ . They are equivalent to the derivatives of  $f$  with respect to the local coordinate chart on  $\Omega_q$ ; see Section 2.3 for a detailed review.

Let  $A_{jk}$  denote the  $(j, k)$  entry of a matrix  $A \in \mathbb{R}^{m \times n}$ . Then, the Frobenius norm is  $\|A\|_F = \sqrt{\sum_{j,k} A_{jk}^2} = \sqrt{\text{tr}(A^T A)}$ , where  $\text{tr}(A^T A)$  is the trace of the square matrix  $A^T A$ , and the operator norm is  $\|A\| = \sup_{\|\mathbf{x}\|=1} \|A\mathbf{x}\|$ . In most cases, we consider the  $L_2$  (operator) norm  $\|\cdot\|_2$ . We define  $\|A\|_{\max} = \max_{j,k} |A_{jk}|$ . The inequality relationships between the above matrix norms are  $\|A\|_2 \leq \|A\|_F \leq \sqrt{n} \|A\|_2$ ,  $\|A\|_{\max} \leq \|A\|_2 \leq \sqrt{mn} \|A\|_{\max}$ , and  $\|A\|_F \leq \sqrt{mn} \|A\|_{\max}$ .

We use the big-O notation  $h(x) = O(g(x))$  if the absolute value of  $h(x)$  is upper bounded by a positive constant multiple of  $g(x)$  for all sufficiently large  $x$ . In contrast,  $h(x) = o(g(x))$  when  $\lim_{x \rightarrow \infty} \frac{|h(x)|}{g(x)} = 0$ . For random vectors, the notation  $o_P(1)$  is short for a sequence of random vectors that converges to zero in probability. The expression  $O_P(1)$  denotes a sequence that is bounded in probability; see Section 2.2 of [van der Vaart \(1998\)](#) for details.

**2. Preliminaries.** In this section, we review the KDE with Euclidean and directional data as well as some differential geometry concepts on  $\Omega_q$ .

**2.1. Euclidean KDE.** Let  $\{\mathbf{X}_1, \dots, \mathbf{X}_n\}$  be a random sample from a distribution with density  $p$  supported on a compact set in  $\mathbb{R}^D$ . We call the sample  $\{\mathbf{X}_1, \dots, \mathbf{X}_n\}$  Euclidean data in the sequel. The (Euclidean) KDE at point  $\mathbf{x} \in \mathbb{R}^D$  with a kernel (function)  $K$  and bandwidth parameter  $h \equiv h(n)$  is written as ([Wasserman, 2006](#); [Scott, 2015](#); [Chen, 2017](#)):

$$(2) \quad \hat{p}_n(\mathbf{x}) = \frac{1}{nh^D} \sum_{i=1}^n K\left(\frac{\mathbf{x} - \mathbf{X}_i}{h}\right).$$

The kernel  $K : \mathbb{R}^D \rightarrow \mathbb{R}$  is generally a unimodal function satisfying the following properties:

- (K1)  $\int_{\mathbb{R}^D} K(\mathbf{x}) d\mathbf{x} = 1$ .
- (K2)  $K(\mathbf{x})$  is (radially) symmetric, i.e.,  $\int_{\mathbb{R}^D} \mathbf{x} K(\mathbf{x}) d\mathbf{x} = 0$ .
- (K3)  $\lim_{\|\mathbf{x}\|_2 \rightarrow \infty} \|\mathbf{x}\|_2^D K(\mathbf{x}) = 0$  and  $\int_{\mathbb{R}^D} \|\mathbf{x}\|_2^2 K(\mathbf{x}) d\mathbf{x} < \infty$ , where  $\|\cdot\|_2$  is the usual Euclidean norm in  $\mathbb{R}^D$ .

One possible approach to construct a multivariate kernel  $K(\mathbf{x})$  with the above properties is to derive it from a kernel profile as follows:

$$(3) \quad K(\mathbf{x}) = c_{k,D} \cdot k\left(\|\mathbf{x}\|_2^2\right),$$

where  $c_{k,D}$  is the normalizing constant such that  $K$  satisfies (K1) and the function  $k : [0, \infty) \rightarrow [0, \infty)$  is called the *profile* of the kernel. An important example of the profile function is  $k_N(x) = \exp(-\frac{x}{2})$  for  $x \geq 0$ , leading to the multivariate Gaussian kernel  $K_N(\mathbf{x}) = \frac{1}{(2\pi)^{\frac{D}{2}}} \exp\left(-\frac{\|\mathbf{x}\|_2^2}{2}\right)$ .

Another approach of designing a multivariate kernel function is to leverage the product kernel technique as  $K(\mathbf{x}) = K_1(x_1) \cdots K_D(x_D)$ , where  $K_1, \dots, K_D$  are kernels function defined on  $\mathbb{R}$  satisfying the properties (K1-3). This leads to a multivariate KDE as

$$(4) \quad \hat{p}_n(\mathbf{x}) = \frac{1}{nh^D} \sum_{i=1}^n K_1\left(\frac{x_1 - X_{i,1}}{h}\right) \cdots K_D\left(\frac{x_D - X_{i,D}}{h}\right).$$

In fact, the multivariate Gaussian kernel  $K_N$  can be obtained by defining its kernel profile as  $k_N(x) = \exp(-\frac{x}{2})$  for  $x \geq 0$  or taking  $K_1(x) = \cdots = K_D(x) = \frac{1}{\sqrt{2\pi}} \exp(-\frac{x^2}{2})$ . In practice, the multivariate KDE (2) with Gaussian kernel is the most popular nonparametric density estimator with Euclidean data. The most crucial part in applying the KDE is to select the bandwidth parameter  $h$ ; see Jones et al. (1996); Sheather (2004) for related discussions.

**2.2. Kernel Density Estimation with Directional Data.** The Euclidean KDE (2) exhibits some salient drawbacks in dealing with directional data samples; see Section B in the supplement (Zhang and Chen, 2021) for detailed discussions. Fortunately, the theory of kernel density estimation with directional data has been well-studied since late 1970s (Beran, 1979; Hall et al., 1987; Bai et al., 1988; Zhao and Wu, 2001; García-Portugués, 2013; Pewsey and García-Portugués, 2021). Let  $\mathbf{X}_1, \dots, \mathbf{X}_n \in \Omega_q \subset \mathbb{R}^{q+1}$  be a random sample generated from an underlying directional density function  $f$  on  $\Omega_q$  with  $\int_{\Omega_q} f(\mathbf{x}) \omega_q(d\mathbf{x}) = 1$ , where  $\omega_q$  is the Lebesgue measure on  $\Omega_q$ . The directional KDE is given by:

$$(5) \quad \hat{f}_h(\mathbf{x}) = \frac{c_{h,q}(L)}{n} \sum_{i=1}^n L\left(\frac{1 - \mathbf{x}^T \mathbf{X}_i}{h^2}\right),$$

where  $L$  is a directional kernel (a rapidly decaying function with nonnegative values and defined on  $(-\delta_L, \infty) \subset \mathbb{R}$  for some constant  $\delta_L > 0$ ),  $h > 0$  is the bandwidth parameter, and  $c_{h,q}(L)$  is a normalizing constant satisfying  $c_{h,q}(L)^{-1} = \int_{\Omega_q} L\left(\frac{1 - \mathbf{x}^T \mathbf{y}}{h^2}\right) \omega_q(d\mathbf{x})$ .

As in the Euclidean KDE, the bandwidth selection is a critical part in determining the performances of directional KDEs (Hall et al., 1987; Bai et al., 1988; Taylor, 2008; Marzio et al., 2011; Oliveira et al., 2012; García-Portugués, 2013; Saavedra-Nieves and María Crujeiras, 2020). On the contrary, the choice of the kernel is less crucial and a popular candidate is the so-called von Mises kernel  $L(r) = e^{-r}$ . Its name originates from the famous  $q$ -von Mises-Fisher distribution on  $\Omega_q$ , which is denoted by  $\text{vMF}(\boldsymbol{\mu}, \nu)$  and has the density

$$(6) \quad f_{\text{vMF}}(\mathbf{x}; \boldsymbol{\mu}, \nu) = C_q(\nu) \cdot \exp(\nu \boldsymbol{\mu}^T \mathbf{x}) \quad \text{with} \quad C_q(\nu) = \frac{\nu^{\frac{q-1}{2}}}{(2\pi)^{\frac{q+1}{2}} \mathcal{I}_{\frac{q-1}{2}}(\nu)},$$

where  $\boldsymbol{\mu} \in \Omega_q$  is the directional mean,  $\nu \geq 0$  is the concentration parameter, and  $\mathcal{I}_\alpha(\nu)$  is the modified Bessel function of the first kind at order  $\nu$ . For more details on statistical properties of the von Mises-Fisher distribution and directional KDE, we refer the interested reader to Mardia and Jupp (2000); Banerjee et al. (2005); García-Portugués et al. (2013).

**2.3. Riemannian Gradient, Hessian, and Exponential Map on  $\Omega_q$ .** Given that the unit hypersphere  $\Omega_q$  is a nonlinear manifold, the Riemannian gradient and Hessian of a smooth



function  $f$  on  $\Omega_q$  are defined within its tangent spaces. They are different from but also interconnected with the total gradient and Hessian of  $f$  in the ambient Euclidean space  $\mathbb{R}^{q+1}$ .

• **Riemannian Gradient on  $\Omega_q$ .** Let  $T_x$  be the tangent space of  $\Omega_q$  at point  $x \in \Omega_q$ , which consists of all the vectors starting from  $x$  and tangent to  $\Omega_q$ . Given a smooth function  $f : \Omega_q \rightarrow \mathbb{R}$ , its *Riemannian gradient*  $\text{grad } f(x) \in T_x$  is defined as

$$(7) \quad \langle v, \text{grad } f(x) \rangle_x = df_x(v)$$

for any (unit) vector  $v \in T_x$ , where  $\langle \cdot, \cdot \rangle_x$  is the inner product (or Riemannian metric) in  $T_x$  and  $df_x : T_x \rightarrow \mathbb{R}$  is the differential operator of  $f$  at  $x \in \Omega_q$ ; see, e.g., Section 3.1 in [Banyaga and Hurtubise \(2004\)](#) for more details. If  $f$  is smooth in an open neighborhood containing  $\Omega_q$  and we consider  $\text{grad } f(x), v \in T_x$  as vectors in  $\mathbb{R}^{q+1}$ , then the inner product in  $T_x$  reduces to the usual one in  $\mathbb{R}^{q+1}$  and the Riemannian gradient  $\text{grad } f(x)$  can be expressed in terms of the total gradient  $\nabla f(x)$  as

$$(8) \quad \text{grad } f(x) = (I_{q+1} - xx^T) \nabla f(x),$$

where  $I_{q+1} \in \mathbb{R}^{(q+1) \times (q+1)}$  is the identity matrix. The left-hand side of (8) is the projection of the total gradient  $\nabla f(x)$  onto the tangent space  $T_x$  at  $x \in \Omega_q$ .

• **Riemannian Hessian on  $\Omega_q$ .** The *Riemannian Hessian*  $\mathcal{H}f(x)$  at point  $x \in \Omega_q$  is a symmetric bilinear map  $\mathcal{H}f(x) : T_x \times T_x \rightarrow \mathbb{R}$  satisfying

$$(9) \quad \mathcal{H}f(x)(v, u) = \langle \text{grad } \langle \text{grad } f(x), v \rangle_x, u \rangle_x.$$

Similar to  $\text{grad } f(x)$ , the Riemannian Hessian  $\mathcal{H}f(x)$  has the following explicit formula when viewed in the ambient Euclidean space  $\mathbb{R}^{q+1}$ :

$$(10) \quad \mathcal{H}f(x) = (I_{q+1} - xx^T) [\nabla \nabla f(x) - \nabla f(x)^T x I_{q+1}] (I_{q+1} - xx^T),$$

where  $\nabla f(x)$  and  $\nabla \nabla f(x)$  are the total gradient and Hessian of  $f$  in  $\mathbb{R}^{q+1}$ . This formula can be derived via the Riemannian connection and Weingarten map on  $\Omega_q$  ([Absil et al., 2013](#)) or geodesics on  $\Omega_q$  ([Zhang and Chen, 2020](#)).

• **Exponential Map.** An *exponential map*  $\text{Exp}_x : T_x \rightarrow \Omega_q$  at  $x \in \Omega_q$  is a mapping that takes a vector  $v \in T_x$  to a point  $y := \text{Exp}_x(v) \in \Omega_q$  with  $\gamma(0) = x$ ,  $\gamma(1) = y$  and  $\gamma'(0) = v$ . Here,  $\gamma : [0, 1] \rightarrow \Omega_q$  is a curve of minimum length between  $x$  and  $y$  (i.e., the so-called geodesic on  $\Omega_q$ ). An intuitive way of thinking of the exponential map  $\text{Exp}_x$  evaluated at  $v$  on  $\Omega_q$  is that starting at point  $x$ , we identify another point  $y$  on  $\Omega_q$  along the geodesic/great circle in the direction of  $v$  so that the geodesic distance between  $x$  and  $y$  is  $\|v\|_2$ . The inverse of an exponential map (or logarithmic map) is defined within a small neighborhood  $U \subset \Omega_q$  around  $x$  as a mapping  $\text{Exp}_x^{-1} : U \rightarrow T_x$  such that  $\text{Exp}_x^{-1}(y)$  represents the vector in  $T_x$  starting at  $x$ , pointing to  $y$ , and with its length equal to the geodesic distance between  $x$  and  $y$ .

**3. Linear Convergence of the SCMS Algorithm with Euclidean Data.** Given the definition (1) of a order- $d$  ridge  $R_d$  of density  $p$  with a compact support in  $\mathbb{R}^D$  (not restricted to  $\Omega_q$ ), we introduce, in this section, some commonly assumed conditions to regularize  $R_d$  and its stability theorem. After revisiting the frameworks of Euclidean mean shift and SCMS algorithms as well as deriving the SCMS algorithm as the SCGA algorithm with an adaptive step size, we present our main theorem on the linear convergence of the SCGA algorithm without imposing any extra condition.

**3.1. Assumptions and Stability of Euclidean Density Ridge.** Under the spectral decomposition on the Hessian  $\nabla\nabla p(\mathbf{x})$  as  $\nabla\nabla p(\mathbf{x}) = V(\mathbf{x})\Lambda(\mathbf{x})V(\mathbf{x})^T$ , we know that  $V(\mathbf{x}) = [\mathbf{v}_1(\mathbf{x}), \dots, \mathbf{v}_D(\mathbf{x})] \in \mathbb{R}^{D \times D}$  is a real orthogonal matrix with the eigenvectors of  $\nabla\nabla p(\mathbf{x})$  as its columns and  $\Lambda(\mathbf{x}) = \text{Diag}[\lambda_1(\mathbf{x}), \dots, \lambda_D(\mathbf{x})]$  is a diagonal matrix with  $\lambda_1(\mathbf{x}) \geq \dots \geq \lambda_D(\mathbf{x})$ . Given that  $V_d(\mathbf{x}) = [\mathbf{v}_{d+1}(\mathbf{x}), \dots, \mathbf{v}_D(\mathbf{x})] \in \mathbb{R}^{D \times (D-d)}$ , we let  $U_d(\mathbf{x}) \equiv V_d(\mathbf{x})V_d(\mathbf{x})^T$  be the projection matrix onto the column space of  $V_d(\mathbf{x})$  and  $U_d^\perp(\mathbf{x}) = \mathbf{I}_D - V_d(\mathbf{x})V_d(\mathbf{x})^T = V_\diamond(\mathbf{x})V_\diamond(\mathbf{x})^T$  be the projection matrix onto the complement space, where  $V_\diamond(\mathbf{x}) = [\mathbf{v}_1(\mathbf{x}), \dots, \mathbf{v}_d(\mathbf{x})] \in \mathbb{R}^{D \times d}$  and  $\mathbf{I}_D$  is the identity matrix in  $\mathbb{R}^{D \times D}$ . Then, the order- $d$  principal gradient  $G_d(\mathbf{x})$  (or projected gradient in [Genovese et al. \(2014\)](#); [Chen et al. \(2015\)](#)) is defined as:

$$(11) \quad G_d(\mathbf{x}) = U_d(\mathbf{x})\nabla p(\mathbf{x}) = V_d(\mathbf{x})V_d(\mathbf{x})^T\nabla p(\mathbf{x}),$$

and  $U_d^\perp(\mathbf{x})\nabla p(\mathbf{x})$  will be called the residual gradient. The order- $d$  density ridge can be equivalently defined as:

$$(12) \quad R_d = \{\mathbf{x} \in \mathbb{R}^D : G_d(\mathbf{x}) = \mathbf{0}, \lambda_{d+1}(\mathbf{x}) < 0\}.$$

It follows that the 0-ridge  $R_0$  is the set of local modes of  $p$ , whose statistical properties and practical estimation algorithm have been well-studied in [Arias-Castro et al. \(2016\)](#); [Chen et al. \(2016\)](#). Thus, we only consider the case when  $1 \leq d < D$  in the sequel. We define the projection from point  $\mathbf{x} \in \mathbb{R}^D$  onto a ridge  $R_d$  by  $\pi_{R_d}(\mathbf{x}) = \arg \min_{\mathbf{y} \in R_d} \|\mathbf{x} - \mathbf{y}\|_2$  and the distance from point  $\mathbf{x}$  to  $R_d$  by  $d_E(\mathbf{x}, R_d) = \|\mathbf{x} - \pi_{R_d}(\mathbf{x})\|_2 = \min_{\mathbf{y} \in R_d} \|\mathbf{x} - \mathbf{y}\|_2$ . Note that the projection from point  $\mathbf{x} \in \mathbb{R}^D$  to  $R_d$  may not be unique. To guarantee the uniqueness of the projection, we introduce a concept called the *reach* ([Federer, 1959](#); [Cuevas, 2009](#)) as:

$$(13) \quad \text{reach}(R_d) = \inf \{\delta > 0 : \forall \mathbf{x} \in R_d \oplus \delta, \mathbf{x} \text{ has a unique projection onto } R_d\},$$

where  $R_d \oplus \delta = \cup_{\mathbf{x} \in R_d} \text{Ball}_D(\mathbf{x}, \delta)$  and  $\text{Ball}_D(\mathbf{x}, \delta) = \{\mathbf{z} \in \mathbb{R}^D : \|\mathbf{z} - \mathbf{x}\|_2 \leq \delta\}$  is a  $D$ -dimensional ball of radius  $\delta$  centered at  $\mathbf{x}$ . To obtain a well-behaved ridge  $R_d$ , some assumptions need imposing on the underlying density  $p$  around a small neighborhood of  $R_d$ .

- **(A1) (Differentiability)** We assume that  $p$  is at least four times differentiable with bounded partial derivatives up to the fourth order for every  $\mathbf{x} \in \mathbb{R}^D$ .
- **(A2) (Eigengap)** We assume that there exist constants  $\rho > 0$  and  $\beta_0 > 0$  such that  $\lambda_{d+1}(\mathbf{y}) \leq -\beta_0$  and  $\lambda_d(\mathbf{y}) - \lambda_{d+1}(\mathbf{y}) \geq \beta_0$  for any  $\mathbf{y} \in R_d \oplus \rho$ .
- **(A3) (Path Smoothness)** Under the same  $\rho, \beta_0 > 0$  in (A2), we assume that there exists another constant  $\beta_1 \in (0, \beta_0)$  such that

$$D^{\frac{3}{2}} \left\| U_d^\perp(\mathbf{y})\nabla p(\mathbf{y}) \right\|_2 \left\| \nabla^3 p(\mathbf{y}) \right\|_{\max} \leq \frac{\beta_0^2}{4},$$

$$d \cdot D^{\frac{3}{2}} \left\| \nabla p(\mathbf{x}) \right\|_2 \left\| \nabla^3 p(\mathbf{x}) \right\|_{\max} \leq \beta_0(\beta_0 - \beta_1)$$

for all  $\mathbf{y} \in R_d \oplus \rho$  and  $\mathbf{x} \in R_d$ .

Condition (A1) is a natural differentiability assumption under the context of ridge estimation. Condition (A2) is a curvature assumption on the true density  $p$ , ensuring that  $p$  is “strongly concave” around  $R_d$  inside the  $(D - d)$ -dimensional linear space spanned by the columns of  $V_d(\mathbf{y})$ . We call this property “subspace constrained strong concavity”. It is critical in the linear convergence of the SCGA algorithm; see Section 3.3 for details. Condition (A3) incorporates some third derivative assumptions that constrain the gradient from being too steep around the ridge  $R_d$ . They are also imposed by [Genovese et al. \(2014\)](#) for characterizing a quadratic behavior and stability of ridges, as well as by [Chen et al. \(2015\)](#) for discussing some properties of the normal space and local uncertainty of  $R_d$ . Compared to the

corresponding condition in [Genovese et al. \(2014\)](#), we shrink the upper bound by a factor  $\frac{1}{2}$  on the right-hand side of the first inequality in (A3) only for the convenience of our linear convergence proof. As the condition is local, such adjustment induces no extra strictness. Notice that the inequality assumptions in (A3) depend on both the ambient dimension  $D$  and intrinsic dimension  $d$  of the ridge  $R_d$ . The larger the dimensions  $D$  and  $d$  are, the harder the assumptions will hold. This phenomenon, in some sense, reflects the *curse of dimensionality* in nonparametric ridge estimation.

Given conditions (A1-3), the ridge  $R_d$  will be stable under small perturbations of the underlying density  $p$  and its derivatives, which is summarized in the following lemma. Such stability of  $R_d$  is generally measured by the Hausdorff distance defined as

$$(14) \quad \text{Haus}(A, B) = \inf \{ \epsilon > 0 : A \subset B \oplus \epsilon \text{ and } B \subset A \oplus \epsilon \},$$

where  $A, B$  are two sets in  $\mathbb{R}^D$ .

LEMMA 1 (Theorem 4 in [Genovese et al. \(2014\)](#)). *Assume conditions (A1-3) for two densities  $p_1, p_2$ . When  $\|p_1 - p_2\|_{\infty,3}^*$  is sufficiently small, we have*

$$\text{Haus}(R_{d,1}, R_{d,2}) = O\left(\|p_1 - p_2\|_{\infty,2}^*\right),$$

where  $R_{d,1}$  and  $R_{d,2}$  are the  $d$ -ridges of  $p_1$  and  $p_2$ , respectively.

When the true density  $p$  that underlies the Euclidean data  $\{\mathbf{X}_1, \dots, \mathbf{X}_n\} \subset \mathbb{R}^D$  is replaced by the Euclidean KDE  $\hat{p}_n$  in the definition (1) of density ridges, we obtain a natural (plug-in) estimator of the true ridge  $R_d$  as:

$$\hat{R}_d = \left\{ \mathbf{x} \in \mathbb{R}^D : \hat{V}_d(\mathbf{x})^T \nabla \hat{p}_n(\mathbf{x}) = \mathbf{0}, \hat{\lambda}_{d+1}(\mathbf{x}) < 0 \right\}.$$

To regularize statistical behaviors of the estimated ridge  $\hat{R}_d$ , we make the following assumptions on the kernel of its form (3) as:

- **(E1)** We assume that  $k : [0, \infty) \rightarrow [0, \infty)$  is non-increasing and at least three times continuously differentiable with bounded fourth order partial derivatives as well as

$$\int_{\mathbb{R}^d} -k'(|x|_2^2) d\mathbf{x} < \infty \quad \text{and} \quad \int_{\mathbb{R}^d} k'(|x|_2^2)^2 d\mathbf{x} < \infty.$$

- **(E2)** Let

$$\mathcal{K}_E = \left\{ \mathbf{y} \mapsto K^{(\alpha)}\left(\frac{\mathbf{x} - \mathbf{y}}{h}\right) = D^{[\alpha]} \left[ c_{k,D} \cdot k\left(\left\|\frac{\mathbf{x} - \mathbf{y}}{h}\right\|_2^2\right) \right] : \mathbf{x} \in \mathbb{R}^D, |[\alpha]| = 0, 1, 2 \right\}.$$

We assume that  $\mathcal{K}_E$  is a bounded VC (subgraph) class of measurable functions on  $\mathbb{R}^D$ ; that is, there exist constants  $A, v > 0$  such that for any  $0 < \epsilon < 1$ ,

$$\sup_Q N(\mathcal{K}_E, L_2(Q), \epsilon \|F\|_{L_2(Q)}) \leq \left(\frac{A}{\epsilon}\right)^v,$$

where  $N(T, d_T, \epsilon)$  is the  $\epsilon$ -covering number of the pseudometric space  $(T, d_T)$ ,  $Q$  is any probability measure with the same support as  $P$  on  $\mathbb{R}^D$ , and  $F$  is an envelope function of  $\mathcal{K}_E$ . The constants  $A$  and  $v$  are usually called the VC characteristics of  $\mathcal{K}_E$ , and the norm  $\|F\|_{L_2(Q)}$  is defined as  $[\int_{\mathbb{R}^D} |F(\mathbf{x})|^2 dQ(\mathbf{x})]^{\frac{1}{2}}$ .



Condition (E1) can be relaxed such that  $k$  is three times continuously differentiable except for finite number of points on  $[0, \infty)$ . Such relaxation allows us to include the Epanechnikov and other compactly supported kernel. The integrability assumption on  $k$  in condition (E1) is similar to the conditions (K1) and (K3) in Section 2.1 for the purpose of bounding the expectation and variance of the gradient estimator  $\nabla \hat{p}_n(\mathbf{x})$ . Condition (E2) regularizes the complexity of the kernel and its (partial) derivatives, which is essential in establishing the uniform consistency of  $\hat{p}_n$  and its derivatives to the corresponding quantities of  $p$  as in (15).

Given conditions (E1) and (E2), the techniques in [Giné and Guillou \(2002\)](#); [Einmahl and Mason \(2005\)](#); [Chacón et al. \(2011\)](#) can be utilized to show the uniform consistency of the Euclidean KDE  $\hat{p}_n$  and its derivatives as:

$$(15) \quad \|\hat{p}_n - p\|_{\infty}^{(k)} = O(h^2) + O_P \left( \sqrt{\frac{|\log h|}{nh^{D+2k}}} \right) \quad \text{for } k = 0, \dots, 3.$$

**3.2. Mean Shift and SCMS Algorithms with Euclidean Data.** We begin with a quick review on the Euclidean mean shift algorithm, as the SCMS algorithm is built on top of such formulation. Given condition (E1) and the Euclidean KDE  $\hat{p}_n(\mathbf{x}) = \frac{c_{k,D}}{nh^D} \sum_{i=1}^n k \left( \left\| \frac{\mathbf{x} - \mathbf{X}_i}{h} \right\|_2^2 \right)$  with kernel (3), its gradient estimator takes the form as:

$$(16) \quad \begin{aligned} \nabla \hat{p}_n(\mathbf{x}) &= \frac{2c_{k,D}}{nh^{D+2}} \sum_{i=1}^n (\mathbf{x} - \mathbf{X}_i) \cdot k' \left( \left\| \frac{\mathbf{x} - \mathbf{X}_i}{h} \right\|_2^2 \right) \\ &= \frac{2c_{k,D}}{nh^{D+2}} \left[ \sum_{i=1}^n -k' \left( \left\| \frac{\mathbf{x} - \mathbf{X}_i}{h} \right\|_2^2 \right) \right] \left[ \frac{\sum_{i=1}^n \mathbf{X}_i k' \left( \left\| \frac{\mathbf{x} - \mathbf{X}_i}{h} \right\|_2^2 \right)}{\sum_{i=1}^n k' \left( \left\| \frac{\mathbf{x} - \mathbf{X}_i}{h} \right\|_2^2 \right)} - \mathbf{x} \right], \end{aligned}$$

where the first term is a variant of KDEs and the second term is the *mean shift* vector

$$(17) \quad \Xi_h(\mathbf{x}) = \frac{\sum_{i=1}^n \mathbf{X}_i k' \left( \left\| \frac{\mathbf{x} - \mathbf{X}_i}{h} \right\|_2^2 \right)}{\sum_{i=1}^n k' \left( \left\| \frac{\mathbf{x} - \mathbf{X}_i}{h} \right\|_2^2 \right)} - \mathbf{x}.$$

This factorization shows that the mean shift vector aligns with the direction of maximum increase in  $\hat{p}_n$ . Thus, moving a point along its mean shift vector successively yields an ascending path to the local mode ([Cheng, 1995](#); [Comaniciu and Meer, 2002](#); [Li et al., 2007](#)). Let  $\{\hat{\mathbf{x}}^{(t)}\}_{t=0}^{\infty}$  be the mean shift sequence with the Euclidean KDE  $\hat{p}_n$ . (Later, we will use the same notation to denote the SCMS or sample-based SCGA sequence with  $\hat{p}_n$ .) Then, one step iteration of the mean shift algorithm is written as

$$(18) \quad \begin{aligned} \hat{\mathbf{x}}^{(t+1)} \leftarrow \hat{\mathbf{x}}^{(t)} + \Xi_h(\hat{\mathbf{x}}^{(t)}) &= \frac{\sum_{i=1}^n \mathbf{X}_i k' \left( \left\| \frac{\hat{\mathbf{x}}^{(t)} - \mathbf{X}_i}{h} \right\|_2^2 \right)}{\sum_{i=1}^n k' \left( \left\| \frac{\hat{\mathbf{x}}^{(t)} - \mathbf{X}_i}{h} \right\|_2^2 \right)} \\ &= \hat{\mathbf{x}}^{(t)} + \frac{1}{\frac{2c_{k,D}}{nh^{D+2}} \sum_{i=1}^n -k' \left( \left\| \frac{\hat{\mathbf{x}}^{(t)} - \mathbf{X}_i}{h} \right\|_2^2 \right)} \cdot \nabla \hat{p}_n(\hat{\mathbf{x}}^{(t)}), \end{aligned}$$

showing that the mean shift algorithm is a gradient ascent method with an adaptive step size

$$(19) \quad \eta_{n,h}^{(t)} = \frac{1}{\frac{2c_{k,D}}{nh^{D+2}} \sum_{i=1}^n -k' \left( \left\| \frac{\hat{\mathbf{x}}^{(t)} - \mathbf{X}_i}{h} \right\|_2^2 \right)}.$$

We denote by  $\hat{g}_n(\hat{\mathbf{x}}^{(t)}) = \frac{2c_{k,D}}{nh^{D+2}} \sum_{i=1}^n -k' \left( \left\| \frac{\hat{\mathbf{x}}^{(t)} - \mathbf{X}_i}{h} \right\|_2^2 \right)$  the denominator of the adaptive step size  $\eta_{n,h}^{(t)}$ . Lemma 2 below shows that under condition (E1),  $\hat{g}_n(\mathbf{x})$  tends to infinity with probability tending to 1 for any  $\mathbf{x} \in \mathbb{R}^D$  as  $nh^D \rightarrow \infty$  and  $h \rightarrow 0$ . Therefore, the step size  $\eta_{n,h}^{(t)}$  tends to zero in the same manner. The proof of Lemma 2 can be found in Appendix E of the supplement (Zhang and Chen, 2021).

LEMMA 2. *Assume condition (E1) and that the underlying density  $p$  is differentiable. Then, the convergence rate of  $\hat{g}_n(\mathbf{x})$  is*

$$\begin{aligned} h^2 \hat{g}_n(\mathbf{x}) &= -2c_{k,D} \cdot p(\mathbf{x}) \int_{\mathbb{R}^D} k' \left( \|\mathbf{u}\|_2^2 \right) d\mathbf{u} + O(h^2) + O_P \left( \sqrt{\frac{1}{nh^D}} \right) \\ &= O(1) + O(h^2) + O_P \left( \sqrt{\frac{1}{nh^D}} \right) \end{aligned}$$

for any  $\mathbf{x} \in \mathbb{R}^D$  as  $nh^D \rightarrow \infty$  and  $h \rightarrow 0$ .

Let  $\{\hat{\mathbf{x}}^{(t)}\}_{t=0}^\infty$  denote the sequence produced by the SCMS algorithm with initial point  $\hat{\mathbf{x}}^{(0)}$ . Compared to the mean shift iteration (18), the SCMS algorithm updates  $\{\hat{\mathbf{x}}^{(t)}\}_{t=0}^\infty$  through the subspace constrained mean shift vector  $\hat{V}_d(\hat{\mathbf{x}}^{(t)})\hat{V}_d(\hat{\mathbf{x}}^{(t)})^T \Xi_h(\hat{\mathbf{x}}^{(t)})$  as:

$$\begin{aligned} \hat{\mathbf{x}}^{(t+1)} &\leftarrow \hat{\mathbf{x}}^{(t)} + \hat{V}_d(\hat{\mathbf{x}}^{(t)})\hat{V}_d(\hat{\mathbf{x}}^{(t)})^T \Xi_h(\hat{\mathbf{x}}^{(t)}) \\ (20) \quad &= \hat{\mathbf{x}}^{(t)} + \frac{1}{\frac{2c_{k,D}}{nh^{D+2}} \sum_{i=1}^n -k' \left( \left\| \frac{\hat{\mathbf{x}}^{(t)} - \mathbf{X}_i}{h} \right\|_2^2 \right)} \cdot \hat{V}_d(\hat{\mathbf{x}}^{(t)})\hat{V}_d(\hat{\mathbf{x}}^{(t)})^T \nabla \hat{p}_n(\hat{\mathbf{x}}^{(t)}). \end{aligned}$$

See Algorithm 1 in Appendix A of the supplement (Zhang and Chen, 2021) for the entire procedure. This also implies that the SCMS algorithm can be viewed as a SCGA method as:

$$(21) \quad \hat{\mathbf{x}}^{(t+1)} \leftarrow \hat{\mathbf{x}}^{(t)} + \eta_{n,h}^{(t)} \cdot \hat{V}_d(\hat{\mathbf{x}}^{(t)})\hat{V}_d(\hat{\mathbf{x}}^{(t)})^T \nabla \hat{p}_n(\hat{\mathbf{x}}^{(t)})$$

with the same adaptive step size  $\eta_{n,h}^{(t)}$  as the Euclidean mean shift algorithm in (18). Such formulation further sheds light on some convergence properties of the SCMS algorithm.

On the one hand, Proposition 2 in Ghassabeh et al. (2013) has shown that the density estimates  $\{\hat{p}_n(\hat{\mathbf{x}}^{(t)})\}_{t=0}^\infty$  along the SCMS sequence is non-decreasing and converges under condition (E1) and the convexity assumption on the kernel profile  $k$  as well as

$$(22) \quad \lim_{t \rightarrow \infty} \left\| \hat{\mathbf{x}}^{(t+1)} - \hat{\mathbf{x}}^{(t)} \right\|_2 = 0 \quad \text{and} \quad \lim_{t \rightarrow \infty} \left\| \hat{V}_d(\hat{\mathbf{x}}^{(t)})^T \nabla \hat{p}_n(\hat{\mathbf{x}}^{(t)}) \right\|_2 = 0.$$

Under conditions (E1-2) and the consequent uniform consistency results for  $\hat{p}_n$  and its derivatives in (15), it is not difficult to see that when  $\frac{nh^{D+4}}{|\log h|}$  is large enough and  $h$  is sufficiently small, the estimated ridge  $\hat{R}_d$  also satisfies conditions (A1-3); see the proof of Theorem 4 in Genovese et al. (2014) together with Weyl's Theorem (Theorem 4.3.1 in Horn and Johnson (2012)). It ensures that within a small neighborhood of  $\hat{R}_d$ , the equation  $\left\| \hat{V}_d(\mathbf{x})^T \nabla \hat{p}_n(\mathbf{x}) \right\|_2 = 0$  holds only when  $\mathbf{x} \in \hat{R}_d$ . Therefore, together with (22), it follows that there exists a constant  $\rho' > 0$  such that the SCMS algorithm converges to a point in  $\hat{R}_d$  when it is initialized within  $\hat{R}_d \oplus \rho'$ ,  $\frac{nh^{D+4}}{|\log h|}$  is sufficiently large enough, and  $h$  is sufficiently small. The (local) convergence of the SCMS sequence is thus verified.

On the other hand, Lemma 2 already shows that the step size  $\eta_{n,h}^{(t)}$  converges to 0 with probability tending to 1 as  $nh^D \rightarrow \infty$  and  $h \rightarrow 0$ . Since we require  $\frac{nh^{D+4}}{|\log h|} \rightarrow \infty$  and  $h \rightarrow 0$  in order for  $\hat{R}_d$  to satisfy conditions (A2-3) (with probability tending to 1), the step size  $\eta_{n,h}^{(t)}$  is indeed equivalent to  $o_P(1)$  and the SCMS path converges to the subspace constrained gradient flow defined by the principal gradient  $G_d(\mathbf{x}) \approx \hat{G}_d(\mathbf{x})$  (in probability). These flow lines (or integral curves) partition the space, and at each  $\mathbf{x}$  where  $\hat{G}_d(\mathbf{x})$  is nonzero, there is a unique integral curve passing through  $\mathbf{x}$  and converging to  $\hat{R}_d$  (Genovese et al., 2014). It thus, from another perspective, justifies the convergence of the SCMS algorithm.

**3.3. Linear Convergence of Population and Sample-Based SCGA Algorithms.** We have shown in Section 3.2 that the (usual/Euclidean) SCMS algorithm is a variant of the SCGA algorithm with an adaptive step size  $\eta_t$ . To demonstrate the linear convergence of SCMS algorithms with both the true density  $p$  and Euclidean KDE  $\hat{p}_n$ , it suffices to study the linear convergence of SCGA algorithms with objective functions  $p$  and  $\hat{p}_n$ .

Let  $\{\mathbf{x}^{(t)}\}_{t=0}^\infty$  be the sequence defined by the SCGA algorithm with objective function  $p$  and  $\{\hat{\mathbf{x}}^{(t)}\}_{t=0}^\infty$  be the sequence defined by the SCGA algorithm with  $\hat{p}_n$ . Recall that the population SCGA algorithm has its iterative formula as:

$$(23) \quad \mathbf{x}^{(t+1)} = \mathbf{x}^{(t)} + \eta \cdot V_d(\mathbf{x}^{(t)}) V_d(\mathbf{x}^{(t)})^T \nabla p(\mathbf{x}^{(t)}),$$

while the iterative formula of the sample-based SCGA algorithm is already defined in (21). Denote the limiting points of  $\{\mathbf{x}^{(t)}\}_{t=0}^\infty$  and  $\{\hat{\mathbf{x}}^{(t)}\}_{t=0}^\infty$  by  $\mathbf{x}^* \in R_d$  and  $\hat{\mathbf{x}}^* \in \hat{R}_d$ , respectively.

Before stating our main result, we introduce the concepts of Q-linear and R-linear convergence from optimization literature (see, e.g., Appendix A2 in Nocedal and Wright 2006).

**DEFINITION 3 (Linear Rate of Convergence).** We say that the convergence of the sequence  $\{\hat{\mathbf{x}}^{(t)}\}_{t=0}^\infty$  to  $\mathbf{x}^*$  is *Q-linear* if there exists a constant  $\Upsilon \in (0, 1)$  such that

$$\frac{\|\mathbf{x}^{(t+1)} - \mathbf{x}^*\|_2}{\|\mathbf{x}^{(t)} - \mathbf{x}^*\|_2} \leq \Upsilon \quad \text{for all } t \text{ sufficiently large.}$$

We say that the convergence is *R-linear* if there is a sequence of nonnegative scalars  $\{\epsilon_t\}_{t=0}^\infty$  such that

$$\|\mathbf{x}^{(t)} - \mathbf{x}^*\|_2 \leq \epsilon_t \text{ for all } t, \text{ and } \{\epsilon_t\}_{t=0}^\infty \text{ converges Q-linearly to zero.}$$

Conditions (A1-3) in Section 3.1 indicate a quadratic behavior of the residual vector  $U_d^\perp(\mathbf{x}^{(t)}) (\mathbf{x}^* - \mathbf{x}^{(t)})$  as described in Lemma 4 below, whose proof is in Appendix E of the supplement (Zhang and Chen, 2021). This quadratic behavior is essential in establishing the linear convergence of the population SCGA algorithm; see Remark 2 below.

**LEMMA 4.** Assume conditions (A1-3). Then, we have that for any  $\mathbf{x}^{(t)} \in R_d \oplus \rho$ ,

$$\begin{aligned} \left\| U_d^\perp(\mathbf{x}^{(t)}) (\mathbf{x}^* - \mathbf{x}^{(t)}) \right\|_2 &\leq \frac{D^{\frac{3}{2}} \|\nabla^3 p(\mathbf{x}^{(t)})\|_{\max} \|\mathbf{x}^* - \mathbf{x}^{(t)}\|_2^2}{\beta_0} + D^2 \|p\|_\infty^{(4)} \cdot \left\| \mathbf{x}^* - \mathbf{x}^{(t)} \right\|_2^3 \\ &= \frac{D^{\frac{3}{2}} \|\nabla^3 p(\mathbf{x}^{(t)})\|_{\max} \|\mathbf{x}^* - \mathbf{x}^{(t)}\|_2^2}{\beta_0} + o\left(\left\| \mathbf{x}^* - \mathbf{x}^{(t)} \right\|_2^2\right). \end{aligned}$$

Now, we present our linear convergence results for population and sample-based SCGA algorithms.

**THEOREM 5.** Assume that conditions (A1-3) hold and  $\text{reach}(R_d) > 0$  throughout the theorem.

(a) **Q-Linear convergence of  $\|\mathbf{x}^{(t)} - \mathbf{x}^*\|_2$ :** Given a convergence radius  $r_1 > 0$  satisfying

$$r_1 \leq \min \left\{ \rho, \text{reach}(R_d), \frac{\rho \beta_0 \|p\|_\infty^{(2)}}{\sqrt{D} \|p\|_\infty^{(1)} \|p\|_\infty^{(3)} + \beta_0 \|p\|_\infty^{(2)}}, \frac{\beta_0}{8A_\rho D^5 \left( \max \left\{ 1, \|p\|_{\infty,4}^* \right\} \right)^3} \right\},$$

where  $A_\rho > 0$  is a constant that only depends on  $\rho > 0$ , we have that whenever  $0 < \eta \leq \min \left\{ \frac{4}{\beta_0}, \frac{1}{D\|p\|_\infty^{(2)}} \right\}$  and the initial point  $\mathbf{x}^{(0)} \in \text{Ball}_D(\mathbf{x}^*, r_1)$  with  $\mathbf{x}^* \in R_d$ ,

$$\|\mathbf{x}^{(t)} - \mathbf{x}^*\|_2 \leq \Upsilon^t \|\mathbf{x}^{(0)} - \mathbf{x}^*\|_2 \quad \text{with} \quad \Upsilon = \sqrt{1 - \frac{\beta_0 \eta}{4}}.$$

(b) **R-Linear convergence of  $d_E(\mathbf{x}^{(t)}, R_d)$ :** Under the same radius  $r_1 > 0$  in (a), we have that whenever  $0 < \eta \leq \min \left\{ \frac{4}{\beta_0}, \frac{1}{D\|p\|_\infty^{(2)}} \right\}$  and the initial point  $\mathbf{x}^{(0)} \in \text{Ball}_D(\mathbf{x}^*, r_1)$  with  $\mathbf{x}^* \in R_d$ ,

$$d_E(\mathbf{x}^{(t)}, R_d) \leq \Upsilon^t \|\mathbf{x}^{(0)} - \mathbf{x}^*\|_2 \quad \text{with} \quad \Upsilon = \sqrt{1 - \frac{\beta_0 \eta}{4}}.$$

We further assume (E1-2) in the rest of statements. Suppose that  $h \rightarrow 0$  and  $\frac{nh^{D+4}}{|\log h|} \rightarrow \infty$ .

(c) **Q-Linear convergence of  $\|\hat{\mathbf{x}}^{(t)} - \mathbf{x}^*\|_2$ :** Under the same radius  $r_1 > 0$  and  $\Upsilon = \sqrt{1 - \frac{\beta_0 \eta}{4}}$  in (a), we have that

$$\|\hat{\mathbf{x}}^{(t)} - \mathbf{x}^*\|_2 \leq \Upsilon^t \|\hat{\mathbf{x}}^{(0)} - \mathbf{x}^*\|_2 + O(h^2) + O_P \left( \sqrt{\frac{|\log h|}{nh^{D+4}}} \right)$$

with probability tending to 1 whenever  $0 < \eta \leq \min \left\{ \frac{4}{\beta_0}, \frac{1}{D\|p\|_\infty^{(2)}} \right\}$  and the initial point  $\hat{\mathbf{x}}^{(0)} \in \text{Ball}_D(\mathbf{x}^*, r_1)$  with  $\mathbf{x}^* \in R_d$ .

(d) **R-Linear convergence of  $d_E(\hat{\mathbf{x}}^{(t)}, R_d)$ :** Under the same radius  $r_1 > 0$  and  $\Upsilon = \sqrt{1 - \frac{\beta_0 \eta}{4}}$  in (a), we have that

$$d_E(\hat{\mathbf{x}}^{(t)}, R_d) \leq \Upsilon^t \|\hat{\mathbf{x}}^{(0)} - \mathbf{x}^*\|_2 + O(h^2) + O_P \left( \sqrt{\frac{|\log h|}{nh^{D+4}}} \right)$$

with probability tending to 1 whenever  $0 < \eta \leq \min \left\{ \frac{4}{\beta_0}, \frac{1}{D\|p\|_\infty^{(2)}} \right\}$  and the initial point  $\hat{\mathbf{x}}^{(0)} \in \text{Ball}_D(\mathbf{x}^*, r_1)$  with  $\mathbf{x}^* \in R_d$ .

The detailed proof of Theorem 5 can be found in Appendix E of the supplement (Zhang and Chen, 2021). Notice that we describe a threshold value of the convergence radius in (a), under which the population SCGA algorithm converges linearly to  $R_d$ . Such radius generally depends on the data dimension  $D$ , the reach of the ridge  $R_d$ , the effective radius  $\rho$  of condition (A2), and functional norms of  $p$  up to its fourth-order (partial) derivatives. Recall from (20) and Lemma 2 that the adaptive step size  $\eta_{n,h}^{(t)}$  of the SCMS algorithm as a variant of the sampled-based SCGA algorithm can be arbitrarily small with probability tending to 1 when  $h \rightarrow 0$  and  $nh^D \rightarrow \infty$ . Together with Theorem 5, it implies that the Euclidean SCMS algorithm converges (at least) linearly around a small neighborhood of  $R_d$  under some estimation errors; see also Remark 1 below.

REMARK 1. In practice, one may be more interested in the algorithmic convergence rate of the sample-based SCGA algorithm to the estimated ridge  $\widehat{R}_d$ . It can be seen from the uniform bounds (15) that  $\widehat{p}_n$  satisfies conditions (A1-3) with probability tending to 1 as  $h \rightarrow 0$  and  $\frac{nh^{D+6}}{|\log h|} \rightarrow \infty$ , because (E1) implies (A1) and conditions (A2-3) depend only on the first three order partial derivatives of the true density function  $p$ . Thus, one can follow the argument in (a) of Theorem 5 to prove that there exists a positive number  $r_2 \leq \min \left\{ \rho, \text{reach}(\widehat{R}_d) \right\}$  such that for any  $\delta \in (0, 1)$ ,

$$d_E(\widehat{\mathbf{x}}^{(t)}, \widehat{R}_d) \leq \left\| \widehat{\mathbf{x}}^{(t)} - \widehat{\mathbf{x}}^* \right\|_2 \leq \Upsilon^t \left\| \widehat{\mathbf{x}}^{(0)} - \widehat{\mathbf{x}}^* \right\|_2 \quad \text{with} \quad \Upsilon = \sqrt{1 - \frac{\beta_0 \eta}{4}}$$

with probability at least  $1 - \delta$  whenever  $0 < \eta \leq \min \left\{ \frac{4}{\beta_0}, \frac{1}{D \|p\|_{\infty}^{(2)}} \right\}$  and the initial point  $\widehat{\mathbf{x}}^{(0)} \in \widehat{R}_d \oplus r_2$ . In addition, this (estimated) convergence radius  $r_2 > 0$  should be at least approximately the same as the convergence radius  $r_1 > 0$  in (a) of Theorem 5. This is because when  $h \rightarrow 0$  and  $\frac{nh^{D+6}}{|\log h|} \rightarrow \infty$ , the Hausdorff distance  $\text{Haus} \left( R_d, \widehat{R}_d \right) = O(h^2) + O_P \left( \sqrt{\frac{|\log h|}{nh^{D+4}}} \right)$  is a highly order error term and  $d_E(\widehat{\mathbf{x}}^{(t)}, R_d) \approx d_E(\widehat{\mathbf{x}}^{(t)}, \widehat{R}_d)$ ; see Lemma 1 and (15).

REMARK 2. Notice that the standard strong concavity assumption on the objective function (or density function)  $p$  is not sufficient to establish the linear convergence of the (population) SCGA algorithm (23). This is because, under the (weak) strong concavity assumption, the objective function  $p$  should satisfy

$$(24) \quad p(\mathbf{x}^*) - p(\mathbf{y}) \leq \nabla p(\mathbf{y})^T (\mathbf{x}^* - \mathbf{y}) - \frac{A_1}{2} \|\mathbf{x}^* - \mathbf{y}\|_2^2$$

for some constant  $A_1 > 0$ , and those standard proofs of the linear convergence of gradient ascent methods rely on this inequality. However, as indicated in our proof of Theorem 5, the linear convergence of the SCGA algorithm (23) requires the following inequality instead:

$$(25) \quad p(\mathbf{x}^*) - p(\mathbf{y}) \leq \nabla p(\mathbf{y})^T V_d(\mathbf{y}) V_d(\mathbf{y})^T (\mathbf{x}^* - \mathbf{y}) - A_2 \|\mathbf{x}^* - \mathbf{y}\|_2^2 + o \left( \|\mathbf{x}^* - \mathbf{y}\|_2^2 \right)$$

for some constant  $A_2 > 0$ , where  $\mathbf{y}$  is generally chosen to be  $\mathbf{x}^{(t)}$ . We call the function  $p$  satisfying (25) to be “subspace constrained strongly concave”. Since  $\nabla p(\mathbf{y})^T (\mathbf{x}^* - \mathbf{y}) = \nabla p(\mathbf{y})^T V_d(\mathbf{y}) V_d(\mathbf{y})^T (\mathbf{x}^* - \mathbf{y}) + \nabla p(\mathbf{y})^T U_d^\perp(\mathbf{y}) (\mathbf{x}^* - \mathbf{y})$ , the strong concavity assumption (24) will not imply the key inequality (25) for the linear convergence of the population SCGA algorithm unless the residual gradient term  $\nabla p(\mathbf{y})^T U_d^\perp(\mathbf{y}) (\mathbf{x}^* - \mathbf{y})$  can be upper bounded by the second-order error term  $O \left( \|\mathbf{x}^* - \mathbf{y}\|_2^2 \right)$ . As illuminated by our Lemma 4, it is the eigengap condition (A2) that guarantees the establishment of such upper bound.

**4. The SCMS Algorithm with Directional Data.** In this section we generalize the definition (1) of density ridges to directional densities on  $\Omega_q$  and propose our directional SCMS algorithm to identify directional density ridges. In addition, we prove the linear convergence of our directional SCMS algorithm by adjusting the arguments in Section 3.3. Throughout this section,  $\{\mathbf{X}_1, \dots, \mathbf{X}_n\}$  denotes a random sample from a directional distribution with density  $f$  supported on the unit hypersphere  $\Omega_q$  embedded in its ambient Euclidean space  $\mathbb{R}^{q+1}$ .

**4.1. Definitions, Assumptions, and Stability of Directional Density Ridges.** Given the Riemannian gradient  $\text{grad } f(\mathbf{x})$  and Hessian  $\mathcal{H}f(\mathbf{x})$  of a directional density  $f$  supported on  $\Omega_q$  defined in (8) and (10) respectively, we perform the spectral decomposition on  $\mathcal{H}f(\mathbf{x})$  as  $\mathcal{H}f(\mathbf{x}) = \underline{V}(\mathbf{x})\underline{\Lambda}(\mathbf{x})\underline{V}(\mathbf{x})^T$ , where  $\underline{V}(\mathbf{x}) = [\mathbf{x}, \underline{\mathbf{v}}_1(\mathbf{x}), \dots, \underline{\mathbf{v}}_q(\mathbf{x})] \in \mathbb{R}^{(q+1) \times (q+1)}$  is a real orthogonal matrix with columns  $\underline{\mathbf{v}}_1(\mathbf{x}), \dots, \underline{\mathbf{v}}_q(\mathbf{x})$  as the eigenvectors of  $\mathcal{H}f(\mathbf{x})$  that are associated with the eigenvalues  $\underline{\lambda}_1(\mathbf{x}) \geq \dots \geq \underline{\lambda}_q(\mathbf{x})$  and lie within the tangent space  $T_{\mathbf{x}}$  at  $\mathbf{x} \in \Omega_q$ , and  $\underline{\Lambda}(\mathbf{x}) = \text{Diag}[0, \underline{\lambda}_1(\mathbf{x}), \dots, \underline{\lambda}_q(\mathbf{x})]$ . Note that the Riemannian Hessian  $\mathcal{H}f(\mathbf{x})$  has a unit eigenvector  $\mathbf{x}$  that is orthogonal to  $T_{\mathbf{x}}$  and corresponds to eigenvalue 0.

Let  $\underline{V}_d(\mathbf{x}) = [\underline{\mathbf{v}}_{d+1}(\mathbf{x}), \dots, \underline{\mathbf{v}}_q(\mathbf{x})] \in \mathbb{R}^{(q+1) \times (q-d)}$  be the last  $q-d$  columns of  $\underline{V}(\mathbf{x})$ , i.e., the unit eigenvectors inside  $T_{\mathbf{x}}$  corresponding to the  $q-d$  smallest eigenvalues of  $\mathcal{H}f(\mathbf{x})$ . Let  $\underline{U}_d(\mathbf{x}) = \underline{V}_d(\mathbf{x})\underline{V}_d(\mathbf{x})^T$  be the projection matrix onto the linear space spanned by the columns of  $\underline{V}_d(\mathbf{x})$ , and  $\underline{U}_d^\perp(\mathbf{x}) = \mathbf{I}_{q+1} - \underline{V}_d(\mathbf{x})\underline{V}_d(\mathbf{x})^T$ . We define the order- $d$  principal Riemannian gradient  $\underline{G}_d(\mathbf{x})$  by

$$(26) \quad \begin{aligned} \underline{G}_d(\mathbf{x}) &= \underline{V}_d(\mathbf{x})\underline{V}_d(\mathbf{x})^T \text{grad } f(\mathbf{x}) = \underline{V}_d(\mathbf{x})\underline{V}_d(\mathbf{x})^T (\mathbf{I}_{q+1} - \mathbf{x}\mathbf{x}^T) \nabla f(\mathbf{x}) \\ &= \underline{V}_d(\mathbf{x})\underline{V}_d(\mathbf{x})^T \nabla f(\mathbf{x}), \end{aligned}$$

where the last equality follows from the fact that the columns of  $\underline{V}_d(\mathbf{x})$  are orthogonal to the unit vector  $\mathbf{x}$ . The order- $d$  density ridge on  $\Omega_q$  (or *directional density ridge*) is the set of points such that

$$(27) \quad \underline{R}_d = \{\mathbf{x} \in \Omega_q : \underline{G}_d(\mathbf{x}) = \mathbf{0}, \underline{\lambda}_{d+1}(\mathbf{x}) < 0\} = \{\mathbf{x} \in \Omega_q : \underline{V}_d(\mathbf{x})^T \nabla f(\mathbf{x}) = \mathbf{0}, \underline{\lambda}_{d+1}(\mathbf{x}) < 0\}.$$

Our definition of density ridges on  $\Omega_q$  can be arguably generalized to any smooth function  $f$  supported on any arbitrary manifold. It also follows that the 0-ridge  $\underline{R}_0$  is the set of local modes of  $f$  on  $\Omega_q$ , whose statistical properties and practical estimation algorithm are discussed in Zhang and Chen (2020). Therefore, we only focus on the case when  $1 \leq d < q$  in this paper. To regularize a directional density ridge  $\underline{R}_d$ , we modify our assumptions on the regular density ridge  $R_d$  in Section 3.1 as follows:

- **(A1) (Differentiability)** We extend the directional density  $f$  from  $\Omega_q$  to  $\mathbb{R}^{q+1} \setminus \{\mathbf{0}\}$  by defining  $f(\mathbf{x}) \equiv f\left(\frac{\mathbf{x}}{\|\mathbf{x}\|_2}\right)$  for all  $\mathbf{x} \in \mathbb{R}^{q+1} \setminus \{\mathbf{0}\}$ . Under this extension, we assume that the total gradient  $\nabla f(\mathbf{x})$ , total Hessian matrix  $\nabla \nabla f(\mathbf{x})$ , and third-order derivative tensor  $\nabla^3 f(\mathbf{x})$  in  $\mathbb{R}^{q+1}$  exist, and are continuous on  $\mathbb{R}^{q+1} \setminus \{\mathbf{0}\}$  and square integrable on  $\Omega_q$ . We also assume that  $f$  has bounded fourth order derivatives on  $\Omega_q$ .
- **(A2) (Eigengap)** We assume that there exist constants  $\underline{\rho} \in (0, 2]$  and  $\underline{\beta}_0 > 0$  such that  $\underline{\lambda}_{d+1}(\mathbf{y}) \leq -\underline{\beta}_0$ ,  $\underline{\lambda}_d(\mathbf{y}) - \underline{\lambda}_{d+1}(\mathbf{y}) \geq \underline{\beta}_0$  for any  $\mathbf{y} \in \underline{R}_d \oplus \underline{\rho}$ .
- **(A3) (Path Smoothness)** Under the same  $\underline{\rho}, \underline{\beta}_0 > 0$  in (A2), we assume that there exists another constant  $\underline{\beta}_1 \in (0, \underline{\beta}_0)$  such that

$$(q+1)^{\frac{3}{2}} \left\| \underline{U}_d^\perp(\mathbf{y}) \text{grad } f(\mathbf{y}) \right\|_2 \left\| \nabla^3 f(\mathbf{y}) \right\|_{\max} \leq \frac{\underline{\beta}_0^2}{4},$$

$$d(q+1)^{\frac{3}{2}} \left\| \nabla f(\mathbf{x}) \right\|_2 \cdot \left\| \nabla^3 f(\mathbf{x}) \right\|_{\max} \leq \underline{\beta}_0 (\underline{\beta}_0 - \underline{\beta}_1)$$

for all  $\mathbf{y} \in \underline{R}_d \oplus \underline{\rho}$  and  $\mathbf{x} \in \underline{R}_d$ .

The discussions about conditions (A1-3) in Section 3.1 apply to their directional counterparts (A1-3), except that the eigengap condition (A2) is imposed on eigenvalues  $\underline{\lambda}_1(\mathbf{x}) \geq \dots \geq \underline{\lambda}_q(\mathbf{x})$  within the tangent space  $T_{\mathbf{x}}$  at  $\mathbf{x} \in \Omega_q$ . However, since the only eigenvalue of  $\mathcal{H}f(\mathbf{x})$  (associated with the eigenvector) outside the tangent space  $T_{\mathbf{x}}$  is 0, the eigengap condition (A2) is also valid to the entire spectrum of  $\mathcal{H}f(\mathbf{x})$  in the ambient space  $\mathbb{R}^{q+1}$ . The



extension of  $f$  in (A1) has also been used by Zhao and Wu (2001); García-Portugués et al. (2013); García-Portugués (2013). Because the directional density  $f$  remains unchanged along every radial direction of  $\Omega_q$  under the extension, the radial component of its total gradient is  $\text{Rad}(\nabla f(\mathbf{x})) = 0$  for all  $\mathbf{x} \in \Omega_q$ , and the Riemannian gradient (8) of  $f$  on  $\Omega_q$  becomes

$$(28) \quad \text{grad}(\mathbf{x}) = (\mathbf{I}_{q+1} - \mathbf{x}\mathbf{x}^T) \nabla f(\mathbf{x}) = \nabla f(\mathbf{x}).$$

Similarly, the Riemannian Hessian (10) of  $f$  on  $\Omega_q$  reduces to

$$(29) \quad \mathcal{H}f(\mathbf{x}) = (\mathbf{I}_{q+1} - \mathbf{x}\mathbf{x}^T) \nabla \nabla f(\mathbf{x}) (\mathbf{I}_{q+1} - \mathbf{x}\mathbf{x}^T).$$

Both the Riemannian gradient and Hessian of  $f$  on  $\Omega_q$  are invariant under this extension.

Similar to Euclidean density ridges, we also establish the following stability theorem of directional density ridges. To measure the distance between two directional ridges  $\underline{R}_d, \tilde{\underline{R}}_d \subset \Omega_q$  defined by the directional density  $f$  and  $\tilde{f}$ , we adopt the definition (14) of Hausdorff distance between two sets in the ambient Euclidean space  $\mathbb{R}^{q+1}$ . Note that the Euclidean norm used in the definition (14) is upper bounded by the geodesic distance when our interested sets lie on  $\Omega_q$ . We will leverage this property in our proof of Theorem 6; see Appendix H of the supplement (Zhang and Chen, 2021).

**THEOREM 6.** *Suppose that conditions (A1-3) hold for the directional density  $f$  and that condition (A1) holds for  $\tilde{f}$ . When  $\|f - \tilde{f}\|_{\infty,3}^*$  is sufficiently small,*

- (a) *conditions (A2-3) holds for  $\tilde{f}$ .*
- (b)  $\text{Haus}(\underline{R}_d, \tilde{\underline{R}}_d) = O\left(\|f - \tilde{f}\|_{\infty,2}^*\right).$
- (c)  $\text{reach}(\tilde{\underline{R}}_d) \geq \min\left\{\rho/2, \frac{\beta_1^2}{\tilde{A}_2(\|f\|_{\infty}^{(3)} + \|\tilde{f}\|_{\infty}^{(4)})}\right\} + O\left(\|f - \tilde{f}\|_{\infty,3}^*\right)$  for a constant  $\tilde{A}_2 > 0$ .

One natural estimator of the directional density ridge  $\underline{R}_d$  can be obtained by plugging the directional KDE  $\hat{f}_h$  into the definition (27) as:

$$\hat{\underline{R}}_d = \left\{ \mathbf{x} \in \Omega_q : \hat{\underline{V}}_d(\mathbf{x})^T \nabla \hat{f}_h(\mathbf{x}) = \mathbf{0}, \hat{\underline{\lambda}}_{d+1}(\mathbf{x}) < 0 \right\}.$$

To regularize the statistical behavior of the estimated directional ridge  $\hat{\underline{R}}_d$ , we consider the following assumptions that are generalized from conditions (E1-2):

- **(D1)** Assume that  $L : (-\delta_L, \infty) \rightarrow [0, \infty)$  is a bounded and three times continuously differentiable function with bounded fourth order derivatives on  $(-\delta_L, \infty) \subset \mathbb{R}$  for some constant  $\delta_L > 0$  such that

$$0 < \int_0^\infty L^k(r) r^{\frac{q}{2}-1} dr < \infty \quad \text{for all } q \geq 1 \text{ and } k = 1, 2, 3$$

for all  $q \geq 1$  and  $\int_{\epsilon^{-1}}^\infty |L'(r)| r^{\frac{q}{2}} dr = O(\epsilon)$  as  $\epsilon \rightarrow 0$  for any  $\epsilon > 0$ .

- **(D2)** Let

$$\mathcal{K}_D = \left\{ \mathbf{u} \mapsto K\left(\frac{\mathbf{z} - \mathbf{u}}{h}\right) : \mathbf{u}, \mathbf{z} \in \Omega_q, h > 0, K(\mathbf{x}) = D^{[\tau]} L\left(\frac{1}{2}\|\mathbf{x}\|_2^2\right), |\tau| = 0, 1, 2, 3 \right\}.$$

We assume that  $\mathcal{K}_D$  is a bounded VC (subgraph) class of measurable functions on  $\Omega_q$ ; that is, there exist constants  $A, v > 0$  such that for any  $0 < \epsilon < 1$ ,

$$\sup_Q N(\mathcal{K}_D, L_2(Q), \epsilon \|F\|_{L_2(Q)}) \leq \left(\frac{A}{\epsilon}\right)^v,$$

where  $N(T, d_T, \epsilon)$  is the  $\epsilon$ -covering number of the pseudometric space  $(T, d_T)$ ,  $Q$  is any probability measure on  $\Omega_q$ , and  $F$  is an envelope function of  $\mathcal{K}_D$ . The constants  $A$  and  $v$  are usually called the VC characteristics of  $\mathcal{K}_D$  and the norm  $\|F\|_{L_2(Q)}$  is defined as  $\left[ \int_{\Omega_q} |F(\mathbf{x})|^2 dQ(\mathbf{x}) \right]^{\frac{1}{2}}$ .

The differentiability assumption in condition (D1) can be relaxed such that  $L$  is (three times) continuously differentiable except for a set of points with Lebesgue measure 0 on  $[0, \infty)$ . Conditions (D1) and (A1) are generally required for establishing the convergence rate of directional KDE and its derivatives (Hall et al., 1987; Klemelä, 2000; Zhao and Wu, 2001; García-Portugués et al., 2013; García-Portugués, 2013). The rate of convergence assumption on the tail behavior of the integral  $\int_{\epsilon^{-1}}^{\infty} |L'(r)| r^{\frac{q}{2}} dr$  in condition (D1) is imposed for two purposes. First, the asymptotic convergence rates of the bias terms in Tang  $(\nabla \hat{f}_h(\mathbf{x}))$  and  $\mathcal{H} \hat{f}_h(\mathbf{x})$  will be of the order  $O(h^2)$  under this assumption; see those uniform bounds in (30). Second,  $\|\nabla \hat{f}_h(\mathbf{x})\|_2$  appearing in the step sizes  $\eta_{n,h}^{(t)}$  or  $\eta_{n,h}^{(t)'}$  of the directional mean shift or SCMS algorithm can then be shown to diverge at the order  $O(h^{-2}) + O_P\left(\frac{1}{nh^{q+2k}}\right)$  as  $nh^q \rightarrow \infty$  and  $h \rightarrow 0$ ; see Section 4.2 for details. One can justify via integration by parts that the von-Mises kernel  $L(r) = e^{-r}$  and many compactly supported kernels satisfy the entire condition (D1). Condition (D2) regularizes the complexity of kernel  $L$  and its derivatives as in condition (E2).

Given conditions (D1-2), the techniques in Hall et al. (1987); Bai et al. (1988); Zhao and Wu (2001); García-Portugués et al. (2013); García-Portugués (2013); Zhang and Chen (2020) can be utilized to show that

$$(30) \quad \left\| \hat{f}_h - f \right\|_{\infty}^{(k)} = \sup_{\mathbf{x} \in \Omega_q} \left\| \nabla_{T_{\mathbf{x}}}^k \hat{f}_h(\mathbf{x}) - \nabla_{T_{\mathbf{x}}}^k f(\mathbf{x}) \right\|_{\max} = O(h^2) + O_P \left( \sqrt{\frac{|\log h|}{nh^{q+2k}}} \right),$$

where  $\nabla_{T_{\mathbf{x}}}$  is the gradient operator within the tangent space  $T_{\mathbf{x}}$  so that  $\nabla_{T_{\mathbf{x}}} f(\mathbf{x}) = \text{grad } f(\mathbf{x})$ ,  $\nabla_{T_{\mathbf{x}}}^2 f(\mathbf{x}) = \mathcal{H} f(\mathbf{x})$ , and  $\nabla_{T_{\mathbf{x}}}^3 f(\mathbf{x}) = \nabla_{T_{\mathbf{x}}} \mathcal{H} f(\mathbf{x})$ .

**4.2. Mean Shift and SCMS Algorithm with Directional Data.** Before deriving our directional SCMS algorithm, we first review the mean shift algorithm with directional data  $\{\mathbf{X}_1, \dots, \mathbf{X}_n\} \subset \Omega_q$ ; the formal derivation can be found in Section 3 of Zhang and Chen (2020). Given the directional KDE  $\hat{f}_h(\mathbf{x}) = \frac{c_{h,q}(L)}{n} \sum_{i=1}^n L\left(\frac{1-\mathbf{x}^T \mathbf{X}_i}{h^2}\right)$  in (5), the directional mean shift vector can be defined as:

$$(31) \quad \Xi_h(\mathbf{x}) = \frac{\sum_{i=1}^n \mathbf{X}_i L'\left(\frac{1}{2} \left\| \frac{\mathbf{x} - \mathbf{X}_i}{h} \right\|_2^2\right)}{\sum_{i=1}^n L'\left(\frac{1}{2} \left\| \frac{\mathbf{x} - \mathbf{X}_i}{h} \right\|_2^2\right)} - \mathbf{x} = \frac{\sum_{i=1}^n \mathbf{X}_i L'\left(\frac{1-\mathbf{x}^T \mathbf{X}_i}{h^2}\right)}{\sum_{i=1}^n L'\left(\frac{1-\mathbf{x}^T \mathbf{X}_i}{h^2}\right)} - \mathbf{x}.$$

Similar to the Euclidean mean shift vector (17),  $\Xi_h(\mathbf{x})$  also points toward the direction of maximum increase in  $\hat{f}_h(\mathbf{x})$  after being projected onto the tangent space  $T_{\mathbf{x}}$ . Thus, the directional mean shift iteration translates a point  $\mathbf{x} \in \Omega_q$  as  $\mathbf{x} + \Xi_h(\mathbf{x})$  with an extra projection  $\frac{\mathbf{x} + \Xi_h(\mathbf{x})}{\|\mathbf{x} + \Xi_h(\mathbf{x})\|_2}$  to draw the shifted point back to  $\Omega_q$ .

Let  $\{\hat{\mathbf{x}}^{(t)}\}_{t=0}^{\infty}$  denote the sequence defined by the above directional mean shift procedure. (Later, we will use the same notation to denote the directional SCGA/SCMS sequence with  $\hat{f}_h$ .) As  $\nabla \hat{f}_h(\mathbf{x}) = -\frac{c_{h,q}(L)}{nh^2} \sum_{i=1}^n \mathbf{X}_i L'\left(\frac{1-\mathbf{x}^T \mathbf{X}_i}{h^2}\right)$ , some simple algebra shows that the direc-

tional mean shift algorithm can be written into the following fixed-point iteration formula:

$$(32) \quad \hat{\mathbf{x}}^{(t+1)} = -\frac{\sum_{i=1}^n \mathbf{X}_i L' \left( \frac{1 - \mathbf{X}_i^T \hat{\mathbf{x}}^{(t)}}{h^2} \right)}{\left\| \sum_{i=1}^n \mathbf{X}_i L' \left( \frac{1 - \mathbf{X}_i^T \hat{\mathbf{x}}^{(t)}}{h^2} \right) \right\|_2} \quad \text{or} \quad \hat{\mathbf{x}}^{(t+1)} = \frac{\nabla \hat{f}_h(\hat{\mathbf{x}}^{(t)})}{\left\| \nabla \hat{f}_h(\hat{\mathbf{x}}^{(t)}) \right\|_2}.$$

From (32), it is also possible to write the directional mean shift algorithm as a gradient ascent method on  $\Omega_q$  with the iteration formula (Zhang and Sra, 2016):

$$(33) \quad \hat{\mathbf{x}}^{(t+1)} = \text{Exp}_{\hat{\mathbf{x}}^{(t)}} \left( \eta_{n,h}^{(t)} \cdot \text{grad } \hat{f}_h(\hat{\mathbf{x}}^{(t)}) \right),$$

where the adaptive step size  $\eta_{n,h}^{(t)}$  is given by

$$(34) \quad \eta_{n,h}^{(t)} = \arccos \left( \frac{\left( \nabla \hat{f}_h(\hat{\mathbf{x}}^{(t)})^T \hat{\mathbf{x}}^{(t)} \right)}{\left\| \nabla \hat{f}_h(\hat{\mathbf{x}}^{(t)}) \right\|_2} \right) \cdot \frac{1}{\left\| \text{grad } \hat{f}_h(\hat{\mathbf{x}}^{(t)}) \right\|_2} = \frac{\theta_t}{\left\| \nabla \hat{f}_h(\hat{\mathbf{x}}^{(t)}) \right\|_2 \cdot \sin \theta_t}.$$

Here, we denote the angle between  $\nabla \hat{f}_h(\hat{\mathbf{x}}^{(t)})$  and  $\hat{\mathbf{x}}^{(t)}$  by  $\theta_t$ ; see Section 5.2 in Zhang and Chen (2020) for detailed derivations. Within some small neighborhoods around local modes of  $\hat{f}_h$ ,  $\frac{\theta_t}{\sin \theta_t} \approx 1$  and the step size  $\eta_{n,h}^{(t)}$  will be dominated by  $\frac{1}{\left\| \nabla \hat{f}_h(\hat{\mathbf{x}}^{(t)}) \right\|_2}$ . The following lemma characterizes the asymptotic behaviors of  $\left\| \nabla \hat{f}_h(\mathbf{x}) \right\|_2$  on  $\Omega_q$  and consequently,  $\eta_{n,h}^{(t)}$ .

LEMMA 7 (Lemma 10 in Zhang and Chen (2020)). *Assume conditions (D1) and (A1). For any fixed  $\mathbf{x} \in \Omega_q$ , we have*

$$h^2 \cdot \left\| \nabla \hat{f}_h(\mathbf{x}) \right\|_2 = f(\mathbf{x}) \cdot C_{L,q} + o(1) + O_P \left( \sqrt{\frac{1}{nh^q}} \right)$$

as  $nh^q \rightarrow \infty$  and  $h \rightarrow 0$ , where  $C_{L,q} = -\frac{\int_0^\infty L'(r) r^{\frac{q}{2}-1} dr}{\int_0^\infty L(r) r^{\frac{q}{2}-1} dr} > 0$  is a constant depending only on kernel  $L$  and dimension  $q$ .

Lemma 7 indicates that  $\left\| \nabla \hat{f}_h(\mathbf{x}) \right\|_2 \rightarrow \infty$  with probability tending to 1 as  $h \rightarrow 0$  and  $nh^q \rightarrow \infty$  for any  $\mathbf{x} \in \Omega_q$ . Such conclusion may seem counterintuitive at the first glance, but one should be aware that the consistency of  $\nabla \hat{f}_h(\mathbf{x})$  holds only on its tangent component; see (30). The radial component of  $\nabla \hat{f}_h(\mathbf{x})$  that is perpendicular to  $\Omega_q$  diverges, despite the fact that the true directional density  $f$  does not have any radial component. Using Lemma 7, one can argue that the adaptive step size  $\eta_{n,h}^{(t)}$  in (34) can be sufficiently small with high probability, so the linear convergence will eventually occur.

In the sequel, we denote by  $\{\hat{\mathbf{x}}^{(t)}\}_{t=0,1,\dots} \subset \Omega_q$  the iterative sequence generated by our directional SCMS algorithm. There are two different methods of defining a directional SCMS iteration, while we will demonstrate that one of them is superior.

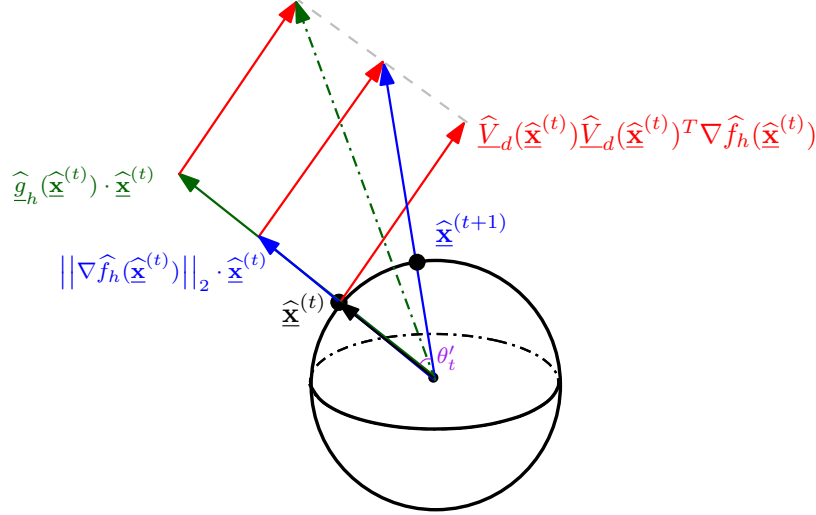


Fig 2: An illustration of one-step iterations under two candidate directional SCMS algorithms

• **Method 1:** As in the Euclidean SCMS algorithm, one can define the directional SCMS sequence by the SCMS vector as:

$$\begin{aligned}
 \hat{\mathbf{x}}^{(t+1)} &\leftarrow \hat{\mathbf{x}}^{(t)} + \hat{\mathbf{V}}_d(\hat{\mathbf{x}}^{(t)}) \hat{\mathbf{V}}_d(\hat{\mathbf{x}}^{(t)})^T \Xi_h(\hat{\mathbf{x}}^{(t)}) \\
 (35) \quad &\stackrel{(31)}{=} \hat{\mathbf{x}}^{(t)} + \hat{\mathbf{V}}_d(\hat{\mathbf{x}}^{(t)}) \hat{\mathbf{V}}_d(\hat{\mathbf{x}}^{(t)})^T \left[ \frac{\sum_{i=1}^n \mathbf{X}_i L' \left( \frac{1 - \mathbf{X}_i^T \hat{\mathbf{x}}^{(t)}}{h^2} \right)}{\sum_{i=1}^n L' \left( \frac{1 - \mathbf{X}_i^T \hat{\mathbf{x}}^{(t)}}{h^2} \right)} \right] \\
 &= \hat{\mathbf{x}}^{(t)} + \hat{\mathbf{V}}_d(\hat{\mathbf{x}}^{(t)}) \hat{\mathbf{V}}_d(\hat{\mathbf{x}}^{(t)})^T \cdot \frac{\nabla \hat{f}_h(\hat{\mathbf{x}}^{(t)})}{\hat{\mathbf{g}}_h(\hat{\mathbf{x}}^{(t)})},
 \end{aligned}$$

where  $\hat{\mathbf{g}}_h(\mathbf{x}) \equiv \frac{c_{h,q}(L)}{nh^2} \sum_{i=1}^n -L' \left( \frac{1 - \mathbf{x}^T \mathbf{X}_i}{h^2} \right)$ ,  $\nabla \hat{f}_h(\mathbf{x}) = -\frac{c_{h,q}(L)}{nh^2} \sum_{i=1}^n \mathbf{X}_i L' \left( \frac{1 - \mathbf{x}^T \mathbf{X}_i}{h^2} \right)$ , and  $\hat{\mathbf{V}}_d(\mathbf{x})$  is the estimated version of  $\mathbf{V}_d(\mathbf{x})$  by the directional KDE  $\hat{f}_h$ .

Unlike the Euclidean SCMS algorithm, we need an extra standardization step  $\hat{\mathbf{x}}^{(t+1)} \leftarrow \frac{\hat{\mathbf{x}}^{(t+1)}}{\|\hat{\mathbf{x}}^{(t+1)}\|_2}$  to project the updated point back to  $\Omega_q$ , which leads to the following fixed-point iteration:

$$(36) \quad \hat{\mathbf{x}}^{(t+1)} = \frac{\hat{\mathbf{V}}_d(\hat{\mathbf{x}}^{(t)}) \hat{\mathbf{V}}_d(\hat{\mathbf{x}}^{(t)})^T \nabla \hat{f}_h(\hat{\mathbf{x}}^{(t)}) + \hat{\mathbf{g}}_h(\hat{\mathbf{x}}^{(t)}) \cdot \hat{\mathbf{x}}^{(t)}}{\left\| \hat{\mathbf{V}}_d(\hat{\mathbf{x}}^{(t)}) \hat{\mathbf{V}}_d(\hat{\mathbf{x}}^{(t)})^T \nabla \hat{f}_h(\hat{\mathbf{x}}^{(t)}) + \hat{\mathbf{g}}_h(\hat{\mathbf{x}}^{(t)}) \cdot \hat{\mathbf{x}}^{(t)} \right\|_2},$$

where the components  $\hat{\mathbf{V}}_d(\mathbf{x}) \hat{\mathbf{V}}_d(\mathbf{x})^T \nabla \hat{f}_h(\mathbf{x})$  and  $\hat{\mathbf{g}}_h(\mathbf{x}) \cdot \mathbf{x}$  are always orthogonal for any  $\mathbf{x} \in \Omega_q$ ; see Figure 2 for a graphical illustration.

• **Method 2:** The fixed-point iteration formula (32) of the directional mean shift algorithm suggests a more efficient formulation of the directional SCMS algorithm:

$$(37) \quad \hat{\mathbf{x}}^{(t+1)} \leftarrow \hat{\mathbf{x}}^{(t)} + \hat{\mathbf{V}}_d(\hat{\mathbf{x}}^{(t)}) \hat{\mathbf{V}}_d(\hat{\mathbf{x}}^{(t)})^T \cdot \frac{\nabla \hat{f}_h(\hat{\mathbf{x}}^{(t)})}{\left\| \nabla \hat{f}_h(\hat{\mathbf{x}}^{(t)}) \right\|_2} \quad \text{and} \quad \hat{\mathbf{x}}^{(t+1)} \leftarrow \frac{\hat{\mathbf{x}}^{(t+1)}}{\left\| \hat{\mathbf{x}}^{(t+1)} \right\|_2},$$

where we replace the directional mean shift vector  $\Xi_h(\mathbf{x})$  with the standardized total gradient estimator  $\frac{\nabla \hat{f}_h(\mathbf{x})}{\|\nabla \hat{f}_h(\mathbf{x})\|_2}$  in (35). This directional SCMS is again a fixed-point iteration as:

$$(38) \quad \hat{\mathbf{x}}^{(t+1)} = \frac{\hat{V}_d(\hat{\mathbf{x}}^{(t)})\hat{V}_d(\hat{\mathbf{x}}^{(t)})^T \nabla \hat{f}_h(\hat{\mathbf{x}}^{(t)}) + \left\| \nabla \hat{f}_h(\hat{\mathbf{x}}^{(t)}) \right\|_2 \cdot \hat{\mathbf{x}}^{(t)}}{\left\| \hat{V}_d(\hat{\mathbf{x}}^{(t)})\hat{V}_d(\hat{\mathbf{x}}^{(t)})^T \nabla \hat{f}_h(\hat{\mathbf{x}}^{(t)}) + \left\| \nabla \hat{f}_h(\hat{\mathbf{x}}^{(t)}) \right\|_2 \cdot \hat{\mathbf{x}}^{(t)} \right\|_2}.$$

A direct computation demonstrates that, by the non-increasing property of kernel  $L$ ,

$$(39) \quad \begin{aligned} \left\| \nabla \hat{f}_h(\mathbf{x}) \right\|_2 &= \left\| -\frac{c_{h,q}(L)}{nh^2} \sum_{i=1}^n \mathbf{X}_i L' \left( \frac{1 - \mathbf{x}^T \mathbf{X}_i}{h^2} \right) \right\|_2 \\ &\leq \frac{c_{h,q}(L)}{nh^2} \sum_{i=1}^n \left\| \mathbf{X}_i L' \left( \frac{1 - \mathbf{x}^T \mathbf{X}_i}{h^2} \right) \right\|_2 \\ &= -\frac{c_{h,q}(L)}{nh^2} \sum_{i=1}^n L' \left( \frac{1 - \mathbf{x}^T \mathbf{X}_i}{h^2} \right) = \hat{g}_h(\mathbf{x}). \end{aligned}$$

Because the radial components in directional SCMS iterative formulae make no contributions in moving the point  $\hat{\mathbf{x}}^{(t)}$  on  $\Omega_q$ , the inequality (39) indicates that the directional SCMS algorithm with iterative formula (38) will be superior to (36); see also Figure 2 for a graphical demonstration. We thus choose **Method 2** as our directional SCMS algorithm. Algorithm 2 in the supplement (Zhang and Chen, 2021) provides a detailed guideline of implementing Method 2 in practice.

Now, we demonstrate the ascending property of our directional SCMS algorithm (37) and two convergent results similar to (22).

**PROPOSITION 8.** *We assume that the directional kernel  $L$  is non-increasing, twice continuously differentiable, and convex with  $L(0) < \infty$ . Given the directional KDE  $\hat{f}_h(\mathbf{x}) = \frac{c_{h,q}(L)}{n} \sum_{i=1}^n L \left( \frac{1 - \mathbf{x}^T \mathbf{X}_i}{h^2} \right)$  and the directional SCMS sequence  $\{\hat{\mathbf{x}}^{(t)}\}_{t=0}^\infty$  defined by (37) or (38), we have the following properties:*

- (a) *The estimated density sequence  $\{\hat{f}_h(\hat{\mathbf{x}}^{(t)})\}_{t=0}^\infty$  is non-decreasing and thus converges.*
- (b)  $\lim_{t \rightarrow \infty} \left\| \hat{V}_d(\hat{\mathbf{x}}^{(t)})^T \nabla \hat{f}_h(\hat{\mathbf{x}}^{(t)}) \right\|_2 = 0.$
- (c) *If the kernel  $L$  is also strictly decreasing on  $[0, \infty)$ , then  $\lim_{t \rightarrow \infty} \left\| \hat{\mathbf{x}}^{(t+1)} - \hat{\mathbf{x}}^{(t)} \right\|_2 = 0.$*

The proof is deferred to Appendix I in the supplement (Zhang and Chen, 2021); our proof is similar to but different from the proof of Proposition 2 in Ghassabeh et al. (2013).

**REMARK 3.** Our results (b) and (c) in Proposition 8 demonstrates that the stopping criterion of our directional SCMS algorithm can be based on either the norm of the (scaled) principal Riemannian gradient estimator or the (Euclidean) distance  $\left\| \hat{\mathbf{x}}^{(t+1)} - \hat{\mathbf{x}}^{(t)} \right\|_2$  between two consecutive iterative points, where the latter one requires a strictly decreasing kernel such as the von Mises kernel  $L(r) = e^{-r}$ .

Under conditions (D1-2) and the uniform bounds (30) of directional KDE  $\hat{f}_h$  as well as its derivatives, the estimated directional ridge  $\hat{R}_d$  also satisfies condition (A1-3) with a probability tending to 1 asymptotically. It guarantees that, within a small neighborhood of  $\hat{R}_d$ ,

the equation  $\left\| \widehat{V}_d(\mathbf{x})^T \nabla \widehat{f}_h(\mathbf{x}) \right\|_2 = 0$  holds only when  $\mathbf{x} \in \widehat{R}_d$ . Therefore, Proposition 8 demonstrates that there exists a radius  $\rho' > 0$  such that our directional SCMS algorithm will converge to a point on  $\widehat{R}_d$  when it is initialized within  $\widehat{R}_d \oplus \rho'$ .

Motivated by the iterative formula (33) for the gradient ascent algorithm on  $\Omega_q$ , we consider writing our directional SCMS algorithm as a variant of the SCGA algorithm on  $\Omega_q$  with an iterative formula:

$$(40) \quad \widehat{\mathbf{x}}^{(t+1)} = \text{Exp}_{\widehat{\mathbf{x}}^{(t)}} \left( \eta_{n,h}^{(t)'} \cdot \widehat{V}_d(\widehat{\mathbf{x}}^{(t)}) \widehat{V}_d(\widehat{\mathbf{x}}^{(t)})^T \text{grad } \widehat{f}_h(\widehat{\mathbf{x}}^{(t)}) \right).$$

Note that  $\text{Exp}_{\mathbf{x}}$  is the exponential map at  $\mathbf{x} \in \Omega_q$  and  $\eta_{n,h}^{(t)'}$  is the step size. To derive  $\eta_{n,h}^{(t)'}$ , we recall the fixed-point equation (38) of our directional SCMS algorithm and compute the geodesic distance between  $\widehat{\mathbf{x}}^{(t+1)}$  and  $\widehat{\mathbf{x}}^{(t)}$  (one-step directional SCMS update) as:

$$\begin{aligned} \arccos \left( \left( \widehat{\mathbf{x}}^{(t+1)} \right)^T \widehat{\mathbf{x}}^{(t)} \right) &= \arccos \left( \frac{\left\| \nabla \widehat{f}_h(\widehat{\mathbf{x}}^{(t)}) \right\|_2}{\left\| \widehat{V}_d(\widehat{\mathbf{x}}^{(t)}) \widehat{V}_d(\widehat{\mathbf{x}}^{(t)})^T \nabla \widehat{f}_h(\widehat{\mathbf{x}}^{(t)}) + \left\| \nabla \widehat{f}_h(\widehat{\mathbf{x}}^{(t)}) \right\|_2 \cdot \widehat{\mathbf{x}}^{(t)} \right\|_2} \right) \\ &= \left\| \eta_{n,h}^{(t)'} \cdot \widehat{V}_d(\widehat{\mathbf{x}}^{(t)}) \widehat{V}_d(\widehat{\mathbf{x}}^{(t)})^T \text{grad } \widehat{f}_h(\widehat{\mathbf{x}}^{(t)}) \right\|_2, \end{aligned}$$

where we equate the geodesic distance between  $\widehat{\mathbf{x}}^{(t+1)}$  and  $\widehat{\mathbf{x}}^{(t)}$  to the norm of the tangent vector inside the exponential map in (40) to obtain the second equality. This shows that our directional SCMS algorithm is a SCGA algorithm with adaptive step size

$$(41) \quad \eta_{n,h}^{(t)'} = \frac{\arccos \left( \frac{\left\| \nabla \widehat{f}_h(\widehat{\mathbf{x}}^{(t)}) \right\|_2}{\left\| \widehat{V}_d(\widehat{\mathbf{x}}^{(t)}) \widehat{V}_d(\widehat{\mathbf{x}}^{(t)})^T \nabla \widehat{f}_h(\widehat{\mathbf{x}}^{(t)}) + \left\| \nabla \widehat{f}_h(\widehat{\mathbf{x}}^{(t)}) \right\|_2 \cdot \widehat{\mathbf{x}}^{(t)} \right\|_2} \right)}{\left\| \widehat{V}_d(\widehat{\mathbf{x}}^{(t)}) \widehat{V}_d(\widehat{\mathbf{x}}^{(t)})^T \nabla \widehat{f}_h(\widehat{\mathbf{x}}^{(t)}) \right\|_2} = \frac{\theta'_t}{\left\| \widehat{f}_h(\widehat{\mathbf{x}}^{(t)}) \right\|_2 \cdot \tan \theta'_t}$$

for  $t = 0, 1, \dots$ , where  $\theta'_t$  denotes the angle between  $\widehat{\mathbf{x}}^{(t+1)}$  and  $\widehat{\mathbf{x}}^{(t)}$ . Note that the above derivation is based on the orthogonality between  $\widehat{\mathbf{x}}^{(t)}$  and the subspace constrained Riemannian gradient estimator

$$\widehat{V}_d(\widehat{\mathbf{x}}^{(t)}) \widehat{V}_d(\widehat{\mathbf{x}}^{(t)})^T \text{grad } \widehat{f}_h(\widehat{\mathbf{x}}^{(t)}) = \widehat{V}_d(\widehat{\mathbf{x}}^{(t)}) \widehat{V}_d(\widehat{\mathbf{x}}^{(t)})^T \nabla \widehat{f}_h(\widehat{\mathbf{x}}^{(t)});$$

see Figure 2 for a graphical illustration. When the directional SCMS algorithm approaches the estimated ridge  $\widehat{R}_d$ ,  $\theta'_t$  tends to 0 and  $\frac{\theta'_t}{\tan \theta'_t}$  is approximately equal to 1. Thus, the step size  $\eta_{n,h}^{(t)'}$  is also controlled by  $\left\| \widehat{f}_h(\widehat{\mathbf{x}}^{(t)}) \right\|_2$  as in the directional mean shift scenario; see Equation (34). Therefore, Lemma 7 is still effective to argue that the step size  $\eta_{n,h}^{(t)'}$  converges to 0 with probability tending to 1 when  $h \rightarrow 0$  and  $nh^q \rightarrow \infty$ .

**4.3. Linear Convergence of Population and Sample-Based SCGA Algorithms on  $\Omega_q$ .** As we have shown that our proposed directional SCMS algorithm is a variant of a SCGA method with directional KDE  $\widehat{f}_h$  on  $\Omega_q$  in Section 4.2, it remains to prove the linear convergence of such SCGA algorithm on  $\Omega_q$ .

Let  $\{\mathbf{x}^{(t)}\}_{t=0}^{\infty}$  be the sequence defined by the population SCGA algorithm with objective function  $f$  on  $\Omega_q$  and  $\{\widehat{\mathbf{x}}^{(t)}\}_{t=0}^{\infty}$  be the sequence defined by the sample-based SCGA



algorithm with objective function  $\hat{f}_h$  on  $\Omega_q$ . Denote their limiting points by  $\underline{\mathbf{x}}^*$  and  $\hat{\underline{\mathbf{x}}}^*$ , respectively. Recall that the population SCGA algorithm on  $\Omega_q$  has its iterative formula as:

$$(42) \quad \underline{\mathbf{x}}^{(t+1)} = \text{Exp}_{\underline{\mathbf{x}}^{(t)}} \left( \eta \cdot \underline{V}_d(\underline{\mathbf{x}}^{(t)}) \underline{V}_d(\underline{\mathbf{x}}^{(t)})^T \text{grad } f(\underline{\mathbf{x}}^{(t)}) \right)$$

with a suitable choice of the step size  $\eta$ . The sample-based version substitutes the subspace constrained Riemannian gradient  $\underline{V}_d(\underline{\mathbf{x}}) \underline{V}_d(\underline{\mathbf{x}})^T \text{grad } f(\underline{\mathbf{x}})$  with its estimator  $\hat{\underline{V}}_d(\underline{\mathbf{x}}) \hat{\underline{V}}_d(\underline{\mathbf{x}})^T \text{grad } \hat{f}_h(\underline{\mathbf{x}})$ ; see (40). The definition of linear convergence of any converging sequence on  $\Omega_q$  (or an arbitrary manifold) is similar to the one in the flat Euclidean space  $\mathbb{R}^D$  (see Definition 3), except that we need to replace the Euclidean distance with the geodesic distance on  $\Omega_q$  in the definition; see Section 4.5 in Absil et al. (2008).

Analogous to Euclidean SCGA algorithms, conditions (A1-3) in Section 4.1 also imply a quadratic behavior of the residual vector  $\underline{U}_d^\perp(\underline{\mathbf{x}}^{(t)}) \text{Exp}_{\underline{\mathbf{x}}^{(t)}}^{-1}(\underline{\mathbf{x}}^*)$  in the tangent space  $T_{\underline{\mathbf{x}}^{(t)}}$ .

LEMMA 9. Assume conditions (A1-3). Then, we have that for any  $\underline{\mathbf{x}}^{(t)} \in \underline{R}_d \oplus \underline{\rho}$ ,

$$\begin{aligned} & \left\| \underline{U}_d^\perp(\underline{\mathbf{x}}^{(t)}) \cdot \text{Exp}_{\underline{\mathbf{x}}^{(t)}}^{-1}(\underline{\mathbf{x}}^*) \right\|_2 \\ & \leq \frac{(q+1)^{\frac{3}{2}} \left\| \nabla^3 f(\underline{\mathbf{x}}^{(t)}) \right\|_{\max} \cdot d_g(\underline{\mathbf{x}}^{(t)}, \underline{\mathbf{x}}^*)^2}{\underline{\beta}_0} + (q+1)^2 \|f\|_\infty^{(4)} \cdot d_g(\underline{\mathbf{x}}^*, \underline{\mathbf{x}}^{(t)})^3 \\ & = \frac{(q+1)^{\frac{3}{2}} \left\| \nabla^3 f(\underline{\mathbf{x}}^{(t)}) \right\|_{\max} \cdot d_g(\underline{\mathbf{x}}^{(t)}, \underline{\mathbf{x}}^*)^2}{\underline{\beta}_0} + o\left(d_g(\underline{\mathbf{x}}^{(t)}, \underline{\mathbf{x}}^*)^2\right). \end{aligned}$$

While Lemma 9 is similar to Lemma 4, the proof of Lemma 9 is more intricate due to the fact that  $\Omega_q$  is a nonlinear manifold. We decompose the tangent vector  $\text{Exp}_{\underline{\mathbf{x}}^{(t)}}^{-1}(\underline{\mathbf{x}}^*)$  in  $T_{\underline{\mathbf{x}}^{(t)}}$  into an infinite sum of parallel transported SCGA iterative vectors and leverage the linearity of parallel transport mappings to develop the desired upper bound; see Appendix I in the supplement (Zhang and Chen, 2021) for details. Note that the statement and argument of our Lemma 9 are applicable to the SCGA algorithm (42) on any arbitrary smooth manifold.

Using the notation in Zhang and Sra (2016), we let  $\zeta(1, c) \equiv \frac{c}{\tanh(c)}$ . One can show by differentiating  $\zeta(1, c)$  that  $\zeta(1, c)$  is strictly increasing and  $\zeta(1, c) > 1$  for any  $c > 0$ . With the above notations, we state our linear convergence results for population and sample-based SCGA algorithms on  $\Omega_q$ .

THEOREM 10. Assume that conditions (A1-3) hold and  $\text{reach}(\underline{R}_d) > 0$  throughout the theorem.

(a) **Q-Linear convergence of  $d_g(\underline{\mathbf{x}}^{(t)}, \underline{\mathbf{x}}^*)$ :** Given a convergence radius  $r_3 > 0$  satisfying

$$\begin{aligned} r_3 \leq \min & \left\{ \underline{\rho}, \text{reach}(\underline{R}_d), \frac{\arccos\left(1 - \frac{1}{2}\underline{\rho}^2\right) \cdot \underline{\beta}_0 \|f\|_\infty^{(2)}}{\sqrt{q+1} \|f\|_\infty^{(1)} \|f\|_\infty^{(3)} + \underline{\beta}_0 \|f\|_\infty^{(2)}}, \right. \\ & \left. \sqrt{2 - 2 \cos\left(\underline{\beta}_0 / \left[8\tilde{A}_\rho \cdot (q+1)^5 \left(\max\{1, \|f\|_{\infty,4}^*\}\right)^3\right]\right)} \right\}, \end{aligned}$$

we have that whenever  $0 < \eta \leq \min\left\{\frac{4}{\underline{\beta}_0}, \frac{1}{(q+1)\|f\|_\infty^{(2)} \cdot \zeta(1, \underline{\rho})}\right\}$  and the initial point  $\underline{\mathbf{x}}^{(0)} \in \text{Ball}_{q+1}(\underline{\mathbf{x}}^*, r_3) \cap \Omega_q$  with  $\underline{\mathbf{x}}^* \in \underline{R}_d$ ,

$$d_g(\underline{\mathbf{x}}^{(t)}, \underline{\mathbf{x}}^*) \leq \underline{\Upsilon}^t \cdot d_g(\underline{\mathbf{x}}^{(0)}, \underline{\mathbf{x}}^*) \quad \text{with} \quad \underline{\Upsilon} = \sqrt{1 - \frac{\underline{\beta}_0 \eta}{4}}.$$

(b) **R-Linear convergence of  $d_g(\underline{\mathbf{x}}^{(t)}, \underline{R}_d)$ :** Under the same radius  $r_3 > 0$  in (a), we have that whenever  $0 < \eta \leq \min \left\{ \frac{4}{\underline{\beta}_0}, \frac{1}{(q+1)\|f\|_\infty^{(2)} \cdot \zeta(1, \underline{\rho})} \right\}$  and the initial point  $\underline{\mathbf{x}}^{(0)} \in \text{Ball}_{q+1}(\underline{\mathbf{x}}^*, r_3) \cap \Omega_q$  with  $\underline{\mathbf{x}}^* \in \underline{R}_d$ ,

$$d_g(\underline{\mathbf{x}}^{(t)}, \underline{R}_d) \leq \underline{\Upsilon}^t \cdot d_g(\underline{\mathbf{x}}^{(0)}, \underline{\mathbf{x}}^*) \quad \text{with} \quad \underline{\Upsilon} = \sqrt{1 - \frac{\underline{\beta}_0 \eta}{4}}.$$

We further assume (D1-2) in the rest of statements. Suppose that  $h \rightarrow 0$  and  $\frac{nh^{q+4}}{|\log h|} \rightarrow \infty$ .

(c) **Q-Linear convergence of  $d_g(\widehat{\underline{\mathbf{x}}}^{(t)}, \underline{\mathbf{x}}^*)$ :** Under the same radius  $r_3 > 0$  and  $\underline{\Upsilon} = \sqrt{1 - \frac{\underline{\beta}_0 \eta}{4}}$  in (a), we have that

$$d_g(\widehat{\underline{\mathbf{x}}}^{(t)}, \underline{\mathbf{x}}^*) \leq \underline{\Upsilon}^t \cdot d_g(\widehat{\underline{\mathbf{x}}}^{(0)}, \underline{\mathbf{x}}^*) + O(h^2) + O_P \left( \sqrt{\frac{|\log h|}{nh^{q+4}}} \right)$$

with probability tending to 1 whenever  $0 < \eta \leq \min \left\{ \frac{4}{\underline{\beta}_0}, \frac{1}{(q+1)\|f\|_\infty^{(2)} \cdot \zeta(1, \underline{\rho})} \right\}$  and the initial point  $\widehat{\underline{\mathbf{x}}}^{(0)} \in \text{Ball}_{q+1}(\underline{\mathbf{x}}^*, r_3) \cap \Omega_q$  with  $\underline{\mathbf{x}}^* \in \underline{R}_d$ .

(d) **R-Linear convergence of  $d_g(\widehat{\underline{\mathbf{x}}}^{(t)}, \underline{R}_d)$ :** Under the same radius  $r_3 > 0$  and  $\underline{\Upsilon} = \sqrt{1 - \frac{\underline{\beta}_0 \eta}{4}}$  in (a), we have that

$$d_g(\widehat{\underline{\mathbf{x}}}^{(t)}, \underline{R}_d) \leq \underline{\Upsilon}^t \cdot d_g(\widehat{\underline{\mathbf{x}}}^{(0)}, \underline{\mathbf{x}}^*) + O(h^2) + O_P \left( \sqrt{\frac{|\log h|}{nh^{q+4}}} \right)$$

with probability tending to 1 whenever  $0 < \eta \leq \min \left\{ \frac{4}{\underline{\beta}_0}, \frac{1}{(q+1)\|f\|_\infty^{(2)} \cdot \zeta(1, \underline{\rho})} \right\}$  and the initial point  $\widehat{\underline{\mathbf{x}}}^{(0)} \in \text{Ball}_{q+1}(\underline{\mathbf{x}}^*, r_3) \cap \Omega_q$  with  $\underline{\mathbf{x}}^* \in \underline{R}_d$ .

The proof is in Appendix I of the supplement (Zhang and Chen, 2021). Theorem 10 illuminates both the step size requirement and the convergence radius for the linear convergence of SCGA algorithms on  $\Omega_q$ . Similar to Euclidean SCGA algorithms in Theorem 5, such radius depends on the manifold dimension  $q$ , the reach of  $\underline{R}_d$ , the effective radius  $\underline{\rho}$  of condition (A2), and functional norms of  $f$  up to its fourth-order derivatives. Recall from (41) that our directional SCMS algorithm embraces an adaptive step size  $\eta_{n,h}^{(t)'}$  converging to 0 asymptotically. This, together with Theorem 10, implies that the directional SCMS algorithm will eventually converge (at least) linearly around a small neighborhood of  $\underline{R}_d$  under some estimation errors; see also Remark 4 below.

**REMARK 4.** In practice, one may focus on the algorithmic convergence rate of the sample-based SCGA algorithm on  $\Omega_q$  to the estimated directional ridge  $\widehat{\underline{R}}_d$  due to its resemblance to the directional SCMS algorithm. We know from the uniform bounds (30) that the estimated directional density  $\widehat{f}_h$  satisfies conditions (A1-3) with probability tending to 1 as  $h \rightarrow 0$  and  $\frac{nh^{q+6}}{|\log h|} \rightarrow \infty$ . This is because condition (D1) implies (A1) and conditions (A2-3) involves only the first three order partial derivatives of the directional density  $f$ . Thus, one can follow the argument in (a) of Theorem 10 to demonstrate that there exists a positive number  $r_4 \leq \min \left\{ \underline{\rho}, \text{reach}(\widehat{\underline{R}}_d) \right\}$  such that

$$d_g(\widehat{\underline{\mathbf{x}}}^{(t)}, \widehat{\underline{R}}_d) \leq \left\| \widehat{\underline{\mathbf{x}}}^{(t)} - \widehat{\underline{\mathbf{x}}}^* \right\|_2 \leq \underline{\Upsilon}^t \left\| \widehat{\underline{\mathbf{x}}}^{(0)} - \widehat{\underline{\mathbf{x}}}^* \right\|_2 \quad \text{with} \quad \underline{\Upsilon} = \sqrt{1 - \frac{\underline{\beta}_0 \eta}{4}}$$

TABLE 1

Comparisons between Euclidean and directional mean shift (MS) or SCMS algorithms and summary of the asymptotic convergence rates of their adaptive sizes when viewed as GA/SCGA algorithms in  $\mathbb{R}^D$  or on  $\Omega_q$ .

Algorithms	Recast forms as GA/SCGA (in $\mathbb{R}^D$ or on $\Omega_q$ )	Asymptotic step sizes
MS / SCMS in $\mathbb{R}^D$	$\hat{\mathbf{x}}^{(t+1)} \leftarrow \begin{cases} \hat{\mathbf{x}}^{(t)} + \eta_{n,h}^{(t)} \cdot \nabla \hat{p}_n(\hat{\mathbf{x}}^{(t)}) \\ \hat{\mathbf{x}}^{(t)} + \eta_{n,h}^{(t)} \cdot \hat{V}_d(\hat{\mathbf{x}}^{(t)}) \hat{V}_d(\hat{\mathbf{x}}^{(t)})^T \nabla \hat{p}_n(\hat{\mathbf{x}}^{(t)}) \end{cases}$	$\eta_{n,h}^{(t)} \asymp O(h^2) + o_P(h^2)$ (See Lemma 2)
MS / SCMS on $\Omega_q$	$\hat{\mathbf{x}}^{(t+1)} \leftarrow \begin{cases} \text{Exp}_{\hat{\mathbf{x}}^{(t)}} \left( \eta_{n,h}^{(t)} \cdot \text{grad } \hat{f}_h(\hat{\mathbf{x}}^{(t)}) \right) \\ \text{Exp}_{\hat{\mathbf{x}}^{(t)}} \left( \eta_{n,h}^{(t')} \cdot \hat{V}_d(\hat{\mathbf{x}}^{(t)}) \hat{V}_d(\hat{\mathbf{x}}^{(t)})^T \text{grad } \hat{f}_h(\hat{\mathbf{x}}^{(t)}) \right) \end{cases}$	$\eta_{n,h}^{(t)} \asymp \eta_{n,h}^{(t')}$ $= O(h^2) + o_P(h^2)$ , (See Lemma 7)

with probability tending to 1 whenever  $0 < \eta \leq \min \left\{ \frac{4}{\underline{\beta}_0}, \frac{1}{(q+1)\|f\|_\infty^{(2)} \cdot \zeta(1, \underline{\rho})} \right\}$  and the initial point  $\hat{\mathbf{x}}^{(0)} \in \text{Ball}_{q+1}(\hat{\mathbf{x}}^*, r_4) \cap \Omega_q$  with  $\hat{\mathbf{x}}^* \in \hat{R}_d$ . In addition, this (estimated) convergence radius  $r_4 > 0$  should be at least approximately as large as the convergence radius  $r_3 > 0$  in (a) of Theorem 10. The reason is that when  $h \rightarrow 0$  and  $\frac{nh^{q+6}}{|\log h|} \rightarrow \infty$ , the Hausdorff distance  $\text{Haus}(\underline{R}_d, \hat{R}_d) = O(h^2) + O_P\left(\sqrt{\frac{|\log h|}{nh^{q+4}}}\right)$  is a high order error term and thus,  $d_g(\hat{\mathbf{x}}^{(t)}, \underline{R}_d) \approx d_g(\hat{\mathbf{x}}^{(t)}, \hat{R}_d)$ ; see Theorem 6 and (30).

REMARK 5. Similar to Euclidean SCGA algorithms, the geodesic strong concavity assumption (Zhang and Sra, 2016) on the objective function  $f$  is not sufficient to prove the linear convergence of the SCGA algorithm (42) on  $\Omega_q$ . We instead establish the following “subspace constrained geodesically strong concavity” under some mild conditions (A1-3):

$$(43) \quad f(\underline{\mathbf{x}}^*) - f(\mathbf{y}) \leq \langle \underline{V}_d(\mathbf{y}) \underline{V}_d(\mathbf{y})^T \text{grad } f(\mathbf{y}), \text{Exp}_{\underline{\mathbf{x}}^*}^{-1}(\mathbf{y}) \rangle - A_3 \cdot d_g(\underline{\mathbf{x}}^*, \mathbf{y})^2 + o(d_g(\underline{\mathbf{x}}^*, \mathbf{y})^2)$$

for some constant  $A_3 > 0$ , where  $\mathbf{y}$  is generally chosen to be  $\underline{\mathbf{x}}^{(t)}$ . In fact, Lemma 9 illustrates that the eigengap condition (A2) is critical in establishing such property.

**5. Discussions.** In this paper, we have provided a rigorous proof for the linear convergence of the well-known SCMS algorithm by viewing it as an example of the SCGA algorithm. We have also generalized the definition of density ridges from usual densities supported on compact sets in  $\mathbb{R}^D$  to directional densities supported on  $\Omega_q$  with nonzero curvature. The stability theorem of directional density ridges has been established, and the linear convergence of our proposed directional SCMS algorithm has been proved. Table 1 summarizes the frameworks of considering (directional) mean shift/SCMS algorithm as gradient ascent/SCGA methods (on  $\Omega_q$ ) and our results of asymptotic convergence rates of their corresponding step sizes.

Our theoretical analyses of the SCGA algorithm in the Euclidean space  $\mathbb{R}^D$  and on the unit hypersphere  $\Omega_q$  has potential implications beyond proving the linear convergence of SCMS algorithms. In the optimization literature (Nocedal and Wright, 2006; Absil et al., 2008; Zhang and Sra, 2016; Nesterov et al., 2018), it is well-known that a standard gradient ascent method (on a smooth manifold) will converge linearly given an appropriate step size when the objective function is smooth and (geodesically) strongly concave. However, as we have discussed in Remarks 2 and 5, the smoothness and (geodesically) strong concavity assumptions are not sufficient for the linear convergence of SCGA algorithms. Therefore, identifying density ridges with SCGA algorithms is not only a nonconvex optimization problem,

but also fundamentally more complex than standard gradient ascent methods. The assumptions and proof arguments developed in this paper may give some insights into the linear convergence of SCGA algorithms with other forms of subspace constrained gradients.

There are still many open problems related to the SCMS algorithm. First, a central issue in determining the performance of a SCMS algorithm is bandwidth selection. There is a variety of bandwidth selection mechanisms available to Euclidean KDE and its derivatives in the literature ([Chacón et al., 2011](#); [Scott, 2015](#)), but it is unclear how to apply them to the SCMS algorithm. We plan to specialize or generalize such techniques to the SCMS algorithm under both the Euclidean and directional data. Second, our definition of density ridges is generalizable to any density supported on an arbitrary Riemannian manifold. As [Hauberg \(2015\)](#) has formulated the principal curve on a Riemannian manifold based on its classical definition in [Hastie and Stuetzle \(1989\)](#), it will be interesting to propose a new definition of principal curves from the perspective of density ridges on Riemannian manifolds and derive a more general SCMS algorithm, possibly based on some existing nonlinear mean shift methods on manifolds ([Subbarao and Meer, 2006, 2009](#)).

**Acknowledgements.** YC is supported by NSF DMS - 1810960 and DMS - 195278, NIH U01 - AG0169761.

## REFERENCES

- ABSIL, P. A., MAHONY, R. and SEPULCHRE, R. (2008). *Optimization Algorithms on Matrix Manifolds*. Princeton University Press, Princeton, NJ.
- ABSIL, P. A., MAHONY, R. and TRUMPF, J. (2013). An Extrinsic Look at the Riemannian Hessian. In *Geometric Science of Information* (F. NIELSEN and F. BARBARESCO, eds.) 361–368. Springer Berlin Heidelberg.
- ALIMISIS, F., ORVIETO, A., BÉCIGNEUL, G. and LUCCHI, A. (2020). Practical Accelerated Optimization on Riemannian Manifolds. *arXiv preprint arXiv:2002.04144v1*.
- ARIAS-CASTRO, E., MASON, D. and PELLETIER, B. (2016). On the Estimation of the Gradient Lines of a Density and the Consistency of the Mean-Shift Algorithm. *Journal of Machine Learning Research* **17** 1-28.
- BAI, Z. D., RAO, C. R. and ZHAO, L. C. (1988). Kernel estimators of density function of directional data. *Journal of Multivariate Analysis* **27** 24 - 39.
- BALAKRISHNAN, S., WAINWRIGHT, M. J. and YU, B. (2017). Statistical guarantees for the EM algorithm: From population to sample-based analysis. *Annals of Statistics* **45** 77–120.
- BANERJEE, A., DHILLON, I. S., GHOSH, J. and SRA, S. (2005). Clustering on the Unit Hypersphere using von Mises-Fisher Distributions. *Journal of Machine Learning Research* **6** 1345-1382.
- BANYAGA, A. and HURTUBISE, D. (2004). *Lectures on Morse Homology. Texts in the Mathematical Sciences*. Springer Netherlands.
- BECK, A. and TETRUASHVILI, L. (2013). On the convergence of block coordinate descent type methods. *SIAM journal on Optimization* **23** 2037–2060.
- BERAN, R. (1979). Exponential Models for Directional Data. *The Annals of Statistics* **7** 1162–1178.
- BONNABEL, S. (2013). Stochastic Gradient Descent on Riemannian Manifolds. *IEEE Transactions on Automatic Control* **58** 2217-2229.
- BUBECK, S. (2015). Convex Optimization: Algorithms and Complexity. *Foundations and Trends in Machine Learning* **8** 231-357.
- BURAGO, Y., GROMOV, M. and PEREL'MAN, G. (1992). A.D. Alexandrov spaces with curvature bounded below. *Russian Mathematical Surveys* **47** 1–58.
- CARREIRA-PERPIÑÁN, M. Á. (2007). Gaussian Mean-Shift Is an EM Algorithm. *IEEE Trans. Pattern Anal. Mach. Intell.* **29** 767–776.
- CHACÓN, E. J., DUONG, T. and WAND, P. M. (2011). Asymptotics for general multivariate kernel density derivative estimators. *Statistica Sinica* **21** 807.
- CHEN, Y.-C. (2017). A tutorial on kernel density estimation and recent advances. *Biostatistics & Epidemiology* **1** 161-187.
- CHEN, Y.-C. (2020). Solution Manifold and Its Statistical Applications. *arXiv preprint arXiv:2002.05297*.
- CHEN, Y.-C., GENOVESE, C. R. and WASSERMAN, L. (2015). Asymptotic theory for density ridges. *Annals of Statistics* **43** 1896–1928.

- CHEN, Y.-C., GENOVESE, C. R. and WASSERMAN, L. (2016). A comprehensive approach to mode clustering. *Electronic Journal of Statistics* **10** 210–241.
- CHEN, Y.-C., GENOVESE, C. R., HO, S. and WASSERMAN, L. (2015a). Optimal Ridge Detection using Coverage Risk. In *Advances in Neural Information Processing Systems* **28**. Curran Associates, Inc.
- CHEN, Y.-C., HO, S., FREEMAN, P. E., GENOVESE, C. R. and WASSERMAN, L. (2015b). Cosmic web reconstruction through density ridges: method and algorithm. *Monthly Notices of the Royal Astronomical Society* **454** 1140–1156.
- CHEN, Y.-C., HO, S., BRINKMANN, J., FREEMAN, P. E., GENOVESE, C. R., SCHNEIDER, D. P. and WASSERMAN, L. (2016). Cosmic web reconstruction through density ridges: catalogue. *Monthly Notices of the Royal Astronomical Society* **461** 3896–3909.
- CHENG, Y. (1995). Mean shift, mode seeking, and clustering. *IEEE Transactions on Pattern Analysis and Machine Intelligence* **17** 790–799.
- CHRISMAN, N. R. (2017). Calculating on a round planet. *International Journal of Geographical Information Science* **31** 637–657.
- COMANICIU, D. and MEER, P. (2002). Mean shift: a robust approach toward feature space analysis. *IEEE Transactions on Pattern Analysis and Machine Intelligence* **24** 603–619.
- CRAIG, T. J., JACKSON, J. A., PRIESTLEY, K. and MCKENZIE, D. (2011). Earthquake distribution patterns in Africa: their relationship to variations in lithospheric and geological structure, and their rheological implications. *Geophysical Journal International* **185** 403–434.
- CUEVAS, A. (2009). Set estimation: Another bridge between statistics and geometry. *Bol. Estad. Investig. Oper* **25** 71–85.
- DAMON, J. (1999). Properties of Ridges and Cores for Two-Dimensional Images. *J. Math. Imaging Vis.* **10** 163–174.
- DAVIS, C. and KAHAN, W. M. (1970). The Rotation of Eigenvectors by a Perturbation. III. *SIAM Journal on Numerical Analysis* **7** 1–46.
- DO CARMO, M. P. (2016). *Differential Geometry of Curves and Surfaces: Revised and Updated Second Edition*. Dover Books on Mathematics. Dover Publications.
- DRMAC, Z. (2000). On Principal Angles between Subspaces of Euclidean Space. *SIAM J. Matrix Anal. Appl.* **22** 173–194.
- EBERLY, D. (1996). *Ridges in Image and Data Analysis*. Computational Imaging and Vision. Springer Netherlands.
- EINMAHL, U. and MASON, D. M. (2005). Uniform in bandwidth consistency of kernel-type function estimators. *Annals of Statistics* **33** 1380–1403.
- FEDERER, H. (1959). Curvature measures. *Transactions of the American Mathematical Society* **93** 418–491.
- GARCÍA-PORTUGUÉS, E. (2013). Exact risk improvement of bandwidth selectors for kernel density estimation with directional data. *Electron. J. Stat.* **7** 1655–1685.
- GARCÍA-PORTUGUÉS, E., CRUJEIRAS, R. M. and GONZÁLEZ-MANTEIGA, W. (2013). Kernel Density Estimation for Directional-Linear Data. *Journal of Multivariate Analysis* **121** 152 - 175.
- GENOVESE, C. R., PERONE-PACIFICO, M., VERDINELLI, I. and WASSERMAN, L. (2014). Nonparametric ridge estimation. *Annals of Statistics* **42** 1511–1545.
- ALIYARI GHASSABEH, Y. (2015). A sufficient condition for the convergence of the mean shift algorithm with Gaussian kernel. *Journal of Multivariate Analysis* **135** 1 - 10.
- GHASSABEH, Y. A., LINDER, T. and TAKAHARA, G. (2013). On some convergence properties of the subspace constrained mean shift. *Pattern Recognition* **46** 3140–3147.
- GHASSABEH, Y. A. and RUDZICZ, F. (2020). Modified Subspace Constrained Mean Shift Algorithm. *Journal of Classification* 1–17.
- GINÉ, E. and GUILLOU, A. (2002). Rates of strong uniform consistency for multivariate kernel density estimators. *Annales de l'Institut Henri Poincaré (B) Probability and Statistics* **38** 907 - 921.
- HALL, P., PENG, L. and RAU, C. (2001). Local Likelihood Tracking of Fault Lines and Boundaries. *Journal of the Royal Statistical Society. Series B (Statistical Methodology)* **63** 569–582.
- HALL, P., QIAN, W. and TITTERINGTON, D. M. (1992). Ridge Finding from Noisy Data. *Journal of Computational and Graphical Statistics* **1** 197–211.
- HALL, P., WATSON, G. S. and CABRARA, J. (1987). Kernel density estimation with spherical data. *Biometrika* **74** 751–762.
- HARRIS, R. A. (2017). Large earthquakes and creeping faults. *Reviews of Geophysics* **55** 169–198.
- HASTIE, T. and STUETZLE, W. (1989). Principal curves. *Journal of the American Statistical Association* **84** 502–516.
- HAUBERG, S. (2015). Principal curves on Riemannian manifolds. *IEEE transactions on pattern analysis and machine intelligence* **38** 1915–1921.

- HORN, R. A. and JOHNSON, C. R. (1991). *Topics in Matrix Analysis*. Cambridge University Press.
- HORN, R. A. and JOHNSON, C. R. (2012). *Matrix Analysis*, 2 ed. Cambridge University Press.
- HOSSEINI, R. and SRA, S. (2020). An alternative to EM for Gaussian mixture models: batch and stochastic Riemannian optimization. *Mathematical Programming* 187–223.
- IRWIN, M. C. (2001). *Smooth Dynamical Systems*. WORLD SCIENTIFIC.
- IZENMAN, A. J. (2012). Introduction to manifold learning. *WIREs Computational Statistics* 4 439–446.
- JONES, M. C., MARRON, J. S. and SHEATHER, S. J. (1996). A Brief Survey of Bandwidth Selection for Density Estimation. *Journal of the American Statistical Association* 91 401–407.
- KAFAI, M., MIAO, Y. and OKADA, K. (2010). Directional mean shift and its application for topology classification of local 3D structures. 170 - 177.
- KLEMELÄ, J. (2000). Estimation of Densities and Derivatives of Densities with Directional Data. *Journal of Multivariate Analysis* 73 18 - 40.
- KOZAK, D., BECKER, S., DOOSTAN, A. and TENORIO, L. (2019). Stochastic Subspace Descent. *arXiv preprint arXiv: 1904.01145*.
- KOZAK, D., BECKER, S., DOOSTAN, A. and TENORIO, L. (2020). A stochastic subspace approach to gradient-free optimization in high dimensions. *arXiv preprint arXiv: 2003.02684*.
- LEE, J. M. (2012). *Introduction to Smooth Manifolds*, second ed. *Graduate Texts in Mathematics*. Springer.
- LEY, C. and VERDEBOUT, T. (2017). *Modern directional statistics*. CRC Press.
- LI, X., HU, Z. and WU, F. (2007). A note on the convergence of the mean shift. *Pattern Recognition* 40 1756 - 1762.
- LOWMAN, P., YATES, J., MASUOKA, P., MONTGOMERY, B., O’LEARY, J. and SALISBURY, D. (1999). A digital tectonic activity map of the Earth. *Journal of Geoscience Education* 47 428–437.
- LUO, Z.-Q. and TSENG, P. (1992). On the convergence of the coordinate descent method for convex differentiable minimization. *Journal of Optimization Theory and Applications* 72 7–35.
- MARDIA, K. V. and JUPP, P. E. (2000). *Directional Statistics*. *Wiley Series in Probability and Statistics*. Wiley.
- MARZIO, M. D., PANZERA, A. and TAYLOR, C. C. (2011). Kernel density estimation on the torus. *Journal of Statistical Planning and Inference* 141 2156 - 2173.
- NESTEROV, Y. et al. (2018). *Lectures on convex optimization* 137. Springer.
- NOCEDAL, J. and WRIGHT, S. J. (2006). *Numerical Optimization*, 2 ed. *Springer Series in Operations Research and Financial Engineering*. Springer, New York.
- NORGARD, G. and BREMER, P.-T. (2012). Second derivative ridges are straight lines and the implications for computing Lagrangian coherent structures. *Physica D: Nonlinear Phenomena* 241 1475–1476.
- OBA, S., KATO, K. and ISHII, S. (2005). Multi-scale clustering for gene expression profiling data. In *Fifth IEEE Symposium on Bioinformatics and Bioengineering (BIBE’05)* 210–217.
- OLIVEIRA, M., CRUJEIRAS, R. M. and RODRÍGUEZ-CASAL, A. (2012). A plug-in rule for bandwidth selection in circular density estimation. *Comput. Stat. Data Anal.* 56 3898–3908.
- OZERTEM, U. and ERDOGMUS, D. (2011). Locally Defined Principal Curves and Surfaces. *Journal of Machine Learning Research* 12 1249–1286.
- PEIKERT, R., GÜNTHER, D. and WEINKAUF, T. (2013). Comment on “Second derivative ridges are straight lines and the implications for computing Lagrangian Coherent Structures, Physica D 2012.05. 006”. *Physica D: Nonlinear Phenomena* 242 65–66.
- PENNEC, X. (2006). Intrinsic Statistics on Riemannian Manifolds: Basic Tools for Geometric Measurements. *Journal of Mathematical Imaging and Vision* 25 127–154.
- PEWSEY, A. and GARCÍA-PORTUGUÉS, E. (2021). Recent advances in directional statistics. *TEST* 1–58.
- QIAO, W. (2020). Asymptotic Confidence Regions for Density Ridges. *arXiv preprint arXiv:2004.11354*.
- QIAO, W. and POLONIK, W. (2016). Theoretical analysis of nonparametric filament estimation. *Annals of Statistics* 44 1269–1297.
- QIAO, W. and POLONIK, W. (2021). Algorithms for ridge estimation with convergence guarantees. *arXiv preprint arXiv:2104.12314*.
- RUDIN, W. (1976). *Principles of Mathematical Analysis*, Third edition ed. McGraw-Hill New York.
- SAAVEDRA-NIEVES, P. and MARÍA CRUJEIRAS, R. (2020). Nonparametric estimation of directional highest density regions. *arXiv preprint arXiv:2009.08915*.
- SARAGIH, J. M., LUCEY, S. and COHN, J. F. (2009). Face alignment through subspace constrained mean-shifts. In *2009 IEEE 12th International Conference on Computer Vision* 1034–1041. Ieee.
- SASAKI, H., KANAMORI, T. and SUGIYAMA, M. (2017). Estimating Density Ridges by Direct Estimation of Density-Derivative-Ratios. In *Proceedings of the 20th International Conference on Artificial Intelligence and Statistics* (A. SINGH and J. ZHU, eds.). *Proceedings of Machine Learning Research* 54 204–212. PMLR, Fort Lauderdale, FL, USA.
- SCOTT, D. W. (2015). *Multivariate Density Estimation: Theory, Practice, and Visualization*. *Wiley Series in Probability and Statistics*. Wiley.



- SHEATHER, S. J. (2004). Density Estimation. *Statistical Science* **19** 588–597.
- SNYDER, J. P., VOXLAND, P. M. and ), G. S. U. S. (1989). *An Album of Map Projections. An Album of Map Projections* **1453**. U.S. Government Printing Office.
- SOUSBIE, T., PICHON, C., COURTOIS, H., COLOMBI, S. and NOVIKOV, D. (2007). The Three-dimensional Skeleton of the SDSS. *The Astrophysical Journal* **672** L1–L4.
- SUBARYA, C., CHLIEH, M., PRAWIRODIRDJO, L., AVOUAC, J.-P., BOCK, Y., SIEH, K., MELTZNER, A. J., NATAWIDJAJA, D. H. and MCCAFFREY, R. (2006). Plate-boundary deformation associated with the great Sumatra–Andaman earthquake. *Nature* **440** 46–51.
- SUBBARAO, R. and MEER, P. (2006). Nonlinear mean shift for clustering over analytic manifolds. In *2006 IEEE Computer Society Conference on Computer Vision and Pattern Recognition (CVPR'06)* **1** 1168–1175. IEEE.
- SUBBARAO, R. and MEER, P. (2009). Nonlinear mean shift over Riemannian manifolds. *International journal of computer vision* **84** 1.
- TAYLOR, C. C. (2008). Automatic bandwidth selection for circular density estimation. *Computational Statistics & Data Analysis* **52** 3493 - 3500.
- VAN DER VAART, A. W. (1998). *Asymptotic Statistics. Cambridge Series in Statistical and Probabilistic Mathematics*. Cambridge University Press.
- VON LUXBURG, U. (2007). A Tutorial on Spectral Clustering. *Statistics and Computing* **17** 395–416.
- WASSERMAN, L. (2006). *All of Nonparametric Statistics (Springer Texts in Statistics)*. Springer-Verlag, Berlin, Heidelberg.
- WASSERMAN, L. (2018). Topological Data Analysis. *Annual Review of Statistics and Its Application* **5** 501–532.
- WRIGHT, S. J. (2015). Coordinate descent algorithms. *Mathematical Programming* **151** 3–34.
- YANG, M.-S., CHANG-CHIEN, S.-J. and KUO, H.-C. (2014). On Mean Shift Clustering for Directional Data on a Hypersphere. In *Artificial Intelligence and Soft Computing* 809–818. Springer International Publishing, Cham.
- YOU, S., BAS, E., ERDOGMUS, D. and KALPATHY-CRAMER, J. (2011). Principal Curved Based Retinal Vessel Segmentation towards Diagnosis of Retinal Diseases. In *2011 IEEE First International Conference on Healthcare Informatics, Imaging and Systems Biology* 331–337.
- YU, Y., WANG, T. and SAMWORTH, R. J. (2014). A useful variant of the Davis–Kahan theorem for statisticians. *Biometrika* **102** 315–323.
- ZHANG, Y. and CHEN, Y.-C. (2020). Kernel Smoothing, Mean Shift, and Their Learning Theory with Directional Data. *arXiv preprint arXiv:2010.13523*.
- ZHANG, Y. and CHEN, Y.-C. (2021). Supplement to “Linear Convergence of the Subspace Constrained Mean Shift Algorithm: From Euclidean to Directional Data”.
- ZHANG, H. and SRA, S. (2016). First-order Methods for Geodesically Convex Optimization. *Proceedings of Machine Learning Research* **49** 1617–1638. PMLR, Columbia University, New York, New York, USA.
- ZHAO, L. and WU, C. (2001). Central limit theorem for integrated squared error of kernel estimators of spherical density. *Sci. China Ser. A Math.* **44** 474–483.

## SUPPLEMENT TO “LINEAR CONVERGENCE OF THE SUBSPACE CONSTRAINED MEAN SHIFT ALGORITHM: FROM EUCLIDEAN TO DIRECTIONAL DATA”

### APPENDIX A: ALGORITHMIC SUMMARIES OF EUCLIDEAN AND DIRECTIONAL SCMS ALGORITHMS

We provide an algorithmic summaries of Euclidean and directional SCMS algorithms in this section for practical reference. Algorithm 1 summarizes the entire procedures for carrying out the Euclidean SCMS algorithm from a practical perspective. In practice, when the observational data are noisy, it is common to incorporate an extra denoising step before Step 2 of Algorithm 1 to stabilize the (Euclidean) SCMS algorithm; see [Genovese et al. \(2014\)](#); [Chen et al. \(2015b\)](#) for comparative studies that demonstrate the significance of denoising.

---

#### Algorithm 1 (Euclidean) Subspace Constrained Mean Shift (SCMS) Algorithm

---

**Input:**

- A data sample  $\mathbf{X}_1, \dots, \mathbf{X}_n \sim p(\mathbf{x})$  in  $\mathbb{R}^D$ .
- The order  $d$  of the ridge, smoothing bandwidth  $h > 0$ , and tolerance level  $\epsilon > 0$ .
- A suitable mesh  $\mathcal{M} \subset \mathbb{R}^D$  of initial points. By default,  $\mathcal{M} = \{\mathbf{X}_1, \dots, \mathbf{X}_n\}$ .

**Step 1:** Compute the density estimator  $\hat{p}_n(\mathbf{x}) = \frac{c_{k,D}}{nh^D} \sum_{i=1}^n k\left(\left\|\frac{\mathbf{x}-\mathbf{X}_i}{h}\right\|_2^2\right)$  on the mesh  $\mathcal{M}$ .

**Step 2:** For each initial point  $\hat{\mathbf{x}}^{(0)} \in \mathcal{M}$ , iterate the following SCMS update until convergence:

**while**  $\left\|\hat{\mathbf{V}}_d(\hat{\mathbf{x}}^{(t)})^T \nabla \hat{p}_n(\hat{\mathbf{x}}^{(t)})\right\|_2 > \epsilon$  **do**

**Step 2-1:** Compute the estimated Hessian matrix as:

$$\begin{aligned} \nabla \nabla \hat{p}_n(\hat{\mathbf{x}}^{(t)}) &= \frac{c_{k,D}}{nh^{D+2}} \sum_{i=1}^n \left[ 2\mathbf{I}_D \cdot k' \left( \left\| \frac{\hat{\mathbf{x}}^{(t)} - \mathbf{X}_i}{h} \right\|_2^2 \right) \right. \\ &\quad \left. + \frac{4}{h^2} (\hat{\mathbf{x}}^{(t)} - \mathbf{X}_i)(\hat{\mathbf{x}}^{(t)} - \mathbf{X}_i)^T \cdot k'' \left( \left\| \frac{\hat{\mathbf{x}}^{(t)} - \mathbf{X}_i}{h} \right\|_2^2 \right) \right]. \end{aligned}$$

**Step 2-2:** Perform the spectral decomposition on the Hessian  $\nabla \nabla \hat{p}_n(\hat{\mathbf{x}}^{(t)})$  and obtain that  $\hat{\mathbf{V}}_d(\hat{\mathbf{x}}^{(t)}) = [\mathbf{v}_{d+1}(\hat{\mathbf{x}}^{(t)}), \dots, \mathbf{v}_D(\hat{\mathbf{x}}^{(t)})]$  whose columns are orthonormal eigenvectors associated with the smallest  $(D - d)$  eigenvalues of  $\nabla \nabla \hat{p}_n(\hat{\mathbf{x}}^{(t)})$ .

**Step 2-3:** Update  $\hat{\mathbf{x}}^{(t+1)} \leftarrow \hat{\mathbf{x}}^{(t)} + \hat{\mathbf{V}}_d(\hat{\mathbf{x}}^{(t)}) \hat{\mathbf{V}}_d(\hat{\mathbf{x}}^{(t)})^T \left[ \frac{\sum_{i=1}^n \mathbf{X}_i k' \left( \left\| \frac{\hat{\mathbf{x}}^{(t)} - \mathbf{X}_i}{h} \right\|_2^2 \right)}{\sum_{i=1}^n k' \left( \left\| \frac{\hat{\mathbf{x}}^{(t)} - \mathbf{X}_i}{h} \right\|_2^2 \right)} - \hat{\mathbf{x}}^{(t)} \right]$ .

**end while**

**Output:** An estimated  $d$ -ridge  $\hat{R}_d$  represented by the collection of resulting points.

---

We summarize the directional SCMS algorithm in Algorithm 2. Note that in Step 2-1 of Algorithm 2, we compute the scaled versions  $\frac{nh^2}{c_{h,q}(L)} \hat{G}_d(\mathbf{x})$  and  $\frac{nh^2}{c_{h,q}(L)} \mathcal{H} \hat{f}_h(\mathbf{x})$  for  $\mathbf{x} \in \Omega_q$  because the estimated principal Riemannian gradient  $\hat{G}_d(\mathbf{x})$  and Hessian  $\mathcal{H} \hat{f}_h(\mathbf{x})$  are often very small. Such scaling stabilizes the numerical computation. The spectral decomposition is

thus performed on the scaled Hessian estimator

$$\begin{aligned} \frac{nh^2}{c_{h,q}(L)} \mathcal{H} \hat{f}_h(\mathbf{x}) &= (\mathbf{I}_{q+1} - \mathbf{x}\mathbf{x}^T) \left[ \frac{1}{h^2} \sum_{i=1}^n \mathbf{X}_i \mathbf{X}_i^T \cdot L'' \left( \frac{1 - \mathbf{x}^T \mathbf{X}_i}{h^2} \right) \right. \\ &\quad \left. + \sum_{i=1}^n \mathbf{x}^T \mathbf{X}_i \mathbf{I}_{q+1} \cdot L' \left( \frac{1 - \mathbf{x}^T \mathbf{X}_i}{h^2} \right) \right] (\mathbf{I}_{q+1} - \mathbf{x}\mathbf{x}^T), \end{aligned}$$

and the scaled principal Riemannian gradient estimator is calculated as

$$\begin{aligned} \frac{nh^2}{c_{h,q}(L)} \hat{G}_d(\mathbf{x}) &= \hat{V}_d(\mathbf{x}) \hat{V}_d(\mathbf{x})^T \left[ \sum_{i=1}^n (\mathbf{x} \cdot \mathbf{x}^T \mathbf{X}_i - \mathbf{X}_i) L' \left( \frac{1 - \mathbf{x}^T \mathbf{X}_i}{h^2} \right) \right] \\ &= - \sum_{i=1}^n \hat{V}_d(\mathbf{x}) \hat{V}_d(\mathbf{x})^T \mathbf{X}_i \cdot L' \left( \frac{1 - \mathbf{x}^T \mathbf{X}_i}{h^2} \right), \end{aligned}$$

where  $\hat{V}_d(\mathbf{x}) = [\hat{\mathbf{v}}_{d+1}(\mathbf{x}), \dots, \hat{\mathbf{v}}_q(\mathbf{x})]$  has its columns equal to the orthonormal eigenvectors associated with the  $d$ -smallest eigenvalues of the scaled Hessian estimator  $\frac{nh^2}{c_{h,q}(L)} \mathcal{H} \hat{f}_h(\mathbf{x})$  (or equivalently,  $\mathcal{H} \hat{f}_h(\mathbf{x})$ ) inside the tangent space  $T_{\mathbf{x}}$ .

---

**Algorithm 2** Directional Subspace Constrained Mean Shift (SCMS) Algorithm

---

**Input:**

- A directional data sample  $\mathbf{X}_1, \dots, \mathbf{X}_n \sim f(\mathbf{x})$  on  $\Omega_q$
- The order  $d$  of the directional ridge, smoothing bandwidth  $h > 0$ , and tolerance level  $\epsilon > 0$ .
- A suitable mesh  $\mathcal{M}_D \subset \Omega_q$  of initial points. By default,  $\mathcal{M}_D = \{\mathbf{X}_1, \dots, \mathbf{X}_n\}$ .

**Step 1:** Compute the directional KDE  $\hat{f}_h(\mathbf{x}) = \frac{c_{h,q}(L)}{n} \sum_{i=1}^n L \left( \frac{1 - \mathbf{x}^T \mathbf{X}_i}{h^2} \right)$  on the mesh  $\mathcal{M}_D$ .

**Step 2:** For each  $\hat{\mathbf{x}}^{(0)} \in \widetilde{\mathcal{M}}_D$ , iterate the following directional SCMS update until convergence:

**while**  $\left\| \frac{nh^2}{c_{h,q}(L)} \hat{G}_d(\hat{\mathbf{x}}^{(t)}) \right\|_2 > \epsilon$  **do:**

**Step 2-1:** Compute the scaled version of the estimated Hessian matrix as:

$$\begin{aligned} \frac{nh^2}{c_{h,q}(L)} \mathcal{H} \hat{f}_h(\hat{\mathbf{x}}^{(t)}) &= \left[ \mathbf{I}_{q+1} - \hat{\mathbf{x}}^{(t)} (\hat{\mathbf{x}}^{(t)})^T \right] \left[ \frac{1}{h^2} \sum_{i=1}^n \mathbf{X}_i \mathbf{X}_i^T \cdot L'' \left( \frac{1 - \mathbf{X}_i^T \hat{\mathbf{x}}^{(t)}}{h^2} \right) \right. \\ &\quad \left. + \sum_{i=1}^n \mathbf{X}_i^T \hat{\mathbf{x}}^{(t)} \mathbf{I}_{q+1} \cdot L' \left( \frac{1 - \mathbf{X}_i^T \hat{\mathbf{x}}^{(t)}}{h^2} \right) \right] \left[ \mathbf{I}_{q+1} - \hat{\mathbf{x}}^{(t)} (\hat{\mathbf{x}}^{(t)})^T \right]. \end{aligned}$$

**Step 2-2:** Perform the spectral decomposition on  $\frac{nh^2}{c_{h,q}(L)} \mathcal{H} \hat{f}_h(\hat{\mathbf{x}}^{(t)})$  and compute  $\hat{V}_d(\hat{\mathbf{x}}^{(t)}) = [\hat{\mathbf{v}}_{d+1}(\hat{\mathbf{x}}^{(t)}), \dots, \hat{\mathbf{v}}_q(\hat{\mathbf{x}}^{(t)})]$ , whose columns are orthonormal eigenvectors corresponding to the smallest  $q - d$  eigenvalues inside the tangent space  $T_{\hat{\mathbf{x}}^{(t)}}$ .

**Step 2-3:** Update  $\hat{\mathbf{x}}^{(t+1)} \leftarrow \hat{\mathbf{x}}^{(t)} + \hat{V}_d(\hat{\mathbf{x}}^{(t)}) \hat{V}_d(\hat{\mathbf{x}}^{(t)})^T \left[ \frac{\sum_{i=1}^n \mathbf{X}_i L' \left( \frac{1 - \mathbf{X}_i^T \hat{\mathbf{x}}^{(t)}}{h^2} \right)}{\sum_{i=1}^n \mathbf{X}_i L' \left( \frac{1 - \mathbf{X}_i^T \hat{\mathbf{x}}^{(t)}}{h^2} \right)} \right]$ .

**Step 2-4:** Standardize  $\hat{\mathbf{x}}^{(t+1)}$  as  $\hat{\mathbf{x}}^{(t+1)} \leftarrow \frac{\hat{\mathbf{x}}^{(t+1)}}{\|\hat{\mathbf{x}}^{(t+1)}\|_2}$ .

**end while**

**Output:** An estimated directional  $d$ -ridge  $\hat{R}_d$  represented by the collection of resulting points.

---

## APPENDIX B: LIMITATIONS OF EUCLIDEAN KDE IN HANDLING DIRECTIONAL DATA

In this section, we demonstrate with examples and simulation studies that it is inadequate to analyze directional data with Euclidean KDE (cf. Equation (2) in the main paper) and SCMS algorithm (Algorithm 1). Consider a directional data sample  $\mathbf{X}_1, \dots, \mathbf{X}_n \in \Omega_2 \subset \mathbb{R}^{q+1}$  generated from a directional density  $f$  on  $\Omega_2$ . The random observations  $\mathbf{X}_1, \dots, \mathbf{X}_n$  on  $\Omega_2$  can also be represented by their angular coordinates  $\mathbf{Y}_1, \dots, \mathbf{Y}_n$ , *i.e.*, longitudes  $Y_{i,1}$  and latitudes  $Y_{i,2}$ , where  $\mathbf{Y}_i = (Y_{i,1}, Y_{i,2}) \in [-\pi, \pi) \times [-\frac{\pi}{2}, \frac{\pi}{2})$ .

**B.1. Case I: Density Estimation.** As the angular coordinates  $\{\mathbf{Y}_1, \dots, \mathbf{Y}_n\}$  of the directional dataset  $\{\mathbf{X}_1, \dots, \mathbf{X}_n\} \subset \Omega_q$  have their ranges in a subset  $[-\pi, \pi) \times [-\frac{\pi}{2}, \frac{\pi}{2})$  of the flat Euclidean space  $\mathbb{R}^2$ , it is tempting to apply the Euclidean KDE on  $\{\mathbf{Y}_1, \dots, \mathbf{Y}_n\}$  to construct a density estimator as:

$$\hat{p}_n(\mathbf{y}) = \frac{1}{nh^2} \sum_{i=1}^n K\left(\frac{\mathbf{y} - \mathbf{Y}_i}{h}\right) = \begin{cases} \frac{c_{k,2}}{nh^2} \sum_{i=1}^n k\left(\left\|\frac{\mathbf{y} - \mathbf{Y}_i}{h}\right\|_2\right) := \hat{p}_n^{(1)}(\mathbf{y}), \\ \frac{1}{nh^2} \sum_{i=1}^n K_1\left(\frac{y_1 - Y_{i,1}}{h}\right) \cdot K_2\left(\frac{y_2 - Y_{i,2}}{h}\right) := \hat{p}_n^{(2)}(\mathbf{y}), \end{cases} \quad (44)$$

where  $\hat{p}_n^{(1)}$  uses a radial symmetric kernel with profile  $k$ , and  $\hat{p}_n^{(2)}$  leverages a product kernel. However, the Euclidean KDE  $\hat{p}_n$  in (44) (either  $\hat{p}_n^{(1)}$  or  $\hat{p}_n^{(2)}$ ) exhibits two potential drawbacks of dealing with directional data.

- First,  $\hat{p}_n(\mathbf{y})$  in (44) is an estimator of the directional density  $f$  under its angular representation  $p_f : [-\pi, \pi) \times [-\frac{\pi}{2}, \frac{\pi}{2}) \rightarrow \mathbb{R}$ , which is  $2\pi$ -periodic in its first coordinate and  $\pi$ -periodic in its second coordinate. Then, the bias of  $\hat{p}_n(\mathbf{y})$ , namely  $\mathbb{E}[\hat{p}_n(\mathbf{y})] - p_f(\mathbf{y})$ , equals to  $\frac{h^2}{2} C_K^2 \Delta p_f(\mathbf{y}) + o(h^2)$ , where  $C_K^2 = \int_{\mathbb{R}^2} \|\mathbf{y}\|_2^2 K(\mathbf{y}) d\mathbf{y}$  and  $\Delta p_f = \frac{\partial^2 p_f}{\partial y_1^2} + \frac{\partial^2 p_f}{\partial y_2^2}$  is the Laplacian of  $p_f$  (Chen, 2017). However, the second-order partial derivative  $\frac{\partial^2 p_f}{\partial y_1^2}$  along the lines of constant latitude (or parallels) would tend to infinity as we approach the north and south poles, given that the first-order partial derivative  $\frac{\partial p_f}{\partial y_1}$  is bounded. One method to justify this phenomenon is that the curvatures of these parallels, which are equivalent to the reciprocals of their radii, tend to infinity as these radii shrink. (Recall that the curvature of a function  $y = g(x)$  is defined as  $\kappa := \frac{|g''|}{(1+g'^2)^{\frac{3}{2}}}$ .) Therefore, applying (44) to estimate the angular representation  $p_f$  of the directional density  $f$  will produce high bias as the estimator  $\hat{p}_n$  approaches the high-latitude regions (around the north and south poles); see also Panel (c) of Figure 4.

- Second, the Euclidean KDE  $\hat{p}_n$  applied on a directional dataset leverages the Euclidean distances between query points and observations with their angular coordinates  $\{\mathbf{Y}_1, \dots, \mathbf{Y}_n\} \subset [-\pi, \pi) \times [-\frac{\pi}{2}, \frac{\pi}{2})$  to construct the density estimates, instead of using the (intrinsic) geodesic distances. As a result, some observations that have dramatically different geodesic distances to density query points can have the same density contributions in  $\hat{p}_n$ , as illustrated in Example 1.

**EXAMPLE 1.** Suppose that we want to estimate the density values at  $\mathbf{y}_1 = (0, 0)$  and  $\mathbf{y}_2 = (0, \frac{\pi}{2} - \epsilon)$ , where  $\epsilon > 0$  is of a small value. Consider a random sample consists of only two observations  $\mathbf{Y}_1 = (\frac{\pi}{2}, 0)$  and  $\mathbf{Y}_2 = (\frac{\pi}{2}, \frac{\pi}{2} - \epsilon)$ . If we use the Euclidean distance, the distance between  $(\mathbf{y}_1, \mathbf{Y}_1)$  and the distance between  $(\mathbf{y}_2, \mathbf{Y}_2)$  are the same. Nevertheless, their geodesic distances are very different; see Figure 3 for a graphical illustration. Therefore, we use Euclidean KDE  $\hat{p}_n$ , the contribution of  $\mathbf{Y}_1$  to  $\mathbf{y}_1$  will be the same as the contribution of  $\mathbf{Y}_2$  to  $\mathbf{y}_2$ , which leads to a severely biased density estimate.

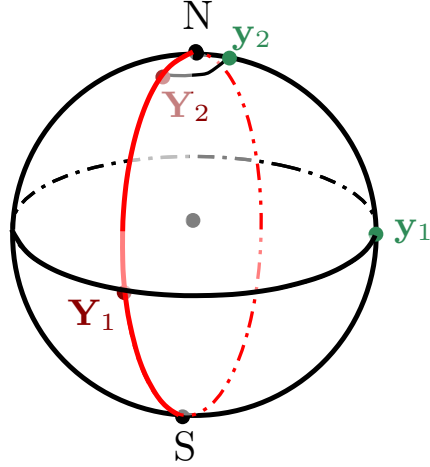


Fig 3: Graphical illustration of geodesic distances between  $y_1$  and  $Y_1$  as well as  $y_2$  and  $Y_2$ .

**B.2. Case II: Ridge-Finding Problem.** We consider a simulated example of identifying a density ridge via the Euclidean SCMS algorithm (Algorithm 1) and our proposed directional SCMS algorithm (Algorithm 2). We generate 1000 data points  $\{\mathbf{X}_1, \dots, \mathbf{X}_{1000}\}$  uniformly from a great circle connecting the north and south poles of  $\Omega_2$  with some i.i.d. additive Gaussian noises  $N(0, 0.2^2)$  to their Cartesian coordinates. Then, all the simulated points will be standardized back to  $\Omega_2$  via  $L_2$  normalization. The angular coordinates of the simulated points are denoted by  $\{\mathbf{Y}_1, \dots, \mathbf{Y}_{1000}\}$  accordingly. Figure 4 presents the result of applying both the Euclidean SCMS (with the Gaussian kernel) and directional SCMS (with the von Mises kernel) algorithms to our simulated dataset. As shown in the panel (b) of Figure 4, the Euclidean SCMS algorithm exhibits high bias in estimating the true circular structure near two poles of  $\Omega_2$ , while our directional SCMS algorithm is able to seek out the true circular structure under negligible errors. The density plot in the panel (c) of Figure 4 also explains the chaotic behaviors of the Euclidean KDE in high-latitude regions.

Other potential issues of analyzing directional data with Euclidean KDEs and ignoring the curvature of  $\Omega_q$  can be found in Chrisman (2017). In summary, it is highly inadequate to apply the Euclidean KDE and SCMS algorithm to handle directional data, which calls for the needs to introduce the directional KDE (5) and propose a well-designed SCMS algorithm for analyzing directional data.

## APPENDIX C: EXPERIMENTS

In this section we validate our linear convergence results of both Euclidean and directional SCMS algorithms on some simulated datasets. Then, we apply these two algorithms to a real-world earthquake dataset in order to identify its density ridges and compare the estimated ridges with boundaries of tectonic plates and fault lines, on which earthquakes are known to happen frequently.

We leverage the Gaussian kernel profile  $k_N(x) = \exp\left(-\frac{x}{2}\right)$  in the Euclidean SCMS algorithm, while the von Mises kernel  $L(r) = e^{-r}$  is applied to the directional SCMS algorithm. In addition, the logarithms of the estimated densities are utilized in our actual implementations (Step 2 in Algorithms 1 and 2) of Euclidean and directional SCMS algorithms because of two advantages. First, using the log-density in the Euclidean SCMS algorithm leads to a faster convergence process (Ghassabeh et al., 2013). The same phenomenon is observed in the directional SCMS iteration, though we do not report here. Second, estimating a hidden manifold with a density ridge defined by a log-density stabilizes the valid region for a

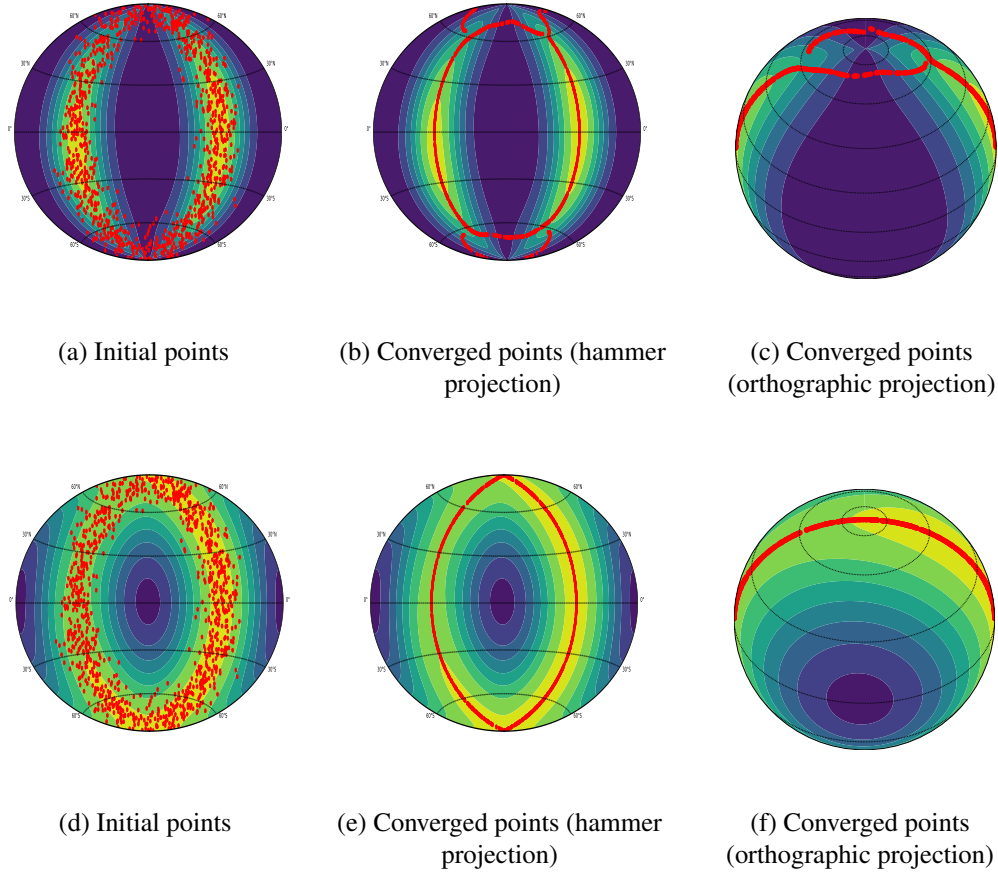


Fig 4: Euclidean and directional SCMS algorithm performed on the simulated dataset. **Panels (a)-(c):** Outcomes of Euclidean SCMS algorithms with the contour plot for the Euclidean KDE. **Panels (d)-(f):** Outcomes of directional SCMS algorithms with the contour plot for the directional KDE. **Panels (a)-(b) and (d)-(e)** are shown in the view of Hammer projections (page 160 in [Snyder et al. \(1989\)](#)), while **Panels (c) and (f)** are presented under the orthographic projections.

well-defined ridge compared to the corresponding ridge defined by the original density; see Theorem 7 (Surrogate theorem) in [Genovese et al. \(2014\)](#).

Unless stated otherwise, we set the default bandwidth parameter of the Euclidean SCMS algorithm to the normal reference rule in [Chacón et al. \(2011\)](#); [Chen et al. \(2016\)](#), which is

$$(45) \quad h_{\text{NR}} = \bar{S}_n \times \left( \frac{4}{D+4} \right)^{\frac{1}{D+6}} n^{-\frac{1}{D+6}}, \quad \bar{S}_n = \frac{1}{D} \sum_{j=1}^D S_{n,j},$$

where  $S_{n,j}$  is the sample standard deviation along  $j$ -th coordinate and  $D$  is the (Euclidean) dimension of the data in  $\mathbb{R}^D$ . The default bandwidth parameter of the directional SCMS algorithm is selected via the rule of thumb in Proposition 2 of [García-Portugués \(2013\)](#), in which the estimated concentration parameter is given by (4.4) in [Banerjee et al. \(2005\)](#). That



is,

$$(46) \quad h_{\text{ROT}} = \left[ \frac{4\pi^{\frac{1}{2}} \mathcal{I}_{\frac{q-1}{2}}(\hat{\nu})^2}{\hat{\nu}^{\frac{q+1}{2}} \left[ 2q \cdot \mathcal{I}_{\frac{q+1}{2}}(2\hat{\nu}) + (q+2)\hat{\nu} \cdot \mathcal{I}_{\frac{q+3}{2}}(2\hat{\nu}) \right] n} \right]^{\frac{1}{q+4}}, \quad \hat{\nu} = \frac{\bar{R}(q+1-\bar{R})}{1-\bar{R}^2},$$

where  $\bar{R} = \frac{\|\sum_{i=1}^n \mathbf{X}_i\|_2}{n}$  given the directional dataset  $\{\mathbf{X}_1, \dots, \mathbf{X}_n\} \subset \Omega_q \subset \mathbb{R}^{q+1}$  and we recall that  $\mathcal{I}_\alpha(\nu)$  is the modified Bessel function of the first kind of order  $\nu$ . The tolerance level is always set to be  $\epsilon = 10^{-9}$  for any SCMS algorithm.

**C.1. Simulation Study on Euclidean SCMS Algorithm.** To evaluate the algorithmic rate of convergence of the Euclidean SCMS algorithm (Algorithm 1), we randomly draw 1000 data points from a Gaussian mixture model with density  $0.4 \cdot N(\boldsymbol{\mu}_1, \Sigma_1) + 0.6 \cdot N(\boldsymbol{\mu}_2, \Sigma_2)$ , where  $\boldsymbol{\mu}_1 = -\boldsymbol{\mu}_2 = (1, 1)^T$ ,  $\Sigma_1 = \text{Diag}(\frac{1}{4}, \frac{1}{4})$ , and  $\Sigma_2 = \begin{pmatrix} \frac{1}{4} & \frac{1}{4} \\ \frac{1}{4} & \frac{1}{4} \end{pmatrix}$ . Another simulated dataset consists of 1000 data points randomly generated from an upper half circle with radius 2 and i.i.d. Gaussian noises  $N(0, 0.3^2)$ . When applying Algorithm 1 with the estimated log-density on these two simulated datasets, we choose each set of initial mesh points as the simulated dataset itself and remove those initial points whose density values are below 25% of the maximum density from each set of mesh points in order to obtain a cleaner ridge structure.

Figure 5 presents Euclidean KDE plots, estimated density ridges from the Euclidean SCMS algorithm, and their corresponding (linear) convergence plots on the two simulated datasets. The linear trends of those plots in the second and third columns of Figure 5 empirically demonstrate the correctness of our Theorem 5 and its related discussion on the linear convergence of the Euclidean SCMS algorithm.

**C.2. Simulation Study on Directional SCMS Algorithm.** Analogous to our simulation study for the linear convergence of the Euclidean SCMS algorithm, we verify the linear convergence of our directional SCMS algorithm (Algorithm 2) on two different simulated datasets. One of them comprises 1000 data points randomly generated from a vMF mixture model  $0.4 \cdot \text{vMF}(\boldsymbol{\mu}_1, \nu_1) + 0.6 \cdot \text{vMF}(\boldsymbol{\mu}_2, \nu_2)$  with  $\boldsymbol{\mu}_1 = (0, 0, 1)^T \in \Omega_2 \subset \mathbb{R}^3$ ,  $\boldsymbol{\mu}_2 = (1, 0, 0)^T \in \Omega_2 \subset \mathbb{R}^3$ , and  $\nu_1 = \nu_2 = 10$ . The other simulated dataset is identical to the example in the right panel of Figure 1 in the main paper as well as the underlying dataset in Figure 4, which consists of 1000 random sampled points from a circle connecting two poles on  $\Omega_2$  with i.i.d. additive Gaussian noises  $N(0, 0.2^2)$  to their Cartesian coordinates and additional  $L_2$  normalization onto  $\Omega_2$ . In our implementation of Algorithm 2 with the directional log-density on the two simulated datasets, we also set each initial mesh as the dataset and remove those points whose density values are below 10% of the maximal density value from each set of mesh points.

Figure 6 shows the directional KDE plots, estimated density ridges on  $\Omega_2$  from the directional SCMS algorithm, and their associated (linear) convergence plots on the aforementioned simulated datasets. Those linear decreasing trends in the convergence plots, possibly after several pilot iterations, illustrate the locally linear convergence of the directional SCMS algorithm that we proved in Theorem 10 and its subsequent discussion. Note that those minor perturbations at the tails of some linear convergence plots in Figure 6 are due to precision errors.

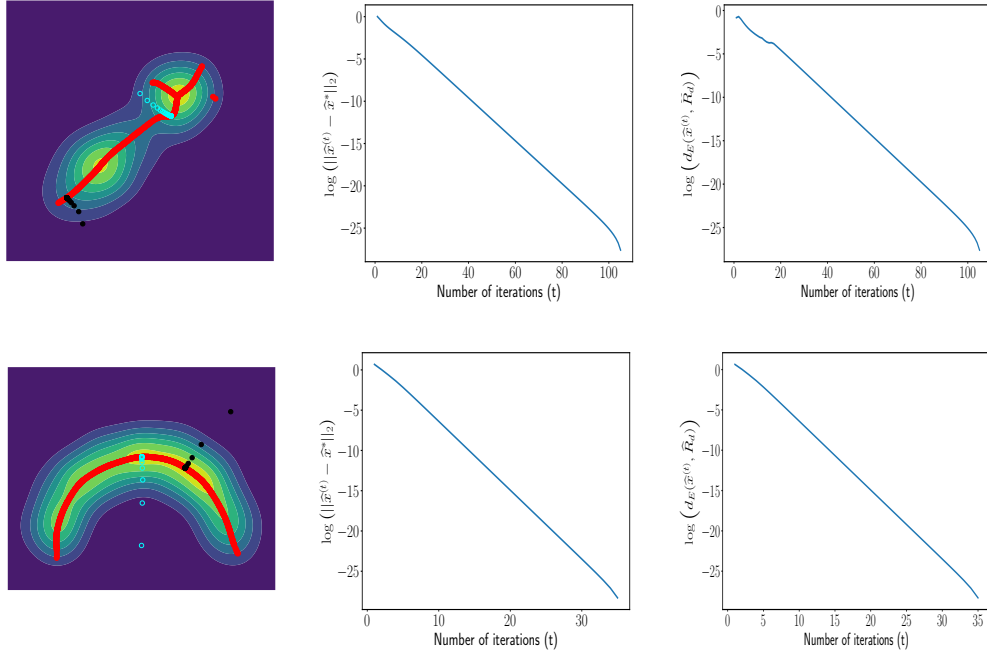


Fig 5: Euclidean SCMS algorithm performed on two simulated datasets and their (linear) convergence plots. Horizontally, the first row displays the results of the simulated Gaussian mixture dataset while the second row presents the results of the half circle simulated dataset. Vertically, the first column includes plots with Euclidean KDE, estimated ridges, and trajectories of SCMS sequences from two (randomly) chosen initial points. The second and third columns present the (linear) convergence plots for the log-distances of points in the highlighted sequences (indicated by hollow cyan points) to their limiting points or estimated ridges.

**C.3. Density Ridges on Earthquake Data.** It is well-known that earthquakes on Earth tend to strike more frequently along the boundaries of tectonic plates and fault lines (*i.e.*, sections of a plate or two plates are moving in different directions); see Panel (c) in Figure 7 and Subarya et al. (2006); Harris (2017) for more details. We analyze earthquakes with magnitudes of 2.5+ occurring between 2020-10-01 00:00:00 UTC and 2021-03-31 23:59:59 UTC, which can be obtained from the Earthquake Catalog (<https://earthquake.usgs.gov/earthquakes/search/>) of the United States Geological Survey. The dataset contains 15049 earthquakes worldwide in this half-year period.

The normal reference rule (45) leads to  $h_{NR} \approx 16.0035$  and the rule of thumb (46) yields  $h_{ROT} \approx 0.1584$  under the earthquake dataset. However, it is known that these methods tend to oversmooth the data, so we decrease the bandwidths for Euclidean and directional SCMS algorithm to  $h_{Eu} = 7.0$  and  $h_{Dir} = 0.1$ , respectively. We generate 5000 points uniformly on the sphere  $\Omega_2$  as the initial mesh points.

Figure 7 displays the density ridges identified by Euclidean and directional SCMS algorithms on the earthquake dataset, both of which coincide with the boundaries of tectonic plates to a large extent. Some extra ridge structures inside a tectonic plate (*e.g.*, the African plate) are also known as the fault lines (Craig et al., 2011). Note that both Euclidean and directional SCMS do not show much difference because most of the observed earthquakes are in the low latitude region (where most human beings live). Yet, the two sets of ridges do show some differences in the high latitude regions.

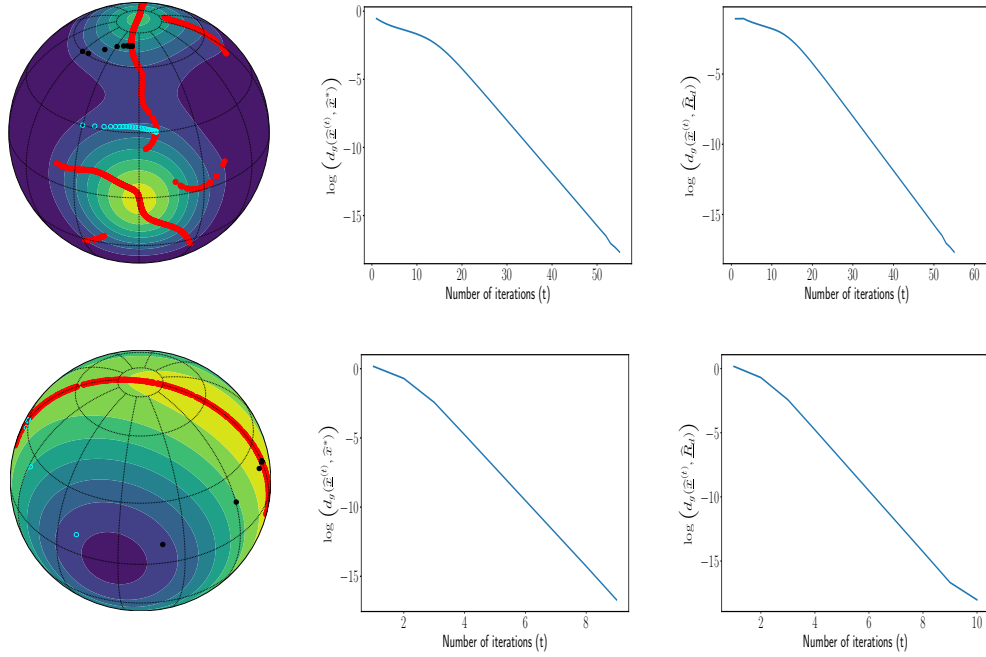


Fig 6: Directional SCMS algorithm performed on two simulated datasets and their (linear) convergence plots. Horizontally, the first row displays the results on the simulated vMF mixture dataset while the second row presents the results on the circular simulated dataset on  $\Omega_2$ . Vertically, the first column includes plots with directional KDE, estimated ridges, and trajectories of directional SCMS sequences from two (randomly) chosen initial points on  $\Omega_2$ . The second and third columns present the (linear) convergence plots for the log-distances of points in the highlighted sequences (indicated by hollow cyan points) to their limiting points or estimated ridges on  $\Omega_2$ .

#### APPENDIX D: NORMAL SPACE OF EUCLIDEAN DENSITY RIDGE

As we will refer to conditions (A1-3) frequently in the next two sections, we restate them here:

- **(A1) (Differentiability)** We assume that  $p$  is at least four times differentiable with bounded partial derivatives up to the fourth order for every  $\mathbf{x} \in \mathbb{R}^D$ .
- **(A2) (Eigengap)** We assume that there exist constants  $\rho > 0$  and  $\beta_0 > 0$  such that  $\lambda_{d+1}(\mathbf{y}) \leq -\beta_0$  and  $\lambda_d(\mathbf{y}) - \lambda_{d+1}(\mathbf{y}) \geq \beta_0$  for any  $\mathbf{y} \in R_d \oplus \rho$ .
- **(A3) (Path Smoothness)** Under the same  $\rho, \beta_0 > 0$  in (A2), we assume that there exists another constant  $\beta_1 \in (0, \beta_0)$  such that

$$D^{\frac{3}{2}} \left\| U_d^\perp(\mathbf{y}) \nabla p(\mathbf{y}) \right\|_2 \left\| \nabla^3 p(\mathbf{y}) \right\|_{\max} \leq \frac{\beta_0^2}{4},$$

$$d \cdot D^{\frac{3}{2}} \left\| \nabla p(\mathbf{x}) \right\|_2 \left\| \nabla^3 p(\mathbf{x}) \right\|_{\max} \leq \beta_0(\beta_0 - \beta_1)$$

for all  $\mathbf{y} \in R_d \oplus \rho$  and  $\mathbf{x} \in R_d$ .

Given a matrix-valued function  $B : \mathbb{R}^D \rightarrow \mathbb{R}^{m \times n}$ , its gradient  $\nabla B(\mathbf{x})$  will be an  $m \times n \times D$  array defined as  $[B(\mathbf{x})]_{ijk} = \frac{\partial}{\partial x_k} B(\mathbf{x})_{ij}$ . The derivative of  $B$  in the directional of a vector

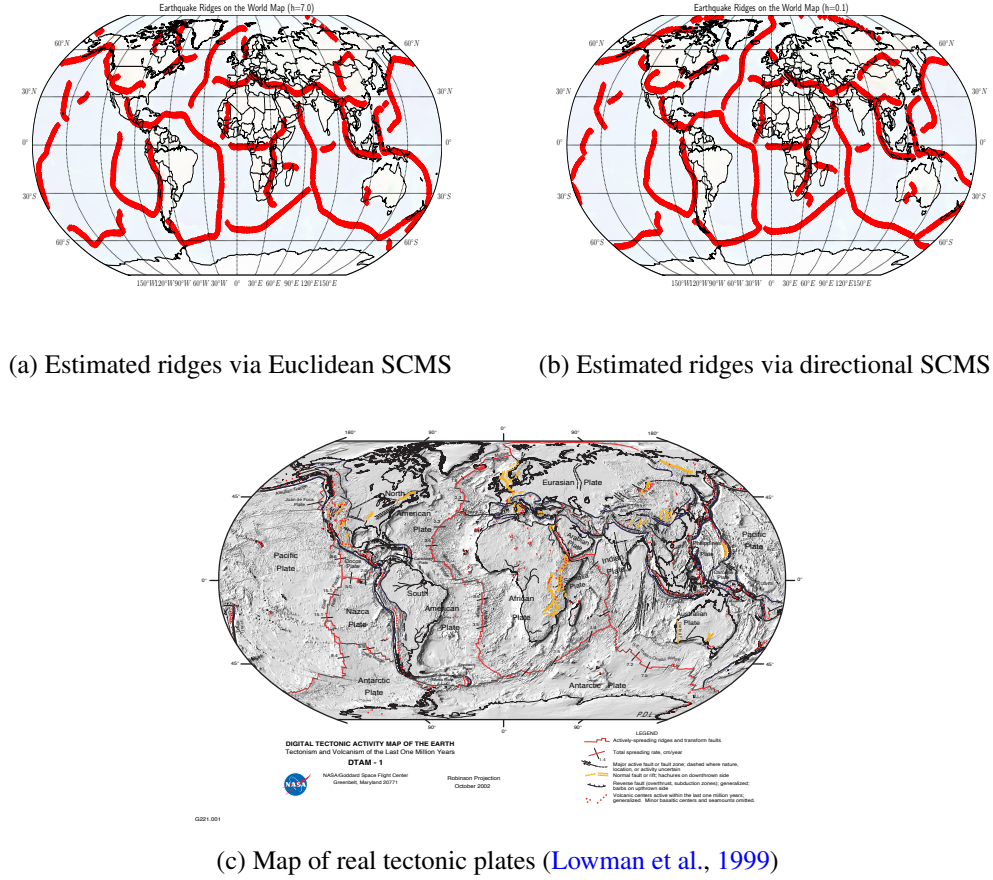


Fig 7: Comparisons between density ridges obtained by the Euclidean SCMS algorithm on angular coordinates and the directional SCMS algorithm on Cartesian coordinates from the earthquake dataset

$z \in \mathbb{R}^D$  is defined as

$$B'(\mathbf{x}; \mathbf{z}) \equiv \lim_{\epsilon \rightarrow 0} \frac{B(\mathbf{x} + \epsilon \mathbf{z}) - B(\mathbf{x})}{\epsilon} = \nabla B(\mathbf{x}) \mathbf{z}.$$

When the matrix  $A(\mathbf{x}) = \nabla \nabla f(\mathbf{x}) \in \mathbb{R}^{D \times D}$ , we will use the notation  $\nabla \nabla f'(\mathbf{x}; \mathbf{z}) = \nabla^3 f(\mathbf{x}) \mathbf{z} \equiv \mathbf{z}^T \nabla^3 f(\mathbf{x})$  interchangeably to denote its directional derivative along  $\mathbf{z}$ .

Recall that an order- $d$  ridge of a density  $p$  in  $\mathbb{R}^D$  is the collection of points defined as:

$$R_d = \{\mathbf{x} \in \mathbb{R}^D : G_d(\mathbf{x}) = \mathbf{0}, \lambda_{d+1}(\mathbf{x}) < 0\} = \{\mathbf{x} \in \mathbb{R}^D : V_d(\mathbf{x})^T \nabla p(\mathbf{x}) = \mathbf{0}, \lambda_{d+1}(\mathbf{x}) < 0\}.$$

Lemma 11 below shows that under conditions (A1-3), the Jacobian matrix  $\nabla [V_d(\mathbf{x})^T \nabla p(\mathbf{x})]$  has rank  $D - d$  at every point of  $R_d$ , and  $R_d$  is a  $d$ -dimensional manifold by the implicit function theorem (Rudin, 1976). Consequently, the row space of  $\nabla [V_d(\mathbf{x})^T \nabla p(\mathbf{x})] \in \mathbb{R}^{(D-d) \times D}$  spans the normal space to  $R_d$ .

If we define  $M(\mathbf{x}) = \nabla [V_d(\mathbf{x})^T \nabla p(\mathbf{x})]^T = [\mathbf{m}_{d+1}(\mathbf{x}), \dots, \mathbf{m}_D(\mathbf{x})] \in \mathbb{R}^{D \times (D-d)}$ , the derivation in pages 60-63 of Eberly (1996) shows that

$$(47) \quad \mathbf{m}_k(\mathbf{x}) = \left[ \lambda_k(\mathbf{x}) \mathbf{I}_D + \sum_{i=1}^d \frac{\mathbf{v}_i(\mathbf{x})^T \nabla p(\mathbf{x})}{\lambda_k(\mathbf{x}) - \lambda_i(\mathbf{x})} \cdot \mathbf{v}_i(\mathbf{x})^T \nabla^3 p(\mathbf{x}) \right] \mathbf{v}_k(\mathbf{x})$$

for  $k = d + 1, \dots, D$ , and the column space of  $M(\mathbf{x})$  spans the normal space to  $R_d$ . Let

$$\begin{aligned}\Lambda_0(\mathbf{x}) &= \text{Diag}[\lambda_{d+1}(\mathbf{x}), \dots, \lambda_D(\mathbf{x})] \\ \Lambda_i(\mathbf{x}) &= \text{Diag}\left[\frac{1}{\lambda_{d+1}(\mathbf{x}) - \lambda_i(\mathbf{x})}, \dots, \frac{1}{\lambda_D(\mathbf{x}) - \lambda_i(\mathbf{x})}\right] \\ T_i(\mathbf{x}) &= [\mathbf{v}_i(\mathbf{x})^T \nabla p(\mathbf{x})] \cdot \mathbf{v}_i(\mathbf{x})^T \nabla^3 p(\mathbf{x})\end{aligned}$$

for  $i = 1, \dots, d$ . Then,

$$(48) \quad M(\mathbf{x}) = V_d(\mathbf{x})\Lambda_0(\mathbf{x}) + \sum_{i=1}^d T_i(\mathbf{x})V_d(\mathbf{x})\Lambda_i(\mathbf{x}).$$

However, the columns of  $M(\mathbf{x})$  are not orthonormal. Thus, we leverage the orthonormalization in [Chen et al. \(2015\)](#) to construct  $N(\mathbf{x})$  whose columns are orthonormal and span the same column space as  $M(\mathbf{x})$  in the following steps. Under the condition that  $M(\mathbf{x}) = \nabla [V_d(\mathbf{x})^T \nabla p(\mathbf{x})]^T$  has full rank  $D - d$  at every point  $\mathbf{x} \in R_d$  (see Lemma 11),  $M(\mathbf{x})^T M(\mathbf{x})$  is positive definite, and we perform the Cholesky decomposition on it, that is,

$$(49) \quad M(\mathbf{x})^T M(\mathbf{x}) = J(\mathbf{x})J(\mathbf{x})^T,$$

where  $J(\mathbf{x}) \in \mathbb{R}^{(D-d) \times (D-d)}$  is a lower triangular matrix whose diagonal elements are positive. We then define

$$(50) \quad N(\mathbf{x}) = M(\mathbf{x}) [J(\mathbf{x})^T]^{-1}.$$

Notice that  $M(\mathbf{x})$ ,  $N(\mathbf{x})$ ,  $J(\mathbf{x})$  intrinsically depend on the dimension  $d$  of the ridge  $R_d$ , but we do not explicate such dependency in their notations. As discussed in [Chen et al. \(2015\)](#),  $M(\mathbf{x})$  might not be unique because the eigenvalues of  $\nabla \nabla p(\mathbf{x})$  can have their multiplicities greater than 1. Any choice of linearly independent unit eigenvectors of  $\nabla \nabla p(\mathbf{x})$  fits into the above construction for  $M(\mathbf{x})$ . However, as will be shown later, this volatility of  $M(\mathbf{x})$  will not affect our results, as we only require the smoothness of  $M(\mathbf{x})^T M(\mathbf{x})$  to develop a lower bound of  $\text{reach}(R_d)$ .

LEMMA 11. Assume conditions (A1-3). Given that  $M(\mathbf{x})$  and  $N(\mathbf{x})$  are defined in (48) and (50), we have the following properties:

(a)  $N(\mathbf{x})$  and  $M(\mathbf{x})$  have the same column space. In addition,

$$N(\mathbf{x})N(\mathbf{x})^T = M(\mathbf{x}) [M(\mathbf{x})^T M(\mathbf{x})]^{-1} M(\mathbf{x})^T.$$

That is,  $N(\mathbf{x})N(\mathbf{x})^T$  is the projection matrix onto the columns of  $M(\mathbf{x})$ .

(b) The columns of  $N(\mathbf{x})$  are orthonormal to each other.

(c) For  $\mathbf{x} \in R_d$ , the column space of  $N(\mathbf{x})$  is normal to the (tangent) direction of  $R_d$  at  $\mathbf{x}$ .

(d) For all  $\mathbf{x} \in R_d$ ,  $\text{rank}(N(\mathbf{x})) = \text{rank}(M(\mathbf{x})) = D - d$ . Moreover,  $R_d$  is a  $d$ -dimensional manifold that contains neither intersections and nor endpoints. Namely,  $R_d$  is a finite union of connected and compact manifold.

(e) For  $\mathbf{x} \in R_d$ ,

$$\left\| [M(\mathbf{x})^T M(\mathbf{x})]^{-1} \right\|_2 \leq \frac{1}{\beta_1^2} \quad \text{and} \quad \left\| [J(\mathbf{x})^T]^{-1} \right\|_2 \leq \frac{1}{\beta_1}.$$

(f) When  $\|\mathbf{x} - \mathbf{y}\|_2$  is sufficiently small and  $\mathbf{x}, \mathbf{y} \in R_d \oplus \rho$ ,

$$\left\| N(\mathbf{x})N(\mathbf{x})^T - N(\mathbf{y})N(\mathbf{y})^T \right\|_{\max} \leq A_0 \left( \|p\|_{\infty}^{(3)} + \|p\|_{\infty}^{(4)} \right)^2 \|\mathbf{x} - \mathbf{y}\|_2$$

for some constant  $A_0 > 0$ .

(g) Assume that another density function  $q$  also satisfies conditions (A1-3), and  $\|p - q\|_{\infty,3}^*$  is sufficiently small. Then

$$\|N_p(\mathbf{x})N_p(\mathbf{x})^T - N_q(\mathbf{x})N_q(\mathbf{x})^T\|_{\max} \leq A_1 \cdot \|p - q\|_{\infty,3}^*$$

for some constant  $A_1 > 0$  and any  $\mathbf{x} \in R_d$ , where  $N_p(\mathbf{x})$  is the matrix defined in (50) with density  $p$ .

(h) The reach of  $R_d$  satisfies

$$\text{reach}(R_d) \geq \min \left\{ \frac{\rho}{2}, \frac{\beta_1^2}{A_2 \left( \|p\|_{\infty}^{(3)} + \|p\|_{\infty}^{(4)} \right)} \right\}$$

for some constant  $A_2 > 0$ .

Lemma 11 is extended from Lemma 2 in [Chen et al. \(2015\)](#) to handle the density ridge  $R_d$  with  $1 < d < D$ . As our conditions (A1-3) imply the imposed conditions of Lemma 2 in [Chen et al. \(2015\)](#), our proof of Lemma 11 essentially follows from their arguments with some minor modifications.

**PROOF OF LEMMA 11.** We adopt and generalize parts of the proof of Lemma 2 in [Chen et al. \(2015\)](#).

The property (a) is a natural corollary of the Cholesky decomposition:

$$N(\mathbf{x})N(\mathbf{x})^T = M(\mathbf{x}) [J(\mathbf{x})^T]^{-1} J(\mathbf{x})^{-1} M(\mathbf{x})^T = M(\mathbf{x}) [M(\mathbf{x})^T M(\mathbf{x})]^{-1} M(\mathbf{x})^T.$$

(b) Some direct calculations show that

$$\begin{aligned} N(\mathbf{x})^T N(\mathbf{x}) &= J(\mathbf{x})^{-1} M(\mathbf{x})^T M(\mathbf{x}) [J(\mathbf{x})^T]^{-1} \\ &= J(\mathbf{x})^{-1} M(\mathbf{x})^T M(\mathbf{x}) [J(\mathbf{x})^T]^{-1} J(\mathbf{x})^{-1} J(\mathbf{x}) \\ &= J(\mathbf{x})^{-1} M(\mathbf{x})^T M(\mathbf{x}) [M(\mathbf{x})^T M(\mathbf{x})]^{-1} J(\mathbf{x}) \\ &= \mathbf{I}_{D-d}. \end{aligned}$$

(c) It can be proved by the argument of Lemma 1 in [Chen et al. \(2015\)](#). Or, we define an arbitrary parametrized curve  $\gamma : (-\epsilon, \epsilon) \rightarrow \mathbb{R}^D$  lying within  $R_d$  for some  $\epsilon > 0$ . Then  $\gamma'(t)$  aligns with the tangent direction at  $\gamma(t) \in R_d$ . Since  $V_d(\gamma(t))^T \nabla p(\gamma(t)) = \mathbf{0}$ , taking the derivative gives us that

$$0 = \frac{d}{dt} [V_d(\gamma(t))^T \nabla p(\gamma(t))] = \nabla [V_d(\mathbf{x})^T \nabla p(\mathbf{x})] \cdot \gamma'(t)$$

with  $\mathbf{x} = \gamma(t)$ . Hence, by the arbitrariness of  $\gamma(t)$ , the column of  $M(\mathbf{x}) = \nabla [V_d(\mathbf{x})^T \nabla p(\mathbf{x})]^T$  is normal to the tangent direction of  $R_d$  at  $\mathbf{x}$ .

(d) We prove that the  $(D - d)$  nonzero singular values of  $M(\mathbf{x}) \in \mathbb{R}^{D \times (D-d)}$  are bounded away from 0. Recall that

$$M(\mathbf{x}) = V_d(\mathbf{x}) \Lambda_0(\mathbf{x}) + \sum_{i=1}^d T_i(\mathbf{x}) V_d(\mathbf{x}) \Lambda_i(\mathbf{x})$$



with

$$\begin{aligned}\Lambda_0(\mathbf{x}) &= \text{Diag}[\lambda_{d+1}(\mathbf{x}), \dots, \lambda_D(\mathbf{x})] \\ \Lambda_i(\mathbf{x}) &= \text{Diag}\left[\frac{1}{\lambda_{d+1}(\mathbf{x}) - \lambda_i(\mathbf{x})}, \dots, \frac{1}{\lambda_D(\mathbf{x}) - \lambda_i(\mathbf{x})}\right] \\ T_i(\mathbf{x}) &= [\mathbf{v}_i(\mathbf{x})^T \nabla p(\mathbf{x})] \cdot \mathbf{v}_i(\mathbf{x})^T \nabla^3 p(\mathbf{x})\end{aligned}$$

for  $i = 1, \dots, d$ . Under condition (A2),

$$\begin{aligned}\left\| \sum_{i=1}^d T_i(\mathbf{x}) V_d(\mathbf{x}) \Lambda_i(\mathbf{x}) \right\|_2 &\leq \sum_{i=1}^d \|T_i(\mathbf{x})\|_2 \cdot \|V_d(\mathbf{x})\|_2 \cdot \frac{1}{\beta_0} \\ &\leq \sum_{i=1}^d \left\| [\mathbf{v}_i(\mathbf{x})^T \nabla p(\mathbf{x})] \cdot \mathbf{v}_i(\mathbf{x})^T \nabla^3 p(\mathbf{x}) \right\|_2 \cdot \frac{1}{\beta_0} \quad \text{since } \|V_d(\mathbf{x})\|_2 = 1 \\ &\leq \frac{d \|\nabla p(\mathbf{x})\|_2 \cdot D^{\frac{3}{2}} \|\nabla^3 p(\mathbf{x})\|_{\max}}{\beta_0} \\ &\leq \beta_0 - \beta_1.\end{aligned}$$

It shows that all the singular values of  $\sum_{i=1}^d T_i(\mathbf{x}) V_d(\mathbf{x}) \Lambda_i(\mathbf{x})$  are less than  $\beta_0 - \beta_1$ . Moreover, under condition (A2) again, all the  $(D - d)$  nonzero singular values of  $V_d(\mathbf{x}) \Lambda_0(\mathbf{x})$  are greater than  $\beta_0$ . By Theorem 3.3.16 in [Horn and Johnson \(1991\)](#), we know that all the  $(D - d)$  nonzero singular values of  $M(\mathbf{x})$  are greater than  $\beta_0 - (\beta_0 - \beta_1) = \beta_1 > 0$ . Therefore,  $\text{rank}(M(\mathbf{x})) = \text{rank}(N(\mathbf{x})) = D - d$ . The rest of the proof follows directly from Claim 4 in [Chen et al. \(2015\)](#).

(e) By the proof of (d), we already know that all the  $(D - d)$  nonzero singular values of  $M(\mathbf{x})$  are greater than  $\beta_1 > 0$ . Thus,  $\left\| [M(\mathbf{x})^T M(\mathbf{x})]^{-1} \right\|_2 \leq \frac{1}{\beta_1^2}$ , and

$$\begin{aligned}\left\| [J(\mathbf{x})^T]^{-1} \right\|_2 &= \sqrt{\frac{1}{\sigma_{\min}(J(\mathbf{x})J(\mathbf{x})^T)}} = \sqrt{\frac{1}{\sigma_{\min}(M(\mathbf{x})^T M(\mathbf{x}))}} \\ &= \sqrt{\left\| [M(\mathbf{x})^T M(\mathbf{x})]^{-1} \right\|_2} \leq \frac{1}{\beta_1},\end{aligned}$$

where  $\sigma_{\min}(A)$  is the smallest singular value of matrix  $A$ .

Finally, the proofs of properties (f), (g), and (h) are essentially the same as the corresponding claims in [Chen et al. \(2015\)](#). We thus omitted them.  $\square$

## APPENDIX E: PROOFS OF LEMMA 2, LEMMA 4, AND THEOREM 5

LEMMA 2. Assume (E1) and that the underlying density  $p$  is differentiable. Then, the convergence rate of  $\hat{g}_n(\mathbf{x})$  is

$$\begin{aligned}h^2 \hat{g}_n(\mathbf{x}) &= -2c_{k,D} \cdot p(\mathbf{x}) \int_{\mathbb{R}^D} k'(\|\mathbf{u}\|_2^2) d\mathbf{u} + O(h^2) + O_P\left(\sqrt{\frac{1}{nh^D}}\right) \\ &= O(1) + O(h^2) + O_P\left(\sqrt{\frac{1}{nh^D}}\right)\end{aligned}$$

for any  $\mathbf{x} \in \mathbb{R}^D$  as  $nh^D \rightarrow \infty$  and  $h \rightarrow 0$ .

Another interpretation of Lemma 2 is that  $\widehat{g}_n(\mathbf{x})$  diverges to infinity at the rate  $O\left(n^{\frac{2}{D+4}}\right) + O_P\left(n^{-\frac{2}{D+4}}\right)$  if we select the bandwidth  $h_{\text{opt}} \asymp O\left(n^{-\frac{1}{D+4}}\right)$  to minimize the asymptotic mean integrated square error (Chen, 2017), where “ $\asymp$ ” stands for the asymptotic equivalence.

PROOF OF LEMMA 2. Note that

$$(51) \quad \widehat{g}_n(\mathbf{x}) = \mathbb{E}[\widehat{g}_n(\mathbf{x})] + \widehat{g}_n(\mathbf{x}) - \mathbb{E}[\widehat{g}_n(\mathbf{x})].$$

Given the differentiability of  $p$ , the expectation of  $\widehat{g}_n(\mathbf{x})$  is given by

$$\begin{aligned} \mathbb{E}[\widehat{g}_n(\mathbf{x})] &= \frac{2c_{k,D}}{h^{D+2}} \int_{\mathbb{R}^D} -k' \left( \left\| \frac{\mathbf{x} - \mathbf{y}}{h} \right\|_2^2 \right) \cdot p(\mathbf{y}) d\mathbf{y} \\ &= \frac{2c_{k,D}}{h^2} \int_{\mathbb{R}^D} -k' \left( \|\mathbf{u}\|_2^2 \right) \cdot p(\mathbf{x} + h\mathbf{u}) d\mathbf{u} \quad \text{by } \mathbf{u} = \frac{\mathbf{y} - \mathbf{x}}{h} \\ &= \frac{2c_{k,D}}{h^2} \int_{\mathbb{R}^D} -k' \left( \|\mathbf{u}\|_2^2 \right) [p(\mathbf{x}) + h\nabla p(\mathbf{x})^T \mathbf{u} + O(h^2)] d\mathbf{u} \\ &= \frac{2c_{k,D} \cdot p(\mathbf{x})}{h^2} \int_{\mathbb{R}^D} -k' \left( \|\mathbf{u}\|_2^2 \right) d\mathbf{u} + O(1). \end{aligned}$$

By condition (E1), the dominating constant  $-2c_{k,D} \cdot p(\mathbf{x}) \int_{\mathbb{R}^D} k' \left( \|\mathbf{u}\|_2^2 \right) d\mathbf{u}$  is finite and therefore,

$$(52) \quad \mathbb{E}[h^2 \widehat{g}_n(\mathbf{x})] = -2c_{k,D} \cdot p(\mathbf{x}) \int_{\mathbb{R}^D} k' \left( \|\mathbf{u}\|_2^2 \right) d\mathbf{u} + O(h^2) = O(1) + O(h^2).$$

In addition, we calculate the variance of  $\widehat{g}_n(\mathbf{x})$  as

$$\begin{aligned} \text{Var}[\widehat{g}_n(\mathbf{x})] &= \frac{4c_{k,D}^2}{nh^{2D+4}} \cdot \text{Var} \left[ k' \left( \left\| \frac{\mathbf{x} - \mathbf{X}_1}{h} \right\|_2^2 \right) \right] \\ &= \frac{4c_{k,D}^2}{nh^{2D+4}} \int_{\mathbb{R}^D} k' \left( \left\| \frac{\mathbf{x} - \mathbf{y}}{h} \right\|_2^2 \right)^2 p(\mathbf{y}) d\mathbf{y} - \frac{1}{n} \{ \mathbb{E}[\widehat{g}_n(\mathbf{x})] \}^2 \\ &= \frac{4c_{k,D}^2}{nh^{D+4}} \int_{\mathbb{R}^D} k' \left( \|\mathbf{u}\|_2^2 \right)^2 \cdot p(\mathbf{x} + h\mathbf{u}) d\mathbf{u} - \frac{1}{n} [O(h^{-2}) + O(1)]^2 \quad \text{by } \mathbf{u} = \frac{\mathbf{y} - \mathbf{x}}{h} \\ &= \frac{4c_{k,D}^2}{nh^{D+4}} \int_{\mathbb{R}^D} k' \left( \|\mathbf{u}\|_2^2 \right)^2 [p(\mathbf{x}) + h\nabla p(\mathbf{x})^T \mathbf{u} + O(h^2)] d\mathbf{u} + O\left(\frac{1}{nh^4}\right) \\ &= \frac{4c_{k,D}^2 \cdot p(\mathbf{x})}{nh^{D+4}} \int_{\mathbb{R}^D} k' \left( \|\mathbf{u}\|_2^2 \right)^2 d\mathbf{u} + o\left(\frac{1}{nh^{D+4}}\right), \end{aligned}$$

Again, by condition (E1), the dominating constant  $4c_{k,D}^2 \cdot p(\mathbf{x}) \int_{\mathbb{R}^D} k' \left( \|\mathbf{u}\|_2^2 \right)^2 d\mathbf{u}$  is finite. Thus, by the central limit theorem,

$$\begin{aligned}
 \widehat{g}_n(\mathbf{x}) - \mathbb{E}[\widehat{g}_n(\mathbf{x})] &= \sqrt{\text{Var}[\widehat{g}_n(\mathbf{x})]} \cdot \frac{\widehat{g}_n(\mathbf{x}) - \mathbb{E}[\widehat{g}_n(\mathbf{x})]}{\sqrt{\text{Var}[\widehat{g}_n(\mathbf{x})]}} \\
 (53) \qquad &= \sqrt{\text{Var}[\widehat{g}_n(\mathbf{x})]} \cdot \mathbf{Z}_n(\mathbf{x}) \\
 &= O_P\left(\sqrt{\frac{1}{nh^{D+4}}}\right),
 \end{aligned}$$

where  $\mathbf{Z}_n(\mathbf{x}) \xrightarrow{d} \mathcal{N}_D(\mathbf{0}, \mathbf{I}_D)$ . Combining (51), (52), and (53), we conclude that

$$\begin{aligned}
 h^2 \widehat{g}_n(\mathbf{x}) &= -2c_{k,D} \cdot p(\mathbf{x}) \int_{\mathbb{R}^D} k'(\|\mathbf{u}\|_2^2) + O(h^2) + O_P\left(\sqrt{\frac{1}{nh^D}}\right) \\
 &= O(1) + O(h^2) + O_P\left(\sqrt{\frac{1}{nh^D}}\right)
 \end{aligned}$$

for any  $\mathbf{x} \in \mathbb{R}^D$  as  $nh^D \rightarrow \infty$  and  $h \rightarrow 0$ .  $\square$

**REMARK 6.** Some previous research papers on the mean shift algorithm (Li et al., 2007; Carreira-Perpiñán, 2007; Aliyari Ghassabeh, 2015) have already justified that the algorithm converges to a local mode of the KDE  $\widehat{p}_n$  when its local modes are isolated and the algorithm starts within some small neighborhoods of these estimated local modes. It is also known that the set of true local modes is well approximated by the set of estimated modes (Chen et al., 2016). Moreover, around the local modes of the true density  $p$ , one can argue easily that  $\widehat{p}_n$  is strongly convex with a Lipschitz gradient by the uniform consistency of  $\nabla \widehat{p}_n$  and  $\nabla \nabla \widehat{p}_n$ ; see Equation (15) in the main paper. Hence, by some standard results in optimization theory (e.g., Chapter 3 in Bubeck (2015)), any gradient ascent algorithm with  $\widehat{p}_n$  converges linearly to (estimated) local modes around their neighborhoods as long as its step size is below some threshold value. Lemma 2 thus provides a probabilistic perspective on the linear convergence of the mean shift algorithm.

The following Davis-Kahan theorem (Davis and Kahan, 1970) is one of the most notable theorems in matrix perturbation theory. We present the theorem in a modified version from von Luxburg (2007); Genovese et al. (2014). Other useful variants of the Davis-Kahan theorem can be found in Yu et al. (2014).

**LEMMA 12 (Davis-Kahan).** *Let  $H$  and  $\widetilde{H}$  be two symmetric matrices in  $\mathbb{R}^{D \times D}$ , whose spectra (Definition 1.1.4 in Horn and Johnson (2012)) are  $\sigma(H)$  and  $\sigma(\widetilde{H})$ , and  $S_1 \subset \mathbb{R}$  be an interval. Denote by  $\sigma_{S_1}(H)$  the set of eigenvalues of  $H$  that are contained in  $S_1$ , and by  $V_1$  the matrix whose columns are the corresponding eigenvectors to  $\sigma_{S_1}(H)$  (more formally,  $V_1$  is the image of the spectral projection induced by  $\sigma_{S_1}(H)$ ). Denote by  $\sigma_{S_1}(\widetilde{H})$  and  $\widetilde{V}_1$  the analogous quantities for  $\widetilde{H}$ . If*

$$\delta := \inf \left\{ |\lambda - \widetilde{\lambda}| : \lambda \in \sigma_{S_1}(H), \widetilde{\lambda} \in \sigma(\widetilde{H}) \setminus \sigma_{S_1}(\widetilde{H}) \right\} > 0,$$

*then the distance  $d(V_1, \widetilde{V}_1) := \left\| \sin \Theta(V_1, \widetilde{V}_1) \right\|$  between two subspaces is bounded by*

$$d(V_1, \widetilde{V}_1) \leq \frac{\left\| H - \widetilde{H} \right\|}{\delta}$$

for any orthogonally invariant norm  $\|\cdot\|$ , such as the Frobenius norm  $\|\cdot\|_F$  and the  $L_2$ -operator norm  $\|\cdot\|_2$ , where  $\Theta(V_1, \tilde{V}_1)$  is a diagonal matrix with the ascending principal angles between the column spaces of  $V_1$  and  $\tilde{V}_1$  on the diagonal.

Note that when we take the Frobenius norm in Lemma 12,  $\left\|\sin \Theta(V_1, \tilde{V}_1)\right\|_F = \sqrt{2} \left\|V_1 V_1^T - \tilde{V}_1 \tilde{V}_1^T\right\|_F$ ; if we take the  $L_2$ -operator norm instead,  $\left\|\sin \Theta(V_1, \tilde{V}_1)\right\|_2 = \left\|V_1 V_1^T - \tilde{V}_1 \tilde{V}_1^T\right\|_2$ ; see Drmac (2000) for details.

LEMMA 4. Assume conditions (A1-3). Then, we have that for any  $\mathbf{x}^{(t)} \in R_d \oplus \rho$ ,

$$\begin{aligned} \left\|U_d^\perp(\mathbf{x}^{(t)}) \left(\mathbf{x}^* - \mathbf{x}^{(t)}\right)\right\|_2 &\leq \frac{D^{\frac{3}{2}} \left\|\nabla^3 p(\mathbf{x}^{(t)})\right\|_{\max} \left\|\mathbf{x}^* - \mathbf{x}^{(t)}\right\|_2^2}{\beta_0} + D^2 \|p\|_\infty^{(4)} \cdot \left\|\mathbf{x}^* - \mathbf{x}^{(t)}\right\|_2^3 \\ &= \frac{D^{\frac{3}{2}} \left\|\nabla^3 p(\mathbf{x}^{(t)})\right\|_{\max} \left\|\mathbf{x}^* - \mathbf{x}^{(t)}\right\|_2^2}{\beta_0} + o\left(\left\|\mathbf{x}^* - \mathbf{x}^{(t)}\right\|_2^2\right). \end{aligned}$$

PROOF OF LEMMA 4. We first decompose the vector  $\mathbf{x}^* - \mathbf{x}^{(t)}$  into an infinite sum of SCGA updates  $\mathbf{x}^{(s+1)} = \mathbf{x}^{(s)} + \eta \cdot V_d(\mathbf{x}^{(s)}) V_d(\mathbf{x}^{(s)})^T \nabla p(\mathbf{x}^{(s)})$  for  $s \geq t$  and compute that

$$\begin{aligned} \mathbf{x}^* - \mathbf{x}^{(t)} &= \sum_{s=t}^{\infty} \left(\mathbf{x}^{(s+1)} - \mathbf{x}^{(s)}\right) \\ &\stackrel{(i)}{=} \sum_{s=t}^{\infty} U_d(\mathbf{x}^{(t)}) \left(\mathbf{x}^{(s+1)} - \mathbf{x}^{(s)}\right) + \sum_{s=t}^{\infty} U_d^\perp(\mathbf{x}^{(t)}) \left(\mathbf{x}^{(s+1)} - \mathbf{x}^{(s)}\right) \\ &= U_d(\mathbf{x}^{(t)}) \left(\mathbf{x}^* - \mathbf{x}^{(t)}\right) + \sum_{s=t}^{\infty} U_d^\perp(\mathbf{x}^{(t)}) \cdot \eta V_d(\mathbf{x}^{(s)}) V_d(\mathbf{x}^{(s)})^T \nabla p(\mathbf{x}^{(s)}) \\ &\stackrel{(ii)}{=} U_d(\mathbf{x}^{(t)}) \left(\mathbf{x}^* - \mathbf{x}^{(t)}\right) \\ &\quad + \sum_{s=t}^{\infty} U_d^\perp(\mathbf{x}^{(t)}) \cdot \eta \left[ V_d(\mathbf{x}^{(s)}) V_d(\mathbf{x}^{(s)})^T - V_d(\mathbf{x}^{(t)}) V_d(\mathbf{x}^{(t)})^T \right] V_d(\mathbf{x}^{(s)}) V_d(\mathbf{x}^{(s)})^T \nabla p(\mathbf{x}^{(s)}), \end{aligned}$$

for any  $\mathbf{x}^{(t)} \in R_d \oplus \rho$ , where we use the equality  $\mathbf{I}_D = U_d(\mathbf{x}^{(t)}) + U_d^\perp(\mathbf{x}^{(t)})$  in (i) and leverage the orthogonality between  $U_d^\perp(\mathbf{x}^{(t)})$  and  $V_d(\mathbf{x}^{(t)}) V_d(\mathbf{x}^{(t)})^T$  as well as the idempotence of  $V_d(\mathbf{x}^{(s)}) V_d(\mathbf{x}^{(s)})^T$  for all  $s \geq t$  in (ii). See Figure 8 for a graphical illustration. Then, by the orthogonality between  $U_d^\perp(\mathbf{x}^{(t)})$  and  $U_d(\mathbf{x}^{(t)})$ , we obtain that

$$\begin{aligned} (54) \quad &U_d^\perp(\mathbf{x}^{(t)}) \left(\mathbf{x}^* - \mathbf{x}^{(t)}\right) \\ &= \sum_{s=t}^{\infty} U_d^\perp(\mathbf{x}^{(t)}) \cdot \eta \left[ V_d(\mathbf{x}^{(s)}) V_d(\mathbf{x}^{(s)})^T - V_d(\mathbf{x}^{(t)}) V_d(\mathbf{x}^{(t)})^T \right] V_d(\mathbf{x}^{(s)}) V_d(\mathbf{x}^{(s)})^T \nabla p(\mathbf{x}^{(s)}) \end{aligned}$$

Now, we intend to develop an upper bound for the right-hand side of (54). On the one hand, since  $\left\|U_d^\perp(\mathbf{x}^{(t)})\right\|_2 = 1$ , we know that

$$\left\| \sum_{s=t}^{\infty} U_d^\perp(\mathbf{x}^{(t)}) \cdot \eta V_d(\mathbf{x}^{(s)}) V_d(\mathbf{x}^{(s)})^T \nabla p(\mathbf{x}^{(s)}) \right\|_2$$

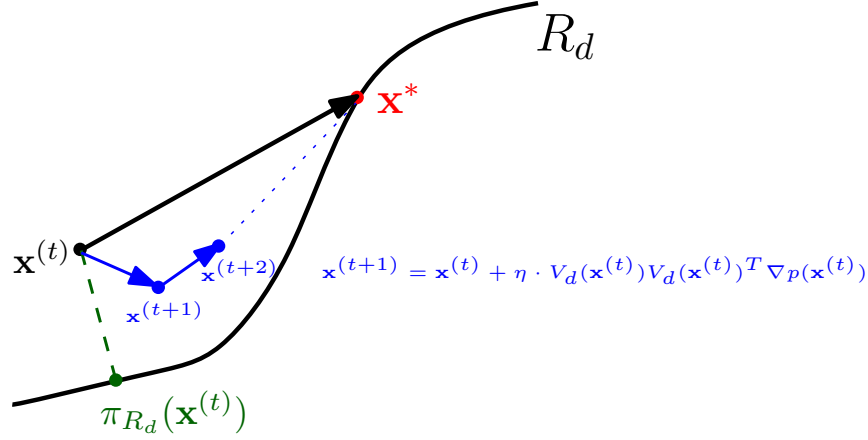


Fig 8: Decomposition of the vector  $\mathbf{x}^* - \mathbf{x}^{(t)}$  into the summation  $\sum_{s=t}^{\infty} (\mathbf{x}^{(s+1)} - \mathbf{x}^{(s)})$  of subspace constrained gradient ascent iterative vectors.

$$\begin{aligned} &\leq \left\| U_d^\perp(\mathbf{x}^{(t)}) \right\|_2 \cdot \left\| \sum_{s=t}^{\infty} \eta V_d(\mathbf{x}^{(s)}) V_d(\mathbf{x}^{(s)})^T \nabla p(\mathbf{x}^{(s)}) \right\|_2 \\ &\leq \left\| \mathbf{x}^* - \mathbf{x}^{(t)} \right\|_2. \end{aligned}$$

On the other hand, by Davis-Kahan theorem (Lemma 12 here) and conditions (A1-3), we deduce that for all  $s \geq t$ ,

$$\begin{aligned} &\left\| V_d(\mathbf{x}^{(s)}) V_d(\mathbf{x}^{(s)})^T - V_d(\mathbf{x}^{(t)}) V_d(\mathbf{x}^{(t)})^T \right\|_2 \\ &\leq \frac{\left\| \nabla \nabla p(\mathbf{x}^{(s)}) - \nabla \nabla p(\mathbf{x}^{(t)}) \right\|_2}{\beta_0} \\ &\leq \frac{\left\| \nabla^3 p(\mathbf{x}^{(t)}) \right\|_2 \left\| \mathbf{x}^{(s)} - \mathbf{x}^{(t)} \right\|_2}{\beta_0} + O\left(\left\| \mathbf{x}^{(s)} - \mathbf{x}^{(t)} \right\|_2^2\right) \\ &\leq \frac{D^{\frac{3}{2}} \left\| \nabla^3 p(\mathbf{x}^{(t)}) \right\|_{\max} \left\| \mathbf{x}^* - \mathbf{x}^{(t)} \right\|_2}{\beta_0} + D^2 \|p\|_{\infty}^{(4)} \cdot \left\| \mathbf{x}^* - \mathbf{x}^{(t)} \right\|_2^2, \end{aligned}$$

where we apply the Taylor's theorem in the second inequality. Given these two facts, we obtain from (54) and Cauchy-Schwarz inequality that

$$\begin{aligned} \left\| U_d^\perp(\mathbf{x}^{(t)}) \left( \mathbf{x}^* - \mathbf{x}^{(t)} \right) \right\|_2 &\leq \frac{D^{\frac{3}{2}} \left\| \nabla^3 p(\mathbf{x}^{(t)}) \right\|_{\max} \left\| \mathbf{x}^* - \mathbf{x}^{(t)} \right\|_2^2}{\beta_0} + D^2 \|p\|_{\infty}^{(4)} \cdot \left\| \mathbf{x}^* - \mathbf{x}^{(t)} \right\|_2^3 \\ &= \frac{D^{\frac{3}{2}} \left\| \nabla^3 p(\mathbf{x}^{(t)}) \right\|_{\max} \left\| \mathbf{x}^* - \mathbf{x}^{(t)} \right\|_2^2}{\beta_0} + o\left(\left\| \mathbf{x}^* - \mathbf{x}^{(t)} \right\|_2^2\right). \end{aligned}$$

The result follows.  $\square$

**THEOREM 5.** Assume that conditions (A1-3) hold and  $\text{reach}(R_d) > 0$  throughout the theorem.

(a) **Q-Linear convergence of  $\|\mathbf{x}^{(t)} - \mathbf{x}^*\|_2$** : Given a convergence radius  $r_1 > 0$  satisfying

$$r_1 \leq \min \left\{ \rho, \text{reach}(R_d), \frac{\rho \beta_0 \|p\|_\infty^{(2)}}{\sqrt{D} \|p\|_\infty^{(1)} \|p\|_\infty^{(3)} + \beta_0 \|p\|_\infty^{(2)}}, \frac{\beta_0}{8A_\rho D^5 \left( \max \left\{ 1, \|p\|_{\infty,4}^* \right\} \right)^3} \right\},$$

where  $A_\rho > 0$  is a constant that only depends on  $\rho > 0$ , we have that whenever  $0 < \eta \leq \min \left\{ \frac{4}{\beta_0}, \frac{1}{D\|p\|_\infty^{(2)}} \right\}$  and the initial point  $\mathbf{x}^{(0)} \in \text{Ball}_D(\mathbf{x}^*, r_1)$  with  $\mathbf{x}^* \in R_d$ ,

$$\|\mathbf{x}^{(t)} - \mathbf{x}^*\|_2 \leq \Upsilon^t \|\mathbf{x}^{(0)} - \mathbf{x}^*\|_2 \quad \text{with} \quad \Upsilon = \sqrt{1 - \frac{\beta_0 \eta}{4}}.$$

(b) **R-Linear convergence of  $d_E(\mathbf{x}^{(t)}, R_d)$** : Under the same radius  $r_1 > 0$  in (a), we have that whenever  $0 < \eta \leq \min \left\{ \frac{4}{\beta_0}, \frac{1}{D\|p\|_\infty^{(2)}} \right\}$  and the initial point  $\mathbf{x}^{(0)} \in \text{Ball}_D(\mathbf{x}^*, r_1)$  with  $\mathbf{x}^* \in R_d$ ,

$$d_E(\mathbf{x}^{(t)}, R_d) \leq \Upsilon^t \|\mathbf{x}^{(0)} - \mathbf{x}^*\|_2 \quad \text{with} \quad \Upsilon = \sqrt{1 - \frac{\beta_0 \eta}{4}}.$$

We further assume (E1-2) in the rest of statements. If  $h \rightarrow 0$  and  $\frac{nh^{D+4}}{|\log h|} \rightarrow \infty$ ,

(c) **Q-Linear convergence of  $\|\hat{\mathbf{x}}^{(t)} - \mathbf{x}^*\|_2$** : under the same radius  $r_1 > 0$  and  $\Upsilon = \sqrt{1 - \frac{\beta_0 \eta}{4}}$  in (a), we have that

$$\|\hat{\mathbf{x}}^{(t)} - \mathbf{x}^*\|_2 \leq \Upsilon^t \|\hat{\mathbf{x}}^{(0)} - \mathbf{x}^*\|_2 + O(h^2) + O_P \left( \sqrt{\frac{|\log h|}{nh^{D+4}}} \right)$$

with probability tending to 1 whenever  $0 < \eta \leq \min \left\{ \frac{4}{\beta_0}, \frac{1}{D\|p\|_\infty^{(2)}} \right\}$  and the initial point  $\hat{\mathbf{x}}^{(0)} \in \text{Ball}_D(\mathbf{x}^*, r_1)$  with  $\mathbf{x}^* \in R_d$ .

(d) **R-Linear convergence of  $d_E(\hat{\mathbf{x}}^{(t)}, R_d)$** : under the same radius  $r_1 > 0$  and  $\Upsilon = \sqrt{1 - \frac{\beta_0 \eta}{4}}$  in (a), we have that

$$d_E(\hat{\mathbf{x}}^{(t)}, R_d) \leq \Upsilon^t \|\hat{\mathbf{x}}^{(0)} - \mathbf{x}^*\|_2 + O(h^2) + O_P \left( \sqrt{\frac{|\log h|}{nh^{D+4}}} \right)$$

with probability tending to 1 whenever  $0 < \eta \leq \min \left\{ \frac{4}{\beta_0}, \frac{1}{D\|p\|_\infty^{(2)}} \right\}$  and the initial point  $\hat{\mathbf{x}}^{(0)} \in \text{Ball}_D(\mathbf{x}^*, r_1)$  with  $\mathbf{x}^* \in R_d$ .

**PROOF OF THEOREM 5.** The entire proof is inspired by some standard results in optimization theory, except that the objective function  $p$  is no longer strongly concave and the SCGA iterations are conducted. We first derive the following two facts.

- *Fact 1.* Given (A1),  $p$  is  $D\|p\|_\infty^{(2)}$ -smooth, that is,  $\nabla p$  is  $D\|p\|_\infty^{(2)}$ -Lipschitz.
- *Fact 2.* Given conditions (A1-3), we know that

$$\left\| V_d(\mathbf{x}^{(t)})^T \nabla p(\mathbf{x}^{(t)}) \right\|_2 > 0 \quad \text{for any } \mathbf{x}^{(t)} \in \text{Ball}_D(\mathbf{x}^*, r_1) \setminus R_d$$

and

$$p(\mathbf{x}^*) - p \left( \mathbf{x}^{(t)} + \frac{1}{D\|p\|_\infty^{(2)}} \cdot V_d(\mathbf{x}^{(t)}) V_d(\mathbf{x}^{(t)})^T \nabla p(\mathbf{x}^{(t)}) \right) \geq 0$$



for any  $\mathbf{x}^{(t)} \in \text{Ball}_D(\mathbf{x}^*, r_1)$ .

As for *Fact 1*, it follows from the differentiability of  $p$  guaranteed by condition (A1) and Taylor's theorem that

$$\begin{aligned} \|\nabla p(\mathbf{x}) - \nabla p(\mathbf{y})\|_2 &\leq \|\nabla \nabla p(\tilde{\mathbf{y}})\|_2 \cdot \|\mathbf{x} - \mathbf{y}\|_2 \\ &\leq D \|p\|_\infty^{(2)} \cdot \|\mathbf{x} - \mathbf{y}\|_2 \end{aligned}$$

for any  $\mathbf{x}, \mathbf{y} \in \mathbb{R}^D$ , where  $\tilde{\mathbf{y}}$  is within a  $\|\mathbf{x} - \mathbf{y}\|_2$ -neighborhood of  $\mathbf{y}$ . Therefore,

$$\begin{aligned} (55) \quad |p(\mathbf{y}) - p(\mathbf{x}) - \nabla p(\mathbf{x})^T(\mathbf{y} - \mathbf{x})| &= \left| \int_0^1 \nabla p(\mathbf{x} + t(\mathbf{y} - \mathbf{x}))^T(\mathbf{y} - \mathbf{x}) dt - \nabla p(\mathbf{x})^T(\mathbf{y} - \mathbf{x}) \right| \\ &\leq \int_0^1 \|\nabla p(\mathbf{x} + t(\mathbf{y} - \mathbf{x})) - \nabla p(\mathbf{x})\|_2 \cdot \|\mathbf{y} - \mathbf{x}\|_2 dt \\ &\leq \frac{D \|p\|_\infty^{(2)}}{2} \cdot \|\mathbf{y} - \mathbf{x}\|_2^2. \end{aligned}$$

Moreover, when  $\eta < \frac{2}{D \|p\|_\infty^{(2)}}$ ,

$$\begin{aligned} (56) \quad p(\mathbf{x}^{(t+1)}) - p(\mathbf{x}^{(t)}) &= p\left(\mathbf{x}^{(t)} + \eta \cdot V_d(\mathbf{x}^{(t)}) V_d(\mathbf{x}^{(t)})^T \nabla p(\mathbf{x}^{(t)})\right) - p(\mathbf{x}^{(t)}) \\ &\geq \nabla p(\mathbf{x}^{(t)})^T \cdot \eta V_d(\mathbf{x}^{(t)}) V_d(\mathbf{x}^{(t)})^T \nabla p(\mathbf{x}^{(t)}) - \frac{D \|p\|_\infty^{(2)}}{2} \eta^2 \left\| V_d(\mathbf{x}^{(t)})^T \nabla p(\mathbf{x}^{(t)}) \right\|_2^2 \quad \text{by (55)} \\ &= \eta \left( 1 - \frac{D \|p\|_\infty^{(2)}}{2} \eta \right) \left\| V_d(\mathbf{x}^{(t)})^T \nabla p(\mathbf{x}^{(t)}) \right\|_2^2 > 0, \end{aligned}$$

showing that the objective function  $p$  is non-decreasing.

*Fact 2* is a natural corollary under conditions (A1-3). This is because the ridge  $R_d$  is the unique projected local mode of  $p$  on the column space of  $V_d(\mathbf{x})$  within  $R_d \oplus \rho$  by condition (A2). In addition, we can derive the following bound:

$$\begin{aligned} &\left\| \frac{1}{D \|p\|_\infty^{(2)}} \cdot V_d(\mathbf{x}^{(t)}) V_d(\mathbf{x}^{(t)})^T \nabla p(\mathbf{x}^{(t)}) \right\|_2 \\ &= \frac{1}{D \|p\|_\infty^{(2)}} \left\| V_d(\mathbf{x}^{(t)}) V_d(\mathbf{x}^{(t)})^T \nabla p(\mathbf{x}^{(t)}) - \underbrace{V_d(\mathbf{x}^*) V_d(\mathbf{x}^*)^T \nabla p(\mathbf{x}^*)}_{=0} \right\|_2 \\ &\leq \frac{1}{D \|p\|_\infty^{(2)}} \left[ \left\| V_d(\mathbf{x}^{(t)}) V_d(\mathbf{x}^{(t)})^T \nabla p(\mathbf{x}^{(t)}) - V_d(\mathbf{x}^*) V_d(\mathbf{x}^*)^T \nabla p(\mathbf{x}^{(t)}) \right\|_2 \right. \\ &\quad \left. + \left\| V_d(\mathbf{x}^*) V_d(\mathbf{x}^*)^T \nabla p(\mathbf{x}^{(t)}) - V_d(\mathbf{x}^*) V_d(\mathbf{x}^*)^T \nabla p(\mathbf{x}^*) \right\|_2 \right] \\ &\stackrel{(i)}{\leq} \frac{\|p\|_\infty^{(1)}}{D \|p\|_\infty^{(2)}} \cdot \frac{\|\nabla \nabla p(\mathbf{x}^{(t)}) - \nabla \nabla p(\mathbf{x}^*)\|_2}{\beta_0} + \frac{\|V_d(\mathbf{x}^*) V_d(\mathbf{x}^*)^T\|_2}{D \|p\|_\infty^{(2)}} \cdot \left\| \nabla p(\mathbf{x}^{(t)}) - \nabla p(\mathbf{x}^*) \right\|_2 \end{aligned}$$

$$\begin{aligned}
&\stackrel{(ii)}{\leq} \frac{\|p\|_\infty^{(1)} D^{\frac{3}{2}} \|p\|_\infty^{(3)}}{D \|p\|_\infty^{(2)} \beta_0} \cdot \left\| \mathbf{x}^{(t)} - \mathbf{x}^* \right\|_2 + \frac{D \|p\|_\infty^{(2)}}{D \|p\|_\infty^{(2)}} \cdot \left\| \mathbf{x}^{(t)} - \mathbf{x}^* \right\|_2 \\
&= \left( \frac{\sqrt{D} \|p\|_\infty^{(1)} \|p\|_\infty^{(3)}}{\beta_0 \|p\|_\infty^{(2)}} + 1 \right) \left\| \mathbf{x}^{(t)} - \mathbf{x}^* \right\|_2 \\
&\stackrel{(iii)}{\leq} \rho,
\end{aligned}$$

where we apply Davis-Khan theorem (Lemma 12 here) in (i), leverage Taylor's theorem and the fact that  $\|V_d(\mathbf{x}^*)V_d(\mathbf{x}^*)^T\|_2 = 1$  in (ii), and use the choice of  $r_1$  to obtain (iii). It implies that one-step SCGA iteration with the step size  $\frac{1}{D\|p\|_\infty^{(2)}}$  will not exit the region  $R_d \oplus \rho$  whenever  $\mathbf{x}^{(t)} \in \text{Ball}_D(\mathbf{x}^*, r_1)$ . Together with the ascending property (56), we conclude that  $p(\mathbf{x}^*) - p\left(\mathbf{x}^{(t)} + \frac{1}{D\|p\|_\infty^{(2)}} \cdot V_d(\mathbf{x}^{(t)})V_d(\mathbf{x}^{(t)})^T \nabla p(\mathbf{x}^{(t)})\right) \geq 0$ .

With the help of these two facts, we start the proofs of (a-d).

(a) We first show that the following claim using Lemma 4: for all  $t \geq 0$  and the initial point  $\mathbf{x}^{(0)} \in \text{Ball}_D(\mathbf{x}^*, r_1)$ ,

$$(57) \quad p(\mathbf{x}^*) - p(\mathbf{x}^{(t)}) \leq \nabla p(\mathbf{x}^{(t)})^T V_d(\mathbf{x}^{(t)}) V_d(\mathbf{x}^{(t)})^T \left( \mathbf{x}^* - \mathbf{x}^{(t)} \right) - \frac{\beta_0}{4} \left\| \mathbf{x}^* - \mathbf{x}^{(t)} \right\|_2^2 + \epsilon_t,$$

where  $\epsilon_t = A_\rho D^5 \left( \max \left\{ 1, \|p\|_{\infty,4}^* \right\} \right)^3 \left\| \mathbf{x}^* - \mathbf{x}^{(t)} \right\|_2^3 = o\left(\left\| \mathbf{x}^* - \mathbf{x}^{(t)} \right\|_2^2\right)$  for some constant  $A_\rho > 0$  that only depends on  $\rho$ . By the differentiability of  $p$  guaranteed by condition (A1) and Taylor's theorem, we have that

$$\begin{aligned}
&p(\mathbf{x}^*) - p(\mathbf{x}^{(t)}) \\
&\leq \nabla p(\mathbf{x}^{(t)})^T (\mathbf{x}^* - \mathbf{x}^{(t)}) + \frac{1}{2} (\mathbf{x}^* - \mathbf{x}^{(t)})^T \nabla \nabla p(\mathbf{x}^{(t)}) (\mathbf{x}^* - \mathbf{x}^{(t)}) + \frac{D^{\frac{3}{2}} \|p\|_\infty^{(3)}}{6} \left\| \mathbf{x}^* - \mathbf{x}^{(t)} \right\|_2^3 \\
&\stackrel{(i)}{=} \nabla p(\mathbf{x}^{(t)})^T V_d(\mathbf{x}^{(t)}) V_d(\mathbf{x}^{(t)})^T (\mathbf{x}^* - \mathbf{x}^{(t)}) + \nabla p(\mathbf{x}^{(t)})^T U_d^\perp(\mathbf{x}^{(t)}) (\mathbf{x}^* - \mathbf{x}^{(t)}) \\
&\quad + \frac{1}{2} (\mathbf{x}^* - \mathbf{x}^{(t)}) \left( V_\diamond(\mathbf{x}^{(t)}), V_d(\mathbf{x}^{(t)}) \right) \begin{pmatrix} \lambda_1(\mathbf{x}^{(t)}) & & \\ & \ddots & \\ & & \lambda_D(\mathbf{x}^{(t)}) \end{pmatrix} \begin{pmatrix} V_\diamond(\mathbf{x}^{(t)}) \\ V_d(\mathbf{x}^{(t)}) \end{pmatrix} (\mathbf{x}^* - \mathbf{x}^{(t)}) \\
&\quad + \frac{D^{\frac{3}{2}} \|p\|_\infty^{(3)}}{6} \left\| \mathbf{x}^* - \mathbf{x}^{(t)} \right\|_2^3 \\
&\stackrel{(ii)}{\leq} \nabla p(\mathbf{x}^{(t)})^T V_d(\mathbf{x}^{(t)}) V_d(\mathbf{x}^{(t)})^T (\mathbf{x}^* - \mathbf{x}^{(t)}) + \nabla p(\mathbf{x}^{(t)})^T U_d^\perp(\mathbf{x}^{(t)}) (\mathbf{x}^* - \mathbf{x}^{(t)}) \\
&\quad + \frac{\lambda_1(\mathbf{x}^{(t)})}{2} \left\| U_d^\perp(\mathbf{x}^{(t)}) (\mathbf{x}^* - \mathbf{x}^{(t)}) \right\|_2^2 - \frac{\beta_0}{2} \left\| V_d(\mathbf{x}^{(t)})^T (\mathbf{x}^* - \mathbf{x}^{(t)}) \right\|_2^2 \\
&\quad + \frac{D^{\frac{3}{2}} \|p\|_\infty^{(3)}}{6} \left\| \mathbf{x}^* - \mathbf{x}^{(t)} \right\|_2^3 \\
&\stackrel{(iii)}{=} \nabla p(\mathbf{x}^{(t)})^T V_d(\mathbf{x}^{(t)}) V_d(\mathbf{x}^{(t)})^T (\mathbf{x}^* - \mathbf{x}^{(t)}) + \nabla p(\mathbf{x}^{(t)})^T U_d^\perp(\mathbf{x}^{(t)}) (\mathbf{x}^* - \mathbf{x}^{(t)}) \\
&\quad + \frac{(\lambda_1(\mathbf{x}^{(t)}) + \beta_0)}{2} \left\| U_d^\perp(\mathbf{x}^{(t)}) (\mathbf{x}^* - \mathbf{x}^{(t)}) \right\|_2^2 - \frac{\beta_0}{2} \left\| \mathbf{x}^* - \mathbf{x}^{(t)} \right\|_2^2 \\
&\quad + \frac{D^{\frac{3}{2}} \|p\|_\infty^{(3)}}{6} \left\| \mathbf{x}^* - \mathbf{x}^{(t)} \right\|_2^3
\end{aligned}$$

$$\begin{aligned}
 & \stackrel{(iv)}{\leq} \nabla p(\mathbf{x}^{(t)})^T V_d(\mathbf{x}^{(t)}) V_d(\mathbf{x}^{(t)})^T (\mathbf{x}^* - \mathbf{x}^{(t)}) \\
 & \quad + \left\| U_d^\perp(\mathbf{x}^{(t)}) \nabla p(\mathbf{x}^{(t)}) \right\|_2 \left[ \frac{D^{\frac{3}{2}} \|\nabla^3 p(\mathbf{x}^{(t)})\|_{\max}}{\beta_0} \left\| \mathbf{x}^* - \mathbf{x}^{(t)} \right\|_2^2 + D^2 \|p\|_\infty^{(4)} \left\| \mathbf{x}^* - \mathbf{x}^{(t)} \right\|_2^3 \right] \\
 & \quad + \frac{(\lambda_1(\mathbf{x}^{(t)}) + \beta_0)}{2} \left[ \frac{D^{\frac{3}{2}} \|\nabla^3 p(\mathbf{x}^{(t)})\|_{\max}}{\beta_0} \left\| \mathbf{x}^* - \mathbf{x}^{(t)} \right\|_2^2 + D^2 \|p\|_\infty^{(4)} \left\| \mathbf{x}^* - \mathbf{x}^{(t)} \right\|_2^3 \right]^2 \\
 & \quad - \frac{\beta_0}{2} \left\| \mathbf{x}^* - \mathbf{x}^{(t)} \right\|_2^2 + \frac{D^{\frac{3}{2}} \|p\|_\infty^{(3)}}{6} \left\| \mathbf{x}^* - \mathbf{x}^{(t)} \right\|_2^3 \\
 & \stackrel{(v)}{\leq} \nabla p(\mathbf{x}^{(t)})^T V_d(\mathbf{x}^{(t)}) V_d(\mathbf{x}^{(t)})^T (\mathbf{x}^* - \mathbf{x}^{(t)}) - \frac{\beta_0}{4} \left\| \mathbf{x}^* - \mathbf{x}^{(t)} \right\|_2^2 \\
 & \quad + \left( D^2 \|p\|_\infty^{(1)} \|p\|_\infty^{(4)} + \frac{D^{\frac{3}{2}} \|p\|_\infty^{(3)}}{6} \right) \left\| \mathbf{x}^* - \mathbf{x}^{(t)} \right\|_2^3 \\
 & \quad + D \|p\|_\infty^{(2)} \rho \left( \frac{D^{\frac{3}{2}} \|p\|_\infty^{(3)}}{\beta_0} + D^2 \|p\|_\infty^{(4)} \rho \right)^2 \left\| \mathbf{x}^* - \mathbf{x}^{(t)} \right\|_2^3 \\
 & \leq \nabla p(\mathbf{x}^{(t)})^T V_d(\mathbf{x}^{(t)}) V_d(\mathbf{x}^{(t)})^T (\mathbf{x}^* - \mathbf{x}^{(t)}) - \frac{\beta_0}{4} \left\| \mathbf{x}^* - \mathbf{x}^{(t)} \right\|_2^2 \\
 & \quad + A'_\rho D^5 \left[ \|p\|_\infty^{(3)} + \|p\|_\infty^{(1)} \|p\|_\infty^{(4)} + \|p\|_\infty^{(2)} \left( \|p\|_{\infty,4}^* \right)^2 \right] \cdot \left\| \mathbf{x}^* - \mathbf{x}^{(t)} \right\|_2^3 \\
 & \leq \nabla p(\mathbf{x}^{(t)})^T V_d(\mathbf{x}^{(t)}) V_d(\mathbf{x}^{(t)})^T (\mathbf{x}^* - \mathbf{x}^{(t)}) - \frac{\beta_0}{4} \left\| \mathbf{x}^* - \mathbf{x}^{(t)} \right\|_2^2 \\
 & \quad + A_\rho D^5 \left( \max \left\{ 1, \|p\|_{\infty,4}^* \right\} \right)^3 \left\| \mathbf{x}^* - \mathbf{x}^{(t)} \right\|_2^3,
 \end{aligned}$$

where we use the equality  $\mathbf{I}_D = V_d(\mathbf{x}^{(t)}) V_d(\mathbf{x}^{(t)})^T + U_d^\perp(\mathbf{x}^{(t)})$  in (i) and (iii), leverage condition (A2) to obtain that  $\lambda_D(\mathbf{x}^{(t)}) \leq \dots \leq \lambda_{d+1}(\mathbf{x}^{(t)}) \leq -\beta_0$  in (ii), apply Lemma 4 to obtain (iv), and apply the first inequality of condition (A3) in (v). We also use the fact that  $\max \{ \beta_0, |\lambda_1(\mathbf{x}^{(t)})| \} \leq D \|p\|_\infty^{(2)}$  and  $\left\| \mathbf{x}^* - \mathbf{x}^{(t)} \right\|_2 \leq \rho$  in (v). Note that  $A'_\rho, A_\rho > 0$  are two constants that depend on  $\rho$  and may be different in general. Claim (57) thus follows.

Given Fact 2 and any  $\mathbf{x}^{(t)} \in \text{Ball}_D(\mathbf{x}^*, r_1)$ ,

$$\begin{aligned}
 & p(\mathbf{x}^{(t)}) - p(\mathbf{x}^*) \\
 & \leq p(\mathbf{x}^{(t)}) - p(\mathbf{x}^*) + p(\mathbf{x}^*) - p \left( \mathbf{x}^{(t)} + \frac{1}{D \|p\|_\infty^{(2)}} V_d(\mathbf{x}^{(t)}) V_d(\mathbf{x}^{(t)})^T \nabla p(\mathbf{x}^{(t)}) \right) \\
 & = - \left[ p \left( \mathbf{x}^{(t)} + \frac{1}{D \|p\|_\infty^{(2)}} \cdot V_d(\mathbf{x}^{(t)}) V_d(\mathbf{x}^{(t)})^T \nabla p(\mathbf{x}^{(t)}) \right) - p(\mathbf{x}^{(t)}) \right] \\
 & \leq - \left[ \nabla p(\mathbf{x}^{(t)})^T \frac{1}{D \|p\|_\infty^{(2)}} V_d(\mathbf{x}^{(t)}) V_d(\mathbf{x}^{(t)})^T \nabla p(\mathbf{x}^{(t)}) - \frac{1}{2D \|p\|_\infty^{(2)}} \left\| V_d(\mathbf{x}^{(t)})^T \nabla p(\mathbf{x}^{(t)}) \right\|_2^2 \right] \\
 & = - \frac{1}{2D \|p\|_\infty^{(2)}} \left\| V_d(\mathbf{x}^{(t)})^T \nabla p(\mathbf{x}^{(t)}) \right\|_2^2,
 \end{aligned}$$

where we apply (55) to obtain the inequality. It implies that

$$(58) \quad \left\| V_d(\mathbf{x}^{(t)})^T \nabla p(\mathbf{x}^{(t)}) \right\|_2^2 \leq 2D \|p\|_\infty^{(2)} \cdot \left[ p(\mathbf{x}^*) - p(\mathbf{x}^{(t)}) \right].$$

Therefore,

$$\begin{aligned} & \left\| \mathbf{x}^{(t+1)} - \mathbf{x}^* \right\|_2^2 \\ &= \left\| \mathbf{x}^{(t)} + \eta V_d(\mathbf{x}^{(t)}) V_d(\mathbf{x}^{(t)})^T \nabla p(\mathbf{x}^{(t)}) - \mathbf{x}^* \right\|_2^2 \\ &= \left\| \mathbf{x}^{(t)} - \mathbf{x}^* \right\|_2^2 + 2\eta \nabla p(\mathbf{x}^{(t)})^T V_d(\mathbf{x}^{(t)}) V_d(\mathbf{x}^{(t)})^T (\mathbf{x}^{(t)} - \mathbf{x}^*) + \eta^2 \left\| V_d(\mathbf{x}^{(t)})^T \nabla p(\mathbf{x}^{(t)}) \right\|_2^2 \\ &\stackrel{(i)}{\leq} \left\| \mathbf{x}^{(t)} - \mathbf{x}^* \right\|_2^2 + 2\eta \left[ p(\mathbf{x}^{(t)}) - p(\mathbf{x}^*) - \frac{\beta_0}{4} \left\| \mathbf{x}^* - \mathbf{x}^{(t)} \right\|_2^2 \right. \\ &\quad \left. + A_\rho D^5 \left( \max \left\{ 1, \|p\|_{\infty,4}^* \right\} \right)^3 \left\| \mathbf{x}^* - \mathbf{x}^{(t)} \right\|_2^3 \right] + \eta^2 \cdot 2D \|p\|_\infty^{(2)} \cdot \left[ p(\mathbf{x}^*) - p(\mathbf{x}^{(t)}) \right] \\ &\stackrel{(ii)}{\leq} \left( 1 - \frac{\beta_0 \eta}{4} \right) \left\| \mathbf{x}^{(t)} - \mathbf{x}^* \right\|_2^2 - 2\eta \left( 1 - \eta D \|p\|_\infty^{(2)} \right) \underbrace{\left[ p(\mathbf{x}^*) - p(\mathbf{x}^{(t)}) \right]}_{\geq 0} \\ &\leq \left( 1 - \frac{\beta_0 \eta}{4} \right) \left\| \mathbf{x}^{(t)} - \mathbf{x}^* \right\|_2^2 \end{aligned}$$

whenever  $0 < \eta \leq \min \left\{ \frac{4}{\beta_0}, \frac{1}{D \|p\|_\infty^{(2)}} \right\}$ , where we apply (57) and (58) in (i) and use the choice of  $r_1 > 0$  to argue that

$$\begin{aligned} A_\rho D^5 \left( \max \left\{ 1, \|p\|_{\infty,4}^* \right\} \right)^3 \left\| \mathbf{x}^* - \mathbf{x}^{(t)} \right\|_2^3 &\leq A_\rho D^5 \left( \max \left\{ 1, \|p\|_{\infty,4}^* \right\} \right)^3 r_1 \left\| \mathbf{x}^* - \mathbf{x}^{(t)} \right\|_2^2 \\ &\leq \frac{\beta_0}{8} \left\| \mathbf{x}^* - \mathbf{x}^{(t)} \right\|_2^2 \end{aligned}$$

in (ii). By telescoping, we conclude that when  $0 < \eta \leq \min \left\{ \frac{4}{\beta_0}, \frac{1}{D \|p\|_\infty^{(2)}} \right\}$  and  $\mathbf{x}^{(0)} \in \text{Ball}_D(\mathbf{x}^*, r_1)$ ,

$$\left\| \mathbf{x}^{(t)} - \mathbf{x}^* \right\|_2 \leq \left( 1 - \frac{\beta_0 \eta}{4} \right)^{\frac{t}{2}} \left\| \mathbf{x}^{(0)} - \mathbf{x}^* \right\|_2.$$

The result follows.

(b) The result follows easily from (a) and the inequality  $d_E(\mathbf{x}^{(t)}, R_d) \leq \left\| \mathbf{x}^{(t)} - \mathbf{x}^* \right\|_2$  for all  $t \geq 0$ .

(c) The proof here is partially inspired by the proof of Theorem 2 in [Balakrishnan et al. \(2017\)](#). We write the spectral decompositions of  $\nabla \nabla p(\mathbf{x})$  and  $\nabla \nabla \hat{p}_n(\mathbf{x})$  as

$$\nabla \nabla p(\mathbf{x}) = V(\mathbf{x}) \Lambda(\mathbf{x}) V(\mathbf{x})^T \quad \text{and} \quad \nabla \nabla \hat{p}_n(\mathbf{x}) = \hat{V}(\mathbf{x}) \hat{\Lambda}(\mathbf{x}) \hat{V}(\mathbf{x})^T.$$

By Weyl's theorem (Theorem 4.3.1 in [Horn and Johnson \(2012\)](#)) and uniform bounds (cf. Equation (15) in the main paper),

$$|\lambda_j(\mathbf{x}) - \hat{\lambda}_j(\mathbf{x})| \leq \max_j |\lambda_j(\nabla \nabla p(\mathbf{x}) - \nabla \nabla \hat{p}_n(\mathbf{x}))|$$

$$\begin{aligned}
 &= \|\nabla \nabla p(\mathbf{x}) - \nabla \nabla \hat{p}_n(\mathbf{x})\|_2 \\
 &\leq D \|p - \hat{p}_n\|_\infty^{(2)} \\
 &= O(h^2) + O_P \left( \sqrt{\frac{|\log h|}{nh^{D+4}}} \right).
 \end{aligned}$$

Thus,  $\hat{p}_n$  satisfies the first two inequalities in condition (A2) when  $h$  is sufficiently small and  $\frac{nh^{D+4}}{|\log h|}$  is sufficiently large. According to Davis-Kahan theorem (Lemma 12 here) and uniform bounds (15),

$$\begin{aligned}
 &\left\| G_d(\mathbf{y}) - \hat{G}_d(\mathbf{y}) \right\|_2 \\
 &= \left\| V_d(\mathbf{y}) V_d(\mathbf{y})^T \nabla p(\mathbf{y}) - \hat{V}_d(\mathbf{y}) \hat{V}_d(\mathbf{y})^T \nabla \hat{p}_n(\mathbf{y}) \right\|_2 \\
 &\leq \left\| \left[ V_d(\mathbf{y}) V_d(\mathbf{y})^T - \hat{V}_d(\mathbf{y}) \hat{V}_d(\mathbf{y})^T \right] \nabla p(\mathbf{y}) \right\|_2 + \left\| \hat{V}_d(\mathbf{y}) \hat{V}_d(\mathbf{y})^T [\nabla p(\mathbf{y}) - \nabla \hat{p}_n(\mathbf{y})] \right\|_2 \\
 &\stackrel{(i)}{\leq} \frac{\|\nabla \nabla p(\mathbf{y}) - \nabla \nabla \hat{p}_n(\mathbf{y})\|_2 \cdot \|\nabla p(\mathbf{y})\|_2}{\beta_0} + \|\nabla p(\mathbf{y}) - \nabla \hat{p}_n(\mathbf{y})\|_2 \\
 &\leq \frac{D \|p - \hat{p}_n\|_\infty^{(2)} \cdot \sqrt{D} \|p\|_\infty^{(1)}}{\beta_0} + \sqrt{D} \|p - \hat{p}_n\|_\infty^{(1)} \\
 &\equiv \epsilon_{n,h} = O(h^2) + O_P \left( \sqrt{\frac{|\log h|}{nh^{D+4}}} \right)
 \end{aligned}$$

for any  $\mathbf{y} \in R_d \oplus r_1$ , where we use the Davis-Kahan theorem and the fact that  $\left\| \hat{V}_d(\mathbf{y}) \hat{V}_d(\mathbf{y})^T \right\|_2 = 1$  to obtain (i). Hence, when  $h \rightarrow 0$  and  $\frac{nh^{D+4}}{|\log h|} \rightarrow \infty$ ,

$$(59) \quad \left\| G_d(\mathbf{y}) - \hat{G}_d(\mathbf{y}) \right\|_2 \leq \epsilon_{n,h} = O(h^2) + O_P \left( \sqrt{\frac{|\log h|}{nh^{D+4}}} \right) \leq \frac{(1 - \Upsilon)r_1}{\eta}$$

with probability tending to 1.

We now claim that  $\left\| \hat{\mathbf{x}}^{(t)} - \mathbf{x}^* \right\|_2 \leq r_1$  and

$$(60) \quad \left\| \hat{\mathbf{x}}^{(t+1)} - \mathbf{x}^* \right\|_2 \leq \Upsilon \left\| \hat{\mathbf{x}}^{(t)} - \mathbf{x}^* \right\|_2 + \eta \cdot \epsilon_{n,h}$$

for all  $t \geq 0$ . We will prove this claim by induction on the iteration number. Note that when  $t = 1$ , we derive from triangle inequality that

$$\begin{aligned}
 &\left\| \hat{\mathbf{x}}^{(1)} - \mathbf{x}^* \right\|_2 \\
 &= \left\| \hat{\mathbf{x}}^{(0)} + \eta \hat{V}_d(\hat{\mathbf{x}}^{(0)}) \hat{V}_d(\hat{\mathbf{x}}^{(0)})^T \nabla \hat{p}_n(\hat{\mathbf{x}}^{(0)}) - \mathbf{x}^* \right\|_2 \\
 &\leq \left\| \hat{\mathbf{x}}^{(0)} + \eta V_d(\hat{\mathbf{x}}^{(0)}) V_d(\hat{\mathbf{x}}^{(0)})^T \nabla p(\hat{\mathbf{x}}^{(0)}) - \mathbf{x}^* \right\|_2 + \eta \left\| G_d(\hat{\mathbf{x}}^{(0)}) - \hat{G}_d(\hat{\mathbf{x}}^{(0)}) \right\|_2 \\
 &\leq \Upsilon \left\| \hat{\mathbf{x}}^{(0)} - \mathbf{x}^* \right\|_2 + \eta \cdot \epsilon_{n,h},
 \end{aligned}$$

where we apply the result in (a) to obtain the last inequality. Moreover, by the choice of  $\hat{\mathbf{x}}^{(0)}$  and (59), we are guaranteed that  $\left\| \hat{\mathbf{x}}^{(1)} - \mathbf{x}^* \right\|_2 \leq r_1$ . In the induction from  $t \mapsto t + 1$ , we suppose that  $\left\| \hat{\mathbf{x}}^{(t)} - \mathbf{x}^* \right\|_2 \leq r_1$  and the claim (60) holds at iteration  $t$ . The same argument

then implies that the claim (60) holds for iteration  $t + 1$  and that  $\|\hat{\mathbf{x}}^{(t+1)} - \mathbf{x}^*\|_2 \leq r_1$ . The claim (60) is thus proved.

Now, given that  $\Upsilon = \sqrt{1 - \frac{\beta_0 \eta}{4}} < 1$ , we iterate the claim (60) to show that

$$\begin{aligned}
\|\hat{\mathbf{x}}^{(t)} - \mathbf{x}^*\|_2 &\leq \Upsilon \|\hat{\mathbf{x}}^{(t-1)} - \mathbf{x}^*\|_2 + \eta \cdot \epsilon_{n,h} \\
&\leq \Upsilon \left[ \Upsilon \|\hat{\mathbf{x}}^{(t-2)} - \mathbf{x}^*\|_2 + \eta \cdot \epsilon_{n,h} \right] + \eta \cdot \epsilon_{n,h} \\
&\leq \Upsilon^t \|\hat{\mathbf{x}}^{(0)} - \mathbf{x}^*\|_2 + \left[ \sum_{s=0}^{t-1} \Upsilon^s \right] \eta \cdot \epsilon_{n,h} \\
&\leq \Upsilon^t \|\hat{\mathbf{x}}^{(0)} - \mathbf{x}^*\|_2 + \frac{\eta \cdot \epsilon_{n,h}}{1 - \Upsilon} \\
&= \Upsilon^t \|\hat{\mathbf{x}}^{(0)} - \mathbf{x}^*\|_2 + O(h^2) + O_P \left( \frac{|\log h|}{nh^{D+4}} \right),
\end{aligned}$$

where the fourth inequality follows by summing the geometric series, and the last equality is due to our notation  $\epsilon_{n,h} = O(h^2) + O_P \left( \frac{|\log h|}{nh^{D+4}} \right)$ . It completes the proof.

(d) The result follows easily from (c) and the inequality  $d_E(\hat{\mathbf{x}}^{(t)}, R_d) \leq \|\hat{\mathbf{x}}^{(t)} - \mathbf{x}^*\|_2$  for all  $t \geq 0$ .  $\square$

## APPENDIX F: OTHER TECHNICAL CONCEPTS OF DIFFERENTIAL GEOMETRY ON $\Omega_q$

• **Taylor’s Theorem on  $\Omega_q$ .** Given a smooth function  $f$  on  $\Omega_q$ , its Taylor’s expansion is often written as (Pennec, 2006):

$$(61) \quad f(\text{Exp}_x(v)) = f(x) + \langle \text{grad } f(x), v \rangle + \frac{1}{2} v^T \mathcal{H}f(x) v + o(\|v\|_2^2)$$

for any  $v \in T_x$ , where  $\text{Exp}_x : T_x \rightarrow \Omega_q$  is the *exponential map* at  $x \in \Omega_q$ . One may replace the exponential map with a more general concept called the *retractions* on an arbitrary manifold; see Section 4.1 in Absil et al. (2008).

• **Parallel Transport.** When comparing vectors in two different tangent spaces  $T_x, T_y$  on  $\Omega_q$ , we leverage the notion of *parallel transport*  $\Gamma_x^y : T_x \rightarrow T_y$  to transport vectors from one tangent space to another along a geodesic (Alimisis et al., 2020), that is,  $\Gamma_x^y(v)$  is a tangent vector in  $T_y$  after being parallel transported from  $v \in T_x$  along a great circle on  $\Omega_q$ . The parallel transport mapping  $\Gamma_x^y$  has two important properties (Hosseini and Sra, 2020): (i)  $\Gamma_x^y(u) = u$  for any  $u \in T_y$ , and (ii) the mapping  $\Gamma_x^y$  is linear.

• **Sectional Curvature.** *Sectional curvature* is the Gaussian curvature of a two-dimensional submanifold formed as the image of a two-dimensional subspace of a tangent space after exponential mapping; see Section 3-2 in do Carmo (2016) for detailed discussions about the Gaussian curvature. It is known that a two dimensional submanifold with positive, zero, or negative sectional curvature is locally isometric to a two dimensional sphere, a Euclidean plane, or a hyperbolic plane with the same Gaussian curvature (Zhang and Sra, 2016).

## APPENDIX G: NORMAL SPACE OF DIRECTIONAL DENSITY RIDGE

As we will refer to conditions (A1-3) frequently in the next three sections, we restate them here:



- **(A1) (Differentiability)** We extend the directional density  $f$  from  $\Omega_q$  to  $\mathbb{R}^{q+1} \setminus \{\mathbf{0}\}$  by defining  $f(\mathbf{x}) \equiv f\left(\frac{\mathbf{x}}{\|\mathbf{x}\|_2}\right)$  for all  $\mathbf{x} \in \mathbb{R}^{q+1} \setminus \{\mathbf{0}\}$ . Under this extension, we assume that the total gradient  $\nabla f(\mathbf{x})$ , total Hessian matrix  $\nabla \nabla f(\mathbf{x})$ , and third-order derivative tensor  $\nabla^3 f(\mathbf{x})$  in  $\mathbb{R}^{q+1}$  exist, and are continuous on  $\mathbb{R}^{q+1} \setminus \{\mathbf{0}\}$  and square integrable on  $\Omega_q$ . We also assume that  $f$  has bounded fourth order derivatives on  $\Omega_q$ .
- **(A2) (Eigengap)** We assume that there exist constants  $\underline{\rho} \in (0, 2]$  and  $\underline{\beta}_0 > 0$  such that  $\underline{\lambda}_{d+1}(\mathbf{y}) \leq -\underline{\beta}_0$ ,  $\underline{\lambda}_d(\mathbf{y}) - \underline{\lambda}_{d+1}(\mathbf{y}) \geq \underline{\beta}_0$  for any  $\mathbf{y} \in \underline{R}_d \oplus \underline{\rho}$ .
- **(A3) (Path Smoothness)** Under the same  $\underline{\rho}, \underline{\beta}_0 > 0$  in (A2), we assume that there exists another constant  $\underline{\beta}_1 \in (0, \underline{\beta}_0)$  such that

$$(q+1)^{\frac{3}{2}} \left\| \underline{U}_d^\perp(\mathbf{y}) \text{grad } f(\mathbf{y}) \right\|_2 \left\| \nabla^3 f(\mathbf{y}) \right\|_{\max} \leq \frac{\underline{\beta}_0^2}{4},$$

$$d(q+1)^{\frac{3}{2}} \left\| \nabla f(\mathbf{x}) \right\|_2 \cdot \left\| \nabla^3 f(\mathbf{x}) \right\|_{\max} \leq \underline{\beta}_0 (\underline{\beta}_0 - \underline{\beta}_1)$$

for all  $\mathbf{y} \in \underline{R}_d \oplus \underline{\rho}$  and  $\mathbf{x} \in \underline{R}_d$ .

Recall that an order- $d$  density ridge of a directional density  $f$  on  $\Omega_q = \{\mathbf{x} \in \mathbb{R}^{q+1} : \|\mathbf{x}\|_2 = 1\}$  is the set of points defined as:

$$(62) \quad \underline{R}_d = \{\mathbf{x} \in \Omega_q : \underline{G}_d(\mathbf{x}) = \mathbf{0}, \underline{\lambda}_{d+1}(\mathbf{x}) < 0\} = \{\mathbf{x} \in \Omega_q : \underline{V}_d(\mathbf{x})^T \nabla f(\mathbf{x}) = \mathbf{0}, \underline{\lambda}_{d+1}(\mathbf{x}) < 0\}.$$

Lemma 13 below shows that under conditions (A1-3), the Jacobian matrices  $\nabla [\underline{V}_d(\mathbf{x})^T \nabla f(\mathbf{x})] \in \mathbb{R}^{(q-d) \times (q+1)}$  and  $(\mathbf{I}_{q+1} - \mathbf{x}\mathbf{x}^T) \nabla [\underline{V}_d(\mathbf{x})^T \nabla f(\mathbf{x})]^T \in \mathbb{R}^{(q+1) \times (q-d)}$  (i.e., projecting the rows of  $\nabla [\underline{V}_d(\mathbf{x})^T \nabla f(\mathbf{x})]$  onto the tangent space  $T_{\mathbf{x}}$ ) both have rank  $q-d$  at every point on  $\underline{R}_d$ , and  $\underline{R}_d$  will be a  $d$ -dimensional submanifold on  $\Omega_q$  by the implicit function theorem (Rudin, 1976; Lee, 2012). Consequently, the row space of  $\nabla [\underline{V}_d(\mathbf{x})^T \nabla f(\mathbf{x})]$  spans the normal space of  $\underline{R}_d$  within the ambient space  $\mathbb{R}^{q+1}$ , and the column space of  $(\mathbf{I}_{q+1} - \mathbf{x}\mathbf{x}^T) \nabla [\underline{V}_d(\mathbf{x})^T \nabla f(\mathbf{x})]^T$  spans the normal space of  $\underline{R}_d$  within the tangent space  $T_{\mathbf{x}}$  at each  $\mathbf{x} \in \underline{R}_d \subset \Omega_q$ .

Analogous to the discussion about the normal space of a Euclidean density ridge in Appendix D, we define

$$\underline{M}(\mathbf{x}) = \nabla [\underline{V}_d(\mathbf{x})^T \nabla f(\mathbf{x})]^T = [\underline{\mathbf{m}}_{d+1}(\mathbf{x}), \dots, \underline{\mathbf{m}}_q(\mathbf{x})] \in \mathbb{R}^{(q+1) \times (q-d)}$$

whose column space spans the normal space of  $\underline{R}_d$  within  $\mathbb{R}^{q+1}$ , and the technique in pages 60-63 of Eberly (1996) is still effective in showing that

$$(63) \quad \underline{\mathbf{m}}_k(\mathbf{x}) = \left[ \underline{\lambda}_k(\mathbf{x}) \mathbf{I}_{q+1} + \sum_{i=1}^d \frac{\underline{\mathbf{v}}_i(\mathbf{x})^T \nabla f(\mathbf{x})}{\underline{\lambda}_k(\mathbf{x}) - \underline{\lambda}_i(\mathbf{x})} \cdot \underline{\mathbf{v}}_i(\mathbf{x})^T \nabla^3 f(\mathbf{x}) + \frac{\mathbf{x}^T \nabla f(\mathbf{x})}{\underline{\lambda}_k(\mathbf{x})} \cdot \mathbf{x}^T \nabla^3 f(\mathbf{x}) \right] \underline{\mathbf{v}}_k(\mathbf{x})$$

$$= \left[ \underline{\lambda}_k(\mathbf{x}) \mathbf{I}_{q+1} + \sum_{i=1}^d \frac{\underline{\mathbf{v}}_i(\mathbf{x})^T \nabla f(\mathbf{x})}{\underline{\lambda}_k(\mathbf{x}) - \underline{\lambda}_i(\mathbf{x})} \cdot \underline{\mathbf{v}}_i(\mathbf{x})^T \nabla^3 f(\mathbf{x}) \right] \underline{\mathbf{v}}_k(\mathbf{x})$$

for  $k = d+1, \dots, q$ , where we use the fact that  $\mathbf{x}^T \nabla f(\mathbf{x}) = \mathbf{x}^T \text{grad } f(\mathbf{x}) = 0$  on  $\Omega_q$  under the extension of  $f$  as in (A1). Let

$$\underline{\Lambda}_0(\mathbf{x}) = \text{Diag} [\underline{\lambda}_{d+1}(\mathbf{x}), \dots, \underline{\lambda}_q(\mathbf{x})],$$

$$\underline{\Lambda}_i(\mathbf{x}) = \text{Diag} \left[ \frac{1}{\underline{\lambda}_{d+1}(\mathbf{x}) - \underline{\lambda}_i(\mathbf{x})}, \dots, \frac{1}{\underline{\lambda}_q(\mathbf{x}) - \underline{\lambda}_i(\mathbf{x})} \right],$$

$$\underline{T}_i(\mathbf{x}) = [\underline{\mathbf{v}}_i(\mathbf{x})^T \nabla f(\mathbf{x})] \cdot \underline{\mathbf{v}}_i(\mathbf{x})^T \nabla^3 f(\mathbf{x})$$

for  $i = 1, \dots, d$ . Then,

$$(64) \quad \underline{M}(\mathbf{x}) = \underline{V}_d(\mathbf{x}) \underline{\Lambda}_0(\mathbf{x}) + \sum_{i=1}^d \underline{T}_i(\mathbf{x}) \underline{V}_d(\mathbf{x}) \underline{\Lambda}_i(\mathbf{x}).$$

As in the Euclidean data case, the columns of  $\underline{M}(\mathbf{x})$  are not orthonormal, and we again leverage the orthonormalization technique in [Chen et al. \(2015\)](#) to construct  $\underline{N}(\mathbf{x})$  that shares the same column space with  $\underline{M}(\mathbf{x})$  but has orthonormal columns. That is, under the condition that  $\underline{M}(\mathbf{x}) = \nabla [\underline{V}_d(\mathbf{x})^T \nabla f(\mathbf{x})]^T$  has full rank  $q - d$  at every point  $\mathbf{x} \in \underline{R}_d$  (see Lemma 13),

$$(65) \quad \underline{N}(\mathbf{x}) = \underline{M}(\mathbf{x}) [\underline{J}(\mathbf{x})^T]^{-1}.$$

with the Cholesky decomposition  $\underline{M}(\mathbf{x})^T \underline{M}(\mathbf{x}) = \underline{J}(\mathbf{x}) \underline{J}(\mathbf{x})^T$ , where  $\underline{J}(\mathbf{x}) \in \mathbb{R}^{(q-d) \times (q-d)}$  is a lower triangular matrix whose diagonal elements are positive. Finally, the non-uniqueness of  $\underline{M}(\mathbf{x})$  will not affect our subsequent discussions about the properties of directional density ridges.

LEMMA 13. Assume conditions (A1-3). Given that  $\underline{M}(\mathbf{x})$  and  $\underline{N}(\mathbf{x})$  are defined in (64) and (65), we have the following properties:

(a)  $\underline{M}(\mathbf{x})$  and  $\underline{N}(\mathbf{x})$  have the same column space. In addition,

$$\underline{N}(\mathbf{x}) \underline{N}(\mathbf{x})^T = \underline{M}(\mathbf{x}) [\underline{M}(\mathbf{x})^T \underline{M}(\mathbf{x})]^{-1} \underline{M}(\mathbf{x})^T.$$

That is,  $\underline{N}(\mathbf{x}) \underline{N}(\mathbf{x})^T$  is the projection matrix onto the columns of  $\underline{M}(\mathbf{x})$ .

(b) The columns of  $\underline{N}(\mathbf{x})$  are orthonormal to each other.

(c) For  $\mathbf{x} \in \underline{R}_d$ , the column space of  $\underline{N}(\mathbf{x})$  is normal to the (tangent) direction of  $\underline{R}_d$  at  $\mathbf{x}$ .

(d) For  $\mathbf{x} \in \underline{R}_d$ ,  $\lambda_{\min}(\underline{M}(\mathbf{x})^T \underline{M}(\mathbf{x})) = \lambda_{\min}(\underline{M}(\mathbf{x})^T (\mathbf{I}_{q+1} - \mathbf{x} \mathbf{x}^T) \underline{M}(\mathbf{x})) \geq \underline{\beta}_1^2 > 0$ , and

$$\text{rank}(\underline{N}(\mathbf{x})) = \text{rank}(\underline{M}(\mathbf{x})) = \text{rank}((\mathbf{I}_{q+1} - \mathbf{x} \mathbf{x}^T) \underline{M}(\mathbf{x})) = q - d.$$

Moreover,  $\underline{R}_d$  is a  $d$ -dimensional submanifold that contains neither intersections and nor endpoints on  $\Omega_q$ . Namely,  $\underline{R}_d$  is a finite union of connected and compact submanifold on  $\Omega_q$ .

(e) For all  $\mathbf{x} \in \underline{R}_d$ ,

$$\left\| [\underline{M}(\mathbf{x})^T (\mathbf{I}_D - \mathbf{x} \mathbf{x}^T) \underline{M}(\mathbf{x})]^{-1} \right\|_2 \leq \frac{1}{\underline{\beta}_1^2} \quad \text{and} \quad \left\| [\underline{J}(\mathbf{x})^T]^{-1} \right\|_2 \leq \frac{1}{\underline{\beta}_1}.$$

(f) When  $\|\mathbf{x} - \mathbf{y}\|_2$  is sufficiently small and  $\mathbf{x}, \mathbf{y} \in \underline{R}_d \oplus \underline{\rho}$ ,

$$\left\| \underline{N}(\mathbf{x}) \underline{N}(\mathbf{x})^T - \underline{N}(\mathbf{y}) \underline{N}(\mathbf{y})^T \right\|_{\max} \leq \tilde{A}_0 \left( \|f\|_{\infty}^{(3)} + \|f\|_{\infty}^{(4)} \right)^2 \|\mathbf{x} - \mathbf{y}\|_2$$

for some constant  $\tilde{A}_0 > 0$ .

(g) Assume that another directional density function  $g$  also satisfies conditions (A1-3) after the extension  $g(\mathbf{x}) \equiv g\left(\frac{\mathbf{x}}{\|\mathbf{x}\|}\right)$  in  $\mathbb{R}^{q+1} \setminus \{\mathbf{0}\}$ , and  $\|f - g\|_{\infty,3}^*$  is sufficiently small. Then,

$$\left\| \underline{N}_f(\mathbf{x}) \underline{N}_f(\mathbf{x})^T - \underline{N}_g(\mathbf{x}) \underline{N}_g(\mathbf{x})^T \right\|_{\max} \leq \tilde{A}_1 \cdot \|f - g\|_{\infty,3}^*$$

for some constant  $\tilde{A}_1 > 0$  and any  $\mathbf{x} \in \underline{R}_d$ , where  $\underline{N}_f(\mathbf{x})$  is the matrix defined in (65) with directional density  $f$ .

(h) The reach of  $\underline{R}_d$  satisfies

$$\text{reach}(\underline{R}_d) \geq \min \left\{ \underline{\rho}/2, \frac{\underline{\beta}_1^2}{\tilde{A}_2 \left( \|f\|_\infty^{(3)} + \|f\|_\infty^{(4)} \right)} \right\}$$

for some constant  $\tilde{A}_2 > 0$ .

This lemma is a direct extension of Lemma 11 to the directional data scenario; thus, its proof is similar to the proof of Lemma 11.

PROOF OF LEMMA 13. The proofs of properties (a), (b), and (c) can be inherited from the corresponding ones in Lemma 11 with mild modifications and we thus omit them.

(d) We will prove that the  $(q-d)$  nonzero singular values of  $\underline{M}(\mathbf{x})$  and  $(\mathbf{I}_{q+1} - \mathbf{x}\mathbf{x}^T) \underline{M}(\mathbf{x}) \in \mathbb{R}^{(q+1) \times (q-d)}$  are bounded away from 0. Recall that

$$\underline{M}(\mathbf{x}) = \underline{V}_d(\mathbf{x}) \underline{\Lambda}_0(\mathbf{x}) + \sum_{i=1}^d \underline{T}_i(\mathbf{x}) \underline{V}_d(\mathbf{x}) \underline{\Lambda}_i(\mathbf{x})$$

with

$$\begin{aligned} \underline{\Lambda}_0(\mathbf{x}) &= \text{Diag} [\lambda_{d+1}(\mathbf{x}), \dots, \lambda_q(\mathbf{x})] \\ \underline{\Lambda}_i(\mathbf{x}) &= \text{Diag} \left[ \frac{1}{\lambda_{d+1}(\mathbf{x}) - \lambda_i(\mathbf{x})}, \dots, \frac{1}{\lambda_q(\mathbf{x}) - \lambda_i(\mathbf{x})} \right] \\ \underline{T}_i(\mathbf{x}) &= [\underline{\mathbf{v}}_i(\mathbf{x})^T \nabla f(\mathbf{x})] \cdot \underline{\mathbf{v}}_i(\mathbf{x})^T \nabla^3 f(\mathbf{x}) \end{aligned}$$

for  $i = 1, \dots, d$ . Under condition (A2),

$$\begin{aligned} & \left\| (\mathbf{I}_{q+1} - \mathbf{x}\mathbf{x}^T) \cdot \sum_{i=1}^d \underline{T}_i(\mathbf{x}) \underline{V}_d(\mathbf{x}) \underline{\Lambda}_i(\mathbf{x}) \right\|_2 \\ & \leq \left\| \sum_{i=1}^d \underline{T}_i(\mathbf{x}) \underline{V}_d(\mathbf{x}) \underline{\Lambda}_i(\mathbf{x}) \right\|_2 \quad \text{since } \|\mathbf{I}_{q+1} - \mathbf{x}\mathbf{x}^T\|_2 = 1 \\ & \leq \sum_{i=1}^d \|\underline{T}_i(\mathbf{x})\|_2 \cdot \|\underline{V}_d(\mathbf{x})\|_2 \cdot \frac{1}{\underline{\beta}_0} \quad \text{by (A2)} \\ & \leq \sum_{i=1}^d \|\underline{\mathbf{v}}_i(\mathbf{x})^T \nabla f(\mathbf{x})\|_2 \cdot \|\underline{\mathbf{v}}_i(\mathbf{x})^T \nabla^3 f(\mathbf{x})\|_2 \quad \text{since } \|\underline{V}_d(\mathbf{x})\|_2 = 1 \\ & \leq \frac{d \|\nabla f(\mathbf{x})\|_2 \cdot (q+1)^{\frac{3}{2}} \|\nabla f(\mathbf{x})\|_{\max}}{\underline{\beta}_0} \\ & \leq \underline{\beta}_0 - \underline{\beta}_1. \end{aligned}$$

It shows that all the singular values of  $(\mathbf{I}_{q+1} - \mathbf{x}\mathbf{x}^T) \sum_{i=1}^d \underline{T}_i(\mathbf{x}) \underline{V}_d(\mathbf{x}) \underline{\Lambda}_i(\mathbf{x})$  or simply  $\sum_{i=1}^d \underline{T}_i(\mathbf{x}) \underline{V}_d(\mathbf{x}) \underline{\Lambda}_i(\mathbf{x})$  are less than  $\underline{\beta}_0 - \underline{\beta}_1$ . Moreover, under condition (A2) again, all the

$(q-d)$  singular values of  $(\mathbf{I}_{q+1} - \mathbf{x}\mathbf{x}^T) \underline{V}_d(\mathbf{x}) \underline{\Lambda}_0(\mathbf{x}) = \underline{V}_d(\mathbf{x}) \underline{\Lambda}_0(\mathbf{x})$  are greater than  $\underline{\beta}_1$ . By Theorem 3.3.16 in [Horn and Johnson \(1991\)](#), we know that all the singular values of  $\underline{M}(\mathbf{x})$  and  $(\mathbf{I}_{q+1} - \mathbf{x}\mathbf{x}^T) \underline{M}(\mathbf{x})$  are greater than

$$\sigma_i(\underline{V}_d(\mathbf{x}) \underline{\Lambda}_0(\mathbf{x})) - \sigma_1\left(\sum_{i=1}^d \underline{T}_i(\mathbf{x}) \underline{V}_d(\mathbf{x}) \underline{\Lambda}_i(\mathbf{x})\right) \geq \underline{\beta}_0 - (\underline{\beta}_0 - \underline{\beta}_1) = \underline{\beta}_1 > 0,$$

where  $\sigma_i(A), i = 1, \dots, q-d$  are singular values of a matrix  $A \in \mathbb{R}^{(q+1) \times (q-d)}$  in their descending order. Therefore, the minimum eigenvalue of  $\underline{M}(\mathbf{x})^T \underline{M}(\mathbf{x})$  satisfies

$$\lambda_{\min}(\underline{M}(\mathbf{x})^T \underline{M}(\mathbf{x})) = \lambda_{\min}(\underline{M}(\mathbf{x})^T (\mathbf{I}_{q+1} - \mathbf{x}\mathbf{x}^T) \underline{M}(\mathbf{x})) \geq \underline{\beta}_1^2 > 0,$$

and  $\text{rank}(\underline{N}(\mathbf{x})) = \text{rank}(\underline{M}(\mathbf{x})) = \text{rank}((\mathbf{I}_{q+1} - \mathbf{x}\mathbf{x}^T) \underline{M}(\mathbf{x})) = q-d$ . Thus, by the implicit function theorem and the extra constraint  $\underline{R}_d \subset \Omega_q$ ,  $\underline{R}_d$  is a  $d$ -dimensional submanifold on  $\Omega_q$ . It also implies that  $\underline{R}_d$  cannot have intersections, because otherwise the intersected points will violate the rank condition.

Finally, we argue by contradiction that  $\underline{R}_d$  has no endpoints. Assume, on the contrary, that  $\underline{R}_d$  has an end point  $\mathbf{x}_0$ . Our preceding argument has shown that  $\underline{M}(\mathbf{x})$ , the derivative of  $\underline{V}_d(\mathbf{x})^T \nabla f(\mathbf{x})$ , is bounded. In addition,  $\mathbf{x}_0 \in \underline{R}_d$ . However, this contradicts to the implicit function theorem indicating that  $\underline{R}_d$  is a  $d$ -dimensional submanifold on  $\Omega_q$ , because at the end point  $\mathbf{x}_0 \in \underline{R}_d$ , there exists no local coordinate chart for  $\underline{R}_d$  defined on an open set in  $\underline{R}_d$ . The results follow.

(e) By the proof of (d), we already know that all the  $(q-d)$  nonzero singular values of  $\underline{M}(\mathbf{x})$  and  $(\mathbf{I}_D - \mathbf{x}\mathbf{x}^T) \underline{M}(\mathbf{x})$  are greater than  $\underline{\beta}_1 > 0$ , so the results follow easily from the argument of (e) in Lemma 11.

Finally, the proofs of properties (f), (g), and (h) are essentially the same as the corresponding claims in [Chen et al. \(2015\)](#). We thus omitted them.  $\square$

REMARK 7. Example 4 in [Chen \(2020\)](#) showed that any Euclidean density ridge  $R_d$  is a concrete example of the solution manifold. It is not difficult to verify that our defined directional density ridge  $\underline{R}_d$  also belongs to the general class of solution manifolds, where we may rewrite  $\underline{R}_d = \{\mathbf{x} \in \mathbb{R}^{q+1} : \Psi(\mathbf{x}) = 0\}$  with

$$\Psi(\mathbf{x}) = \begin{bmatrix} \underline{v}_{d+1}(\mathbf{x})^T \nabla f(\mathbf{x}) \\ \vdots \\ \underline{v}_q(\mathbf{x})^T \nabla f(\mathbf{x}) \\ \mathbf{x}^T \mathbf{x} - 1 \end{bmatrix}.$$

Therefore, the discussions about the normal space and other statistical properties of a generic solution manifold apply to the (directional) density ridge  $R_d$  or  $\underline{R}_d$ .

## APPENDIX H: STABILITY OF DIRECTIONAL DENSITY RIDGE

**H.1. Subspace Constrained Gradient Flows.** This subsection is modified from Section 4 in [Genovese et al. \(2014\)](#) for directional densities and their ridges on  $\Omega_q$ . A map  $\varpi : \mathbb{R} \rightarrow \Omega_q$  is a subspace constrained gradient flow with the projected Riemannian gradient  $\underline{G}_d$  if  $\varpi(0) = \mathbf{x} \in \Omega_q$  and

$$(66) \quad \varpi'(t) = \underline{G}_d(\varpi(t)) = \underline{U}_d(\varpi(t)) \cdot \text{grad } f(\varpi(t)) = \underline{V}_d(\varpi(t)) \underline{V}_d(\varpi(t))^T \nabla f(\varpi(t)).$$

Given the definition of the directional density ridge  $\underline{R}_d$  in (62), it consists of the destinations of the subspace constrained gradient flow  $\varpi: \mathbf{y} \in \underline{R}_d$  if  $\lim_{t \rightarrow \infty} \varpi(t) = \mathbf{y}$  for some  $\varpi$  satisfying (66). It will be convenient to parametrize the subspace constrained gradient ascent path with  $\varpi$  by arc length. Let  $s \equiv s(t)$  be the arc length from  $\varpi(t)$  to  $\varpi(\infty)$ :

$$s(t) = \int_t^\infty \|\varpi'(u)\|_2 du.$$

Denote the inverse of  $s(t)$  by  $t \equiv t(s)$ . Note that

$$t'(s) = \frac{1}{s'(t)} = -\frac{1}{\|\varpi'(t(s))\|_2} = -\frac{1}{\|\underline{G}_d(\varpi(t(s)))\|_2}.$$

With  $\gamma(s) = \varpi(t(s))$ ,

$$(67) \quad \gamma'(s) = -\frac{\underline{G}_d(\gamma(s))}{\|\underline{G}_d(\gamma(s))\|_2},$$

which is a reparametrization of (66) by arc length. Note that  $\gamma$  always lies on  $\Omega_q$  because its velocity is within the tangent space  $T_{\gamma(s)}$  for every  $s \in [0, \infty)$ . Lemma 2 in [Genovese et al. \(2014\)](#) justifies the uniqueness of  $\gamma$  passing through any particular point  $\mathbf{x} \in (\underline{R}_d \oplus \underline{\rho}) \setminus \underline{R}_d$  under conditions (A1-3). The (reversed) subspace constrained gradient flow  $\gamma$  can be lifted onto the directional function  $f$ , as we may define

$$(68) \quad \xi(s) = f(\varpi(\infty)) - f(\varpi(t(s))) = f(\gamma(0)) - f(\gamma(s)).$$

Sometimes, we may add the subscript  $\mathbf{x}$  to the curves  $\varpi_{\mathbf{x}}, \gamma_{\mathbf{x}}, \xi_{\mathbf{x}}$  if we want to emphasize that  $\varpi, \gamma, \xi$  start from or pass through the specific point  $\mathbf{x}$ .

To analyze the behavior of the subspace constrained gradient flow  $\xi$  lifted on  $f$ , we need the derivative of the projection matrix  $\underline{U}(\mathbf{x}) \equiv \underline{U}_d(\mathbf{x})$  along the path  $\gamma$ . Recall that  $\underline{U}(\mathbf{x}) \equiv \underline{U}(\mathcal{H}f(\mathbf{x})) = \underline{V}_d(\mathbf{x})\underline{V}_d(\mathbf{x})^T$ . The collection  $\{\underline{U}(\mathbf{x}) : \mathbf{x} \in \Omega_q\}$  defines a matrix field: there is a matrix  $\underline{U}(\mathbf{x})$  attached to each point  $\mathbf{x}$ . As mentioned earlier, there is a unique path  $\gamma$  and unique  $s > 0$  such that  $\mathbf{x} = \gamma(s)$  for any  $\mathbf{x} \in (\underline{R}_d \oplus \underline{\rho}) \setminus \underline{R}_d$ . Define

$$(69) \quad \dot{\underline{U}}_{\gamma(s)} \equiv \lim_{\epsilon \rightarrow 0} \frac{\underline{U}(\mathcal{H}f(\gamma(s+\epsilon))) - \underline{U}(\mathcal{H}f(\gamma(s)))}{\epsilon} = \lim_{t \rightarrow 0} \frac{\underline{U}(\mathcal{H}f(\gamma(s)) + tE_s) - \underline{U}(\mathcal{H}f(\gamma(s)))}{t},$$

where  $E_s = \frac{d}{ds} \mathcal{H}f(\gamma(s)) = \nabla \mathcal{H}f(\gamma(s)) \cdot \gamma'(s)$ . Under conditions (A1-3),  $\xi$  has a quadratic-like behavior near the directional ridge  $\underline{R}_d$ , analogous to Lemma 3 in [Genovese et al. \(2014\)](#).

**LEMMA 14.** *Assume that conditions (A1-3) holds. For all  $\mathbf{x} \in (\underline{R}_d \oplus \underline{\rho}) \cap \Omega_q$ , we have the following properties:*

- (a)  $\xi(0) = 0$ ,  $\xi'(s) = \|\underline{G}_d(\gamma(s))\|_2$ , and  $\xi'(0) = 0$ . Thus,  $\xi(s)$  is non-decreasing in  $s$ .
- (b) The second derivative of  $\xi$  satisfies  $\xi''(s) \geq \frac{3\beta_0}{4}$ .
- (c)  $\xi(s) \geq \frac{3\beta_0}{8} \|\gamma(0) - \gamma(s)\|_2^2$ .

**PROOF OF LEMMA 14.** The proof is adopted from Lemma 3 in [Genovese et al. \(2014\)](#).

(a) The first property  $\xi(0) = 0$  is obvious from the definition (68). Then,

$$\begin{aligned} \xi'(s) &= -\nabla f(\gamma(s))^T \gamma'(s) = \frac{\nabla f(\gamma(s))^T \underline{G}_d(\gamma(s))}{\|\underline{G}_d(\gamma(s))\|_2} \quad \text{by (67)} \\ &= \frac{\nabla f(\gamma(s))^T \underline{V}_d(\gamma(s)) \underline{V}_d(\gamma(s))^T \nabla f(\gamma(s))}{\|\underline{G}_d(\gamma(s))\|_2} \\ &= \|\underline{G}_d(\gamma(s))\|_2, \end{aligned}$$

since  $\underline{V}_d(\gamma(s))^T \underline{V}_d(\gamma(s)) = \mathbf{I}_{q-d}$  for all  $\gamma(s) \in \Omega_q$ . By the definition of  $\underline{R}_d$  in (1),  $\underline{G}_d(\gamma(s)) = 0$  when  $\gamma(s) \in \underline{R}_d$ . Thus,  $\xi'(0) = 0$  and  $\xi(s)$  is non-decreasing in  $s$ .

(b) Note that

$$\begin{aligned} (\xi'(s))^2 &= \|\underline{G}_d(\gamma(s))\|_2^2 = \nabla f(\gamma(s))^T \underline{V}_d(\gamma(s)) \underline{V}_d(\gamma(s))^T \nabla f(\gamma(s)) \\ &= [\mathbf{grad} f(\gamma(s))]^T \underline{U}(\gamma(s)) [\mathbf{grad} f(\gamma(s))]. \end{aligned}$$

Differentiating both sides of the equation, we have that

$$\begin{aligned} 2\xi'(s)\xi''(s) &= 2\gamma'(s)^T \mathcal{H}f(\gamma(s)) \underline{U}(\gamma(s)) [\mathbf{grad} f(\gamma(s))] \\ &\quad + [\mathbf{grad} f(\gamma(s))]^T \dot{\underline{U}}_{\gamma(s)}(\gamma(s)) [\mathbf{grad} f(\gamma(s))]. \end{aligned}$$

Since  $\underline{U}(\gamma(s)) \cdot \underline{U}(\gamma(s)) = \underline{U}(\gamma(s))$  (idempotent), we have that  $\dot{\underline{U}}_{\gamma(s)} = \underline{U}(\gamma(s)) \dot{\underline{U}}_{\gamma(s)} + \dot{\underline{U}}_{\gamma(s)} \underline{U}(\gamma(s))$ , and hence the second term on the right-hand side of the above equation becomes

$$\begin{aligned} &[\mathbf{grad} f(\gamma(s))]^T \dot{\underline{U}}_{\gamma(s)}(\gamma(s)) [\mathbf{grad} f(\gamma(s))] \\ &= \nabla f(\gamma(s))^T \underline{U}(\gamma(s)) \dot{\underline{U}}_{\gamma(s)}(\gamma(s)) \nabla f(\gamma(s)) + \nabla f(\gamma(s))^T \dot{\underline{U}}_{\gamma(s)}(\gamma(s)) \underline{U}(\gamma(s)) \nabla f(\gamma(s)) \\ &= 2\nabla f(\gamma(s))^T \dot{\underline{U}}_{\gamma(s)} \underline{G}_d(\gamma(s)) \end{aligned}$$

Thus,

$$2\xi'(s)\xi''(s) = 2\gamma'(s)^T \mathcal{H}f(\gamma(s)) \underline{G}_d(\gamma(s)) + 2\nabla f(\gamma(s))^T \dot{\underline{U}}_{\gamma(s)} \underline{G}_d(\gamma(s)).$$

By (a) and (67), we conclude that

$$(70) \quad \xi''(s) = -\frac{\underline{G}_d(\gamma(s))^T \mathcal{H}f(\gamma(s)) \cdot \underline{G}_d(\gamma(s))}{\|\underline{G}_d(\gamma(s))\|_2^2} + \frac{\nabla f(\gamma(s))^T \dot{\underline{U}}_{\gamma(s)} \underline{G}_d(\gamma(s))}{\|\underline{G}_d(\gamma(s))\|_2}.$$

Now, we will bound the two terms in (70), respectively. As for the first term  $-\frac{\underline{G}_d(\gamma(s))^T \mathcal{H}f(\gamma(s)) \cdot \underline{G}_d(\gamma(s))}{\|\underline{G}_d(\gamma(s))\|_2^2}$ , we notice that  $\underline{G}_d(\gamma(s))$  is in the column space of  $\underline{V}_d(\gamma(s))$ . Hence,

$$\underline{G}_d(\gamma(s))^T \mathcal{H}f(\gamma(s)) \cdot \underline{G}_d(\gamma(s)) = \underline{G}_d(\gamma(s))^T [\underline{V}_d(\gamma(s)) \Lambda_{\underline{R}_d}(\gamma(s)) \underline{V}_d(\gamma(s))^T] \underline{G}_d(\gamma(s)),$$

where  $\Lambda_{\underline{R}_d}(\gamma(s)) = \text{Diag} [\lambda_{d+1}(\gamma(s)), \dots, \lambda_q(\gamma(s))]$ . Therefore, from condition (A2),

$$\begin{aligned} \frac{\underline{G}_d(\gamma(s))^T \mathcal{H}f(\gamma(s)) \cdot \underline{G}_d(\gamma(s))}{\|\underline{G}_d(\gamma(s))\|_2^2} &= \frac{\underline{G}_d(\gamma(s))^T [\underline{V}_d(\gamma(s)) \Lambda_{\underline{R}_d}(\gamma(s)) \underline{V}_d(\gamma(s))^T] \underline{G}_d(\gamma(s))}{\|\underline{G}_d(\gamma(s))\|_2^2} \\ &\leq \lambda_{\max} [\underline{V}_d(\gamma(s)) \Lambda_{\underline{R}_d}(\gamma(s)) \underline{V}_d(\gamma(s))^T] \leq -\underline{\beta}_0 \end{aligned}$$

and consequently,

$$-\frac{\underline{G}_d(\gamma(s))^T \mathcal{H}f(\gamma(s)) \cdot \underline{G}_d(\gamma(s))}{\|\underline{G}_d(\gamma(s))\|_2^2} \geq \underline{\beta}_0.$$

As for the second term  $\frac{\nabla f(\gamma(s))^T \dot{\underline{U}}_{\gamma(s)} \underline{G}_d(\gamma(s))}{\|\underline{G}_d(\gamma(s))\|_2}$ , we notice that  $\underline{U}(\gamma(s)) + \underline{U}^\perp(\gamma(s)) = \mathbf{I}_{q+1}$ , where  $\underline{U}^\perp \equiv \underline{U}_d^\perp$ , and  $\underline{U}(\gamma(s)) \cdot \underline{G}_d(\gamma(s)) = \underline{G}_d(\gamma(s))$ . Then,

$$\begin{aligned} &\nabla f(\gamma(s))^T \dot{\underline{U}}_{\gamma(s)} \underline{G}_d(\gamma(s)) \\ &= \nabla f(\gamma(s))^T \underline{U}(\gamma(s)) \dot{\underline{U}}_{\gamma(s)} \underline{G}_d(\gamma(s)) + \nabla f(\gamma(s))^T \underline{U}^\perp(\gamma(s)) \dot{\underline{U}}_{\gamma(s)} \underline{G}_d(\gamma(s)) \\ &= \nabla f(\gamma(s))^T \underline{U}(\gamma(s)) \dot{\underline{U}}_{\gamma(s)} \underline{U}(\gamma(s)) \cdot \underline{G}_d(\gamma(s)) + \nabla f(\gamma(s))^T \underline{U}^\perp(\gamma(s)) \dot{\underline{U}}_{\gamma(s)} \underline{U}(\gamma(s)) \cdot \underline{G}_d(\gamma(s)). \end{aligned}$$

However,  $\left| \nabla f(\gamma(s))^T \underline{U}(\gamma(s)) \dot{\underline{U}}_{\gamma(s)} \underline{U}(\gamma(s)) \cdot \underline{G}_d(\gamma(s)) \right| = 0$ . To see this, note that  $\underline{U}(\gamma(s)) \cdot \underline{U}(\gamma(s)) = \underline{U}(\gamma(s))$  and it implies that

$$\begin{aligned} \underline{U}(\gamma(s)) \dot{\underline{U}}_{\gamma(s)} + \dot{\underline{U}}_{\gamma(s)} \underline{U}(\gamma(s)) &= \dot{\underline{U}}_{\gamma(s)} \\ \implies \underline{U}(\gamma(s)) \dot{\underline{U}}_{\gamma(s)} \underline{U}(\gamma(s)) + \dot{\underline{U}}_{\gamma(s)} \underline{U}(\gamma(s)) &= \dot{\underline{U}}_{\gamma(s)} \underline{U}(\gamma(s)), \end{aligned}$$

showing that  $\underline{U}(\gamma(s)) \dot{\underline{U}}_{\gamma(s)} \underline{U}(\gamma(s)) = \mathbf{0}$ . To bound  $\nabla f(\gamma(s))^T \underline{U}^\perp(\gamma(s)) \dot{\underline{U}}_{\gamma(s)} \underline{U}(\gamma(s)) \cdot \underline{G}_d(\gamma(s))$ , we proceed as follows. As before, we let  $E_s = \frac{d}{ds} \mathcal{H}f(\gamma(s)) = \nabla \mathcal{H}f(\gamma(s)) \cdot \gamma'(s)$ . Then, by the Davis-Kahan theorem (Lemma 12 here),

$$\begin{aligned} & \left| \nabla f(\gamma(s))^T \underline{U}^\perp(\gamma(s)) \dot{\underline{U}}_{\gamma(s)} \underline{U}(\gamma(s)) \cdot \underline{G}_d(\gamma(s)) \right| \\ &= \lim_{t \rightarrow 0} \frac{\left| \nabla f(\gamma(s))^T \underline{U}^\perp(\gamma(s)) \left[ \underline{U}(\mathcal{H}f(\gamma(s)) + tE_s) - \underline{U}(\mathcal{H}f(\gamma(s))) \right] \underline{U}(\gamma(s)) \cdot \underline{G}_d(\gamma(s)) \right|}{t} \\ &\leq \left\| \underline{U}^\perp(\gamma(s)) \nabla f(\gamma(s)) \right\|_2 \cdot \lim_{t \rightarrow 0} \frac{\left\| \underline{U}(\mathcal{H}f(\gamma(s)) + tE_s) - \underline{U}(\mathcal{H}f(\gamma(s))) \right\|_2}{t} \cdot \left\| \underline{G}_d(\gamma(s)) \right\|_2 \\ &\leq \frac{\left\| \underline{U}^\perp(\gamma(s)) \nabla f(\gamma(s)) \right\|_2 \cdot \|E_s\| \cdot \left\| \underline{G}_d(\gamma(s)) \right\|_2}{\underline{\beta}_0}. \end{aligned}$$

Note that  $\|E_s\|_2 \leq \|\nabla \mathcal{H}f(\gamma(s))\|_2 \cdot \|\gamma'(s)\|_2 \leq (q+1)^{\frac{3}{2}} \|\nabla^3 f(\gamma(s))\|_{\max}$ , because  $\|\gamma'(s)\|_2 = 1$ . Thus, from condition (A2),

$$\frac{\left| \nabla f(\gamma(s))^T \dot{\underline{U}}_{\gamma(s)} \underline{G}_d(\gamma(s)) \right|}{\left\| \underline{G}_d(\gamma(s)) \right\|_2} \leq \frac{(q+1)^{\frac{3}{2}} \|\nabla^3 f(\gamma(s))\|_{\max} \left\| \underline{U}^\perp(\gamma(s)) \nabla f(\gamma(s)) \right\|_2}{\underline{\beta}_0} \leq \frac{\underline{\beta}_0}{4}.$$

Therefore,  $\xi''(s) \geq \underline{\beta}_0 - \frac{\underline{\beta}_0}{4} = \frac{3\underline{\beta}_0}{4}$ .

(c) For some  $0 \leq \tilde{s} \leq s$ ,

$$\xi(s) = \xi(0) + s\xi'(0) + \frac{s^2}{2}\xi''(\tilde{s}) = \frac{s^2}{2}\xi''(\tilde{s}) \geq \frac{3\underline{\beta}_0 s^2}{8}$$

by (a) and (b). As  $\gamma$  is parametrized by arc length, we conclude that

$$\xi(s) - \xi(0) \geq \frac{3\underline{\beta}_0}{8} s^2 \geq \frac{3\underline{\beta}_0}{8} \|\gamma(0) - \gamma(s)\|_2^2.$$

The result follows.  $\square$

The quadratic behavior of the subspace constrained gradient flow  $\xi$  lifted onto the directional density  $f$ , guaranteed by conditions (A1-3), enables us to quantify the stability of directional ridges under small perturbations on the density and develop the linear convergence of sample-based SCGA algorithms on  $\Omega_q$ .

**H.2. Proof of Theorem 6.** We now show that if two directional densities  $f$  and  $\tilde{f}$  are close, their corresponding ridges  $\underline{R}_d$  and  $\tilde{\underline{R}}_d$  are also close. We will use  $\underline{G}_d, \underline{U}_d, \dots$ , etc. to refer to the projected gradient, projection matrix with its columns as the eigenvectors corresponding to the smallest  $q-d$  eigenvalues of the Hessian  $\mathcal{H}\tilde{f}$ , defined by  $\tilde{f}$ .

**THEOREM 6.** Suppose that conditions (A1-3) hold for the directional density  $f$  and that condition (A1) holds for  $\tilde{f}$ . When  $\left\| f - \tilde{f} \right\|_{\infty,3}^*$  is sufficiently small,



- (a) conditions (A2-3) holds for  $\tilde{f}$ .  
 (b)  $\text{Haus}(\underline{R}_d, \tilde{R}_d) = O\left(\left\|f - \tilde{f}\right\|_{\infty,2}^*\right)$ .  
 (c)  $\text{reach}(\tilde{R}_d) \geq \min\left\{\rho/2, \frac{\beta_0^2}{\tilde{A}_2(\|f\|_{\infty}^{(3)} + \|\tilde{f}\|_{\infty}^{(4)})}\right\} + O\left(\left\|f - \tilde{f}\right\|_{\infty,3}^*\right)$  for a constant  $\tilde{A}_2 > 0$ .

PROOF OF THEOREM 6. The proof is modified from Theorem 4 in [Genovese et al. \(2014\)](#) and Theorem 4 in [Chen \(2020\)](#).

- (a) We write the spectral decompositions of  $\mathcal{H}f$  and  $\mathcal{H}\tilde{f}$  as

$$\mathcal{H}f = V\Lambda V^T \quad \text{and} \quad \mathcal{H}\tilde{f} = \tilde{V}\tilde{\Lambda}\tilde{V}^T.$$

By Weyl's Theorem (Theorem 4.3.1 in [Horn and Johnson \(2012\)](#)), we know that

$$|\lambda_j - \tilde{\lambda}_j| \leq \left\|\mathcal{H}f - \mathcal{H}\tilde{f}\right\|_2 \leq (q+1) \left\|f - \tilde{f}\right\|_{\infty,2}^*.$$

Thus,  $\tilde{f}$  satisfies condition (A2). Moreover, since condition (A3) depends only on the first and third order derivative of  $f$ , they hold for  $\tilde{f}$  when  $\left\|f - \tilde{f}\right\|_{\infty,3}^*$  is small enough.

- (b) We have two methods of proving this statement, so we include both methods here.

**Method 1:** By the Davis-Kahan theorem (Lemma 12),

$$\begin{aligned} \left\|\underline{U}_d(\mathbf{x}) - \tilde{\underline{U}}_d(\mathbf{x})\right\|_2 &= \left\|\underline{V}_d(\mathbf{x})\underline{V}_d(\mathbf{x})^T - \tilde{\underline{V}}_d(\mathbf{x})\tilde{\underline{V}}_d(\mathbf{x})^T\right\|_2 \\ &\leq \frac{\left\|\mathcal{H}f(\mathbf{x}) - \mathcal{H}\tilde{f}(\mathbf{x})\right\|}{\underline{\beta}_0} \\ &\leq \frac{(q+1) \left\|f - \tilde{f}\right\|_{\infty,2}^*}{\underline{\beta}_0} \end{aligned}$$

for any  $\mathbf{x} \in \Omega_q$ . Then,

$$\begin{aligned} \left\|\underline{G}_d(\mathbf{x}) - \tilde{\underline{G}}_d(\mathbf{x})\right\|_2 &= \left\|\underline{V}_d(\mathbf{x})\underline{V}_d(\mathbf{x})^T \nabla f(\mathbf{x}) - \tilde{\underline{V}}_d(\mathbf{x})\tilde{\underline{V}}_d(\mathbf{x})^T \nabla \tilde{f}(\mathbf{x})\right\|_2 \\ &\leq \left\|\left[\underline{V}_d(\mathbf{x})\underline{V}_d(\mathbf{x})^T - \tilde{\underline{V}}_d(\mathbf{x})\tilde{\underline{V}}_d(\mathbf{x})^T\right] \nabla f(\mathbf{x})\right\|_2 \\ &\quad + \left\|\tilde{\underline{V}}_d(\mathbf{x})\tilde{\underline{V}}_d(\mathbf{x})^T \left[\nabla f(\mathbf{x}) - \nabla \tilde{f}(\mathbf{x})\right]\right\|_2 \\ &\leq \frac{(q+1) \left\|f - \tilde{f}\right\|_{\infty,2}^*}{\underline{\beta}_0} \cdot \|\nabla f(\mathbf{x})\|_2 + (q+1)^{\frac{1}{2}} \left\|f - \tilde{f}\right\|_{\infty,1}^*. \end{aligned}$$

Therefore, by the differentiability of  $f$  from (A1) and the compactness of  $\Omega_q$ , we obtain from the above calculations that

$$\sup_{\mathbf{x} \in \Omega_q} \left\|\underline{G}_d(\mathbf{x}) - \tilde{\underline{G}}_d(\mathbf{x})\right\|_2 \leq C_1 \left\|f - \tilde{f}\right\|_{\infty,2}^*$$

for some constant  $C_1 > 0$ . Now let  $\tilde{\mathbf{x}} \in \tilde{R}_d$ . Then,  $\left\|\tilde{\underline{G}}_d(\tilde{\mathbf{x}})\right\|_2 = 0$ , and  $\left\|\underline{G}_d(\tilde{\mathbf{x}})\right\|_2 \leq C_1 \left\|f - \tilde{f}\right\|_{\infty,2}^*$ . Let  $\gamma$  be the subspace constrained gradient ascent path through  $\tilde{\mathbf{x}}$  as defined in Section H.1 so that  $\gamma(s) = \tilde{\mathbf{x}}$  for some  $s$ . Note that  $\gamma(0) \in \underline{R}_d$ . From property (a) of

Lemma 14, we have that  $\xi'(s) = \|\underline{G}_d(\tilde{\mathbf{x}})\|_2$ . Moreover, by Taylor's theorem,

$$C_1 \left\| f - \tilde{f} \right\|_{\infty,2}^* \geq \|\underline{G}_d(\tilde{\mathbf{x}})\|_2 = \xi'(s) = \xi'(0) + s\xi''(u)$$

for some  $u$  between 0 and  $s$ . Since  $\xi'(0) = 0$ , from property (b) of Lemma 14,

$$C_1 \left\| f - \tilde{f} \right\|_{\infty,2}^* \geq s\xi''(u) \geq \frac{3s\beta_0}{4},$$

and consequently,  $d_g(\gamma(0), \tilde{\mathbf{x}}) \leq s \leq \frac{4C_1}{3\beta_0} \left\| f - \tilde{f} \right\|_{\infty,2}^*$ , where  $d_g(\mathbf{x}, \mathbf{y})$  denotes the geodesic distance between  $\mathbf{x}$  and  $\mathbf{y}$  on  $\Omega_q$ . Therefore,

$$d_E(\tilde{\mathbf{x}}, \underline{R}_d) \leq \|\gamma(0) - \tilde{\mathbf{x}}\|_2 \leq d_g(\gamma(0), \tilde{\mathbf{x}}) \leq \frac{4C_1}{3\beta_0} \left\| f - \tilde{f} \right\|_{\infty,2}^*.$$

Now let  $\mathbf{x} \in \underline{R}_d$ . The same argument shows that  $d_E(\mathbf{x}, \tilde{\underline{R}}_d) \leq \frac{4C_1}{3\beta_0} \left\| f - \tilde{f} \right\|_{\infty,2}^*$  for some constant  $C_2 > 0$  because conditions (A1-3) hold for  $\tilde{f}$ .

As a result,  $\text{Haus}(\underline{R}_d, \tilde{\underline{R}}_d) \leq \frac{4C_1}{3\beta_0} \left\| f - \tilde{f} \right\|_{\infty,2}^* = O\left(\left\| f - \tilde{f} \right\|_{\infty,2}^*\right)$ .

**Method 2:** Since we are only required to bound the maximum Euclidean distance between  $\underline{R}_d$  and  $\tilde{\underline{R}}_d$ , we may view  $\underline{R}_d$  and  $\tilde{\underline{R}}_d$  as solution manifolds in  $\mathbb{R}^{q+1}$  and tentatively ignore the manifold constraint  $\underline{R}_d, \tilde{\underline{R}}_d \subset \Omega_q$ . Define  $h(\mathbf{x}) = \|\underline{V}_d(\mathbf{x})^T \nabla f(\mathbf{x})\|_2 = \sqrt{\nabla f(\mathbf{x})^T \underline{V}_d(\mathbf{x}) \underline{V}_d(\mathbf{x})^T \nabla f(\mathbf{x})}$ . Given that  $\underline{M}(\mathbf{x}) = \nabla [\underline{V}_d(\mathbf{x})^T \nabla f(\mathbf{x})]^T$ , the gradient of  $h(\mathbf{x})$ ,

$$(71) \quad \nabla h(\mathbf{x}) = \frac{\nabla [\underline{V}_d(\mathbf{x})^T \nabla f(\mathbf{x})]^T \underline{V}_d(\mathbf{x})^T \nabla f(\mathbf{x})}{\|\underline{V}_d(\mathbf{x})^T \nabla f(\mathbf{x})\|_2} = \frac{\underline{M}(\mathbf{x}) \underline{V}_d(\mathbf{x})^T \nabla f(\mathbf{x})}{\|\underline{V}_d(\mathbf{x})^T \nabla f(\mathbf{x})\|_2},$$

is a vector in  $\mathbb{R}^{q+1}$ . Let  $\mathbf{z} \in \tilde{\underline{R}}_d$ . We define a flow  $\phi_{\mathbf{z}} : \mathbb{R} \rightarrow \mathbb{R}^{q+1}$  such that

$$\phi_{\mathbf{z}}(0) = \mathbf{z}, \quad \phi'_{\mathbf{z}}(t) = -\nabla h(\phi_{\mathbf{z}}(t)).$$

It can be argued by Theorem 6 in Chen (2020) that  $\phi_{\mathbf{z}}(\infty) \in \underline{R}_d$  when  $\mathbf{z} \in \underline{R}_d \oplus \delta_0$  for some small  $\delta_0 > 0$ . In addition, we can always choose  $\left\| f - \tilde{f} \right\|_{\infty,3}^*$  to be small enough so that  $\tilde{\underline{R}}_d \subset \underline{R}_d \oplus \delta_0$ . By Theorem 3.39 in Irwin (2001),  $\phi_{\mathbf{z}}(t)$  is uniquely defined because the gradient  $\nabla h(\mathbf{z})$  is well-defined for all  $\mathbf{z} \notin \underline{R}_d$ . We can also reparametrize  $\phi_{\mathbf{z}}(t)$  by arc length as:

$$\gamma_{\mathbf{z}}(0) = \mathbf{z}, \quad \gamma'_{\mathbf{z}}(s) = -\frac{\nabla h(\gamma_{\mathbf{z}}(s))}{\|\nabla h(\gamma_{\mathbf{z}}(s))\|_2}.$$

Let  $\mathcal{S}_{\mathbf{z}} = \inf \{s > 0 : \gamma_{\mathbf{z}}(s) \in \underline{R}_d\}$  be the terminal time/arc-length point and let  $\gamma_{\mathbf{z}}(\mathcal{S}_{\mathbf{z}}) \in \underline{R}_d$  be the destination of  $\gamma_{\mathbf{z}}$  on  $\underline{R}_d$ . The above argument also demonstrates that the flows  $\phi_{\mathbf{z}}$  or  $\gamma_{\mathbf{z}}$  converge to the manifold  $\underline{R}_d$  from the normal direction of  $\underline{R}_d$ , because we can write

$$\gamma'_{\mathbf{z}}(\mathcal{S}_{\mathbf{z}}) = -\frac{\nabla h(\gamma_{\mathbf{z}}(\mathcal{S}_{\mathbf{z}}))}{\|\nabla h(\gamma_{\mathbf{z}}(\mathcal{S}_{\mathbf{z}}))\|_2} = -\sum_{k=d+1}^q \mathbf{a}_k \cdot \underline{\mathbf{m}}_k(\gamma_{\mathbf{z}}(\mathcal{S}_{\mathbf{z}}))$$

$$\text{with } \mathbf{a}_k = -\frac{\mathbf{e}_{k-d}^T \underline{V}_d(\gamma_{\mathbf{z}}(\mathcal{S}_{\mathbf{z}})) \nabla f(\gamma_{\mathbf{z}}(\mathcal{S}_{\mathbf{z}}))}{\|\underline{M}(\gamma_{\mathbf{z}}(\mathcal{S}_{\mathbf{z}})) \underline{V}_d(\gamma_{\mathbf{z}}(\mathcal{S}_{\mathbf{z}})) \nabla f(\gamma_{\mathbf{z}}(\mathcal{S}_{\mathbf{z}}))\|_2}$$

and the column space of  $\underline{M}(\gamma_z(\mathcal{S}_z))$  spans the normal space of  $\underline{R}_d$  at  $\gamma_z(\mathcal{S}_z) \in \underline{R}_d$ . The goal now is to bound  $\mathcal{S}_z$  because its length must be greater or equal to  $\|z - \pi_{\underline{R}_d}(z)\|_2$ . We then define  $\vartheta_z(s) = h(\gamma_z(s)) - h(\gamma_z(\mathcal{S}_z)) = h(\gamma_z(s))$ . Differentiating  $\vartheta_z(s)$  with respect to  $s$  leads to

$$\begin{aligned}
 \vartheta'_z(s) &= \frac{d}{ds} h(\gamma_z(s)) = [\nabla h(\gamma_z(s))]^T \gamma'_z(s) \\
 &= -\|\nabla h(\gamma_z(s))\|_2 \\
 (72) \quad &= -\frac{\|\underline{M}(\gamma_z(s))\underline{V}_d(\gamma_z(s))^T \nabla f(\gamma_z(s))\|_2}{\|\underline{V}_d(\gamma_z(s))^T \nabla f(\gamma_z(s))\|_2} \\
 &\leq -\lambda_{\min}(\underline{M}(\gamma_z(s))^T \underline{M}(\gamma_z(s))) \leq -\tilde{\beta}_1
 \end{aligned}$$

by (d) in Lemma 13. (Note that  $0 < \tilde{\beta}_1 \leq \underline{\beta}_1$  because by the continuity of  $\lambda_{\min}(\underline{M}(\mathbf{y})^T \underline{M}(\mathbf{y}))$ , we can always choose  $\delta_0 > 0$  such that  $\lambda_{\min}(\underline{M}(\mathbf{y})^T \underline{M}(\mathbf{y})) \geq \tilde{\beta}_1$  for all  $\mathbf{y} \in \underline{R}_d \oplus \delta_0$ .) As  $z \in \tilde{\underline{R}}_d$ , by the proof of **Method 1**, we know that

$$\begin{aligned}
 C_1 \|f - \tilde{f}\|_{\infty,2}^* &\geq \|G_d(z)\| = \|\underline{V}_d(z)^T \nabla f(z)\|_2 \\
 &= h(\gamma_z(0)) - h(\gamma_z(\mathcal{S}_z)) \quad \text{since } h(\gamma_z(\mathcal{S}_z)) = 0 \\
 &= \vartheta_z(0) - \vartheta_z(\mathcal{S}_z) \quad \text{since } \vartheta_z(\mathcal{S}_z) = 0 \text{ and } \vartheta_z(0) = h(\gamma_z(0)) \\
 &= -\mathcal{S}_z \vartheta'_z(\mathcal{S}_z^*) \quad \text{by the mean value theorem} \\
 &\geq \mathcal{S}_z \tilde{\beta}_1 \quad \text{by (72),}
 \end{aligned}$$

where  $\mathcal{S}_z^*$  is some value between 0 and  $\mathcal{S}_z$ . Hence,  $\mathcal{S}_z \leq \frac{C_1}{\tilde{\beta}_1} \|f - \tilde{f}\|_{\infty,2}^* = O\left(\|f - \tilde{f}\|_{\infty,2}^*\right)$ , which is independent of  $z \in \tilde{\underline{R}}_d$ . This implies that

$$\sup_{z \in \tilde{\underline{R}}_d} d_E(z, \underline{R}_d) \leq \frac{C_1}{\tilde{\beta}_1} \|f - \tilde{f}\|_{\infty,2}^* = O\left(\|f - \tilde{f}\|_{\infty,2}^*\right).$$

We can exchange the role of  $\underline{R}_d$  and  $\tilde{\underline{R}}_d$  and apply the same argument to show that

$$\sup_{x \in \underline{R}_d} d_E(x, \tilde{\underline{R}}_d) = O\left(\|f - \tilde{f}\|_{\infty,2}^*\right).$$

In total, this leads to the conclusion that  $\text{Haus}(\underline{R}_d, \tilde{\underline{R}}_d) = O\left(\|f - \tilde{f}\|_{\infty,2}^*\right)$ .

(c) By (g) in Lemma 13, the reach of  $\underline{R}_d$  has a lower bound,  $\min\left\{\underline{\rho}/2, \frac{\beta_1^2}{A_2(\|f\|_{\infty}^{(3)} + \|f\|_{\infty}^{(4)})}\right\}$ . Note that  $\underline{\rho}$  and  $\underline{\beta}_1$  depend on the first three order derivatives of  $f$ . Thus, the lower bound for the reach of  $\tilde{\underline{R}}_d$  will be identical to the one for  $\underline{R}_d$  with an error rate  $O\left(\|f - \tilde{f}\|_{\infty,3}^*\right)$ .  $\square$

Note that for the stability of directional ridges, one can relax the condition (A1) by requiring  $f$  to be  $\beta$ -Hölder with  $\beta \geq 3$ .

**REMARK 8.** We apply two different methods to establish the stability theorem of directional density ridges. Method 1 utilizes the subspace constrained gradient flow constructed

in Section H.1 and its quadratic behavior (Lemma 14), while Method 2 defines a normal flow to the ridge  $\underline{R}_d$  induced by the column space of  $\underline{M}(\mathbf{x})$ . Each of these two flows has its pros and cons. The subspace constrained gradient flow aligns more coherently with our directional SCMS algorithm (Algorithm 2) to identify the (estimated) directional ridge from data, because it relies only on the first and second order derivatives of the (estimated) density  $f$ . Nevertheless, the subspace constrained gradient flow does not necessarily converge to  $\underline{R}_d$  in the optimal direction, that is, the normal direction to  $\underline{R}_d$ . This can be seen from the explicit formula (64) of  $\underline{M}(\mathbf{x})$ , which spans the normal space of  $\underline{R}_d$ . The normal flow

$$\phi_z(0) = \mathbf{z}, \quad \phi'_z(t) = -\frac{\underline{M}(\phi_z(t))\underline{V}_d(\phi_z(t))^T \nabla f(\phi_z(t))}{\|\underline{V}_d(\phi_z(t))^T \nabla f(\phi_z(t))\|_2}$$

defined in Method 2, however, converges to  $\underline{R}_d$  in its normal direction by construction. In general, the normal flow tends to the ridge  $\underline{R}_d$  faster than the subspace constrained gradient flow, but such normal flow is rarely used in any practical ridge-finding task due to its involvement with third order derivatives of the (estimated) density  $f$ .

#### APPENDIX I: PROOFS OF PROPOSITION 8, LEMMA 9, AND THEOREM 10

**PROPOSITION 8.** We assume that the directional kernel  $L$  is non-increasing, twice continuously differentiable, and convex with  $L(0) < \infty$ . Given the directional KDE  $\hat{f}_h(\mathbf{x}) = \frac{c_{h,q}(L)}{n} \sum_{i=1}^n L\left(\frac{1-\mathbf{x}^T \mathbf{X}_i}{h^2}\right)$  and the directional SCMS sequence  $\{\hat{\mathbf{x}}^{(t)}\}_{t=0}^\infty$  defined by

$$\hat{\mathbf{x}}^{(t+1)} \leftarrow \hat{\mathbf{x}}^{(t)} + \hat{\underline{V}}_d(\hat{\mathbf{x}}^{(t)})\hat{\underline{V}}_d(\hat{\mathbf{x}}^{(t)})^T \cdot \frac{\nabla \hat{f}_h(\hat{\mathbf{x}}^{(t)})}{\|\nabla \hat{f}_h(\hat{\mathbf{x}}^{(t)})\|_2} \quad \text{and} \quad \hat{\mathbf{x}}^{(t+1)} \leftarrow \frac{\hat{\mathbf{x}}^{(t+1)}}{\|\hat{\mathbf{x}}^{(t+1)}\|_2},$$

we have the following properties:

- (a) The estimated density sequence  $\{\hat{f}_h(\hat{\mathbf{x}}^{(t)})\}_{t=0}^\infty$  is non-decreasing and thus converges.
- (b)  $\lim_{t \rightarrow \infty} \|\hat{\underline{V}}_d(\hat{\mathbf{x}}^{(t)})^T \nabla \hat{f}_h(\hat{\mathbf{x}}^{(t)})\|_2 = 0$ .
- (c) If the kernel  $L$  is also strictly decreasing on  $[0, \infty)$ , then  $\lim_{t \rightarrow \infty} \|\hat{\mathbf{x}}^{(t+1)} - \hat{\mathbf{x}}^{(t)}\|_2 = 0$ .

**PROOF OF PROPOSITION 8.** (a) The sequence  $\{\hat{f}_h(\hat{\mathbf{x}}^{(t)})\}_{t=0}^\infty$  is bounded if the kernel  $L$  is non-increasing with  $L(0) < \infty$ . Hence, it suffices to show that it is non-decreasing. The convexity and differentiability of kernel  $L$  imply that

$$(73) \quad L(x_2) - L(x_1) \geq L'(x_1) \cdot (x_2 - x_1)$$

for all  $x_1, x_2 \in [0, \infty)$ . Then, with  $\nabla \hat{f}_h(\mathbf{x}) = -\frac{c_{h,q}(L)}{nh^2} \sum_{i=1}^n \mathbf{X}_i L'\left(\frac{1-\mathbf{x}^T \mathbf{X}_i}{h^2}\right)$  and the iterative formula (38) in the main paper, we derive that

$$\begin{aligned} & \hat{f}_h(\hat{\mathbf{x}}^{(t+1)}) - \hat{f}_h(\hat{\mathbf{x}}^{(t)}) \\ &= \frac{c_{h,q}(L)}{n} \sum_{i=1}^n \left[ L\left(\frac{1 - \mathbf{X}_i^T \hat{\mathbf{x}}^{(t+1)}}{h^2}\right) - L\left(\frac{1 - \mathbf{X}_i^T \hat{\mathbf{x}}^{(t)}}{h^2}\right) \right] \\ &\geq \frac{c_{h,q}(L)}{nh^2} \sum_{i=1}^n L'\left(\frac{1 - \mathbf{X}_i^T \hat{\mathbf{x}}^{(t)}}{h^2}\right) \mathbf{X}_i^T (\hat{\mathbf{x}}^{(t)} - \hat{\mathbf{x}}^{(t+1)}) \end{aligned}$$

$$\begin{aligned}
&= \nabla \hat{f}_h(\hat{\mathbf{x}}^{(t)})^T \left( \hat{\mathbf{x}}^{(t+1)} - \hat{\mathbf{x}}^{(t)} \right) \\
&= \nabla \hat{f}_h(\hat{\mathbf{x}}^{(t)})^T \left[ \frac{\hat{\mathbf{V}}_d(\hat{\mathbf{x}}^{(t)}) \hat{\mathbf{V}}_d(\hat{\mathbf{x}}^{(t)})^T \nabla \hat{f}_h(\hat{\mathbf{x}}^{(t)}) + \left\| \nabla \hat{f}_h(\hat{\mathbf{x}}^{(t)}) \right\|_2 \cdot \hat{\mathbf{x}}^{(t)}}{\left\| \hat{\mathbf{V}}_d(\hat{\mathbf{x}}^{(t)}) \hat{\mathbf{V}}_d(\hat{\mathbf{x}}^{(t)})^T \nabla \hat{f}_h(\hat{\mathbf{x}}^{(t)}) + \left\| \nabla \hat{f}_h(\hat{\mathbf{x}}^{(t)}) \right\|_2 \cdot \hat{\mathbf{x}}^{(t)} \right\|_2} - \hat{\mathbf{x}}^{(t)} \right] \\
&\stackrel{(i)}{=} \frac{\left\| \hat{\mathbf{V}}_d(\hat{\mathbf{x}}^{(t)})^T \nabla \hat{f}_h(\hat{\mathbf{x}}^{(t)}) \right\|_2^2}{\sqrt{\left\| \hat{\mathbf{V}}_d(\hat{\mathbf{x}}^{(t)})^T \nabla \hat{f}_h(\hat{\mathbf{x}}^{(t)}) \right\|_2^2 + \left\| \nabla \hat{f}_h(\hat{\mathbf{x}}^{(t)}) \right\|_2^2}} \\
&\quad + \frac{\left[ \left\| \nabla \hat{f}_h(\hat{\mathbf{x}}^{(t)}) \right\|_2 - \sqrt{\left\| \hat{\mathbf{V}}_d(\hat{\mathbf{x}}^{(t)})^T \nabla \hat{f}_h(\hat{\mathbf{x}}^{(t)}) \right\|_2^2 + \left\| \nabla \hat{f}_h(\hat{\mathbf{x}}^{(t)}) \right\|_2^2} \right] \cdot \nabla \hat{f}_h(\hat{\mathbf{x}}^{(t)})^T \hat{\mathbf{x}}^{(t)}}{\sqrt{\left\| \hat{\mathbf{V}}_d(\hat{\mathbf{x}}^{(t)})^T \nabla \hat{f}_h(\hat{\mathbf{x}}^{(t)}) \right\|_2^2 + \left\| \nabla \hat{f}_h(\hat{\mathbf{x}}^{(t)}) \right\|_2^2}} \\
&\stackrel{(ii)}{=} \frac{\left\| \hat{\mathbf{V}}_d(\hat{\mathbf{x}}^{(t)})^T \nabla \hat{f}_h(\hat{\mathbf{x}}^{(t)}) \right\|_2^2}{\sqrt{\left\| \hat{\mathbf{V}}_d(\hat{\mathbf{x}}^{(t)})^T \nabla \hat{f}_h(\hat{\mathbf{x}}^{(t)}) \right\|_2^2 + \left\| \nabla \hat{f}_h(\hat{\mathbf{x}}^{(t)}) \right\|_2^2}} \\
&\quad \times \frac{\left[ \left\| \nabla \hat{f}_h(\hat{\mathbf{x}}^{(t)}) \right\|_2 + \sqrt{\left\| \hat{\mathbf{V}}_d(\hat{\mathbf{x}}^{(t)})^T \nabla \hat{f}_h(\hat{\mathbf{x}}^{(t)}) \right\|_2^2 + \left\| \nabla \hat{f}_h(\hat{\mathbf{x}}^{(t)}) \right\|_2^2} - \nabla \hat{f}_h(\hat{\mathbf{x}}^{(t)})^T \hat{\mathbf{x}}^{(t)} \right]}{\left\| \nabla \hat{f}_h(\hat{\mathbf{x}}^{(t)}) \right\|_2 + \sqrt{\left\| \hat{\mathbf{V}}_d(\hat{\mathbf{x}}^{(t)})^T \nabla \hat{f}_h(\hat{\mathbf{x}}^{(t)}) \right\|_2^2 + \left\| \nabla \hat{f}_h(\hat{\mathbf{x}}^{(t)}) \right\|_2^2}} \\
&\stackrel{(iii)}{\geq} \frac{\left\| \hat{\mathbf{V}}_d(\hat{\mathbf{x}}^{(t)})^T \nabla \hat{f}_h(\hat{\mathbf{x}}^{(t)}) \right\|_2^2}{\left\| \nabla \hat{f}_h(\hat{\mathbf{x}}^{(t)}) \right\|_2 + \sqrt{\left\| \hat{\mathbf{V}}_d(\hat{\mathbf{x}}^{(t)})^T \nabla \hat{f}_h(\hat{\mathbf{x}}^{(t)}) \right\|_2^2 + \left\| \nabla \hat{f}_h(\hat{\mathbf{x}}^{(t)}) \right\|_2^2}} \\
&\stackrel{(iv)}{\geq} \frac{\left\| \hat{\mathbf{V}}_d(\hat{\mathbf{x}}^{(t)})^T \nabla \hat{f}_h(\hat{\mathbf{x}}^{(t)}) \right\|_2^2}{(1 + \sqrt{2}) \cdot \left\| \nabla \hat{f}_h(\hat{\mathbf{x}}^{(t)}) \right\|_2} \\
&\geq 0,
\end{aligned}$$

where we use the orthogonality between  $\hat{\mathbf{V}}_d(\hat{\mathbf{x}}^{(t)}) \hat{\mathbf{V}}_d(\hat{\mathbf{x}}^{(t)})^T$  and  $\hat{\mathbf{x}}^{(t)}$  in (i), multiply  $\left\| \nabla \hat{f}_h(\hat{\mathbf{x}}^{(t)}) \right\|_2 + \sqrt{\left\| \hat{\mathbf{V}}_d(\hat{\mathbf{x}}^{(t)})^T \nabla \hat{f}_h(\hat{\mathbf{x}}^{(t)}) \right\|_2^2 + \left\| \nabla \hat{f}_h(\hat{\mathbf{x}}^{(t)}) \right\|_2^2}$  on both the numerators and denominators to obtain (ii), leverage the fact that  $\left\| \nabla \hat{f}_h(\hat{\mathbf{x}}^{(t)}) \right\|_2 \geq \nabla \hat{f}_h(\hat{\mathbf{x}}^{(t)})^T \hat{\mathbf{x}}^{(t)}$  in (iii), use the inequality  $\left\| \hat{\mathbf{V}}_d(\hat{\mathbf{x}}^{(t)})^T \nabla \hat{f}_h(\hat{\mathbf{x}}^{(t)}) \right\|_2 \leq \left\| \nabla \hat{f}_h(\hat{\mathbf{x}}^{(t)}) \right\|_2$  in (iv). It thus completes the proof of (a).

(b) Our derivation in (a) already shows that

$$\left\| \hat{\mathbf{V}}_d(\hat{\mathbf{x}}^{(t)})^T \nabla \hat{f}_h(\hat{\mathbf{x}}^{(t)}) \right\|_2 \leq \sqrt{(1 + \sqrt{2}) \cdot \left\| \nabla \hat{f}_h(\hat{\mathbf{x}}^{(t)}) \right\|_2 \cdot \left[ \hat{f}_h(\hat{\mathbf{x}}^{(t+1)}) - \hat{f}_h(\hat{\mathbf{x}}^{(t)}) \right]}.$$

Notice that, on the one hand, the differentiability of kernel  $L$  and the compactness of  $\Omega_q$  imply that  $\left\| \nabla \hat{f}_h(\mathbf{x}) \right\|_2 \leq B_{h,L}$  for all  $\mathbf{x} \in \Omega_q$ , where  $B_{h,L} > 0$  only depends on the bandwidth  $h$  and kernel  $L$ . On the other hand, our argument in (a) already proves the convergence of  $\left\{ \hat{f}_h(\hat{\mathbf{x}}^{(t)}) \right\}_{t=0}^\infty$ . Therefore,

$$\left\| \hat{\mathbf{V}}_d(\hat{\mathbf{x}}^{(t)})^T \nabla \hat{f}_h(\hat{\mathbf{x}}^{(t)}) \right\|_2 \leq \sqrt{(1 + \sqrt{2}) B_{h,L} \cdot \left[ \hat{f}_h(\hat{\mathbf{x}}^{(t+1)}) - \hat{f}_h(\hat{\mathbf{x}}^{(t)}) \right]} \rightarrow 0$$

as  $t \rightarrow \infty$ . The result follows.

(c) Given the iterative formula (38) in the main paper, we deduce that

$$\begin{aligned} & \left\| \hat{\mathbf{x}}^{(t+1)} - \hat{\mathbf{x}}^{(t)} \right\|_2^2 \\ &= \left\| \frac{\hat{\mathbf{V}}_d(\hat{\mathbf{x}}^{(t)}) \hat{\mathbf{V}}_d(\hat{\mathbf{x}}^{(t)})^T \nabla \hat{f}_h(\hat{\mathbf{x}}^{(t)}) + \left\| \nabla \hat{f}_h(\hat{\mathbf{x}}^{(t)}) \right\|_2 \cdot \hat{\mathbf{x}}^{(t)}}{\left\| \hat{\mathbf{V}}_d(\hat{\mathbf{x}}^{(t)}) \hat{\mathbf{V}}_d(\hat{\mathbf{x}}^{(t)})^T \nabla \hat{f}_h(\hat{\mathbf{x}}^{(t)}) + \left\| \nabla \hat{f}_h(\hat{\mathbf{x}}^{(t)}) \right\|_2 \cdot \hat{\mathbf{x}}^{(t)} \right\|_2} - \hat{\mathbf{x}}^{(t)} \right\|_2^2 \\ &\stackrel{(i)}{=} \frac{\left\| \hat{\mathbf{V}}_d(\hat{\mathbf{x}}^{(t)}) \hat{\mathbf{V}}_d(\hat{\mathbf{x}}^{(t)})^T \nabla \hat{f}_h(\hat{\mathbf{x}}^{(t)}) + \left[ \left\| \nabla \hat{f}_h(\hat{\mathbf{x}}^{(t)}) \right\|_2 - \sqrt{\left\| \hat{\mathbf{V}}_d(\hat{\mathbf{x}}^{(t)})^T \nabla \hat{f}_h(\hat{\mathbf{x}}^{(t)}) \right\|_2^2 + \left\| \nabla \hat{f}_h(\hat{\mathbf{x}}^{(t)}) \right\|_2^2} \right] \hat{\mathbf{x}}^{(t)} \right\|_2^2}{\left\| \hat{\mathbf{V}}_d(\hat{\mathbf{x}}^{(t)})^T \nabla \hat{f}_h(\hat{\mathbf{x}}^{(t)}) \right\|_2^2 + \left\| \nabla \hat{f}_h(\hat{\mathbf{x}}^{(t)}) \right\|_2^2} \\ &\stackrel{(ii)}{=} \frac{2 \left\| \hat{\mathbf{V}}_d(\hat{\mathbf{x}}^{(t)})^T \nabla \hat{f}_h(\hat{\mathbf{x}}^{(t)}) \right\|_2^2}{\left\| \hat{\mathbf{V}}_d(\hat{\mathbf{x}}^{(t)})^T \nabla \hat{f}_h(\hat{\mathbf{x}}^{(t)}) \right\|_2^2 + \left\| \nabla \hat{f}_h(\hat{\mathbf{x}}^{(t)}) \right\|_2^2} \\ &\quad + \underbrace{\frac{2 \left\| \nabla \hat{f}_h(\hat{\mathbf{x}}^{(t)}) \right\|_2^2 - 2 \left\| \nabla \hat{f}_h(\hat{\mathbf{x}}^{(t)}) \right\|_2 \cdot \sqrt{\left\| \hat{\mathbf{V}}_d(\hat{\mathbf{x}}^{(t)})^T \nabla \hat{f}_h(\hat{\mathbf{x}}^{(t)}) \right\|_2^2 + \left\| \nabla \hat{f}_h(\hat{\mathbf{x}}^{(t)}) \right\|_2^2}}{\left\| \hat{\mathbf{V}}_d(\hat{\mathbf{x}}^{(t)})^T \nabla \hat{f}_h(\hat{\mathbf{x}}^{(t)}) \right\|_2^2 + \left\| \nabla \hat{f}_h(\hat{\mathbf{x}}^{(t)}) \right\|_2^2}}_{\leq 0} \\ &\leq \frac{2 \left\| \hat{\mathbf{V}}_d(\hat{\mathbf{x}}^{(t)})^T \nabla \hat{f}_h(\hat{\mathbf{x}}^{(t)}) \right\|_2^2}{\left\| \hat{\mathbf{V}}_d(\hat{\mathbf{x}}^{(t)})^T \nabla \hat{f}_h(\hat{\mathbf{x}}^{(t)}) \right\|_2^2 + \left\| \nabla \hat{f}_h(\hat{\mathbf{x}}^{(t)}) \right\|_2^2}, \end{aligned}$$

where we leverage the orthogonality between  $\hat{\mathbf{V}}_d(\hat{\mathbf{x}}^{(t)}) \hat{\mathbf{V}}_d(\hat{\mathbf{x}}^{(t)})^T \nabla \hat{f}_h(\hat{\mathbf{x}}^{(t)})$  and  $\hat{\mathbf{x}}^{(t)}$  to obtain (i) and (ii). Under the assumption that the kernel  $L$  is strictly decreasing and (twice) continuously differentiable, we know that  $\left\| \nabla \hat{f}_h(\mathbf{x}) \right\|_2$  is lower bounded away from 0 on  $\Omega_q$ . Therefore, with the result in (b), the above calculation indicates that

$$\left\| \hat{\mathbf{x}}^{(t+1)} - \hat{\mathbf{x}}^{(t)} \right\|_2 \leq \frac{\sqrt{2} \left\| \hat{\mathbf{V}}_d(\hat{\mathbf{x}}^{(t)})^T \nabla \hat{f}_h(\hat{\mathbf{x}}^{(t)}) \right\|_2}{\sqrt{\left\| \hat{\mathbf{V}}_d(\hat{\mathbf{x}}^{(t)})^T \nabla \hat{f}_h(\hat{\mathbf{x}}^{(t)}) \right\|_2^2 + \left\| \nabla \hat{f}_h(\hat{\mathbf{x}}^{(t)}) \right\|_2^2}} \rightarrow 0$$

as  $t \rightarrow \infty$ . The result follows.  $\square$

**REMARK 9.** The conditions imposed on kernel  $L$  in Proposition 8 is satisfied by some commonly used kernels, such as the von Mises kernel  $L(r) = e^{-r}$ . However, they can be

further relaxed. On the one hand, it is sufficient to assume that the kernel  $L$  is twice continuously differentiable except for finitely many points on  $[0, \infty)$ . On the other hand, as long as the kernel  $L$  satisfies  $C_{L,q} = -\frac{\int_0^\infty L'(r)r^{\frac{q}{2}-1}dr}{\int_0^\infty L(r)r^{\frac{q}{2}-1}dr} > 0$  and the true directional density  $f$  is always positive on  $\Omega_q$ , Lemma 7 demonstrates that  $\|\nabla \hat{f}_h(\mathbf{x})\|_2 \rightarrow \infty$  with probability tending to 1 when  $h \rightarrow 0$  and  $nh^q \rightarrow \infty$ . Therefore, our upper bound on  $\|\hat{\mathbf{x}}^{(t+1)} - \hat{\mathbf{x}}^{(t)}\|_2$  in our proof of (c) will be asymptotically valid for all  $t \geq 0$ , even without the strict decreasing property of kernel  $L$ . Under such relaxation, our conclusions in Proposition 8 are applicable to directional SCMS algorithms using other kernels with bounded supports on  $[0, \infty)$ .

The nonzero curvature structure of the unit (hyper-sphere)  $\Omega_q$ , on which the objective function (or density)  $f$  lies, induces an extra challenge in establishing the linear convergence of population and sample-based SCGA algorithms. Some useful techniques used in analyzing non-asymptotic convergence of first-order methods in  $\mathbb{R}^{q+1}$ , such as the law of cosines and linearizations of the objective function, would fail on  $\Omega_q$  (Zhang and Sra, 2016). Therefore, we first introduce a practical trigonometric distance bound for an Alexandrov space (Burago et al., 1992) with its sectional curvature bounded from below.

LEMMA 15 (Lemma 5 in Zhang and Sra (2016); see also Bonnabel (2013)). *If  $a, b, c$  are the sides (i.e., side lengths) of a geodesic triangle in an Alexandrov space with sectional curvature lower bounded by  $\kappa$ , and  $A$  is the angle between sides  $b$  and  $c$ , then*

$$(74) \quad a^2 \leq \frac{\sqrt{|\kappa|}c}{\tanh(\sqrt{|\kappa|}c)}b^2 + c^2 - 2bc \cos(A).$$

The sketching proof of Lemma 15 can be founded in Lemma 5 of Zhang and Sra (2016). Note that the sectional curvature  $\kappa = 1$  on  $\Omega_q$ . We inherit the notation in Zhang and Sra (2016) and denote  $\frac{\sqrt{|\kappa|}c}{\tanh(\sqrt{|\kappa|}c)}$  by  $\zeta(\kappa, c)$  for the curvature dependent quantity in the inequality (74). One can show by differentiating  $\zeta(\kappa, c)$  with respect to  $c$  that  $\zeta(\kappa, c)$  is strictly increasing and greater than 1 for any  $c > 0$  and fixed  $\kappa \neq 0$ . With Lemma 15 in hand, we are able to state a straightforward corollary indicating an important relation between two consecutive points in the SCGA sequence  $\{\underline{\mathbf{x}}^{(t)}\}_{t=0}^\infty$  on  $\Omega_q$  defined by (cf. Equation (42) in the main paper):

$$(75) \quad \underline{\mathbf{x}}^{(t+1)} = \text{Exp}_{\underline{\mathbf{x}}^{(t)}} \left( \eta \cdot \underline{V}_d(\underline{\mathbf{x}}^{(t)}) \underline{V}_d(\underline{\mathbf{x}}^{(t)})^T \text{grad } f(\underline{\mathbf{x}}^{(t)}) \right).$$

COROLLARY 16. *For any point  $\mathbf{y}, \underline{\mathbf{x}}^{(t)}$  in a geodesically convex set on  $\Omega_q$ , the update in (75) satisfies*

$$\begin{aligned} & 2\eta \left\langle \underline{V}_d(\underline{\mathbf{x}}^{(t)}) \underline{V}_d(\underline{\mathbf{x}}^{(t)})^T \nabla f(\underline{\mathbf{x}}^{(t)}), \text{Exp}_{\underline{\mathbf{x}}^{(t)}}^{-1}(\mathbf{y}) \right\rangle \\ & \leq d_g(\underline{\mathbf{x}}^{(t)}, \mathbf{y})^2 - d_g(\underline{\mathbf{x}}^{(t+1)}, \mathbf{y})^2 + \zeta \left( 1, d_g(\underline{\mathbf{x}}^{(t)}, \mathbf{y}) \right) \cdot \eta^2 \left\| \underline{V}_d(\underline{\mathbf{x}}^{(t)})^T \text{grad } f(\underline{\mathbf{x}}^{(t)}) \right\|_2^2, \end{aligned}$$

where  $d_g(\mathbf{x}, \mathbf{y}) = \sqrt{\langle \text{Exp}_{\mathbf{x}}^{-1}(\mathbf{y}), \text{Exp}_{\mathbf{x}}^{-1}(\mathbf{y}) \rangle} = \|\text{Exp}_{\mathbf{x}}^{-1}(\mathbf{y})\|_2$  is the geodesic distance between  $\mathbf{x}$  and  $\mathbf{y}$  on  $\Omega_q$ .

Note that  $\underline{R}_d \oplus \underline{\rho}$  in our conditions (A2-3) is a geodesically convex set, where the minimal geodesic between two points in the set  $\underline{R}_d \oplus \underline{\rho}$  always lies within the set.



PROOF OF COROLLARY 16. Recall from (75) that the SCGA iterative formula on  $\Omega_q$  is  $\underline{\mathbf{x}}^{(t+1)} = \text{Exp}_{\underline{\mathbf{x}}^{(t)}}(\eta \cdot \underline{V}_d(\underline{\mathbf{x}}^{(t)}) \underline{V}_d(\underline{\mathbf{x}}^{(t)})^T \text{grad } f(\underline{\mathbf{x}}^{(t)}))$ . Note that for the geodesic triangle  $\triangle \underline{\mathbf{x}}^{(t)} \underline{\mathbf{x}}^{(t+1)} \mathbf{y}$  with  $\mathbf{y} \in \Omega_q$ , we have

$$d_g(\underline{\mathbf{x}}^{(t)}, \underline{\mathbf{x}}^{(t+1)}) = \eta \left\| \underline{V}_d(\underline{\mathbf{x}}^{(t)}) \underline{V}_d(\underline{\mathbf{x}}^{(t)})^T \text{grad } f(\underline{\mathbf{x}}^{(t)}) \right\|_2 = \eta \left\| \underline{V}_d(\underline{\mathbf{x}}^{(t)})^T \text{grad } f(\underline{\mathbf{x}}^{(t)}) \right\|_2$$

and

$$\begin{aligned} & d_g(\underline{\mathbf{x}}^{(t)}, \underline{\mathbf{x}}^{(t+1)}) \cdot d_g(\underline{\mathbf{x}}^{(t)}, \mathbf{y}) \cdot \cos(\angle \underline{\mathbf{x}}^{(t+1)} \underline{\mathbf{x}}^{(t)} \mathbf{y}) \\ &= \left\langle \eta \underline{V}_d(\underline{\mathbf{x}}^{(t)}) \underline{V}_d(\underline{\mathbf{x}}^{(t)})^T \text{grad } f(\underline{\mathbf{x}}^{(t)}), \text{Exp}_{\underline{\mathbf{x}}^{(t)}}^{-1}(\mathbf{y}) \right\rangle. \end{aligned}$$

By letting  $a = \overline{\underline{\mathbf{x}}^{(t+1)} \mathbf{y}}$ ,  $b = \overline{\underline{\mathbf{x}}^{(t+1)} \underline{\mathbf{x}}^{(t)}}$ ,  $c = \overline{\underline{\mathbf{x}}^{(t)} \mathbf{y}}$ , and  $A = \angle \mathbf{y}_{s+1} \mathbf{y}_s \mathbf{x}$  in Lemma 15, we obtain that

$$\begin{aligned} d_g(\underline{\mathbf{x}}^{(t+1)}, \mathbf{y})^2 &\leq \zeta(1, d_g(\underline{\mathbf{x}}^{(t)}, \mathbf{x})) \cdot \eta^2 \left\| \underline{V}_d(\underline{\mathbf{x}}^{(t)})^T \text{grad } f(\underline{\mathbf{x}}^{(t)}) \right\|_2^2 \\ &\quad + d_g(\underline{\mathbf{x}}^{(t)}, \mathbf{y})^2 - 2\eta \left\langle \underline{V}_d(\underline{\mathbf{x}}^{(t)}) \underline{V}_d(\underline{\mathbf{x}}^{(t)})^T \text{grad } f(\underline{\mathbf{x}}^{(t)}), \text{Exp}_{\underline{\mathbf{x}}^{(t)}}^{-1}(\mathbf{y}) \right\rangle. \end{aligned}$$

Some rearrangements will yield the final display.  $\square$

LEMMA 9. Assume conditions (A1-3). Then, we have that for any  $\underline{\mathbf{x}}^{(t)} \in \underline{R}_d \oplus \underline{\rho}$ ,

$$\begin{aligned} & \left\| \underline{U}_d^\perp(\underline{\mathbf{x}}^{(t)}) \cdot \text{Exp}_{\underline{\mathbf{x}}^{(t)}}^{-1}(\underline{\mathbf{x}}^*) \right\|_2 \\ & \leq \frac{(q+1)^{\frac{3}{2}} \left\| \nabla^3 f(\underline{\mathbf{x}}^{(t)}) \right\|_{\max} \cdot d_g(\underline{\mathbf{x}}^{(t)}, \underline{\mathbf{x}}^*)^2}{\underline{\beta}_0} + (q+1)^2 \|f\|_\infty^{(4)} \cdot d_g(\underline{\mathbf{x}}^*, \underline{\mathbf{x}}^{(t)})^3 \\ & = \frac{(q+1)^{\frac{3}{2}} \left\| \nabla^3 f(\underline{\mathbf{x}}^{(t)}) \right\|_{\max} \cdot d_g(\underline{\mathbf{x}}^{(t)}, \underline{\mathbf{x}}^*)^2}{\underline{\beta}_0} + o(d_g(\underline{\mathbf{x}}^{(t)}, \underline{\mathbf{x}}^*)^2). \end{aligned}$$

PROOF OF LEMMA 9. We first decompose the tangent vector  $\text{Exp}_{\underline{\mathbf{x}}^{(t)}}^{-1}(\underline{\mathbf{x}}^*)$  into an infinite sum of SCGA updates (75) on  $\Omega_q$  as

$$\text{Exp}_{\underline{\mathbf{x}}^{(t)}}^{-1}(\underline{\mathbf{x}}^*) = \sum_{s=t}^{\infty} \Gamma_{\underline{\mathbf{x}}^{(s)}}^{\underline{\mathbf{x}}^{(t)}} \left( \text{Exp}_{\underline{\mathbf{x}}^{(s)}}^{-1}(\underline{\mathbf{x}}^{(s+1)}) \right).$$

See Figure 9 for a graphical illustration. This equation is valid because parallel transports preserve inner products and are linear. Using (75) and the fact that  $\underline{U}_d(\underline{\mathbf{x}}^{(t)}) + \underline{U}_d^\perp(\underline{\mathbf{x}}^{(t)}) = \mathbf{I}_{q+1}$ , we obtain that

(76)

$$\begin{aligned} \text{Exp}_{\underline{\mathbf{x}}^{(t)}}^{-1}(\underline{\mathbf{x}}^*) &= \sum_{s=t}^{\infty} \Gamma_{\underline{\mathbf{x}}^{(s)}}^{\underline{\mathbf{x}}^{(t)}} \left( \mathbf{I}_{q+1} \cdot \eta \underline{V}_d(\underline{\mathbf{x}}^{(s)}) \underline{V}_d(\underline{\mathbf{x}}^{(s)})^T \text{grad } f(\underline{\mathbf{x}}^{(s)}) \right) \\ &= \sum_{s=t}^{\infty} \Gamma_{\underline{\mathbf{x}}^{(s)}}^{\underline{\mathbf{x}}^{(t)}} \left( \left[ \underline{U}_d(\underline{\mathbf{x}}^{(t)}) + \underline{U}_d^\perp(\underline{\mathbf{x}}^{(t)}) \right] \cdot \eta \underline{V}_d(\underline{\mathbf{x}}^{(s)}) \underline{V}_d(\underline{\mathbf{x}}^{(s)})^T \text{grad } f(\underline{\mathbf{x}}^{(s)}) \right) \\ &= \sum_{s=t}^{\infty} \Gamma_{\underline{\mathbf{x}}^{(s)}}^{\underline{\mathbf{x}}^{(t)}} \left( \underline{U}_d(\underline{\mathbf{x}}^{(t)}) \cdot \eta \underline{V}_d(\underline{\mathbf{x}}^{(s)}) \underline{V}_d(\underline{\mathbf{x}}^{(s)})^T \text{grad } f(\underline{\mathbf{x}}^{(s)}) \right) \\ &\quad + \sum_{s=t}^{\infty} \Gamma_{\underline{\mathbf{x}}^{(s)}}^{\underline{\mathbf{x}}^{(t)}} \left( \underline{U}_d^\perp(\underline{\mathbf{x}}^{(t)}) \cdot \eta \underline{V}_d(\underline{\mathbf{x}}^{(s)}) \underline{V}_d(\underline{\mathbf{x}}^{(s)})^T \text{grad } f(\underline{\mathbf{x}}^{(s)}) \right), \end{aligned}$$

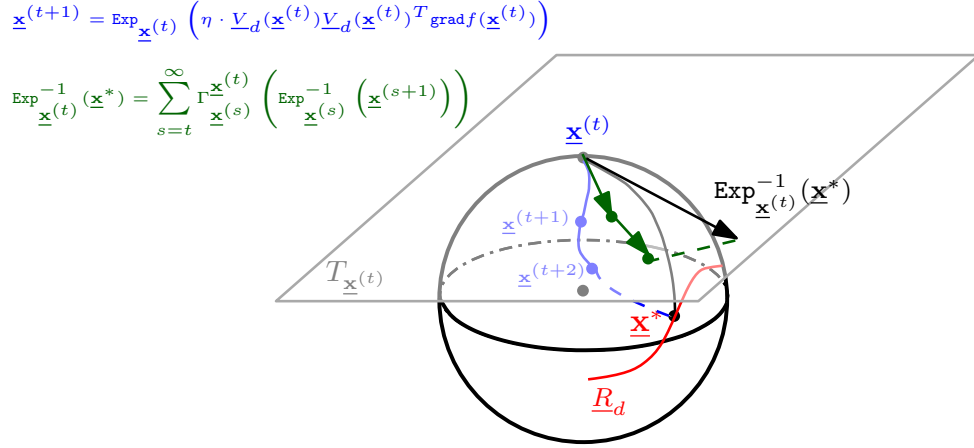


Fig 9: Decomposition of the vector  $\text{Exp}_{\underline{x}^{(t)}}^{-1}(\underline{x}^*)$  within the tangent space  $T_{\underline{x}^{(t)}}$  into the summation  $\sum_{s=t}^{\infty} \Gamma_{\underline{x}^{(s)}}^{\underline{x}^{(t)}} \left( \text{Exp}_{\underline{x}^{(s)}}^{-1}(\underline{x}^{(s+1)}) \right)$  of parallel transported SCGA iterative vectors. Here, the blue curves on  $\Omega_q$  are iterative paths of the SCGA algorithm, while the green vectors are tangent vectors  $\text{Exp}_{\underline{x}^{(s)}}^{-1}(\underline{x}^{(s+1)}) \in T_{\underline{x}^{(s)}}$  after being parallel transported to  $T_{\underline{x}^{(t)}}$ .

where we utilize the linearity of parallel transport mappings  $\Gamma_{\underline{x}^{(s)}}^{\underline{x}^{(t)}}$  for all  $s \geq t$  to obtain the last equality. Now, recall that  $\underline{U}_d(\underline{x}^{(t)}) = \underline{V}_d(\underline{x}^{(t)}) \underline{V}_d(\underline{x}^{(t)})^T$  is a projection matrix onto the last  $(q - d)$  eigenspace of  $\mathcal{H}f(\underline{x}^{(t)})$  within the tangent space  $T_{\underline{x}^{(t)}}$ . Thus, the vector

$$\underline{U}_d(\underline{x}^{(t)}) \cdot \eta \underline{V}_d(\underline{x}^{(s)}) \underline{V}_d(\underline{x}^{(s)})^T \text{grad } f(\underline{x}^{(s)})$$

already lies within  $T_{\underline{x}^{(t)}}$  for any  $s \geq t$ , and by Property (i) of parallel transports in Appendix F, the first term in (76) can be written as:

$$\begin{aligned} & \sum_{s=t}^{\infty} \Gamma_{\underline{x}^{(s)}}^{\underline{x}^{(t)}} \left( \underline{U}_d(\underline{x}^{(t)}) \cdot \eta \underline{V}_d(\underline{x}^{(s)}) \underline{V}_d(\underline{x}^{(s)})^T \text{grad } f(\underline{x}^{(s)}) \right) \\ &= \underline{U}_d(\underline{x}^{(t)}) \sum_{s=t}^{\infty} \eta \underline{V}_d(\underline{x}^{(s)}) \underline{V}_d(\underline{x}^{(s)})^T \text{grad } f(\underline{x}^{(s)}). \end{aligned}$$

Under this important equality, we obtain from (76) and the orthogonality between  $\underline{U}_d(\underline{x}^{(t)})$  and  $\underline{U}_d^{\perp}(\underline{x}^{(t)})$  that

$$\underline{U}_d^{\perp}(\underline{x}^{(t)}) \cdot \text{Exp}_{\underline{x}^{(t)}}^{-1}(\underline{x}^*) = \underline{U}_d^{\perp}(\underline{x}^{(t)}) \cdot \sum_{s=t}^{\infty} \Gamma_{\underline{x}^{(s)}}^{\underline{x}^{(t)}} \left( \underline{U}_d^{\perp}(\underline{x}^{(t)}) \cdot \eta \underline{V}_d(\underline{x}^{(s)}) \underline{V}_d(\underline{x}^{(s)})^T \text{grad } f(\underline{x}^{(s)}) \right). \quad (77)$$

Now, we focus on developing an upper bound for the right-hand side of (77). On the one hand, using the fact that  $\|\underline{U}_d^{\perp}(\underline{x}^{(t)})\|_2 = 1$ , we know that

$$\begin{aligned} & \left\| \underline{U}_d^{\perp}(\underline{x}^{(t)}) \cdot \sum_{s=t}^{\infty} \Gamma_{\underline{x}^{(s)}}^{\underline{x}^{(t)}} \left( \underline{U}_d^{\perp}(\underline{x}^{(t)}) \cdot \eta \underline{V}_d(\underline{x}^{(s)}) \underline{V}_d(\underline{x}^{(s)})^T \text{grad } f(\underline{x}^{(s)}) \right) \right\|_2 \\ & \leq \left\| \sum_{s=t}^{\infty} \Gamma_{\underline{x}^{(s)}}^{\underline{x}^{(t)}} \left( \underline{U}_d^{\perp}(\underline{x}^{(t)}) \cdot \eta \underline{V}_d(\underline{x}^{(s)}) \underline{V}_d(\underline{x}^{(s)})^T \text{grad } f(\underline{x}^{(s)}) \right) \right\|_2 \end{aligned}$$

$$\begin{aligned} &\leq \left\| \sum_{s=t}^{\infty} \Gamma_{\underline{\mathbf{x}}^{(s)}}^{\underline{\mathbf{x}}^{(t)}} \left( \eta \underline{V}_d(\underline{\mathbf{x}}^{(s)}) \underline{V}_d(\underline{\mathbf{x}}^{(s)})^T \mathbf{grad} f(\underline{\mathbf{x}}^{(s)}) \right) \right\|_2 \\ &= d_g(\underline{\mathbf{x}}^{(t)}, \underline{\mathbf{x}}^*), \end{aligned}$$

because the norm of the sum of those vectors will be upper bounded by  $\left\| \text{Exp}_{\underline{\mathbf{x}}^{(t)}}^{-1}(\underline{\mathbf{x}}^*) \right\|_2 = d_g(\underline{\mathbf{x}}^{(t)}, \underline{\mathbf{x}}^*)$  due to the property of parallel transports. On the other hand, by Davis-Kahan theorem (Lemma 12 here) and conditions (A1-3), we have that for all  $s \geq t$ ,

$$\begin{aligned} &\left\| \underline{V}_d(\underline{\mathbf{x}}^{(s)}) \underline{V}_d(\underline{\mathbf{x}}^{(s)})^T - \underline{V}_d(\underline{\mathbf{x}}^{(t)}) \underline{V}_d(\underline{\mathbf{x}}^{(t)})^T \right\|_2 \\ &\leq \frac{\left\| \mathcal{H}f(\underline{\mathbf{x}}^{(s)}) - \mathcal{H}f(\underline{\mathbf{x}}^{(t)}) \right\|_2}{\underline{\beta}_0} \\ &\leq \frac{\left\| \nabla^3 f(\underline{\mathbf{x}}^{(t)}) \right\|_2 d_g(\underline{\mathbf{x}}^{(s)}, \underline{\mathbf{x}}^{(t)})}{\underline{\beta}_0} + O\left(d_g(\underline{\mathbf{x}}^{(s)}, \underline{\mathbf{x}}^{(t)})^2\right) \\ &\leq \frac{(q+1)^{\frac{3}{2}} \left\| \nabla^3 f(\underline{\mathbf{x}}^{(t)}) \right\|_{\max} d_g(\underline{\mathbf{x}}^*, \underline{\mathbf{x}}^{(t)})}{\underline{\beta}_0} + (q+1)^2 \|f\|_{\infty}^{(4)} \cdot d_g(\underline{\mathbf{x}}^*, \underline{\mathbf{x}}^{(t)})^2 \end{aligned}$$

for all  $s \geq t$ , where we apply the Taylor's theorem for function  $f$  on  $\Omega_q$  in the second inequality. Combining these two results, we can bound (77) as:

$$\begin{aligned} &\left\| \underline{U}_d^{\perp}(\underline{\mathbf{x}}^{(t)}) \cdot \text{Exp}_{\underline{\mathbf{x}}^{(t)}}^{-1}(\underline{\mathbf{x}}^*) \right\|_2 \\ &= \left\| \underline{U}_d^{\perp}(\underline{\mathbf{x}}^{(t)}) \cdot \sum_{s=t}^{\infty} \Gamma_{\underline{\mathbf{x}}^{(s)}}^{\underline{\mathbf{x}}^{(t)}} \left( \underline{U}_d^{\perp}(\underline{\mathbf{x}}^{(t)}) \cdot \eta \underline{V}_d(\underline{\mathbf{x}}^{(s)}) \underline{V}_d(\underline{\mathbf{x}}^{(s)})^T \mathbf{grad} f(\underline{\mathbf{x}}^{(s)}) \right) \right\|_2 \\ &\stackrel{(i)}{\leq} \left\| \sum_{s=t}^{\infty} \Gamma_{\underline{\mathbf{x}}^{(s)}}^{\underline{\mathbf{x}}^{(t)}} \left( \underline{U}_d^{\perp}(\underline{\mathbf{x}}^{(t)}) \cdot \eta \underline{V}_d(\underline{\mathbf{x}}^{(s)}) \underline{V}_d(\underline{\mathbf{x}}^{(s)})^T \mathbf{grad} f(\underline{\mathbf{x}}^{(s)}) \right) \right\|_2 \\ &\stackrel{(ii)}{=} \left\| \sum_{s=t}^{\infty} \Gamma_{\underline{\mathbf{x}}^{(s)}}^{\underline{\mathbf{x}}^{(t)}} \left( \underline{U}_d^{\perp}(\underline{\mathbf{x}}^{(t)}) \left[ \underline{V}_d(\underline{\mathbf{x}}^{(s)}) \underline{V}_d(\underline{\mathbf{x}}^{(s)})^T - \underline{V}_d(\underline{\mathbf{x}}^{(t)}) \underline{V}_d(\underline{\mathbf{x}}^{(t)})^T \right] \right. \right. \\ &\quad \left. \left. \times \eta \underline{V}_d(\underline{\mathbf{x}}^{(s)}) \underline{V}_d(\underline{\mathbf{x}}^{(s)})^T \mathbf{grad} f(\underline{\mathbf{x}}^{(s)}) \right) \right\|_2 \\ &\stackrel{(iii)}{\leq} \sup_{s \geq t} \left\| \underline{V}_d(\underline{\mathbf{x}}^{(s)}) \underline{V}_d(\underline{\mathbf{x}}^{(s)})^T - \underline{V}_d(\underline{\mathbf{x}}^{(t)}) \underline{V}_d(\underline{\mathbf{x}}^{(t)})^T \right\|_2 \\ &\quad \times \left\| \sum_{s=t}^{\infty} \Gamma_{\underline{\mathbf{x}}^{(s)}}^{\underline{\mathbf{x}}^{(t)}} \left( \eta \underline{V}_d(\underline{\mathbf{x}}^{(s)}) \underline{V}_d(\underline{\mathbf{x}}^{(s)})^T \mathbf{grad} f(\underline{\mathbf{x}}^{(s)}) \right) \right\|_2 \\ &\leq \frac{(q+1)^{\frac{3}{2}} \left\| \nabla^3 f(\underline{\mathbf{x}}^{(t)}) \right\|_{\max} d_g(\underline{\mathbf{x}}^*, \underline{\mathbf{x}}^{(t)})^2}{\underline{\beta}_0} + (q+1)^2 \|f\|_{\infty}^{(4)} \cdot d_g(\underline{\mathbf{x}}^*, \underline{\mathbf{x}}^{(t)})^3, \end{aligned}$$

where we use the fact that  $\left\| \underline{U}_d^{\perp}(\underline{\mathbf{x}}^{(t)}) \right\|_2 = 1$  to derive (i), apply the orthogonality between  $\underline{U}_d^{\perp}(\underline{\mathbf{x}}^{(t)})$  and  $\underline{V}_d(\underline{\mathbf{x}}^{(t)}) \underline{V}_d(\underline{\mathbf{x}}^{(t)})^T$  as well as the idempotence of  $\underline{V}_d(\underline{\mathbf{x}}^{(s)}) \underline{V}_d(\underline{\mathbf{x}}^{(s)})^T$  for all  $s \geq t$  in (ii), and Cauchy-Schwarz inequality in (iii). It thus completes our proof.  $\square$

**THEOREM 10.** Assume that conditions (A1-3) hold and  $\text{reach}(\underline{R}_d) > 0$  throughout the theorem.

(a) **Q-Linear convergence of  $d_g(\underline{\mathbf{x}}^{(t)}, \underline{\mathbf{x}}^*)$ :** Given a convergence radius  $r_3 > 0$  satisfying

$$r_3 \leq \min \left\{ \underline{\rho}, \text{reach}(\underline{R}_d), \frac{\arccos(1 - \frac{1}{2}\underline{\rho}^2) \cdot \underline{\beta}_0 \|f\|_\infty^{(2)}}{\sqrt{q+1} \|f\|_\infty^{(1)} \|f\|_\infty^{(3)} + \underline{\beta}_0 \|f\|_\infty^{(2)}}, \right. \\ \left. \sqrt{2 - 2 \cos \left( \underline{\beta}_0 / \left[ 8\tilde{A}_{\underline{\rho}} \cdot (q+1)^5 \left( \max \{1, \|f\|_{\infty,4}^*\} \right)^3 \right] \right)} \right\},$$

we have that whenever  $0 < \eta \leq \min \left\{ \frac{4}{\underline{\beta}_0}, \frac{1}{(q+1)\|f\|_\infty^{(2)} \cdot \zeta(1, \underline{\rho})} \right\}$  and the initial point  $\underline{\mathbf{x}}^{(0)} \in \text{Ball}_{q+1}(\underline{\mathbf{x}}^*, r_3) \cap \Omega_q$  with  $\underline{\mathbf{x}}^* \in \underline{R}_d$ ,

$$d_g(\underline{\mathbf{x}}^{(t)}, \underline{\mathbf{x}}^*) \leq \underline{\Upsilon}^t \cdot d_g(\underline{\mathbf{x}}^{(0)}, \underline{\mathbf{x}}^*) \quad \text{with} \quad \underline{\Upsilon} = \sqrt{1 - \frac{\underline{\beta}_0 \eta}{4}}.$$

(b) **R-Linear convergence of  $d_g(\underline{\mathbf{x}}^{(t)}, \underline{R}_d)$ :** Under the same radius  $r_3 > 0$  in (a), we have that whenever  $0 < \eta \leq \min \left\{ \frac{4}{\underline{\beta}_0}, \frac{1}{(q+1)\|f\|_\infty^{(2)} \cdot \zeta(1, \underline{\rho})} \right\}$  and the initial point  $\underline{\mathbf{x}}^{(0)} \in \text{Ball}_{q+1}(\underline{\mathbf{x}}^*, r_3) \cap \Omega_q$  with  $\underline{\mathbf{x}}^* \in \underline{R}_d$ ,

$$d_g(\underline{\mathbf{x}}^{(t)}, \underline{R}_d) \leq \underline{\Upsilon}^t \cdot d_g(\underline{\mathbf{x}}^{(0)}, \underline{\mathbf{x}}^*) \quad \text{with} \quad \underline{\Upsilon} = \sqrt{1 - \frac{\underline{\beta}_0 \eta}{4}}.$$

We further assume (D1-2) in the rest of statements. Suppose that  $h \rightarrow 0$  and  $\frac{nh^{q+4}}{|\log h|} \rightarrow \infty$ .

(c) **Q-Linear convergence of  $d_g(\hat{\underline{\mathbf{x}}}^{(t)}, \underline{\mathbf{x}}^*)$ :** Under the same radius  $r_3 > 0$  and  $\underline{\Upsilon} = \sqrt{1 - \frac{\underline{\beta}_0 \eta}{4}}$  in (a), we have that

$$d_g(\hat{\underline{\mathbf{x}}}^{(t)}, \underline{\mathbf{x}}^*) \leq \underline{\Upsilon}^t \cdot d_g(\hat{\underline{\mathbf{x}}}^{(0)}, \underline{\mathbf{x}}^*) + O(h^2) + O_P \left( \sqrt{\frac{|\log h|}{nh^{q+4}}} \right)$$

with probability tending to 1 whenever  $0 < \eta \leq \min \left\{ \frac{4}{\underline{\beta}_0}, \frac{1}{(q+1)\|f\|_\infty^{(2)} \cdot \zeta(1, \underline{\rho})} \right\}$  and the initial point  $\hat{\underline{\mathbf{x}}}^{(0)} \in \text{Ball}_{q+1}(\underline{\mathbf{x}}^*, r_3) \cap \Omega_q$  with  $\underline{\mathbf{x}}^* \in \underline{R}_d$ .

(d) **R-Linear convergence of  $d_g(\hat{\underline{\mathbf{x}}}^{(t)}, \underline{R}_d)$ :** Under the same radius  $r_3 > 0$  and  $\underline{\Upsilon} = \sqrt{1 - \frac{\underline{\beta}_0 \eta}{4}}$  in (a), we have that

$$d_g(\hat{\underline{\mathbf{x}}}^{(t)}, \underline{R}_d) \leq \underline{\Upsilon}^t \cdot d_g(\hat{\underline{\mathbf{x}}}^{(0)}, \underline{\mathbf{x}}^*) + O(h^2) + O_P \left( \sqrt{\frac{|\log h|}{nh^{q+4}}} \right)$$

with probability tending to 1 whenever  $0 < \eta \leq \min \left\{ \frac{4}{\underline{\beta}_0}, \frac{1}{(q+1)\|f\|_\infty^{(2)} \cdot \zeta(1, \underline{\rho})} \right\}$  and the initial point  $\hat{\underline{\mathbf{x}}}^{(0)} \in \text{Ball}_{q+1}(\underline{\mathbf{x}}^*, r_3) \cap \Omega_q$  with  $\underline{\mathbf{x}}^* \in \underline{R}_d$ .

**PROOF OF THEOREM 10.** The proof is similar to our argument in Theorem 5, except that the objective function  $f$  is supported on a nonlinear manifold  $\Omega_q$  here. The key arguments are credited to Corollary 16 and Lemma 9. We first derive the following two properties.

- *Property 1.* Given (A1), the function  $f$  is  $(q+1)\|f\|_\infty^{(2)}$ -smooth, that is,  $\text{grad } f$  is  $(q+1)\|f\|_\infty^{(2)}$ -Lipschitz.
- *Property 2.* Given conditions (A1-3), we know that

$$\left\| V_d(\underline{x}^{(t)})^T \text{grad } f(\underline{x}^{(t)}) \right\|_2 > 0 \quad \text{for any } \underline{x}^{(t)} \in (\text{Ball}_{q+1}(\underline{x}^*, r_3) \cap \Omega_q) \setminus \underline{R}_d$$

and

$$f(\underline{x}^*) - f\left(\text{Exp}_{\underline{x}^{(t)}}\left(\frac{1}{(q+1)\|f\|_\infty^{(2)}} \cdot V_d(\underline{x}^{(t)})V_d(\underline{x}^{(t)})^T \text{grad } f(\underline{x}^{(t)})\right)\right) \geq 0$$

for any  $\underline{x}^{(t)} \in \text{Ball}_{q+1}(\underline{x}^*, r_3) \cap \Omega_q$  with  $\underline{x}^* \in \underline{R}_d$ .

As for *Property 1*, it follows from the differentiability of  $f$  guaranteed by condition (A1) and Taylor's theorem that

$$\begin{aligned} \|\text{grad } f(\underline{y}) - \Gamma_{\underline{x}}^{\underline{y}}(\text{grad } f(\underline{x}))\|_2 &\leq \|\mathcal{H}f(\underline{y})\|_2 \cdot \|\text{Exp}_{\underline{y}}^{-1}(\tilde{\underline{x}})\|_2 \\ &\leq (q+1)\|f\|_\infty^{(2)} \cdot \|\text{Exp}_{\underline{y}}^{-1}(\underline{x})\|_2 \end{aligned}$$

for any  $\underline{x}, \underline{y} \in \Omega_q$ , where  $\tilde{\underline{x}}$  lies within a  $d_g(\underline{y}, \underline{x})$ -neighborhood of  $\underline{y}$  on  $\Omega_q$ . It implies that (Zhang and Sra, 2016; Alimisis et al., 2020):

$$(78) \quad f(\underline{y}) - f(\underline{x}) - \langle \text{grad } f(\underline{x}), \text{Exp}_{\underline{x}}^{-1}(\underline{y}) \rangle \geq -\frac{(q+1)\|f\|_\infty^{(2)}}{2} \|\text{Exp}_{\underline{x}}^{-1}(\underline{y})\|_2^2.$$

Moreover, when  $0 < \eta \leq \frac{2}{(q+1)\|f\|_\infty^{(2)}}$ ,

$$\begin{aligned} &f(\underline{x}^{(t+1)}) - f(\underline{x}^{(t)}) \\ &= f\left(\text{Exp}_{\underline{x}^{(t)}}\left(\eta V_d(\underline{x}^{(t)})V_d(\underline{x}^{(t)})^T \text{grad } f(\underline{x}^{(t)})\right)\right) - f(\underline{x}^{(t)}) \\ &\geq \left\langle \text{grad } f(\underline{x}^{(t)}), \eta V_d(\underline{x}^{(t)})V_d(\underline{x}^{(t)})^T \text{grad } f(\underline{x}^{(t)}) \right\rangle \\ &\quad - \frac{(q+1)\|f\|_\infty^{(2)}}{2} \cdot \eta^2 \left\| V_d(\underline{x}^{(t)})^T \text{grad } f(\underline{x}^{(t)}) \right\|_2^2 \\ &= \eta \left(1 - \frac{(q+1)\|f\|_\infty^{(2)}}{2}\right) \left\| V_d(\underline{x}^{(t)})^T \text{grad } f(\underline{x}^{(t)}) \right\|_2^2 > 0, \end{aligned}$$

showing that the objective function  $f$  is non-decreasing along the subspace constrained gradient ascent path on  $\Omega_q$ .

*Property 2* is a natural corollary under conditions (A1-3). This is because  $\underline{R}_d$  is the unique projected local mode of  $f$  on the column space of  $V_d(\underline{x})$  within  $\underline{R}_d \oplus \underline{\rho}$  on  $\Omega_q$  by condition

(A2). In addition, we develop the following bound:

$$\begin{aligned}
(79) \quad & \left\| \frac{1}{(q+1)\|f\|_\infty^{(2)}} \cdot \underline{V}_d(\underline{\mathbf{x}}^{(t)}) \underline{V}_d(\underline{\mathbf{x}}^{(t)})^T \text{grad } f(\underline{\mathbf{x}}^{(t)}) \right\|_2 \\
& \stackrel{(i)}{=} \frac{1}{(q+1)\|f\|_\infty^{(2)}} \left\| \underline{V}_d(\underline{\mathbf{x}}^{(t)}) \underline{V}_d(\underline{\mathbf{x}}^{(t)})^T \nabla f(\underline{\mathbf{x}}^{(t)}) - \underbrace{\underline{V}_d(\underline{\mathbf{x}}^*) \underline{V}_d(\underline{\mathbf{x}}^*)^T \nabla f(\underline{\mathbf{x}}^*)}_{=0} \right\|_2 \\
& \leq \frac{1}{(q+1)\|f\|_\infty^{(2)}} \left[ \left\| \underline{V}_d(\underline{\mathbf{x}}^{(t)}) \underline{V}_d(\underline{\mathbf{x}}^{(t)})^T - \underline{V}_d(\underline{\mathbf{x}}^*) \underline{V}_d(\underline{\mathbf{x}}^*)^T \right\|_2 \cdot \left\| \nabla f(\underline{\mathbf{x}}^{(t)}) \right\|_2 \right. \\
& \quad \left. + \left\| \underline{V}_d(\underline{\mathbf{x}}^*) \underline{V}_d(\underline{\mathbf{x}}^*)^T \right\|_2 \cdot \left\| \nabla f(\underline{\mathbf{x}}^{(t)}) - \nabla f(\underline{\mathbf{x}}^*) \right\|_2 \right] \\
& \stackrel{(ii)}{\leq} \frac{1}{(q+1)\|f\|_\infty^{(2)}} \left[ \|f\|_\infty^{(1)} \cdot \frac{\left\| \nabla \nabla f(\underline{\mathbf{x}}^{(t)}) - \nabla \nabla f(\underline{\mathbf{x}}^*) \right\|}{\underline{\beta}_0} + \left\| \nabla f(\underline{\mathbf{x}}^{(t)}) - \nabla f(\underline{\mathbf{x}}^*) \right\|_2 \right] \\
& \stackrel{(iii)}{\leq} \frac{1}{(q+1)\|f\|_\infty^{(2)}} \left[ \frac{(q+1)^{\frac{3}{2}} \|f\|_\infty^{(3)} \|f\|_\infty^{(1)}}{\underline{\beta}_0} + (q+1)\|f\|_\infty^{(2)} \right] \cdot \left\| \underline{\mathbf{x}}^{(t)} - \underline{\mathbf{x}}^* \right\|_2 \\
& = \left( \frac{\sqrt{q+1} \|f\|_\infty^{(3)} \|f\|_\infty^{(1)}}{\underline{\beta}_0 \|f\|_\infty^{(2)}} + 1 \right) \cdot r_3 \\
& \stackrel{(iv)}{\leq} \arccos \left( 1 - \frac{1}{2} \rho^2 \right),
\end{aligned}$$

where we apply the fact that  $\underline{V}_d(\underline{\mathbf{x}}^{(t)})^T \text{grad } f(\underline{\mathbf{x}}^{(t)}) = \underline{V}_d(\underline{\mathbf{x}}^{(t)})^T \nabla f(\underline{\mathbf{x}}^{(t)})$  (c.f., (28) in the main paper) and the definition of  $\underline{R}_d$  in (i), leverage the Davis-Kahan and Taylor's theorem in (ii) and (iii), and use our choice of  $r_3$  to obtain (iv). It indicates that the one-step SCGA iteration  $\text{Exp}_{\underline{\mathbf{x}}^{(t)}} \left( \frac{1}{(q+1)\|f\|_\infty^{(2)}} \cdot \underline{V}_d(\underline{\mathbf{x}}^{(t)}) \underline{V}_d(\underline{\mathbf{x}}^{(t)})^T \text{grad } f(\underline{\mathbf{x}}^{(t)}) \right)$  on  $\Omega_q$  will stay within the region  $\underline{R}_d \oplus \underline{\rho}$  whenever  $\underline{\mathbf{x}}^{(t)} \in \text{Ball}_{q+1}(\underline{\mathbf{x}}^*, r_3) \cap \Omega_q$ . Notice that the notation  $\underline{R}_d \oplus \underline{\rho}$  is defined via the Euclidean metric and the geodesic distance from a point on the boundary  $\partial(\underline{R}_d \oplus \underline{\rho})$  to the directional ridge  $\underline{R}_d$  is  $\arccos(1 - \frac{1}{2}\rho^2)$ . Together with the ascending property (79), we conclude that  $f(\underline{\mathbf{x}}^*) - f(\text{Exp}_{\underline{\mathbf{x}}^{(t)}} \left( \frac{1}{(q+1)\|f\|_\infty^{(2)}} \cdot \underline{V}_d(\underline{\mathbf{x}}^{(t)}) \underline{V}_d(\underline{\mathbf{x}}^{(t)})^T \text{grad } f(\underline{\mathbf{x}}^{(t)}) \right)) \geq 0$  whenever  $\underline{\mathbf{x}}^{(t)} \in \text{Ball}_{q+1}(\underline{\mathbf{x}}^*, r_3) \cap \Omega_q$ .

With the help of these two properties, we start the proofs of (a-d).

(a) We first prove the following claim using Lemma 9: for all  $t \geq 0$  and  $\underline{\mathbf{x}}^{(0)} \in \text{Ball}_{q+1}(\underline{\mathbf{x}}^*, r_3) \cap \Omega_q$ ,

$$(80) \quad f(\underline{\mathbf{x}}^*) - f(\underline{\mathbf{x}}^{(t)}) \leq \left\langle \underline{V}_d(\underline{\mathbf{x}}^{(t)}) \underline{V}_d(\underline{\mathbf{x}}^{(t)})^T \text{grad } f(\underline{\mathbf{x}}^{(t)}), \text{Exp}_{\underline{\mathbf{x}}^{(t)}}^{-1}(\underline{\mathbf{x}}^*) \right\rangle - \frac{\underline{\beta}_0}{4} d_g(\underline{\mathbf{x}}^*, \underline{\mathbf{x}}^{(t)})^2 + \epsilon_t,$$

where  $\epsilon_t = \tilde{A}_{\underline{\rho}} \cdot (q+1)^5 \left( \max \left\{ 1, \|f\|_{\infty,4}^* \right\} \right)^3 d_g(\underline{\mathbf{x}}^*, \underline{\mathbf{x}}^{(t)})^3 = o(d_g(\underline{\mathbf{x}}^*, \underline{\mathbf{x}}^{(t)})^2)$  for some constant  $\tilde{A}_{\underline{\rho}} > 0$  that depends on  $\underline{\rho}$ . By the differentiability of  $f$  ensured by condition (A1)

and Taylor's theorem, we deduce that

$$\begin{aligned}
 & f(\underline{\mathbf{x}}^*) - f(\underline{\mathbf{x}}^{(t)}) \\
 & \leq \left\langle \text{grad } f(\underline{\mathbf{x}}^{(t)}), \text{Exp}_{\underline{\mathbf{x}}^{(t)}}^{-1}(\underline{\mathbf{x}}^*) \right\rangle + \frac{1}{2} \text{Exp}_{\underline{\mathbf{x}}^{(t)}}^{-1}(\underline{\mathbf{x}}^*)^T \left[ \mathcal{H}f(\underline{\mathbf{x}}^{(t)}) \right] \text{Exp}_{\underline{\mathbf{x}}^{(t)}}^{-1}(\underline{\mathbf{x}}^*) \\
 & \quad + \frac{(q+1)^{\frac{3}{2}} \|f\|_{\infty}^{(3)}}{6} \cdot \left\| \text{Exp}_{\underline{\mathbf{x}}^{(t)}}^{-1}(\underline{\mathbf{x}}^*) \right\|_2^3 \\
 & \stackrel{(i)}{=} \left\langle \underline{V}_d(\underline{\mathbf{x}}^{(t)}) \underline{V}_d(\underline{\mathbf{x}}^{(t)})^T \text{grad } f(\underline{\mathbf{x}}^{(t)}), \text{Exp}_{\underline{\mathbf{x}}^{(t)}}^{-1}(\underline{\mathbf{x}}^*) \right\rangle + \left\langle \underline{U}_d^\perp(\underline{\mathbf{x}}^{(t)}) \text{grad } f(\underline{\mathbf{x}}^{(t)}), \text{Exp}_{\underline{\mathbf{x}}^{(t)}}^{-1}(\underline{\mathbf{x}}^*) \right\rangle \\
 & \quad + \frac{1}{2} \text{Exp}_{\underline{\mathbf{x}}^{(t)}}^{-1}(\underline{\mathbf{x}}^*)^T \left( \underline{V}_\diamond(\underline{\mathbf{x}}^{(t)}), \underline{V}_d(\underline{\mathbf{x}}^{(t)}) \right) \begin{pmatrix} 0 & & \\ & \lambda_1(\underline{\mathbf{x}}^{(t)}) & \\ & & \ddots \\ & & & \lambda_q(\underline{\mathbf{x}}^{(t)}) \end{pmatrix} \begin{pmatrix} \underline{V}_\diamond(\underline{\mathbf{x}}^{(t)}) \\ \underline{V}_d(\underline{\mathbf{x}}^{(t)}) \end{pmatrix} \text{Exp}_{\underline{\mathbf{x}}^{(t)}}^{-1}(\underline{\mathbf{x}}^*) \\
 & \quad + \frac{(q+1)^{\frac{3}{2}} \|f\|_{\infty}^{(3)}}{6} \cdot d_g(\underline{\mathbf{x}}^*, \underline{\mathbf{x}}^{(t)})^3 \\
 & \stackrel{(ii)}{\leq} \left\langle \underline{V}_d(\underline{\mathbf{x}}^{(t)}) \underline{V}_d(\underline{\mathbf{x}}^{(t)})^T \text{grad } f(\underline{\mathbf{x}}^{(t)}), \text{Exp}_{\underline{\mathbf{x}}^{(t)}}^{-1}(\underline{\mathbf{x}}^*) \right\rangle + \text{grad } f(\underline{\mathbf{x}}^{(t)})^T \underline{U}_d^\perp(\underline{\mathbf{x}}^{(t)}) \text{Exp}_{\underline{\mathbf{x}}^{(t)}}^{-1}(\underline{\mathbf{x}}^*) \\
 & \quad + \frac{\max\{0, \lambda_1(\underline{\mathbf{x}}^{(t)})\}}{2} \left\| \underline{U}_d^\perp(\underline{\mathbf{x}}^{(t)}) \text{Exp}_{\underline{\mathbf{x}}^{(t)}}^{-1}(\underline{\mathbf{x}}^*) \right\|_2^2 - \frac{\beta_0}{2} \left\| \underline{V}_d(\underline{\mathbf{x}}^{(t)})^T \text{Exp}_{\underline{\mathbf{x}}^{(t)}}^{-1}(\underline{\mathbf{x}}^*) \right\|_2^2 \\
 & \quad + \frac{(q+1)^{\frac{3}{2}} \|f\|_{\infty}^{(3)}}{6} \cdot d_g(\underline{\mathbf{x}}^*, \underline{\mathbf{x}}^{(t)})^3 \\
 & \stackrel{(iii)}{\leq} \left\langle \underline{V}_d(\underline{\mathbf{x}}^{(t)}) \underline{V}_d(\underline{\mathbf{x}}^{(t)})^T \text{grad } f(\underline{\mathbf{x}}^{(t)}), \text{Exp}_{\underline{\mathbf{x}}^{(t)}}^{-1}(\underline{\mathbf{x}}^*) \right\rangle \\
 & \quad + \left\| \underline{U}_d^\perp(\underline{\mathbf{x}}^{(t)}) \text{grad } f(\underline{\mathbf{x}}^{(t)}) \right\|_2 \cdot \left\| \underline{U}_d^\perp(\underline{\mathbf{x}}^{(t)}) \text{Exp}_{\underline{\mathbf{x}}^{(t)}}^{-1}(\underline{\mathbf{x}}^*) \right\|_2 \\
 & \quad + \frac{(\beta_0 + \max\{0, \lambda_1(\underline{\mathbf{x}}^{(t)})\})}{2} \left\| \underline{U}_d^\perp(\underline{\mathbf{x}}^{(t)}) \text{Exp}_{\underline{\mathbf{x}}^{(t)}}^{-1}(\underline{\mathbf{x}}^*) \right\|_2^2 - \frac{\beta_0}{2} \left\| \text{Exp}_{\underline{\mathbf{x}}^{(t)}}^{-1}(\underline{\mathbf{x}}^*) \right\|_2^2 \\
 & \quad + \frac{(q+1)^{\frac{3}{2}} \|f\|_{\infty}^{(3)}}{6} \cdot d_g(\underline{\mathbf{x}}^*, \underline{\mathbf{x}}^{(t)})^3 \\
 & \stackrel{(iv)}{\leq} \left\langle \underline{V}_d(\underline{\mathbf{x}}^{(t)}) \underline{V}_d(\underline{\mathbf{x}}^{(t)})^T \text{grad } f(\underline{\mathbf{x}}^{(t)}), \text{Exp}_{\underline{\mathbf{x}}^{(t)}}^{-1}(\underline{\mathbf{x}}^*) \right\rangle \\
 & \quad + \left\| \underline{U}_d^\perp(\underline{\mathbf{x}}^{(t)}) \text{grad } f(\underline{\mathbf{x}}^{(t)}) \right\|_2 \left[ \frac{(q+1)^{\frac{3}{2}} \|\nabla^3 f(\underline{\mathbf{x}}^{(t)})\|_{\max}}{\beta_0} \cdot d_g(\underline{\mathbf{x}}^*, \underline{\mathbf{x}}^{(t)})^2 \right. \\
 & \quad \quad \left. + (q+1)^2 \|f\|_{\infty}^{(4)} d_g(\underline{\mathbf{x}}^*, \underline{\mathbf{x}}^{(t)})^3 \right] \\
 & \quad + \frac{(\beta_0 + \max\{0, \lambda_1(\underline{\mathbf{x}}^{(t)})\})}{2} \left[ \frac{(q+1)^{\frac{3}{2}} \|\nabla^3 f(\underline{\mathbf{x}}^{(t)})\|_{\max}}{\beta_0} \cdot d_g(\underline{\mathbf{x}}^*, \underline{\mathbf{x}}^{(t)})^2 \right. \\
 & \quad \quad \left. + (q+1)^2 \|f\|_{\infty}^{(4)} d_g(\underline{\mathbf{x}}^*, \underline{\mathbf{x}}^{(t)})^3 \right]^2
 \end{aligned}$$



$$\begin{aligned}
& -\frac{\beta_0}{2}d_g(\underline{\mathbf{x}}^*, \underline{\mathbf{x}}^{(t)})^2 + \frac{(q+1)^{\frac{3}{2}}\|f\|_\infty^{(3)}}{6} \cdot d_g(\underline{\mathbf{x}}^*, \underline{\mathbf{x}}^{(t)})^3 \\
& \stackrel{(v)}{\leq} \left\langle \underline{V}_d(\underline{\mathbf{x}}^{(t)})\underline{V}_d(\underline{\mathbf{x}}^{(t)})^T \mathbf{grad} f(\underline{\mathbf{x}}^{(t)}), \mathbf{Exp}_{\underline{\mathbf{x}}^{(t)}}^{-1}(\underline{\mathbf{x}}^*) \right\rangle - \frac{\beta_0}{4}d_g(\underline{\mathbf{x}}^*, \underline{\mathbf{x}}^{(t)})^2 \\
& + \left[ (q+1)^2\|f\|_\infty^{(1)}\|f\|_\infty^{(4)} + \frac{(q+1)^{\frac{3}{2}}\|f\|_\infty^{(3)}}{6} \right] d_g(\underline{\mathbf{x}}^*, \underline{\mathbf{x}}^{(t)})^3 \\
& + (q+1)\|f\|_\infty^{(2)} \arccos\left(1 - \frac{1}{2}\rho^2\right) \left[ \frac{(q+1)^{\frac{3}{2}}\|f\|_\infty^{(3)}}{\beta_0} \right. \\
& \quad \left. + (q+1)^2\|f\|_\infty^{(4)} \arccos\left(1 - \frac{1}{2}\rho^2\right) \right]^2 d_g(\underline{\mathbf{x}}^*, \underline{\mathbf{x}}^{(t)})^3 \\
& \leq \left\langle \underline{V}_d(\underline{\mathbf{x}}^{(t)})\underline{V}_d(\underline{\mathbf{x}}^{(t)})^T \mathbf{grad} f(\underline{\mathbf{x}}^{(t)}), \mathbf{Exp}_{\underline{\mathbf{x}}^{(t)}}^{-1}(\underline{\mathbf{x}}^*) \right\rangle - \frac{\beta_0}{4}d_g(\underline{\mathbf{x}}^*, \underline{\mathbf{x}}^{(t)})^2 \\
& + \tilde{A}_\rho \cdot (q+1)^5 \left( \max\left\{1, \|f\|_{\infty,4}^*\right\} \right)^3 d_g(\underline{\mathbf{x}}^*, \underline{\mathbf{x}}^{(t)})^3,
\end{aligned}$$

where we leverage the equality  $\mathbf{I}_{q+1} = \underline{V}_d(\underline{\mathbf{x}}^{(t)})\underline{V}_d(\underline{\mathbf{x}}^{(t)})^T + \underline{U}_d^\perp(\underline{\mathbf{x}}^{(t)})$  in (i) and (iii), use condition (A2) that  $\underline{\lambda}_q(\underline{\mathbf{x}}^{(t)}) \leq \dots \leq \underline{\lambda}_{d+1}(\underline{\mathbf{x}}^{(t)})$  in (ii), apply Lemma 9 to obtain (iv), and use the first inequality of condition (A3) in (v). We also use the fact that  $\max\left\{\frac{\beta_0}{2}, 0, \underline{\lambda}_1(\underline{\mathbf{x}}^{(t)})\right\} \leq (q+1)\|f\|_\infty^{(2)}$  and  $d_g(\underline{\mathbf{x}}^*, \underline{\mathbf{x}}^{(t)}) \leq \arccos\left(1 - \frac{1}{2}\rho^2\right)$  in (v). Our claim (80) is thus proved.

In addition, given *Property 2* and any  $\underline{\mathbf{x}}^{(t)} \in \underline{R}_d \oplus r_3$ , we derive that

$$\begin{aligned}
& f(\underline{\mathbf{x}}^{(t)}) - f(\underline{\mathbf{x}}^*) \\
& \leq f(\underline{\mathbf{x}}^{(t)}) - f(\underline{\mathbf{x}}^*) + f(\underline{\mathbf{x}}^*) - f\left(\mathbf{Exp}_{\underline{\mathbf{x}}^{(t)}}\left(\frac{1}{(q+1)\|f\|_\infty^{(2)}} \cdot \underline{V}_d(\underline{\mathbf{x}}^{(t)})\underline{V}_d(\underline{\mathbf{x}}^{(t)})^T \mathbf{grad} f(\underline{\mathbf{x}}^{(t)})\right)\right) \\
& = -\left[f\left(\mathbf{Exp}_{\underline{\mathbf{x}}^{(t)}}\left(\frac{1}{(q+1)\|f\|_\infty^{(2)}} \cdot \underline{V}_d(\underline{\mathbf{x}}^{(t)})\underline{V}_d(\underline{\mathbf{x}}^{(t)})^T \mathbf{grad} f(\underline{\mathbf{x}}^{(t)})\right)\right) - f(\underline{\mathbf{x}}^{(t)})\right] \\
& \leq -\left[\left\langle \mathbf{grad} f(\underline{\mathbf{x}}^{(t)}), \frac{1}{(q+1)\|f\|_\infty^{(2)}} \underline{V}_d(\underline{\mathbf{x}}^{(t)})\underline{V}_d(\underline{\mathbf{x}}^{(t)})^T \mathbf{grad} f(\underline{\mathbf{x}}^{(t)}) \right\rangle \right. \\
& \quad \left. - \frac{(q+1)\|f\|_\infty^{(2)}}{2} \cdot \left\| \frac{1}{(q+1)\|f\|_\infty^{(2)}} \underline{V}_d(\underline{\mathbf{x}}^{(t)})\underline{V}_d(\underline{\mathbf{x}}^{(t)})^T \mathbf{grad} f(\underline{\mathbf{x}}^{(t)}) \right\|_2^2 \right] \\
& = -\frac{1}{2(q+1)\|f\|_\infty^{(2)}} \left\| \underline{V}_d(\underline{\mathbf{x}}^{(t)})^T \mathbf{grad} f(\underline{\mathbf{x}}^{(t)}) \right\|_2^2,
\end{aligned}$$

where we apply (78) to obtain the inequality. This indicates that

$$(81) \quad \left\| \underline{V}_d(\underline{\mathbf{x}}^{(t)})^T \mathbf{grad} f(\underline{\mathbf{x}}^{(t)}) \right\|_2^2 \leq 2(q+1)\|f\|_\infty^{(2)} [f(\underline{\mathbf{x}}^*) - f(\underline{\mathbf{x}}^{(t)})]$$

for any  $\underline{\mathbf{x}}^{(t)} \in \underline{R}_d \oplus r_3$ . Therefore, by Corollary 16, we obtain that

$$\begin{aligned}
& d_g(\underline{\mathbf{x}}^{(t+1)}, \underline{\mathbf{x}}^*) \\
& \stackrel{(i)}{\leq} d_g(\underline{\mathbf{x}}^{(t)}, \underline{\mathbf{x}}^*) - 2\eta \left\langle \underline{V}_d(\underline{\mathbf{x}}^{(t)})\underline{V}_d(\underline{\mathbf{x}}^{(t)})^T \mathbf{grad} f(\underline{\mathbf{x}}^{(t)}) \right\rangle
\end{aligned}$$

$$\begin{aligned}
 & + \zeta(1, \rho) \cdot \eta^2 \left\| \underline{V}_d(\underline{\mathbf{x}}^{(t)})^T \mathbf{grad} f(\underline{\mathbf{x}}^{(t)}) \right\|_2^2 \\
 & \stackrel{(ii)}{\leq} d_g(\underline{\mathbf{x}}^{(t)}, \underline{\mathbf{x}}^*)^2 + 2\eta \left[ f(\underline{\mathbf{x}}^{(t)}) - f(\underline{\mathbf{x}}^*) - \frac{\beta_0}{4} d_g(\underline{\mathbf{x}}^*, \underline{\mathbf{x}}^{(t)})^2 \right. \\
 & \quad \left. + \tilde{A}_\rho \cdot (q+1)^5 \left( \max \left\{ 1, \|f\|_{\infty,4}^* \right\} \right)^3 d_g(\underline{\mathbf{x}}^*, \underline{\mathbf{x}}^{(t)})^3 \right] \\
 & \quad + \zeta(1, \rho) \cdot \eta^2 \cdot 2(q+1) \|f\|_\infty^{(2)} \left[ f(\underline{\mathbf{x}}^*) - f(\underline{\mathbf{x}}^{(t)}) \right] \\
 & \stackrel{(iii)}{\leq} \left( 1 - \frac{\beta_0 \eta}{4} \right) \cdot d_g(\underline{\mathbf{x}}^*, \underline{\mathbf{x}}^{(t)})^2 - 2\eta \left[ 1 - \eta \cdot \zeta(1, \rho) \cdot (q+1) \|f\|_\infty^{(2)} \right] \cdot \left[ f(\underline{\mathbf{x}}^*) - f(\underline{\mathbf{x}}^{(t)}) \right] \\
 & \leq \left( 1 - \frac{\beta_0 \eta}{4} \right) \cdot d_g(\underline{\mathbf{x}}^*, \underline{\mathbf{x}}^{(t)})^2
 \end{aligned}$$

whenever  $0 < \eta \leq \min \left\{ \frac{4}{\beta_0}, \frac{1}{(q+1)\|f\|_\infty^{(2)}\zeta(1,\rho)} \right\}$ , where we utilize Corollary 16 and the monotonicity of  $\zeta(1, c)$  with respect to  $c$  in (i), apply (80) and (81) to obtain (ii), and use the choice of  $r_3$  to argue that

$$\begin{aligned}
 & \tilde{A}_\rho \cdot (q+1)^5 \left( \max \left\{ 1, \|f\|_{\infty,4}^* \right\} \right)^3 d_g(\underline{\mathbf{x}}^*, \underline{\mathbf{x}}^{(t)})^3 \\
 & \leq \tilde{A}_\rho \cdot (q+1)^5 \left( \max \left\{ 1, \|f\|_{\infty,4}^* \right\} \right)^3 d_g(\underline{\mathbf{x}}^*, \underline{\mathbf{x}}^{(t)})^2 \cdot \arccos \left( 1 - \frac{1}{2} r_3^2 \right) \\
 & \leq \frac{\beta_0}{8} \cdot d_g(\underline{\mathbf{x}}^*, \underline{\mathbf{x}}^{(t)})^2
 \end{aligned}$$

in (iii). By telescoping, we conclude that when  $0 < \eta \leq \min \left\{ \frac{4}{\beta_0}, \frac{1}{(q+1)\|f\|_\infty^{(2)}\zeta(1,\rho)} \right\}$  and  $\underline{\mathbf{x}}^{(0)} \in \underline{R}_d \oplus r_3$ ,

$$d_g(\underline{\mathbf{x}}^*, \underline{\mathbf{x}}^{(t)}) \leq \left( 1 - \frac{\beta_0 \eta}{4} \right)^{\frac{t}{2}} d_g(\underline{\mathbf{x}}^*, \underline{\mathbf{x}}^{(0)}).$$

The result follows.

(b) The result follows obviously from (a) and the fact that  $d_g(\underline{\mathbf{x}}^{(t)}, \underline{R}_d) \leq d_g(\underline{\mathbf{x}}^{(t)}, \underline{\mathbf{x}}^*)$  for all  $t \geq 0$ .

(c) The proof is logically similar to the proof of (c) in Theorem 5. We write the spectral decompositions of  $\mathcal{H}f(\mathbf{x})$  and  $\mathcal{H}\hat{f}_h(\mathbf{x})$  as:

$$\mathcal{H}f(\mathbf{x}) = \underline{V}(\mathbf{x})\underline{\Lambda}(\mathbf{x})\underline{V}(\mathbf{x})^T \quad \text{and} \quad \mathcal{H}\hat{f}_h(\mathbf{x}) = \hat{\underline{V}}(\mathbf{x})\hat{\underline{\Lambda}}(\mathbf{x})\hat{\underline{V}}(\mathbf{x})^T.$$

By Weyl's theorem (Theorem 4.3.1 in Horn and Johnson (2012)) and uniform bounds (cf. Equation (30) in the main paper),

$$\begin{aligned}
 |\lambda_j(\mathbf{x}) - \hat{\lambda}_j(\mathbf{x})| & \leq \left\| \mathcal{H}f(\mathbf{x}) - \mathcal{H}\hat{f}_h(\mathbf{x}) \right\|_2 \\
 & \leq (q+1) \left\| f(\mathbf{x}) - \hat{f}_h(\mathbf{x}) \right\|_\infty^{(2)} \\
 & = O(h^2) + O_P \left( \sqrt{\frac{|\log h|}{nh^{q+4}}} \right).
 \end{aligned}$$

Thus,  $\hat{f}_h$  will satisfy conditions (A2) when  $h$  is sufficiently small and  $\frac{nh^{q+4}}{|\log h|}$  is sufficiently large. According to Davis-Kahan theorem (Lemma 12 here), uniform bounds (30), and the continuity of exponential maps, we have that

$$\begin{aligned}
& d_g \left( \text{Exp}_{\mathbf{y}} \left( \eta \hat{V}_d(\mathbf{y}) \hat{V}_d(\mathbf{y})^T \text{grad } \hat{f}_h(\mathbf{y}) \right), \text{Exp}_{\mathbf{y}} \left( \eta V_d(\mathbf{y}) V_d(\mathbf{y})^T \text{grad } f(\mathbf{y}) \right) \right) \\
& \leq \eta C_3 \left\| \hat{V}_d(\mathbf{y}) \hat{V}_d(\mathbf{y})^T \text{grad } \hat{f}_h(\mathbf{y}) - V_d(\mathbf{y}) V_d(\mathbf{y})^T \text{grad } f(\mathbf{y}) \right\|_2 \\
& \leq \eta C_3 \left\| \hat{V}_d(\mathbf{y}) \hat{V}_d(\mathbf{y})^T \left[ \text{grad } \hat{f}_h(\mathbf{y}) - \text{grad } f(\mathbf{y}) \right] \right\|_2 \\
& \quad + \eta C_3 \left\| \left[ \hat{V}_d(\mathbf{y}) \hat{V}_d(\mathbf{y})^T - V_d(\mathbf{y}) V_d(\mathbf{y})^T \right] \text{grad } f(\mathbf{y}) \right\|_2 \\
& \stackrel{(i)}{\leq} \eta C_3 \left\| \text{grad } \hat{f}_h(\mathbf{y}) - \text{grad } f(\mathbf{y}) \right\|_2 + \eta C_3 \cdot \frac{\left\| \mathcal{H}f(\mathbf{y}) - \mathcal{H}\hat{f}_h(\mathbf{y}) \right\|_2 \cdot \|\text{grad } f(\mathbf{y})\|}{\underline{\beta}_0} \\
& \leq \eta C_3 \sqrt{q+1} \left\| \hat{f}_h - f \right\|_\infty^{(1)} + \eta C_3 \cdot \frac{(q+1) \left\| \hat{f}_h - f \right\|_\infty^{(2)} \sqrt{q+1} \|f\|_\infty^{(1)}}{\underline{\beta}_0} \\
& \equiv \epsilon_{n,h} = O(h^2) + O_P \left( \sqrt{\frac{|\log h|}{nh^{q+4}}} \right)
\end{aligned}$$

for any  $\mathbf{y} \in \text{Ball}_{q+1}(\mathbf{x}^*, r_3) \cap \Omega_q$ , where we utilize the Davis-Kahan theorem and the fact that  $\left\| \hat{V}_d(\mathbf{y}) \hat{V}_d(\mathbf{y})^T \right\|_2 = 1$  in (i). Hence, when  $h \rightarrow 0$  and  $\frac{nh^{q+4}}{|\log h|} \rightarrow \infty$ ,

$$\begin{aligned}
& d_g \left( \text{Exp}_{\mathbf{y}} \left( \eta \hat{V}_d(\mathbf{y}) \hat{V}_d(\mathbf{y})^T \text{grad } \hat{f}_h(\mathbf{y}) \right), \text{Exp}_{\mathbf{y}} \left( \eta V_d(\mathbf{y}) V_d(\mathbf{y})^T \text{grad } f(\mathbf{y}) \right) \right) \\
(82) \quad & \leq \epsilon_{n,h} = O(h^2) + O_P \left( \sqrt{\frac{|\log h|}{nh^{q+4}}} \right) \leq (1 - \Upsilon) \cdot \arccos \left( 1 - \frac{1}{2} r_3^2 \right)
\end{aligned}$$

with probability tending to 1.

We now claim that  $d_g(\hat{\mathbf{x}}^{(t)}, \mathbf{x}^*) \leq \arccos \left( 1 - \frac{r_3^2}{2} \right)$  and

$$(83) \quad d_g(\hat{\mathbf{x}}^{(t+1)}, \mathbf{x}^*) \leq \Upsilon \cdot d_g(\hat{\mathbf{x}}^{(t)}, \mathbf{x}^*) + \epsilon_{n,h}$$

for all  $t \geq 0$ . We again prove this claim by induction on the iteration number. Note that when  $t = 1$ , we derive that

$$\begin{aligned}
& d_g(\hat{\mathbf{x}}^{(1)}, \mathbf{x}^*) \\
& = d_g \left( \text{Exp}_{\hat{\mathbf{x}}^{(0)}} \left( \eta \hat{V}_d(\hat{\mathbf{x}}^{(0)}) \hat{V}_d(\hat{\mathbf{x}}^{(0)})^T \text{grad } \hat{f}_h(\hat{\mathbf{x}}^{(0)}) \right), \mathbf{x}^* \right) \\
& \stackrel{(i)}{\leq} d_g \left( \text{Exp}_{\hat{\mathbf{x}}^{(0)}} \left( \eta V_d(\hat{\mathbf{x}}^{(0)}) V_d(\hat{\mathbf{x}}^{(0)})^T \text{grad } f(\hat{\mathbf{x}}^{(0)}) \right), \mathbf{x}^* \right) \\
& \quad + d_g \left( \text{Exp}_{\hat{\mathbf{x}}^{(0)}} \left( \eta \hat{V}_d(\hat{\mathbf{x}}^{(0)}) \hat{V}_d(\hat{\mathbf{x}}^{(0)})^T \text{grad } \hat{f}_h(\hat{\mathbf{x}}^{(0)}) \right), \text{Exp}_{\hat{\mathbf{x}}^{(0)}} \left( \eta V_d(\hat{\mathbf{x}}^{(0)}) V_d(\hat{\mathbf{x}}^{(0)})^T \text{grad } f(\hat{\mathbf{x}}^{(0)}) \right) \right) \\
& \stackrel{(ii)}{\leq} \Upsilon \cdot d_g(\hat{\mathbf{x}}^{(0)}, \mathbf{x}^*) + \epsilon_{n,h},
\end{aligned}$$

where we apply the triangle inequality in (i) and leverage the result in (a) and (82) to obtain (ii). The triangle inequality is valid in this context because the geodesic measures the

minimal distance between two points on  $\Omega_q$ . Moreover, by the choice of  $\hat{\underline{x}}^{(0)}$  and (82), we are ensured that  $d_g(\hat{\underline{x}}^{(1)}, \underline{x}^*) \leq \arccos\left(1 - \frac{r_3^2}{2}\right)$ . In the induction from  $t \mapsto t + 1$ , we suppose that  $d_g(\hat{\underline{x}}^{(t)}, \underline{x}^*) \leq \arccos\left(1 - \frac{r_3^2}{2}\right)$  and the claim (83) holds at iteration  $t$ . The same argument then implies that the claim (83) holds for iteration  $t + 1$  and that  $d_g(\hat{\underline{x}}^{(t+1)}, \underline{x}^*) \leq \arccos\left(1 - \frac{r_3^2}{2}\right)$ . The claim (83) is thus verified.

Now, given that  $\Upsilon = \sqrt{1 - \frac{\beta_0 \eta}{4}} < 1$ , we iterate the claim (83) to show that

$$\begin{aligned} d_g(\hat{\underline{x}}^{(t)}, \underline{x}^*) &\leq \Upsilon \cdot d_g(\hat{\underline{x}}^{(t-1)}, \underline{x}^*) + \epsilon_{n,h} \\ &\leq \Upsilon \left[ \Upsilon \cdot d_g(\hat{\underline{x}}^{(t-2)}, \underline{x}^*) + \epsilon_{n,h} \right] + \epsilon_{n,h} \\ &\leq \Upsilon^t \cdot d_g(\hat{\underline{x}}^{(0)}, \underline{x}^*) + \left[ \sum_{s=0}^{t-1} \Upsilon^s \right] \epsilon_{n,h} \\ &\leq \Upsilon^t \cdot d_g(\hat{\underline{x}}^{(0)}, \underline{x}^*) + \frac{\epsilon_{n,h}}{1 - \Upsilon} \\ &= \Upsilon^t \cdot d_g(\hat{\underline{x}}^{(0)}, \underline{x}^*) + O(h^2) + O_P \left( \sqrt{\frac{|\log h|}{nh^{q+4}}} \right), \end{aligned}$$

where the fourth inequality follows by summing the geometric series, and the last equality is due to our notation  $\epsilon_{n,h} = O(h^2) + O_P \left( \sqrt{\frac{|\log h|}{nh^{q+4}}} \right)$ . It completes the proof.

(d) The result follows directly from (c) and the inequality  $d_g(\hat{\underline{x}}^{(t)}, \underline{R}_d) \leq d_g(\hat{\underline{x}}^{(t)}, \underline{x}^*)$  for all  $t \geq 0$ .  $\square$